

การจำแนกและการตรวจวินิจฉัยระดับโมเลกุลของเชื้อไวรัสไข้หวัดนก
สายพันธุ์ H5N1 และไข้หวัดสุนัขสายพันธุ์ H3N8



นาย สัตยชัย พยุงภร

สถาบันวิทยบริการ

จุฬาลงกรณ์มหาวิทยาลัย

วิทยานิพนธ์นี้เป็นส่วนหนึ่งของการศึกษาตามหลักสูตรปริญญาวิทยาศาสตรดุษฎีบัณฑิต

สาขาวิชาชีวเวชศาสตร์ (สหสาขาวิชา)

บัณฑิตวิทยาลัย จุฬาลงกรณ์มหาวิทยาลัย

ปีการศึกษา 2549

ลิขสิทธิ์ของจุฬาลงกรณ์มหาวิทยาลัย

MOLECULAR CHARACTERIZATION AND MOLECULAR DIAGNOSIS OF
RECENTLY EMERGED INFLUENZA A VIRUSES (H5N1 & H3N8)



Mr. Sunchai Payungporn

สถาบันวิทยบริการ
จุฬาลงกรณ์มหาวิทยาลัย

A Dissertation Submitted in Partial Fulfillment of the Requirements
for the Degree of Doctor of Philosophy Program in Biomedical Sciences

(Interdisciplinary Program)

Graduate School

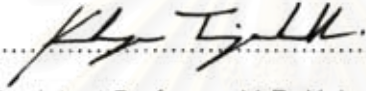
Chulalongkorn University

Academic Year 2006


Copyright of Chulalongkorn University


Thesis Title Molecular characterization and molecular diagnosis of
recently emerged influenza A viruses (H5N1 & H3N8)
By Mr. Sunchai Payungporn
Field of Study Biomedical Sciences
Thesis Advisor Professor Yong Poovorawan, M.D.
Thesis Co-advisor Assistant Professor Alongkorn Amonsin, D.V.M., Ph.D.


Accepted by the Graduate School, Chulalongkorn University in Partial
Fulfillment of the Requirements for the Doctoral Degree

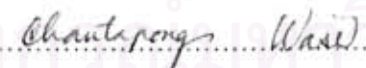
..... Dean of the Graduate School
(Assistant Professor M.R. Kalaya Tingsabadh, Ph.D.)

THESIS COMMITTEE

..... Chairman
(Professor Apiwat Mutirangura, M.D., Ph.D.)

..... Thesis Advisor
(Professor Yong Poovorawan, M.D.)

..... Thesis Co-advisor
(Assistant Professor Alongkorn Amonsin, D.V.M., Ph.D.)

..... Member
(Associate Professor Chantapong Wasi, M.D.)

..... Member
(Associate Professor Kanisak Oraveerakul, D.V.M., Ph.D.)

..... Member
(Associate Professor Parvapan Bhattarakosol, Ph.D.)

สัญญาชัย พยุงภร : การจำแนกและการตรวจวินิจฉัยระดับโมเลกุลของเชื้อไวรัสไข้หวัดนกสายพันธุ์ H5N1 และไข้หวัดสุนัขสายพันธุ์ H3N8 (MOLECULAR CHARACTERIZATION AND MOLECULAR DIAGNOSIS OF RECENTLY EMERGED INFLUENZA A VIRUSES (H5N1 & H3N8)) อ.ที่ปรึกษา: ศ.นพ.ยง ภู่วรวรรณ, อ.ที่ปรึกษาร่วม: ผศ.น.สพ. อลงกร อมรศิลป์, 202หน้า.

การศึกษานี้ได้จำแนกลักษณะทางพันธุกรรมของไวรัสไข้หวัดนกสายพันธุ์ H5N1 ที่ระบาดในประเทศไทย ในช่วงต้นปี พ.ศ. 2547 จากการวิเคราะห์รหัสพันธุกรรมและความสัมพันธ์เชิงวงศ์วานวิทยาพบว่าสายพันธุ์ของไวรัสไข้หวัดนกในประเทศไทยเป็นสายพันธุ์ที่ก่อโรครุนแรงโดยพบว่ามีส่วนของกรดอะมิโนที่มีคุณสมบัติเป็นเบสหลาย ๆ ตัวที่บริเวณ cleavage site ของโมเลกุล hemagglutinin และมีการขาดหายไปของกรดอะมิโน 20 ตัวในส่วนของโมเลกุล neuraminidase นอกจากนี้ยังพบว่ามีกรดอะมิโนขาดหายไปของกรดอะมิโน 5 ตัวในส่วนของ non-structural protein ด้วย จากนั้นได้ทำการพัฒนาการตรวจวินิจฉัยระดับโมเลกุลของเชื้อไวรัสไข้หวัดนกสายพันธุ์ H5N1 โดยใช้เทคนิคต่าง ๆ เช่น multiplex RT-PCR, multiplex real-time RT-PCR และ melting curve analysis

นอกจากนี้ได้ทำการศึกษาเชื้อไวรัสไข้หวัดสุนัขสายพันธุ์ H3N8 จากการระบาดของเชื้อไวรัสในสุนัขที่รัฐฟลอริดา ประเทศสหรัฐอเมริกา โดยได้ทำการแยกเชื้อและจำแนกลักษณะพันธุกรรมของเชื้อไวรัสจากการวิเคราะห์พบว่าเชื้อไวรัสนี้มีลักษณะทางพันธุกรรมใกล้เคียงกับเชื้อไข้หวัดสุนัขที่แยกได้จากสุนัขพันธุ์ Greyhound จากนั้นได้ทำการพัฒนาการตรวจวินิจฉัยระดับโมเลกุลของเชื้อไวรัสไข้หวัดสุนัขสายพันธุ์ H3N8 โดยใช้เทคนิค real-time RT-PCR

โดยสรุปแล้วการศึกษานี้รายงานข้อมูลเกี่ยวกับการจำแนกและวิเคราะห์ลักษณะทางพันธุกรรม พร้อมทั้งพัฒนาการตรวจวินิจฉัยระดับโมเลกุล ทำให้สามารถตรวจสอบการติดเชื้อได้อย่างรวดเร็ว แม่นยำ มีความไวและความจำเพาะสูง จึงมีความเหมาะสมในการตรวจวินิจฉัย และมีความสำคัญต่อการควบคุมและป้องกันการแพร่ระบาดของเชื้อไวรัสไข้หวัดนกสายพันธุ์ H5N1 และไข้หวัดสุนัขสายพันธุ์ H3N8

สาขาวิชา ชีวเวชศาสตร์
ปีการศึกษา 2549

ลายมือชื่อนิสิตสัญญาชัย.....
ลายมือชื่ออาจารย์ที่ปรึกษาอ.ยง.....
ลายมือชื่ออาจารย์ที่ปรึกษาร่วม

#458 96830 20 : MAJOR BIOMEDICAL SCIENCES

KEY WORD: INFLUENZA, H5N1, H3N8, REAL-TIME RT-PCR

SUNCHAI PAYUNGORN: MOLECULAR CHARACTERIZATION AND MOLECULAR DIAGNOSIS OF RECENTLY EMERGED INFLUENZA A VIRUSES (H5N1 & H3N8)
 THESIS ADVISOR: PROF. YONG POOVORAWAN, M.D., THESIS CO-ADVISOR:
 ASST. PROF. ALONGKORN AMORNSIN, D.V.M., Ph.D., 202 pp.

In this report, the genome of A/Chicken/Nakorn-Pathom/Thailand/CU-K2/04 (H5N1), the virus responsible for the avian influenza outbreak during January 2004 in Thailand, was sequenced followed by the phylogenetic analysis. Molecular characterization of this virus showed evidence of highly pathogenic based on polybasic amino acids within the cleavage site of the hemagglutinin (H5), a 20-codon deletion in the neuraminidase (N1) and a 5-codon deletion in the non-structural protein, respectively. Molecular diagnosis for H5N1 influenza detection based on multiplex RT-PCR, multiplex real-time RT-PCR and real-time PCR with melting curve analysis were developed and validated.

We also investigated two outbreaks of respiratory disease in an animal shelter and veterinary clinic in the State of Florida that involved dog breeds other than greyhounds. Influenza A virus subtype H3N8 was isolated and characterized genetically. Comparison of the nucleotide sequence of the hemagglutinin (H3) revealed that the new canine influenza isolates were closely related but distinguishable from earlier virus isolates from greyhound dogs. Moreover, a single step real-time RT-PCR for rapid detection of H3N8 canine influenza A virus was also evaluated.

In conclusion, this study reported the molecular characterization providing crucial information of the nucleotide and deduced amino acid sequences while the molecular diagnosis based on RT-PCR and real-time RT-PCR were rapid, specific and sensitive assays suitable for immediate detection and large scale screening in order to control and prevent severe outbreaks of H5N1 avian influenza and H3N8 canine influenza viruses.

Field of Study: Biomedical sciences

Academic Year: 2006

Student's Signature: *Sunchai Payungorn*

Advisor's Signature: *Yong Poovoran*

Co-advisor's Signature: *Alongkorn Amornsinn*

ACKNOWLEDGEMENTS

I would like to express my deepest gratitude and appreciation to my advisor, Professor Yong Poovorawan, for his competent supervision, guidance, encouragement and criticism which have inspired me to accomplish my study.

I am extremely grateful to my thesis co-advisor, Assistant Professor Dr. Alongkorn Amonsin, for his valuable suggestion, support and encouragement for the completeness of this thesis. I am very grateful to my supervisory committee, Professor Dr. Apiwat Mutirangura, Associate Professor Chantapong Wasi, Associate Professor Dr. Parvapan Bhattarakosol and Associate Professor Dr. Kanisak Oraveerakul for their valuable suggestions and criticisms.

My sincere appreciation is also expressed to Dr. Ruben O. Donis for his valuable advice, excellent ideas and kindness support during one year of my research in the Centers for Disease Control and Prevention, Atlanta, GA. Special thanks must also be extended to Dr. Cynda Crawford and Dr. Li-mei Chen for their advices and suggestions.

I am indebted to Ms. Apiradee Theamboonlers, Ms. Pojchanad Jantaradsamee, Ms. Jutatip Keawcharoen, Mr. Rachod Tantilertcharoen, Ms. Sumitra Wattanodorn and Ms. Soraya Panklom for their technical instructions and sincere helpful during my study. I would like to thank Ms. Salin Chutinimitkul, Ms. Piraya Phakdeewirot, Mr. Kamol Suwannakarn, Mr. Thaweesak Chieochansin, Ms. Nuananong Pariyothorn, Ms. Cheunsakon Choatrakol and Ms. Piyada Linsuwanon for their assistances of some materials and logistic works.

I am particularly indebted to the Royal Golden Jubilee (RGJ) Ph.D. program, Thailand Research Fund (TRF) and the National Center for Genetic Engineering and Biotechnology for scholarship and funding supports. Special appreciation must also be extended to the Centre of Excellence in Clinical Virology, Department of Paediatrics, Faculty of Medicine, Chulalongkorn University; Faculty of Veterinary, Chulalongkorn University and Centers for Disease Control and Prevention, Atlanta, GA.

Finally, I would like take this opportunity to express the profound gratitude from the bottom of my heart to my beloved parents, family and friends for their love, encouragements and moral supports throughout this study.

TABLE OF CONTENTS

	Page
ABSTRACT (THAI).....	IV
ABSTRACT (ENGLISH).....	V
ACKNOWLEDGEMENTS.....	VI
TABLE OF CONTENTS.....	VII
LIST OF TABLES.....	VIII
LIST OF FIGURES.....	IX
LIST OF ABBREVIATIONS.....	XI
CHAPTER	
I. INTRODUCTION.....	1
II. REVIEW OF RELATED LITERATURE.....	8
III. MATERIALS AND METHODS	38
IV. RESULTS.....	61
V. CONCLUSION AND DISCUSSION.....	113
REFERENCES.....	132
APPENDICES.....	145
APPENDIX A.....	146
APPENDIX B.....	171
APPENDIX C.....	180
BIOGRAPHY.....	202

LIST OF TABLES

Table		Page
1	Characteristics of RNA segments and gene products of influenza	11
2	Pandemics of influenza A viruses during the 20 th century	16
3	Previous outbreaks of highly pathogenic avian influenza worldwide	21
4	Number of human cases of H5N1 avian influenza reported to WHO	24
5	Primers used for whole genome amplification and sequencing	62
6	Summary of amino acid sequences analysis	75
7	Primers compositions in each multiplex RT-PCR systems	82
8	Multiplex RT-PCR primers set for H5N1 influenza A virus detection	85
9	Multiplex real-time PCR primers/probes for H5N1 influenza detection	90
10	Specificity test of multiplex real-time RT-PCR	95
11	Primers used for discrimination of HPAI and LPAI by melting analysis	97
12	Intra- and inter-assay variation of melting temperature (T _m)	101
13	H3 Amino acid differences between canine and equine influenza	106
14	H3 primers/probe for canine influenza detection by real-time RT-PCR	108
15	Specificity test of canine H3 primers/probe set	109
16	Properties of molecular methods suitable for detection of influenza	116
17	Normalized viral RNA in different tissue organs of infected tigers	121
18	Guidelines for agarose gel analysis of multiplex PCR products	149
19	Multiplex fluorescence reporters dyes suitable for each instrument	155
20	Spectrophotometric conversions for nucleic acid templates	158
21	Common fluorescence reporters & quenchers in real-time PCR	163
22	pGEM-T Easy Vector sequence reference points	164
23	Data used to calculate TCID ₅₀ and EID ₅₀	176
24	Specific primers and probes for GAPDH and Cyclophilin B	186
25	Silencing efficiency of the optimization plate	186
26	Quantitation of M gene by real-time RT-PCR	188
27	Membrane trafficking gene families	190
28	Means of delta Ct values from relative quantitation of M gene	194
29	Possible roles of genes involving in the replication of influenza virus	200

LIST OF FIGURES

Figure		Page
1	Structure of influenza A virus particle	10
2	Various subtypes of influenza A viruses	13
3	Mechanism of antigenic diversity of influenza A viruses	15
4	Polybasic amino acid insertion at the cleavage site of HA	19
5	Replication cycle of influenza A viruses	26
6	Specific primers for amplification of H5N1 influenza A virus	63
7	Phylogenetic tree of HA (H5) gene	66
8	Phylogenetic tree of NA (N1) gene	67
9	Phylogenetic tree of PB2 gene	68
10	Phylogenetic tree of PB1 gene	69
11	Phylogenetic tree of PA gene	70
12	Phylogenetic tree of NP gene	71
13	Phylogenetic tree of M gene	72
14	Phylogenetic tree of NS gene	73
15	Alignments of amino acid sequences of the HA cleavage site	76
16	Alignments of deduced amino acid sequences of the NA stalk region	77
17	Alignments of deduced amino acid sequence of NS	78
18	Schematic maps of candidate primers used in multiplex RT-PCR	81
19	Band patterns amplified by 12 systems of multiplex RT-PCR	82
20	Construction of positive controls	83
21	Interpretation of influenza A virus detection by multiplex RT-PCR	85
22	Specificity test of multiplex RT-PCR	86
23	Representative results of H5N1 multiplex RT-PCR detection	87
24	Sensitivity of multiplex RT-PCR detection	88
25	Maps of primers and probes used in multiplex real-time RT-PCR	90
26	Representative results obtained from multiplex real-time RT-PCR	93
27	Nucleotide sequences alignment between HPAI and LPAI	97
28	Discrimination between HPAI and LPAI by melting analysis	99

LIST OF FIGURES (CONT.)

Figure		Page
29	Phylogenetic tree of H3 gene of canine influenza	102
30	Phylogenetic relationships of H3 hemagglutinin genes	105
31	Sensitivity test of H3 gene detection by real-time RT-PCR	110
32	Standard curves of H3 gene obtained from real-time RT-PCR	111
33	Standard curve of matrix and 28S rRNA based on real-time RT-PCR	120
34	Multiple alignments of matrix primers and probe	124
35	Multiple alignments of neuraminidase (N1) primers and probe	125
36	Multiple alignments of hemagglutinin (H5) primers and probe	126
37	Variations of multiple basic amino acids within cleavage site of HA	128
38	Schematic diagram of the PCR process	147
39	Schematic diagram of reverse transcription process	148
40	Amplification plot obtained by real-time PCR analysis	150
41	Detection chemistries commonly used in real-time PCR	153
42	Representative result of real-time PCR with melting curve analysis	154
43	Representative of absolute quantitation by real-time PCR	157
44	Primer and probe spanning of an intron / exon boundary	162
45	Circle map of pGEM-T Easy vector (Promega)	164
46	Model for RNA interference triggered by dsRNA	166
47	Silencing reagents for RNAi screening	166
48	Designation of effective siRNA	169
49	Schematic diagram represent anatomy of embryonated egg	172
50	Example of result obtained by Hemagglutination assay	179
51	Transfection of siRNAs by reverse transfection format	183
52	Optimization of siRNA transfection and silencing efficiency	184
53	Results of MTT assay obtained from the optimization plate	185
54	Optimization of condition for virus infection	188
55	Relative quantification of M gene by real-time RT-PCR	195
56	Proposed roles of genes involving in the replication of influenza virus	201

LIST OF ABBREVIATIONS

μg	=	microgram
μl	=	microlitre
cDNA	=	Complementary deoxyribonucleic acid
CF	=	Complement fixation
CIV	=	Canine Influenza Virus
cRNA	=	Complementary ribonucleic acid
DEPC	=	Diethylpyrocarbonate
DMEM	=	Dulbecco's Modified Eagle Medium
DNA	=	Deoxyribonucleic acid
EDTA	=	Ethylene Diamine Tetraacetic Acid
EIA	=	Enzyme Immunoassay
EID	=	Egg Infective Dose
FBS	=	Fetal Bovine Serum
FDA	=	Food and Drug Administration
GTC	=	Guanidine Thiocyanate
HA	=	Haemagglutinin
HI	=	Haemagglutination Inhibition
HPAI	=	High pathogenic avian influenza
IAA	=	Iso-Amyl Alcohol
ICTV	=	International Committee on Taxonomy of Viruses
IFA	=	Immunofluorescence assay
IPTG	=	Isopropyl-Thio-B-D-Galactopyranoside
LPAI	=	Low pathogenic avian influenza
M	=	Matrix protein
MDCK	=	Madin-Darby Canine Kidney
mg	=	milligram
ml	=	millilitre

LIST OF ABBREVIATIONS (CONT.)

mRNA	=	Messenger ribonucleic acid
NA	=	Neuraminidase
NEP	=	Nuclear Export Protein
nm	=	nanometre
NP	=	Nucleoprotein
NS	=	Non-structural protein
OIE	=	Office International des Epizooties
PA	=	Polymerase Acidic protein
PB1	=	Polymerase Basic protein 1
PB2	=	Polymerase Basic protein 2
PBS	=	Phosphate Buffered Saline
PCR	=	Polymerase Chain Reaction
RNA	=	Ribonucleic acid
RNAi	=	RNA Interference
RNP	=	Ribonucleoprotein
rRNA	=	Ribosomal ribonucleic acid
RT	=	Reverse Transcription
RTF	=	Reverse Transfection Format
SDS	=	Sodium Dodecyl Sulfate
siRNA	=	Short Interfering RNA
TCID	=	Tissue Culture Infective Dose
tRNA	=	Transfer ribonucleic acid
TSR	=	Template Suppression Reagent
vRNA	=	Viral ribonucleic acid
WHO	=	World Health Organization

CHAPTER I

INTRODUCTION

BACKGROUND AND RATIONALE

Influenza virus infection is a major public health problem worldwide, causing millions of cases in severe illness associated with various respiratory syndromes and approximately 500,000 deaths annually [1]. Globally, about 20% of children and 5% of adults develop symptomatic influenza each year [2]. In humans, influenza A virus infection occurs in the upper respiratory tract and in the lungs [3]. There are three major types of influenza viruses-A, B and C according to differences in their nucleoproteins and matrix proteins. Of the three types, most pandemics of influenza are associated with type A [4].

Influenza A viruses infection

Influenza A viruses threat as a pathogen depends on some of the virus's unique properties. Firstly, the virus can easily spread by aerosol. Second, accumulations of point mutations "antigenic drift" in the virus' principal antigens HA and NA are frequent, enabling the virus to readily escape protective immunity of host [5]. Third, new strains of virus markedly different antigenically can be generated by genetic reassortment "antigenic shift" [6]. When influenza viruses from two species, such as human and swine, infect the same cell, hybrid (reassortant) viruses containing RNA segments from the two species can emerge [7]. The hybrid virus, with the resulting major antigenic alteration, can be especially virulent, because it is not restrained by host immunity to previously prevalent strains of the virus. The mortality due to influenza virus infection is generally found in infants, adults over 65 years of age, and immunocompromised patients [8]. As the population ages in industrialized countries, influenza virus infection and its associated complications and mortality will likely become an even larger public health problem.

Influenza A viruses can be classified into various subtypes on the basis of antigenic differences between their two surface glycoproteins, haemagglutinin (HA) and neuraminidase (NA). Serologically, 16 subtypes of HA (H1-H16) and 9 subtypes of NA (N1-N9) have been identified. All of these occur in viruses that circulate in aquatic birds, and these species serve as the natural reservoir for all influenza A viruses [1]. Normally, only H1N1, H2N2, and H3N2 viruses were known to have circulated extensively in humans. During the past few years, various subtypes of influenza A viruses including H5N1, H7N7, H7N3 and H9N2 have been reported to infect humans [9]. In addition, H5N1 avian influenza A virus has been recently reported to infect canine and felines (cats, tigers and leopards) [10 -12]. Moreover, H3N8 equine influenza A virus also directly transmitted from equine to canine species [13].

Outbreaks of H5N1 avian influenza A viruses

In 1997, the outbreak of influenza A virus subtype H5N1 caused a fulminating and rapidly fatal systemic disease in domestic poultry. Although this virus spread directly from poultry to humans in Hong Kong and killed 6 of 18 infected humans [14], the poultry depopulation policy of the Hong Kong government had successfully terminated this virus. However, in 2001, Hong Kong reported a re-emergence of highly pathogenic avian influenza (HPAI) H5N1 in the live-bird markets. In early February 2003, the second occurrence of human infection with avian influenza virus (H5N1) was reported. Thereafter, H5N1 influenza A virus repeatedly caused several epidemics in 10 different Asian countries including Korea, Vietnam, Japan, Taipei, Laos, Cambodia, China, Pakistan, Indonesia and Thailand in early 2004. As a consequence, avian influenza A (H5N1) has cross-infected humans and killed 16 children and adults in Vietnam [15]. Similarly, this virus has emerged in Thailand causing a major economic loss in the poultry industry. Moreover, it has killed several persons diagnosed with the infection and over 30 million poultry from both industry and backyards had to be slaughtered [16].

According to the early 2004 outbreak of H5N1 avian influenza A virus in Thailand, there is a requirement for sensitive and rapid diagnostic techniques to verify the clinical diagnosis of H5N1 influenza A virus and improve the quality of surveillance systems. One thing must be done before developing accurate and specific diagnostic methods is to characterize the genome organization and strain of this virus in order to design specific primers and probes used in molecular diagnosis.

Outbreaks of H3N8 canine influenza A viruses

Influenza A subtype H3N8 virus has recently emerged as a respiratory pathogen in dogs in association with outbreaks of acute respiratory disease in racing greyhounds [13]. The disease is caused by a novel virus closely related to contemporary equine influenza A subtype H3N8 viruses with which it shares $\geq 96\%$ nucleotide sequence identity, suggesting that the entire virus was directly transmitted from horses to dogs without reassortment with other strains [13, 17, 18]. It was first identified in greyhounds in Florida in January 2004 and was later reported from other states in the USA, including Texas, New York and Iowa [19]. The initial reports of CIV in racetracks were followed by outbreaks in shelters, day-care centers, veterinary clinics, and related facilities. Clinical signs such as 'kennel cough', nasal discharge and low-grade fever can be seen. Most infected dogs experience a mild form of disease while some develop clinical signs of acute pneumonia [13, 20].

Infection with canine influenza virus induces a humoral antibody response that can be readily detected in convalescent serum samples as early as seven days after infection. Although canine influenza vaccines are likely to be protective, they have not yet become commercially available. Twenty percent of infected dogs can have a subclinical infection and serve as carriers without showing any clinical sign [21]. Therefore, disease control practices are currently centered on hygiene and isolation.

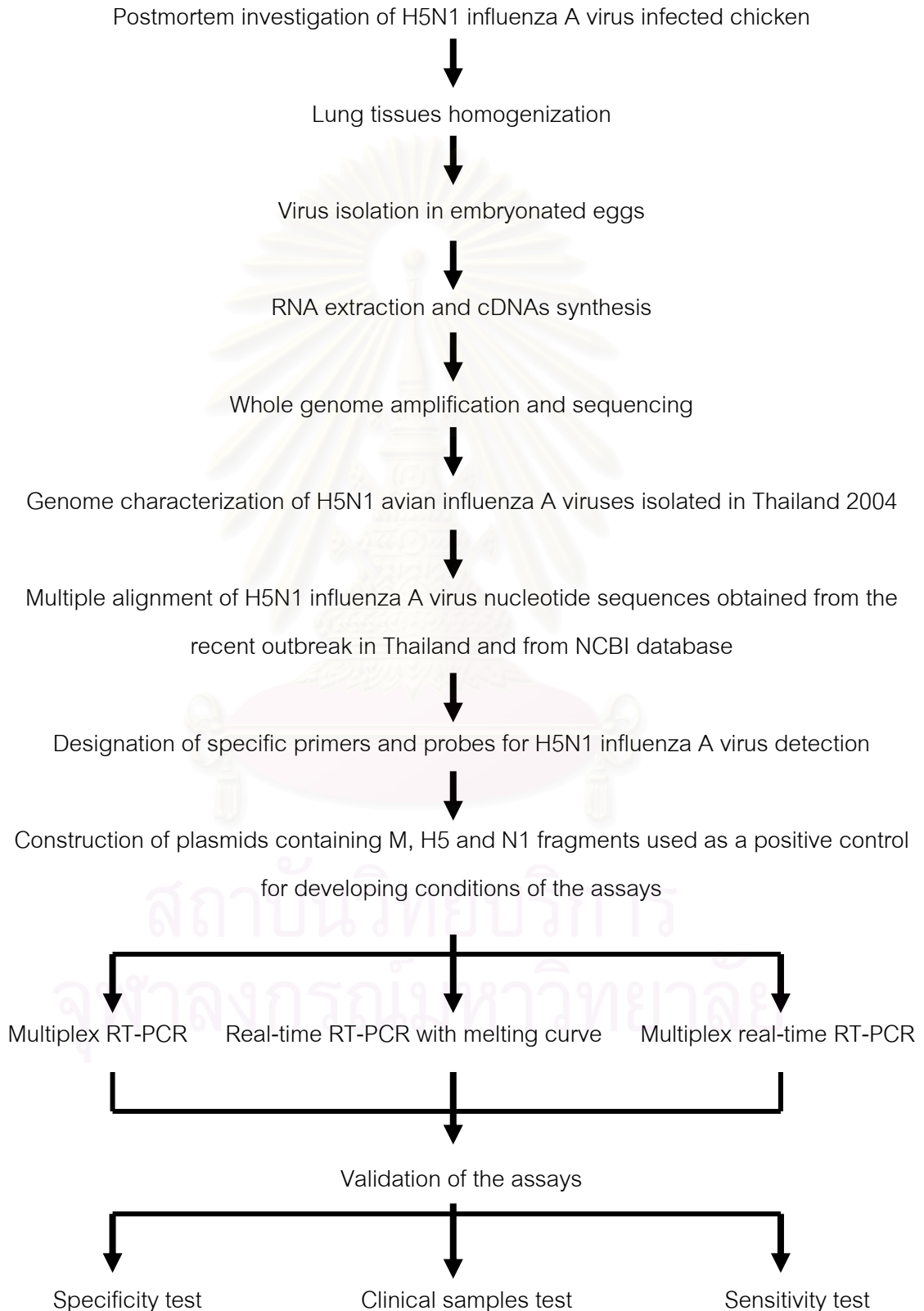
In this study, we characterized the genome sequences of influenza A viruses that recently emerged during the past few years, which including H5N1 avian influenza and H3N8 canine influenza. Then we developed molecular diagnostic assays based on RT-PCR and real-time RT-PCR for rapid and specific detection of both H5N1 avian influenza and H3N8 canine influenza.

Objectives

1. To characterize and analyze the genome sequence of H5N1 avian influenza A virus during the first outbreak in Thailand
2. To develop a rapid and cost-effective assay based on Multiplex RT-PCR for H5N1 avian influenza A virus detection
3. To develop a rapid and sensitive assay based on Multiplex real-time RT-PCR for H5N1 avian influenza A virus detection
4. To develop a rapid and effective assay based on real-time RT-PCR with melting curve analysis for discrimination between highly pathogenic avian influenza (HPAI) and low pathogenic avian influenza (LPAI) subtype H5
5. To characterize and analyze the genome sequence of H3N8 canine influenza A viruses isolated from non-greyhound dogs
6. To develop a rapid and sensitive assay based on real-time RT-PCR for H3N8 canine influenza A virus

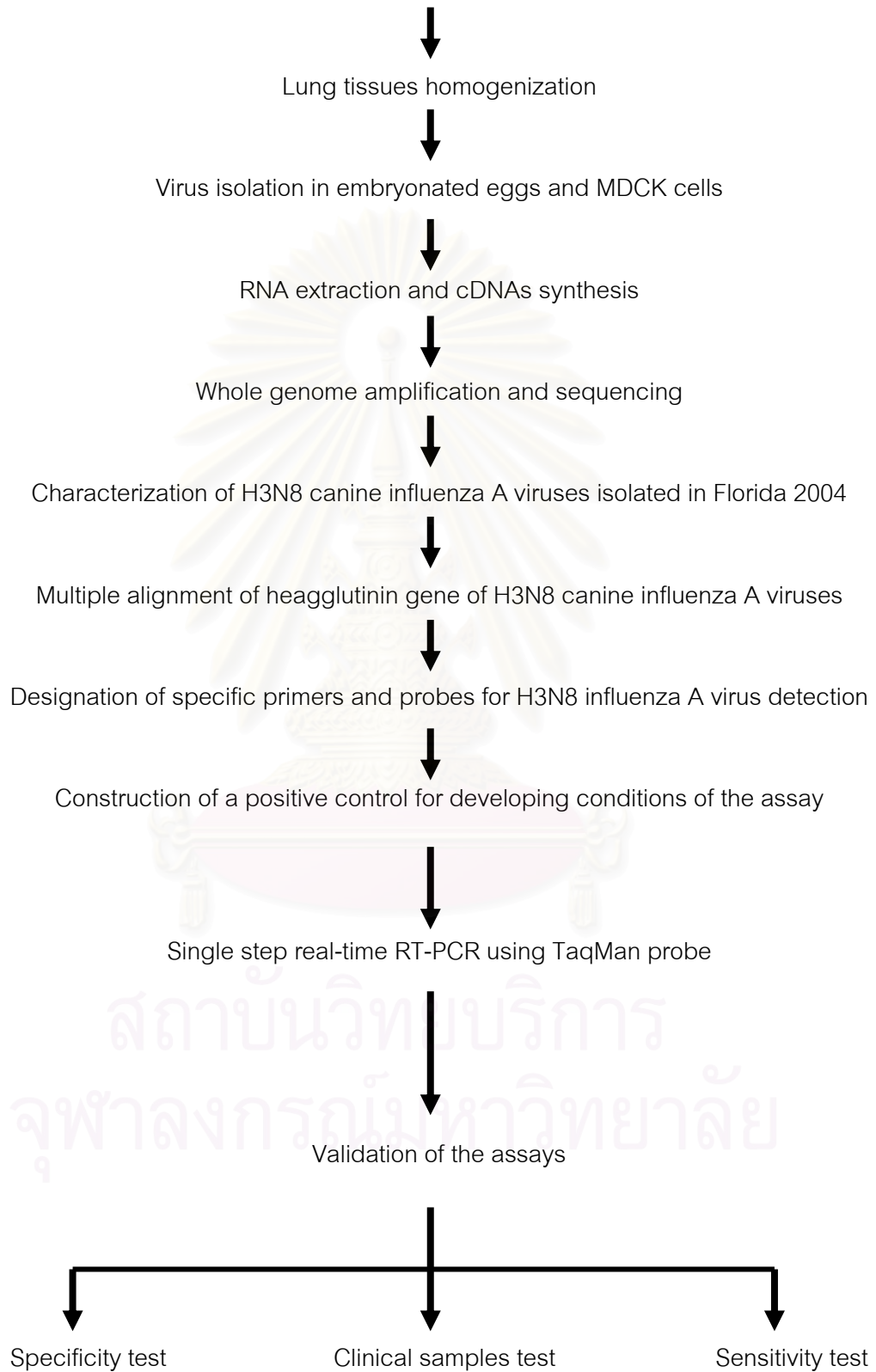
Conceptual Framework

1. Molecular characterization and diagnosis of H5N1 avian influenza A virus



2. Molecular characterization and diagnosis of H3N8 canine influenza A virus

Postmortem investigation of H3N8 influenza A virus infected non-greyhound dogs



Key Words

Influenza A virus, H5N1, H3N8, molecular characterization, molecular diagnosis, multiplex RT-PCR, real-time RT-PCR

Expected Benefits

1. Genome sequences of the virus (H5N1 avian influenza and H3N8 canine influenza) will be submitted into GenBank database for further epidemiological and phylogenetic analysis representing genetic evolution and relationship among several virus strains isolated from different hosts or outbreaks.
2. The nucleotide and deduced amino acid sequences analysis may represent general and particular characteristics of the viruses in terms of subtyping, antigenicity, pathogenicity, binding affinity, ability of transmission and resistance against anti-viral treatment.
3. Molecular diagnosis techniques based on RT-PCR and real-time RT-PCR can be applied for rapid, specific and sensitive detection of the viruses from clinical specimens in order to control and prevent severe outbreaks of H5N1 avian influenza and H3N8 canine influenza viruses.

สถาบันวิทยบริการ
จุฬาลงกรณ์มหาวิทยาลัย

CHAPTER II

REVIEW OF RELATED LITERATURE

Taxonomy of influenza viruses

According to the International Committee on Taxonomy of Viruses (ICTV), influenza viruses can be classified into group V, which is a negative single stranded RNA virus and belonged to the *Orthomyxoviridae* family. From the Greek, 'myxa' means mucus, represents the special association of the virus with mucosal surfaces. The family of *Orthomyxoviridae* consists of 3 types of influenza viruses, including A, B & C and Thogovirus [3]. Influenza A, B and C were originally distinguished serologically into three distinct types based on antigenic differences between their nucleoproteins and matrix proteins. Moreover, the genome organization of influenza A and B viruses consist of 8 segmented RNA genomes whereas influenza C virus contains only 7 RNA segments. Of the three types, most pandemics of influenza are associated with type A [4].

Structure and genome organization of influenza A viruses

Influenza A viruses are enveloped single-stranded RNA viruses with a spherical or filamentous in structure, ranging from 80-120 nm in diameter. The envelope of the virus is a lipid bilayer membrane which originates from the virus-producing cell and which contains prominent projections of haemagglutinin (HA) and neuraminidase (NA), as well as the M2 protein cover the surface of the particle. They contain a genome composed of eight segments of negative-sense RNA that encode ten functional viral proteins (Table 1 & Figure 1). The followings are the characteristics and functions of each genes of influenza A viruses [22].

- The three largest gene segments encode the Polymerase basic protein 2 (PB2), Polymerase basic protein 1 (PB1) and Polymerase acidic protein (PA) which form the viral polymerase complex responsible for transcription of messenger RNAs (mRNAs), synthesizing positive-sense complementary RNA templates (cRNAs), and transcribing the cRNAs into the virion RNA segments (vRNAs) that are incorporated into progeny viruses.
- The fourth segment encodes the hemagglutinin glycoprotein (HA), which play a crucial role for binding of the virus to sialic acid-containing cell-surface receptors and for membrane fusion during virus entry into host cells. Moreover, it is the major antigenic determinant and also the principal target for neutralizing antibodies.
- The nucleoprotein (NP) is the product of the fifth gene segment. This is the protein that encapsidates cRNAs and vRNAs, which is necessary for them to be recognized as templates for the viral polymerase.
- The product of the sixth gene segment is the neuraminidase (NA), which cleaves sialic acid from virus and host cell glycoconjugates at the end of the virus life cycle to allow mature virions to be released from the host cells.
- The seventh segment generates two gene products, the matrix protein (M1), and the ion channel (M2) protein. M1 mRNA is an unspliced transcript, and its product is the most abundant structural component in the virion and it is thought to play a fundamental role in viral assembly. The M2-ion channel is a small transmembrane protein derived from spliced mRNA. It has proton channel activity that aids in virus uncoating during the initial stages of infection.
- The last gene segment also encodes two proteins due to alternative splicing. These proteins are referred to nonstructural proteins (NS1) and (NS2). The NS1 has several functions including a regulator of both mRNA splicing and translation, and it also plays a critical role in the modulation of the host's interferon responses against viral infection. The function of NS2 is to mediate the export of newly synthesized ribonucleoproteins (RNPs) from the nucleus, so it is also referred to as a nuclear export protein (NEP).

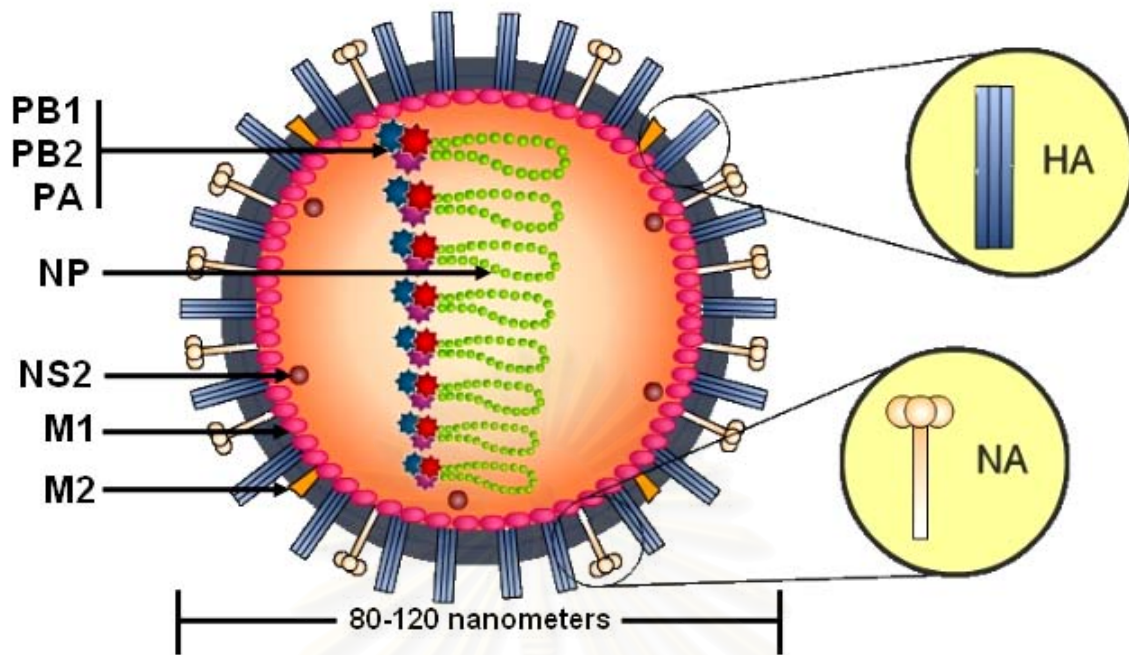


Figure 1 Structure of influenza A virus particle. The nucleoprotein (NP) associates with each of the eight viral RNA (vRNA) segments to form ribonucleoprotein (RNP) complexes. The subunits of the viral RNA-dependent RNA-polymerase complex PB1, PB2 and PA are also associated with the RNPs. The viral glycoproteins, hemagglutinin (HA) and neuraminidase (NA), are exposed on the virus surface as trimers and tetramers, respectively. Matrix-protein-1 (M1) is derived from a colinear mRNA of segment 7 and forms the inner layer of the virion. A spliced mRNA of the same segment gives rise to the transmembrane M2 protein, which is a pH-dependent ion channel. Alternative splicing of segment 8 yields the non-structural protein 1 (NS1) and the nuclear export protein (NEP; also known as NS2) [Modified from 23].

จุฬาลงกรณ์มหาวิทยาลัย

Table 1 General characteristics of RNA segments and gene products of influenza A virus [Modified from 24].

Segment	RNA (bp)	Gene Product	Size (kDa)	Localization & features	Functions
1	2350	PB2	96	Virion interior, infected cell nuclei	Form heterotrimeric polymerase complex;
2	2350	PB1	87	Virion interior, infected cell nuclei	Associated with NP & virion RNA;
3	2250	PA	85.5	Virion interior, infected cell nuclei	Responsible for transcription & replication of viral RNA
4	1780	HA	73	Virion envelope, infected cell surface; Form homotrimers bear antigenic sites & receptor binding site;	Binding to sialic acid-containing receptors on host cell; Membrane fusion of virus and cells membranes; Major antigenic determinant
5	1575	NP	55	Virion interior; Associated with Polymerase complex & viral RNA to form ribonucleoproteins (RNPs)	Major component of nucleocapsid; Role in vRNA replication, virus maturation & packaging
6	1420	NA	60	Virion envelope, infected cell surface; Form homotetramers bear antigenic sites & enzyme active site	Digesting mucin to enable virus to reach target epithelium & facilitating release of infectious progeny virus; Antigenic molecule
7	1050	M1	28	Beneath lipid bilayer of virion envelope; Associates with vRNPs to form nucleocapsid	Central role in replication & virus assembly, modulating nuclear transport of viral RNPs
		M2	15	Virion envelope, infected cell surface (abundant)	Form homotetramers contain membrane cation channel activity
8	900	NS1	25	Infected cell nuclei	Inhibit host mRNA translation & Down-regulate anti-viral response
		NS2	14	Associated with core components of virion; cytoplasm of infected cells	Mediates nuclear export of viral RNPs

Classification of influenza A virus into various subtypes

Influenza A viruses can be classified into various subtypes on the basis of antigenic differences between their two transmembrane glycoproteins, haemagglutinin (HA) and neuraminidase (NA). Serologically, influenza A viruses are further subdivided into 16 subtypes of HA (H1-H16) [25] and 9 subtypes of NA (N1-N9). All of these subtypes occur in viruses that circulate in aquatic birds, and these species serve as the natural reservoir for all influenza A viruses [3]. However, influenza viruses that have become established in mammals show a restricted combination of HA and NA types.

Natural hosts of influenza A viruses

Wild aquatic birds, notably members of the orders *Anseriformes* (ducks and geese) and *Charadriiformes* (gulls and shorebirds), are carriers of the full variety of influenza virus A subtypes, and thus, most probably constitute the natural reservoir of all influenza A viruses [5]. While all bird species are thought to be susceptible, some domestic poultry species including chickens, turkey, guinea fowl, quail and pheasants are known to be especially susceptible to the sequelae of infection. As influenza viruses are normally highly species specific, they only rarely spill over to cause infection in other species, due to differences in the use of cellular receptors. Avian influenza viruses bind to cell-surface glycoproteins containing sialyl-galactosyl residues linked by a 2-3-linkage, whereas human influenza viruses bind to receptors that contain terminal 2-6-linked sialyl-galactosyl moieties [24]. For an avian virus to be easily transmitted between humans, it is fundamental that it acquires the ability to bind cells that display the 2-6 receptors so that it can enter the cell and replicate in them. Usually, only H1N1, H2N2, and H3N2 influenza A viruses were known to have circulated extensively in humans. During the past few years, various subtypes of avian influenza A virus including H5N1, H7N3, H7N7 and H9N2 have been reported to infect humans [9]. In addition, H5N1 avian influenza A virus has been recently reported to infect canine and felines (cats, tigers and leopards) [10-12]. Moreover, H3N8 equine influenza A virus also directly transmitted from equine to canine species [13] (Figure 2).

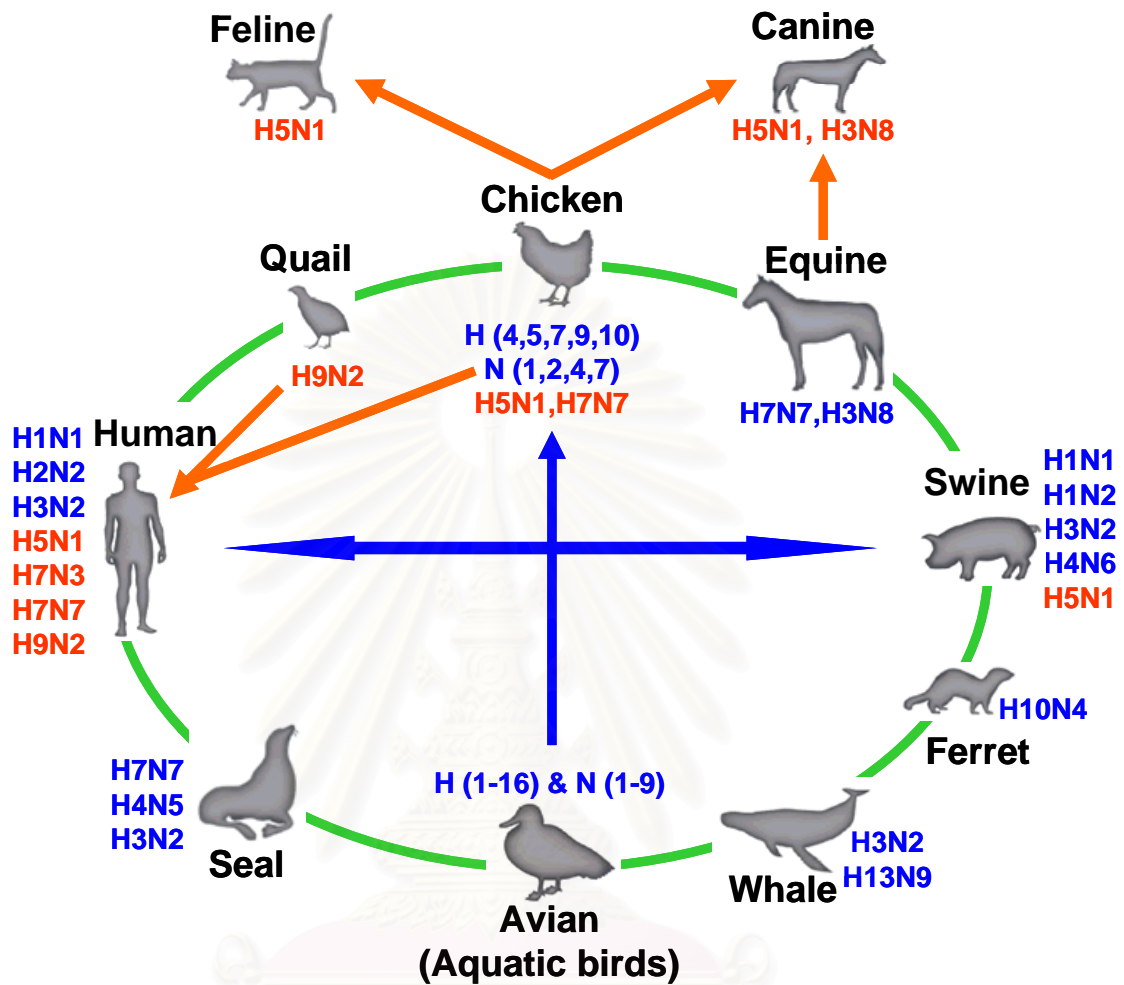


Figure 2 Various subtypes of influenza A viruses that can be isolated from different host species.

Nomenclature of influenza viruses

The full nomenclature for influenza virus isolates requires connotation of the influenza virus type (influenza A, B or C), the original host of origin (omitted if human in origin), the place of virus isolation, the strain number and the year of isolation. For influenza A viruses, the subtypes of the HA and NA antigens required to be included in brackets [14].

- Thus, A/Hong Kong/156/1997 (H5N1) is a human strain of influenza A virus isolated in Hong Kong, strain number 156 in 1997, with haemagglutinin type 5 and neuraminidase type 1.
- A/Chicken/Nakorn-Pathom/Thailand/CU-K2/2004 (H5N1) is a strain of influenza A virus isolated from chicken in Nakorn-Pathom province, Thailand, strain number CU-K2, in 2004, with haemagglutinin type 5 and neuraminidase type 1.
- B/Hong Kong/330/2001 is the influenza B strain isolated from human in Hong Kong, strain number 330, in 2001.

Antigenic diversity of influenza A viruses

Influenza viruses are unique among respiratory viruses in their segmented genome and great antigenic diversity. The antigenic variability of influenza viruses are the results of 2 processes including antigenic 'drift' and antigenic 'shift'.

- "Antigenic drift" is the accumulations of gene mutations in the viruses' principal antigens (HA and NA) that are selected in response to immune pressure from host antibodies, enabling the virus to readily escape protective immunity of host, thereby allowing a new strain to spread within a non-immune population [5]. This phenomenon occurs in all influenza types but is more frequent in type A influenza.
- "Antigenic shift" is the phenomenon that generates new strains of antigenic different virus by genetic reassortment. This process can occur when influenza viruses from different species such as human and avian, co-infect a single host-possibly a pig which serves as a 'mixing vessel'. Because influenza virus possesses a genome with eight separate segments, gene reassortment with 256 possible gene combinations may occur during co-infection, and a hybrid (reassortant) viruses containing RNA segments from the two parental strains can emerge [7]. This process results in strains of unpredictable pathogenicity, but it may lead to the generation of virus that remains virulent and possesses 'new' surface antigens from the non-human virus. The hybrid virus, with the resulting major antigenic alteration, can be especially virulent, because it is not restrained by host immunity to previously prevalent strains of the virus.

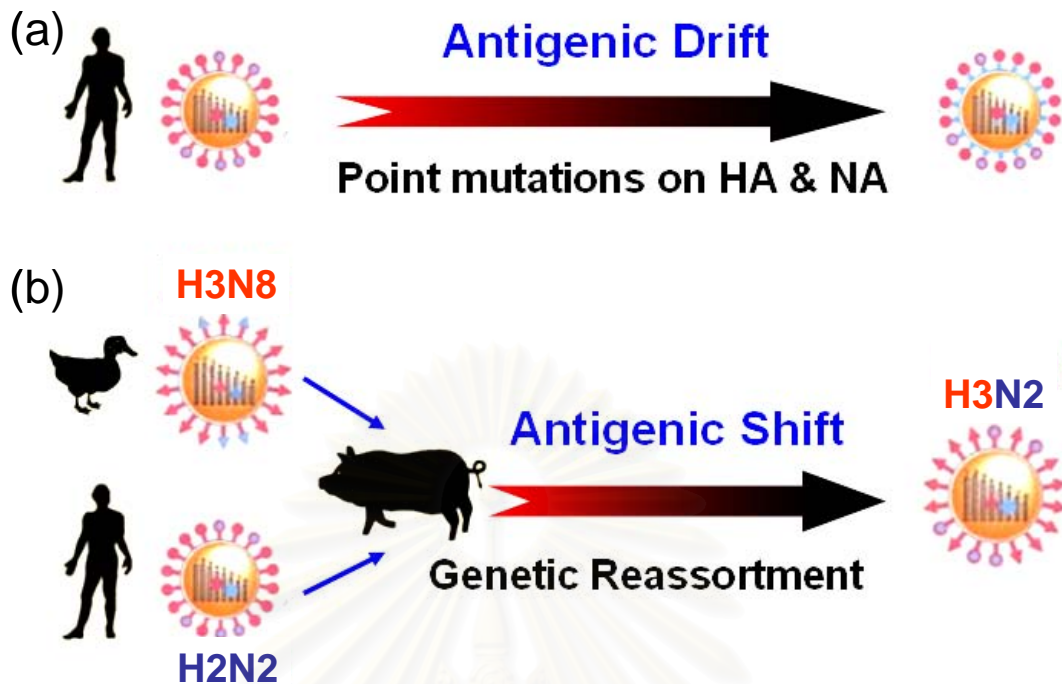


Figure 3 Mechanism of antigenic diversity of influenza A viruses. (a) Antigenic drift accumulates point mutations within the HA and NA genes, enabling the virus to escape host's protective immune response. (b) Antigenic shift occurs when influenza viruses from different species such as human (H2N2) and avian (H3N8), co-infect a pig, yielding the reassortant virus (H3N2) containing RNA segments from the two parental strains.

Epidemics and Pandemics of influenza

Influenza is a serious respiratory illness which can be debilitating and cause complications that lead to hospitalization and death, especially in the elderly. Every year, the global burden of influenza epidemics is believed to be 3-5 million cases of severe illness and 300,000-500,000 deaths. The risk of serious illness and mortality due to influenza virus infection generally is found in infants, adults over 65 years of age, children aged <2 years and immunocompromised patients [8].

New epidemic influenza A strains arise every 1 to 2 years by the introduction of selected point mutations within two surface glycoproteins: haemagglutinin (HA) and neuraminidase (NA). The new variants are able to evade human host defenses and there is therefore no lasting immunity against the virus, neither after natural infection nor after vaccination, as is the case with smallpox, yellow fever, polio, and measles. These permanent and usually small changes in the antigenicity of influenza A viruses are termed “antigenic drift” and are the basis for the regular occurrence of influenza epidemics. In addition, there is now evidence that multiple lineages of the same virus subtype can co-circulate, persist, and reassort in epidemiologically significant ways [26].

In contrast to epidemics, pandemics are rare events that occur every 10 to 50 years. During the twentieth century, three influenza pandemics occurred (Table 2). Their mortality impact ranged from devastating to moderate or mild. The 1918 pandemic was caused by a H1N1 virus of apparently avian origin [27], whereas the subsequent pandemic strains H2N2 in 1957 and H3N2 in 1968 were reassortant viruses containing genes from avian viruses: three in 1957 (haemagglutinin, neuraminidase, and the RNA polymerase PB1) and two (haemagglutinin and PB1) in 1968 [28]. These major changes in the antigenicity of an influenza virus are called “antigenic shift”.

One hallmark of pandemic influenza is a mortality shift towards younger age groups. Half of influenza-related deaths during the 1968 pandemic and large proportions of influenza-related deaths during the 1957 and the 1918 pandemics occurred among persons < 65 years old.

Table 2 Pandemics of influenza A viruses during the 20th century

Year	Designation	Subtype	Resulting Pandemic	Death Toll
1918	“Spanish Flu”	H1N1	Devastating	50-100 million
1957	“Asian Flu”	H2N2	Moderate	1 million
1968	“Hong Kong Flu”	H3N2	Mild	1 million

Avian influenza A viruses

Highly pathogenic avian influenza, or, as it was termed originally, 'fowl plague', was initially recognized as an infectious disease of birds in chickens in Italy, 1878. In 1955, Schäfer characterized these agents as influenza A viruses. In the natural reservoir hosts of avian influenza viruses, wild water birds, the infection generally runs an entirely asymptomatic course as influenza A virus biotypes of low pathogenicity co-exist in almost perfect balance with these hosts [5, 29].

Properties of avian influenza viruses

Influenza pandemics are caused by the emergence of a virus that possess an HA subtype to which most of the population lacks immunity. Recently, purely avian influenza viruses, including the H5N1, H9N2 and H7N7 subtypes, have been directly transmitted to humans, raising concern over the possibility of a new influenza pandemic among the world's immunologically naive populations. As most of the viruses responsible for pandemics in the past century were all characterized by the acquisition of HAs from avian viruses, clues to the molecular changes that give rise to human pandemic strains can be found in the avian reservoir.

Pathogenicity of avian influenza viruses

Avian influenza viruses can be further differentiated as highly pathogenic avian influenza (HPAI) and low pathogenic avian influenza (LPAI) on the basis of specific molecular genetic and pathogenesis criteria that require specific testing. The HPAI viruses cause systemic lethal infection, killing birds as soon as 24 hours post-infection, and usually within one week, whereas LPAI viruses cause local infection with rarely generate outbreaks of severe disease in the field, and their associated morbidity and mortality rates are lower than those of HPAI viruses [5]. Without exception, all of the HPAI viruses belong to the H5 or H7 subtype, for reasons that are still unclear. There do not seem to be any associations of specific NA subtypes with HPAI viruses.

When low pathogenic avian influenza (LPAI) viruses are transmitted from avian reservoir hosts to highly susceptible poultry species such as chickens and turkeys (an interspecies transmission step), only mild symptoms are induced in general. However, in cases where the poultry species supports several cycles of infection, these strains may undergo a series of mutation events resulting in adaptation to their new hosts. Influenza A viruses of the subtypes H5 and H7 not only run through a host adaptation phase but may have the capability to switch by insertional mutations into a highly pathogenic form highly pathogenic avian influenza (HPAI) viruses inducing overwhelming systemic and rapidly fatal disease. Such HPAI viruses may arise unpredictably de novo in poultry infected with LPAI progenitors of H5 and H7 subtypes.

The HA protein appears to be the most important protein in determining the virulence of avian influenza viruses. For the virus to become infectious, cleavage of a precursor of HA (HA0) into HA1 and HA2 subunits is required, since cell fusion is mediated by the free amino-terminus of the HA2 subunit [30]. Comparison of the complete sequence of HA from the two virus strains responsible for the different degrees of severity of the disease, demonstrated that the highly pathogenicity was determined by the insertion and substitution of polybasic amino acid residues (arginine and/or lysine) in the HA cleavage site (Figure 4) [31] which renders it processible for subtilysin-like endoproteases specific for a minimal consensus sequence of -R-X-K/R-R- [32]. Proteases of this type (e.g. furin, proprotein-convertases) are active in virtually every tissue throughout the body. Therefore, viruses carrying these mutations have an advantage for replicating unrestrictedly in a systemic manner. In contrast, the cleavage site of the HA of low pathogenic viruses is composed of two basic amino acids at positions -1/-4 (H5) and -1/-3 (H7) [33]. These sites are accessible to tissue-specific trypsin-like proteases which are preferentially expressed at the surface of respiratory and gastrointestinal epithelia. Therefore, efficient replication of LPAIVs is believed to be largely confined to these sites, at least in their natural hosts.

Differences in tissue tropism of low and highly pathogenic AI viruses reflect diversity in the pathogenic mechanisms which lead to clinical disease and death of infected chickens, and are related with differences in the proteolytic cleavage site of HA [34]. LPAI infections can be asymptomatic or cause a wide range of clinical signs varying from mild to severe signs of disease affecting respiratory, urogenital and/or enteric systems. Whereas clinical signs of HPAI include various combinations of decreased activity and feed consumption, emaciation, decreased egg production, coughing, sneezing, rales, sinusitis, cyanosis of unfeathered skin, central nervous system disorders, and finally, severe disease with high morbidity and mortality [35].

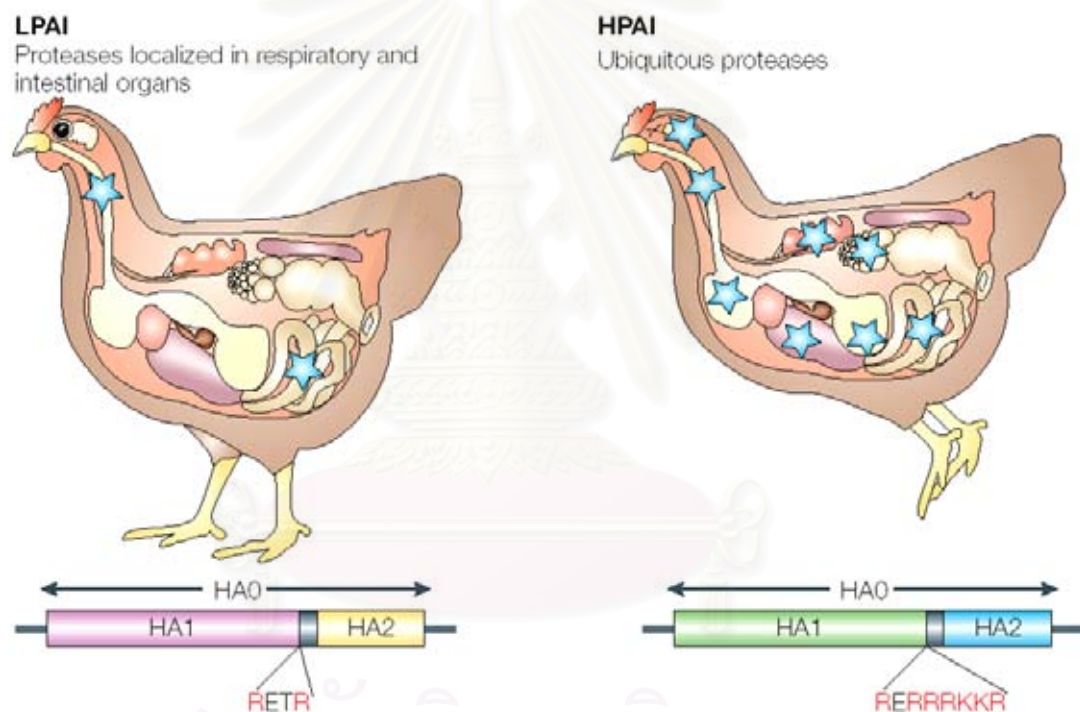


Figure 4 Polybasic amino acid insertion at the cleavage site of haemagglutinin (HA) as a major molecular determinant of the pathogenicity of avian influenza viruses in poultry. The HAs of low-pathogenicity avian influenza (LPAI) viruses do not contain a series of basic amino acid at the protease cleavage site and thus are cleaved by only proteases that are localized in respiratory and intestinal organs, resulting in mild localized infections. By contrast, the HAs of high-pathogenicity avian influenza (HPAI) viruses possess multiple basic amino acids at the cleavage site (RERRRKKR), which are cleaved by ubiquitous proteases in a wide range of organs, resulting in lethal systemic infection [36].

Criteria for High Pathogenicity

The standard method used by the Office International des Epizooties (OIE) and U.S. Animal Health Association to determine whether an avian influenza virus is highly pathogenic involves the intravenous inoculation of a minimum of eight susceptible 4- to 8-week old chickens with infectious virus. If the virus lethal for at least 75% (six of the eight) chickens within 10 days, the virus strain is considered to be highly pathogenic. An additional test involves sequencing of HA gene of the virus. All highly pathogenic avian influenza viruses contain a multiple basic amino acid insertion at the cleavage site, which known to be associated with high lethality.

Outbreaks of the highly pathogenic avian influenza

HPAI in poultry is characterized by a sudden onset, severe illness of a short duration, and a mortality approaching virtually 100 % in susceptible species. Due to excessive economical losses to the poultry industry, HPAI receives immense attention in the veterinary world and is globally treated as a disease immediately notifiable on suspicion to the authorities. Because of their potential to give rise to HPAIV, LPAI caused by subtypes H5 and H7 is also considered notifiable. Before 1997, HPAI was fortunately a rare disease, with only 24 recorded primary outbreaks globally since the 1950s (Table 3).

Outbreaks of H5N1 avian influenza A viruses

In 1997, the outbreak of influenza A virus subtype H5N1 caused a fulminating and rapidly fatal systemic disease in domestic poultry. Moreover, this virus spread directly from poultry to human in Hong Kong and killed 6 of 18 infected cases [14]. The clinical features of infection included onset of fever and upper-respiratory-tract infection, typical of classical influenza. Some patients had severe complications, mainly pneumonia, gastrointestinal manifestations, elevated liver enzymes and renal failure [37]. Epidemiological studies suggested direct transmission of the virus from birds and serological evidence of human-to-human transmission was limited to a few cases [38], indicating that the virus had not become fully adapted to the human host. The slaughter of all poultry in Hong Kong successfully terminated the treat of major outbreak of the H5N1 virus infection.

Table 3 Previous outbreaks of highly pathogenic avian influenza worldwide

Year	City / Country	Strains of virus
1959	Scotland	A/chicken/Scotland/59 (H5N1)
1963	England	A/turkey/England/63 (H7N3)
1966	Ontario/ Canada	A/turkey/Ontario/7732/66 (H5N9)
1976	Victoria/ Australia	A/chicken/Victoria/76 (H7N7)
1979	Germany	A/chicken/Germany/79 (H7N7)
1979	England	A/turkey/England/199/79 (H7N7)
1983-1985	Pennsylvania/ USA	A/chicken/Pennsylvania/1370/83 (H5N2)
1983	Ireland	A/turkey/Ireland/1378/83 (H5N8)
1985	Victoria/ Australia	A/chicken/Victoria/85 (H7N7)
1991	England	A/turkey/England/50-92/91(H5N1)
1992	Victoria/ Australia	A/chicken/Victoria/1/92 (H7N3)
1994	Queensland/ Australia	A/chicken/Queensland/667-6/94 (H7N3)
1994-1995	Mexico	A/chicken/Puebla/8623-607/94 (H5N2)
1994	Pakistan	A/chicken/Pakistan/447/95 (H7N3)
1997	Hong Kong SAR	A/chicken/Hong Kong/220/97 (H5N1)
1997	New South Wales/ Australia	A/chicken/New South Wales/1651/97 (H7N4)
1997	Italy	A/chicken/Italy/330/97 (H5N2)
1999-2000	Italy	A/turkey/Italy/99 (H7N1)
2002	Chile	A/chicken/Chile/2002 (H7N3)
2003	Netherlands	A/chicken/Netherlands/2003 (H7N7)
2004	British Col./ Canada	A/chicken/Canada-BC/ 2004 (H7N3)
2004	USA	A/chicken/USA-TX/2004 (H5N2)
2004	South Africa	A/ostrich/South Africa/2004 (H5N2)

The H5N1 avian influenza viruses isolated from human were not reassortants like the H2N2 (Asian Flu in 1957) and H3N2 (Hong Kong Flu in 1968) pandemic strains. Instead, all of the H5N1 viral genes originated from a Eurasian avian virus [39]. The HA gene was derived from a H5N1 virus first isolated from a goose that died in Guangdong Province, China (A/goose/Guangdong/1/96) [40]. During 1997-2001, H5N1 viruses with an HA of the same genetic lineage continued to circulate in birds in southeastern China [41]. In 2002, another H5N1 avian influenza virus showing antigenic drift emerged in Hong Kong and was highly pathogenic in ducks and other aquatic birds [42]. In early 2003, the second occurrence of human infection with avian influenza virus (H5N1) was reported in Hong Kong [43].

Thereafter, the most devastating outbreak of H5N1 highly pathogenic avian influenza occurred in 2003-2004 in several Asian countries, including Vietnam, Thailand, Indonesia, Cambodia, Laos, Korea, Japan, Pakistan, China and Malaysia [44]. As a consequence, this virus has emerged in Thailand causing a major economic loss and over 30 million poultry from both industry and backyards had to be slaughtered.

Extensive phylogenetic analysis of the viruses isolated from poultry in Hong Kong and China revealed multiple genetic reassortants representing multiple genotypes, including A, B, C, D, E, V, W, X, Y, Z and Z⁺, although each of the reassortant viruses possessed an HA similar to that of the HA from the A/goose/Guangdong/1/96 strain [45]. The H5N1 avian influenza viruses with a dominant Z genotype were responsible for the outbreaks in Vietnam, Thailand and Indonesia [16, 45]. By contrast, viruses isolated in 2004 in Japan and Korea belonged to the genotype V. Their polymerase acid protein (PA) gene segments differed considerably from those of the genotype Z virus, although the remaining segments are related to this virus [46]. Therefore, at least two genotypes (Z and V) of H5N1 avian influenza seem to be responsible for the Asian outbreak in 2003-2004. Taken together, these observations indicate that domestic ducks and land-based poultry in southern China probably had a central role in the generation and maintenance of the H5N1 avian influenza virus and wild birds might have contributed to the broad spread of the virus.

In April 2005, yet another level of the epizootic was reached, when, for the first time, the H5N1 strain obtained access to wild bird populations on a larger scale [47]. At Qinghai Lake in North Western China, several thousands of bar-headed geese, a migratory species, succumbed to the infection. Several species of gulls as well as cormorants were affected as well at this location. Additional outbreaks of H5N1 highly pathogenic avian influenza were reported in seven countries including, Russia, Kazakhstan, Mongolia, Turkey, Romania, Croatia and Ukraine. This marked the beginning of the spread of H5N1 influenza virus from Asia to Eurasia. Both poultry and wild aquatic birds were found to be affected. Presently, it can only be speculated as to whether wild aquatic birds can carry the virus over long distances during the incubation period, or whether some species indeed remain mobile despite an H5N1 infection.

By May 2006, H5N1 virus had spread among poultry stocks throughout Eurasia and more recently, in Africa so that Iraq, Nigeria, Azerbaijan, Bulgaria, Greece, Italy, Slovenia, Iran, Austria, Germany, Egypt, India, France, Hungary, Slovakia, Bosnia-Herzegovina, Georgia, Niger, Switzerland, Serbia-Montenegro, Poland, Albania, Cameroon, Myanmar, Denmark, Sweden, Afghanistan, Israel, Pakistan, Jordan, Czech Republic, Burkina Faso, United Kingdom, Sudan, Kuwait, Côte d'Ivoire and Djibouti all reported incidences of this new and virulent strain of avian influenza virus. Moreover, H5N1 was identified in human cases from Turkey, Azerbaijan, Egypt and Djibouti [44].

Transmission of H5N1 avian influenza to human

Transmission of avian influenza viruses to humans, leading to the development of clinically overt disease is a rare event. However, there was substantial transmission to humans; resulting in a total of 170 deaths from 288 infected persons in several countries (Table 4) [48]. The clinical presentations include fever, cough, diarrhoea, shortness of breath, rapid respiratory rate, lymphopaenia and abnormalities on chest radiography. The risk of direct transmission of the H5N1 virus from birds to humans seems to be greatest in persons who have close contact with live infected poultry, or surfaces and objects heavily contaminated with their droppings.

Exposure risk is considered substantial during slaughter, defeathering, butchering and preparation of poultry for cooking. The highly pathogenic H5N1 avian influenza virus can be found in all tissues - including the meat – throughout the bird's carcass. To date, there is no evidence that properly cooked poultry meat or poultry products are a source of human infection by the Asian lineage H5N1. As a general rule, the WHO recommends that meat be thoroughly cooked, so that all parts of the meat reach an internal temperature of 70°C. At this temperature, influenza viruses are inactivated, thus rendering safe any raw poultry meat contaminated with the H5N1 virus.

Table 4 Cumulative number of confirmed human cases of H5N1 avian influenza reported to WHO (Updated on 2nd April 2007)

Country	2003		2004		2005		2006		2007		Total	
	Cases	Deaths	Cases	Deaths	Cases	Deaths	Cases	Deaths	Cases	Deaths	Cases	Deaths
Azerbaijan	0	0	0	0	0	0	8	5	0	0	8	5
Cambodia	0	0	0	0	4	4	2	2	0	0	6	6
China	1	1	0	0	8	5	13	8	2	1	24	15
Djibouti	0	0	0	0	0	0	1	0	0	0	1	0
Egypt	0	0	0	0	0	0	18	10	14	3	32	13
Indonesia	0	0	0	0	20	13	55	45	6	5	81	63
Iraq	0	0	0	0	0	0	3	2	0	0	3	2
Lao PDR	0	0	0	0	0	0	0	0	2	2	2	2
Nigeria	0	0	0	0	0	0	0	0	1	1	1	1
Thailand	0	0	17	12	5	2	3	3	0	0	25	17
Turkey	0	0	0	0	0	0	12	4	0	0	12	4
Viet Nam	3	3	29	20	61	19	0	0	0	0	93	42
Total	4	4	46	32	98	43	115	79	25	12	288	170

Transmission of H5N1 avian influenza to other mammals

Natural infection with H5N1 was described in tigers (*Panthera tigris*) and leopards (*Panthera pardus*) at a zoo in Suphanburi, Thailand after the animals were fed with virus-positive chicken carcasses [10]. The animals showed clinical signs, including high fever and respiratory distress, to which they unexpectedly succumbed. Severe disease accompanied by high mortality ensued.

In 2004, there was a second outbreak of H5N1 virus infection at the Sriracha tiger zoo, the biggest tiger zoo in Thailand. An outbreak occurred among zoo tigers have been fed with chicken carcasses. Also, possible of tiger-to-tiger transmission has apparently occurred in the same zoo [49]. Another feline affected by H5N1 viral infection was a domestic cat in Thailand [11]. The cat had eaten a pigeon carcass 5 days before the onset of symptoms, including body temperature of 41°C, convulsions and ataxia to which it succumbed after 2 days. Clinical signs and pathology observed on the infected cat were similar to those found in household European short hair cats that experimentally infected with the H5N1 avian influenza virus [50]. Furthermore, fatal infection of H5N1 influenza was also found in dog following ingestion of a virus infected duck in Thailand [12]. Avian influenza viruses have never been detected in rats, rabbits and various other mammals present at live bird markets in Hong Kong where 20 % of the chickens were found positive for the Asian lineage H5N1 [51].

Outbreaks of H3N8 canine influenza A viruses

Influenza A subtype H3N8 virus has recently emerged as a respiratory pathogen in dogs in association with outbreaks of acute respiratory disease in racing greyhounds [13]. The disease is caused by a novel virus closely related to contemporary equine influenza A subtype H3N8 viruses with which it shares $\geq 96\%$ nucleotide sequence identity, suggesting that the entire virus was directly transmitted from horses to dogs without reassortment with other strains [13]. Most of the greyhounds had clinical signs associated with virus infection of the upper respiratory tract, including a 'kennel cough' for 10 to 30 days, nasal discharge, and a low grade fever with subsequent recovery. However, many dogs suffered peracute death associated with extensive hemorrhage in the lungs, mediastinum, and pleural cavity. Histological examination revealed tracheitis, bronchitis, bronchiolitis, and suppurative bronchopneumonia associated with extensive erosion of epithelial cells and neutrophil infiltration. The isolation of four closely related influenza A subtype H3N8 viruses from fatal cases in different geographic locations over a 25-month period, together with substantial serological evidence of widespread infection among racing greyhounds in 9 states, suggested sustained circulation of CIV in this population by dog-to-dog transmission [13, 19].

Replication cycle of influenza A viruses

The replication cycle of influenza A viruses can be divided into 6 major steps, beginning with the attachment of the virus with host cell's receptors, entry of the virus into a host cell, followed by uncoating of the viral components into the cytoplasm. After that the viral RNAs and viral proteins are synthesized by using host cell machinery, then the viral RNAs and proteins are assemble into a new viral progeny and finally release of the infectious progeny virus (Figure 5). The time from virus entry to production of new virus is approximately 6 hours. The details of each replication step are discussed below.

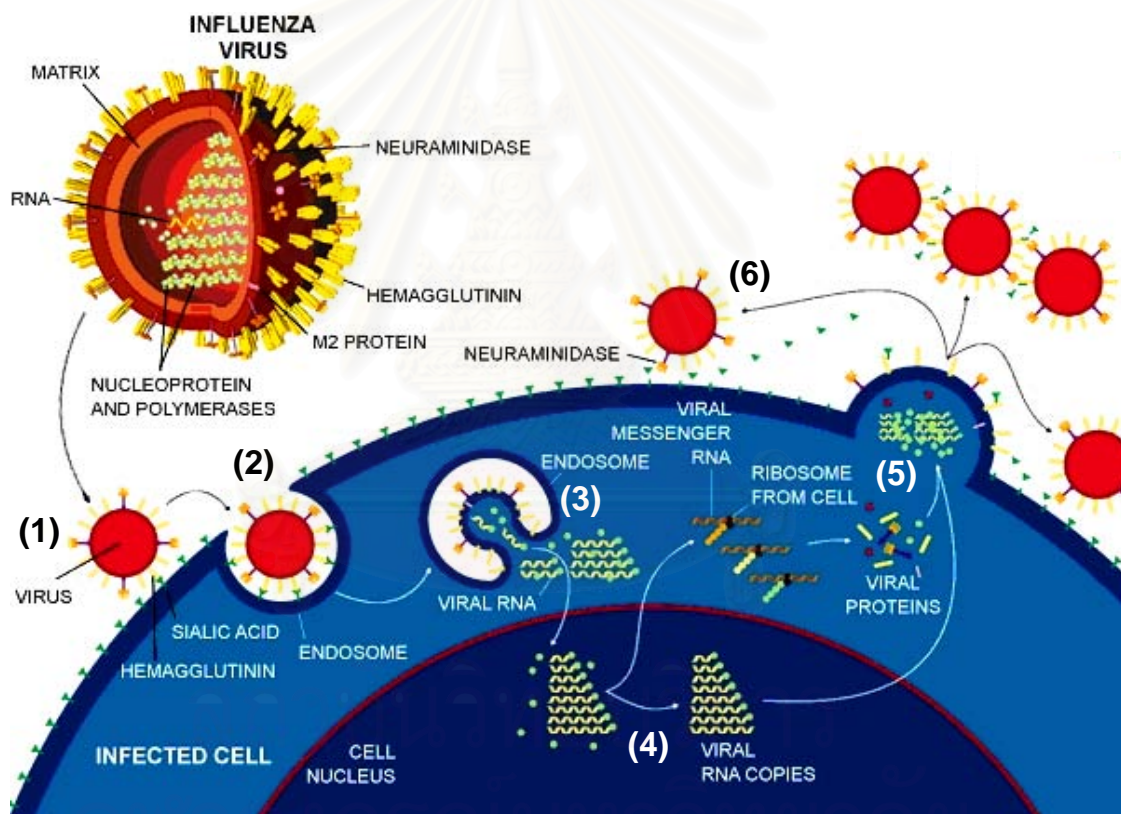


Figure 5 Replication cycle of influenza A viruses consists of 6 main steps. (1) Attachment of the virus with a host cell; (2) Entry of the virus into a host cell; (3) Uncoating of the virus; (4) Synthesis of viral RNA and viral proteins; (5) Assembly of the progeny viral particle; and (6) Release of the infectious progeny viruses.

1. Attachment of the virus with a host cell

The influenza virus particle binds its target cell through interaction between the outer top of viral homotrimerized haemagglutinin (HA) molecules and sialic acid (N-acetyl- or N-glycolylneuraminic acid) receptors on the host cell surface. The sialic acid linkage to the penultimate galactose, either alpha 2,3 (in birds) or alpha 2,6 (in human), determines host specificity [52, 53]. Since sialic acid-presenting carbohydrates are present on several cells of the organism, the binding capacity of the HA explains why multiple cell types in an organism may be infected. A variety of different sialyloligosaccharides are expressed with restriction to tissue and species origin in the different hosts of influenza viruses. Adaptation in both the viral HA and the NA glycoprotein to the specific receptor type(s) of a certain host species is a prerequisite for efficient replication [54]. Avian influenza viruses generally show the highest affinities for alpha-2-3 linked sialic acid as this is the dominating receptor type in epithelial tissues of endodermic origin (gut, lung) in those birds that are targeted by these viruses [55]. In contrast, human-adapted influenza viruses primarily access 2-6 linked residues which predominate on non-ciliated epithelial cells of the human airway. These receptors define part of a species barrier preventing hassle-free transmission of avian viruses to humans [56].

2. Entry of the virus into a host cell

After successful attachment, the virus is taken up into a host cell endosome, via a clathrin-coated receptor-mediated endocytosis and clathrin-independent mechanisms [57]. When internalised, the clathrin molecules are liberated and the vesicle harbouring the whole virus fuses with endosomes. The contents of the vesicle are usually digested through a stepwise lowering of the pH within the phagosome.

3. Uncoating of the virus

When a certain pH level is reached around 5.0, the lowering of the pH is stopped by proton transport of the viral M2- ion channel which allows a low pH-dependent conformational change in the HA exposes the 'fusion peptide' leading to fusion of the virus and host cell membranes [58]. The ion influx from the endosome to the virus particle leads to dissociation of the different viral proteins; M1-protein aggregation is disrupted and the viral ribonucleoproteins (each RNA segment bounds to NP) no longer adhere to the M1-matrix protein, leading to the release of viral ribonucleoproteins (RNPs) into the cytoplasm.

4. Synthesis of viral RNA and viral proteins

The viral RNPs are transported into the nucleus for transcription of viral mRNAs and replication of genomic RNA in a complex process which is delicately regulated by viral and cellular factors [59]. The RNA-dependent RNA polymerase (RdRp) is formed by a complex of the viral PB1, PB2 and PA proteins, and requires ribonucleoprotein (RNPs) for this task. The polymerase complex binds to viral RNA (vRNA), cleaves viral RNA by its endonuclease activity, and simultaneously synthesizes positive-sense complementary RNA (cRNA) templates. Then the cRNAs serve as templates for transcription of mRNA and production of negative anti-sense viral RNA (vRNA). According to the error-prone activity of the viral RdRp, a high mutation rate of $\geq 5 \times 10^{-5}$ nucleotide changes per nucleotide and replication cycle, thus approaching almost one nucleotide exchange per genome per replication, is observed among the influenza viruses [60]. The mRNAs are then transported to the cytoplasm, where viral proteins are generated at the ribosome. Parts of the viral mRNAs (segment 7 and 8) are spliced by cellular enzymes so that finally viral proteins, such as M2 and NS2, can be synthesized without any further cleavage. Some of the newly synthesized viral proteins (NP and polymerase complex) are transported into the nucleus and bound to viral RNA to form RNPs. Other newly synthesized viral proteins (HA, NA and M2) are processed in the endoplasmic reticulum and the Golgi apparatus where glycosylation occurs.

5. Assembly of the progeny viral particle

After post translational modification, the modified proteins are transported and anchored in regions of the plasma membrane. When the concentrations of these proteins are high enough, RNPs and M1-matrix proteins aggregate to the regions of plasma membrane. Arrangements between helical nucleocapsids and viral envelope proteins are mediated by the viral M1-matrix protein which forms a shell-like structure just beneath the viral envelope and then condense to form the new virion.

6. Release of the infectious progeny viruses

The sialylated progeny virions are initially aggregated at the host cell membrane but finally, the infectious progeny virions will be released from the membrane by the enzymatic activity of the neuraminidase (NA).

Shedding of the influenza viruses

Immunohistological pictures show that foci of virus-producing cells are clustered in the mucous layer of the respiratory tract, in the gut and even in endothelial layers, myocardium and brain. Within nasal secretions, millions of virus particles per ml are shed, so that a 0.1 μ l aerosol particle contains more than 100 virus particles. A single HID (human infectious dose) of influenza virus might be between 100 and 1,000 particles. At least during the early course of influenza infection, the virus can be found also in the blood and in other body fluids.

Infectivity of influenza viruses

Infectivity of influenza virus particles is preserved depending on temperature, pH and salinity of the water, and UV irradiation. At 4°C, the half-life of infectivity is about 2-3 weeks in water. Due to the conformation of the lipid bilayer, survival under normal environmental conditions should be shorter. Infectivity of the influenza virus particle is easily inactivated by all alcoholic disinfectants, chlorine and aldehydes. As far as is known, temperatures above 70°C will destroy infectivity in a few seconds.

Highly pathogenic avian viruses can survive in the environment for long periods, especially in low temperatures (i.e., in manure-contaminated water). In water, the virus can survive for up to four days at 22°C, and more than 30 days at 0°C. In frozen material, the virus probably survives indefinitely. Recent studies indicate that the H5N1 viruses isolated in 2004 have become more stable, surviving at 37°C for 6 days- isolates from the 1997 outbreak survived just 2 days. The virus is killed by heat (56°C for 3 hours or 60°C for 30 minutes) and common disinfectants, such as formalin and iodine compounds.

Transmission of influenza A viruses

Influenza viruses are primarily transmitted from person to person through droplets (> 5 µm in diameter) from coughing and sneezing of an infected person. Particles do not remain suspended in the air, and close contact (up to 3-6 feet) is required for transmission. Transmission may also occur via direct skin-to-skin contact or indirect contact with respiratory secretions (touching contaminated surfaces then touching the eyes, nose or mouth). The viruses are able to penetrate the mucin layer of the outer surface of the respiratory tract, entering respiratory epithelial cells, as well as other cell types. Replication is very quick: after only 6 hours, the first influenza viruses are shed from infected cells. Individuals may spread influenza virus from up to two days before to approximately 5 days after onset of symptoms. Children can spread the virus for 10 days or longer.

Influenza vaccines

The only effective protection against influenza virus infection now available is vaccination [61]. Currently, influenza vaccines are recommended for all individuals at risk of complications of influenza including patients with chronic underlying diseases (asthma, chronic obstructive pulmonary disease, congenital heart disease, chronic heart failure, ischaemic heart disease, liver cirrhosis, etc.), elderly persons (aged 65 or older), healthcare workers and immunosuppressed patients and their household contacts [62].

Compositions of the current influenza vaccines

The primary target for the immune response against influenza virus is the viral hemagglutinin protein (HA). The rapid antigenic changes in HA render the previous year's vaccine ineffective against currently circulating viruses. Therefore, each year during interpandemic periods the existing vaccine strains need to be reformulated to provide antigenically well-matched vaccines. The World Health Organization (WHO) publishes semiannual recommendations for reviewing vaccine compositions and updating the antigenic content of the prevalent circulating strains for the Northern and Southern hemispheres. Influenza virus vaccines are usually trivalent, including 2 strains of influenza type A (H1N1 and H3N2) and 1 strain of influenza type B. Currently, the 2006-2007 vaccine formulation for the Northern hemisphere consists of the A/New Caledonia/20/1999 (H1N1), A/Wisconsin/67/2005 (H3N2), and B/Malaysia/2506/2004-like viruses whereas the 2006 influenza vaccine for the Southern hemisphere contains the A/New Caledonia/20/1999 (H1N1), A/California/7/2004 (H3N2) and B/Malaysia/2506/2004-like viruses [63].

Approved influenza vaccines at the present time

- **Inactivated influenza vaccine**

Inactivated influenza vaccines can be classified into 3 formulations including whole-virus, split-product and surface-antigen subunit. Although whole-virus vaccines provide higher antigenicity than split-product vaccines, they are usually associated with increased undesirable reactions, especially in children, and hence are rarely used. Most influenza vaccines are split-product vaccines generated from detergent-treated, highly purified influenza virus or surface-antigen vaccines containing purified haemagglutinin and neuraminidase. Current influenza vaccines produced in the United States and Europe are prepared by propagating the vaccine seed strains in embryonated eggs, inactivation by formaldehyde and chemical disruption of the purified viruses with a nonionic detergent such as Triton X-100. However, only high-yielding egg-grown strains such as A/Puerto Rico/8/34 (H1N1) can be used as a seed virus to produce a vaccine according to this procedure. Therefore, annual influenza vaccines are typically derived from 6:2 reassortant viruses containing HA and NA genes of the currently circulating strain and the 6 remaining genes from A/Puerto Rico/8/34 virus [64].

- **Live-attenuated influenza vaccine**

The only FDA (Food and Drug Administration)-licensed live vaccine against influenza is the cold-adapted attenuated vaccine. The cold-adapted, temperature-sensitive influenza virus can be passaged at 25°C in chicken kidney cells and in embryonated eggs. The annually updated live-attenuated vaccine strains can be generated by reassortment between a cold-adapted strain such as A/Ann Arbor/6/60 (H2N2) and virus closely related to the prevalent circulating strain. As a result, the selected vaccine strain is (6:2) reassortant virus containing 6 internal genes derived from the cold-adapted master strain and 2 antigenic determinant genes (HA and NA) obtained from the circulating virus [65, 66]. Intranasal administration of live-attenuated cold-adapted influenza vaccines provides systemic and local mucosal neutralizing immunity and cell-mediated responses which may be longer lasting and more cross-protective than those obtained by inactivated vaccines.

Antiviral drugs for treatment of influenza infection

Treatment of influenza infection is similar to other respiratory diseases caused by viral infection. At present, there are two major classes of antiviral drugs available against influenza viruses, including Adamantane derivatives and neuraminidase inhibitors.

- **Adamantane derivatives:** The Adamantane derivatives include amantadine and rimantadine, which are inhibitors of M2-ion channel protein. These drugs inhibit virus replication during the early stage of infection by inactivating the ion channel formed by the M2 protein of influenza A viruses; however these drugs have no effect against influenza B viruses. Substitution of one of the five amino acids (positions 26, 27, 30, 31, and 34) within the transmembrane domain of M2 has been reported for association with drug-resistance strains [67].

- **Neuraminidase inhibitors:** The neuraminidase inhibitors consist of Zanamivir and Oseltamivir. Zanamivir is available as a powder for inhalation whereas Oseltamivir is the first orally active antiviral drug. Oseltamivir imitates natural neuraminidase substrate molecules and binds to the active site of the enzyme in addition to interfering with the release of progeny influenza virus from infected host cells [68]. However, Oseltamivir-resistant virus might survive and propagate since the chemical structure of Oseltamivir could facilitate the development of resistant mutations that would permit neuraminidase to function. Molecular characterization of amino acids within the neuraminidase protein revealed that rotation at E276 and bond with R224 to form the side chain of Oseltamivir. The substitution of R292K, N294S, and H274Y (N2 numbering system) inhibit this rotation and prevent the chain from forming, resulting in Oseltamivir resistance. An E119V mutation may permit the binding of a water molecule in the space created by the smaller valine, also interfering with oseltamivir binding. In contrast, the binding of Zanamivir does not require any reorientation of amino acids [68].

Laboratory Diagnosis

There are several diagnostic techniques can be applied for influenza virus detection. Many factors should be considered in deciding which tests to use. Sensitivity, specificity, turn-around-time, reproducibility, ease of performance and costs should all be taken into account.

Direct methods

Different methods exist for direct detection of influenza viruses. Some methods such as enzyme immunoassays (EIAs) can be suitable for bedside testing, others such as direct immunofluorescence allow for the preparation of slides onsite in clinics and posting of fixed slides to a central laboratory [69]. RT-PCR can only be performed in well equipped laboratory facilities by trained personnel. These methods can either detect both influenza A and B or differentiate between types (influenza A or B). The only direct technique that has the potential to differentiate between subtypes (i.e. on the basis of haemagglutinin and neuraminidase) is RT-PCR.

- **Immunofluorescence**

For direct immunofluorescence, potentially infected respiratory epithelial cells are fixed to a slide and viral antigens contained in the cells is detected by specific antibodies which are either directly conjugated to a fluorescent dye (direct immunofluorescence) or detected by anti-antibodies linked to a fluorescent dye (indirect immunofluorescence). In both cases reactions are visualised under the fluorescence microscope and positive cells are distinguished on colour intensity and morphology of fluorescent areas. Direct immunofluorescence tends to allow faster results but is generally less sensitive than indirect immunofluorescence. Indirect immunofluorescence also has the advantage that pooled antisera can be used to screen for viral infection using a single anti-antibody conjugated to a fluorescent dye (fluorescein isothiocyanate-conjugated anti-mouse antibodies are commonly used). Immunofluorescence allows for the rapid diagnosis of respiratory specimens as long as sufficient respiratory epithelial cells are present in the specimens. However, inter-individual variation in reporting of immunofluorescence tests exists since interpretation is subjective and accuracy depends on the competence and experience of the operator.

- **Enzyme immuno assays or Immunochromatography assays**

Enzyme immunoassays (EIAs) utilise antibodies directed against viral antigen that are conjugated to an enzyme. An incubation step with a chromogenic substrate follows and a colour change is indicative of the presence of viral antigen. Certain enzyme immunoassays as well as similar assays using immunochromatography allow for bedside testing taking 10-30 minutes. These rapid assays are generally more expensive than direct immunofluorescence or virus culture. Sensitivities of EIAs vary between 64% and 78% [69]. Different rapid tests can detect either influenza A or B virus without distinguishing the type, influenza A virus only or detect both influenza A and B and identify the type. However non of these rapid tests can differentiate between subtypes that infect humans (H1N1 and H3N2) or avian influenza subtypes

- **Reverse transcription polymerase chain reaction (RT-PCR)**

RT-PCR is a process whereby RNA is first converted to complementary DNA (cDNA) and a section of the genome is then amplified through the use of primers that bind specifically to this target area. This allows for exponential amplification of small amounts of nucleic acid, through the action of a thermo stable DNA polymerase enzyme, which enables highly sensitive detection of minute amounts of viral genome. Not only does RT-PCR have superior sensitivity [70] but it can also be used to differentiate between subtypes and conduct phylogenetic analysis [69]. RNA degradation of archival samples can decrease the sensitivity of RT-PCR [71]. Therefore specimens should be processed as fast as possible after collection. RT-PCR reactions that required a gel electrophoresis step were initially time consuming but the relatively recent development of real-time technology made RT-PCR diagnosis within about two hours possible.

Virus isolation methods

Virus isolation or culture is a technique whereby a specimen is inoculated in a live culture system and the presence of virus infection is then detected in this culture system. Since culture amplifies the amount of virus it is more sensitive than direct methods with the exception of RT-PCR (that also employs amplification). Virus isolation is only of use if the live system or cells are sensitive for the virus that one intends to isolate. Isolation requires the rapid transport of specimens to the laboratory since delays may lead to inactivation of virus [69].

- **Embryonated egg culture**

Specimens are inoculated into the amniotic cavity of 10-12 day embryonated chicken eggs. High yields of virus can be harvested after 3 days of incubation. Since this technique requires the supply of fertilized chicken eggs and special incubators it is no longer used for the routine diagnosis of influenza infection. However egg isolation provides high quantities of virus and is a very sensitive culture system. Reference laboratories therefore utilize this culture system to ensure high sensitivity and to enable the production of virus stocks for epidemiological monitoring.

- **Cell culture**

Conventional culture: Various cell-lines are utilised to isolate influenza viruses, most commonly primary monkey kidney cells and Madin-Darby canine kidney (MDCK) cells. Some authors recommend the use of trypsin to aid virus entry into the cell lines [72]. Conventional cell culture takes up to two weeks but has a very high sensitivity. Cytopathic effects such as syncytia and intracytoplasmic basophilic inclusion bodies are observed. The presence of influenza virus can be ascertained using haemadsorption using guinea pig red blood cells or immunofluorescence on cultured cells. The latter can also be used to type the isolated virus. Immunofluorescence has a higher sensitivity in detection of positive cultures than haemadsorption.

Serology

Serology refers to the detection of influenza virus-specific antibodies in serum (or other body fluids). Serology can either detect total antibodies or be class-specific (IgG, IgA, or IgM). Different serological techniques are available for influenza diagnosis: haemagglutination inhibition (HI), complement fixation (CF), enzyme immunoassays (EIA) and indirect immunofluorescence. Serological diagnosis has little value in diagnosing acute influenza. In order to diagnose acute infection, an at least four-fold rise in titre needs to be demonstrated, which necessitates both an acute and a convalescent specimen. However it may have value in diagnosing recently infected patients. Serology is also used to determine the response to influenza vaccination. Serology has greater clinical value in paediatric patients without previous exposure to influenza since previous exposure can lead to heterologous antibody responses [70].

- **Complement fixation (CF)**

Complement fixation tests are based on the ability of antigen-antibody complexes to consume complement - which results in no complement being available to lyse sensitised sheep red blood cells. These assays are labour intensive and necessitate controls for each procedure but reagents are cheap and widely available. CF assays are less sensitive than HI both in the diagnosis of acute infection and the determination of immunity after vaccination.

- **Haemagglutination inhibition (HI)**

HI assays are labour intensive and time consuming assays that require several controls for standardisation. However the assay reagents are cheap and widely available. Various red blood cells such as guinea pig, fowl and human blood group "O" erythrocytes are used. A 0.4-0.5% red blood cell dilution is generally used. Serum is pre-treated to remove non-specific haemagglutinins and inhibitors. A viral haemagglutinin preparation that produces visible haemagglutination (usually 4 haemagglutination units) is then pre-incubated with two-fold dilutions of the serum specimen. The lowest dilution of serum that inhibits haemagglutination is the HI titer. HI is more sensitive than complement fixation and has the added advantage that it is more specific in differentiating between HA subtypes [73].

- **Ezyme immuno assays (EIA)**

EIAs are more sensitive than HI or CF assays (Bishai and Galli 1978). Various commercial EIAs are available. Assays that detect IgG and IgA are more sensitive than IgM assays [74] but are not indicative of acute infection.

Rapid tests

The clinical value of a diagnostic test for influenza is to a large extent dependent on the particular test is turnaround time. The first diagnostic tests that were developed for influenza diagnosis were virus isolation and serological assays. At that stage it took more than two weeks to exclude influenza infection. Although shell vial tests have reduced the turn-around time of isolation, they are not generally regarded as rapid tests. The development of direct tests such as immunofluorescence enabled the diagnosis within a few hours (1 to 2 incubation and wash steps). Immunofluorescence tests however necessitate skilled laboratory workers and the availability of immunofluorescence microscopes. The revolution in rapid diagnosis of influenza was brought about by the development of rapid antigen assays (most of which work on an EIA or immunochromatography principle). These assays enable the diagnosis of influenza within 10-30 minutes. Some of these tests are so easy to perform that even non-laboratory trained people can perform these tests in the clinic, which is referred to as bedside or point of-care testing. Although antigen assays are generally the most user-friendly, they are not as sensitive as immunofluorescence, isolation or RT-PCR.

CHAPTER III

MATERIALS AND METHODS

Materials

1. Materials and reagents required for mammalian cells culture and virus isolation

- A549 (human alveolar epithelial) cell lines (kindly provided by Dr. Ruben O Donis; Influenza Branch, Center for Disease Control and Prevention, USA)
- MDCK (Madin-Darby canine kidney) cell lines (kindly provided by Associate Prof. Kanisak Oraveerakul; Faculty of Veterinary, Chulalongkorn University)
- Embryonated chicken eggs
- Dulbecco's Modified Eagle Medium (D-MEM), high glucose (1X), liquid, with L-glutamine, without sodium pyruvate (GIBCO, Cat no. 11965-084)
- Foetal Bovine Serum EU Approved Origin (GIBCO, Cat no. 10270-098)
- 0.05% Trypsin-EDTA (1X)(GIBCO, Cat no. 25300-054)
- Trypsin, TPCK treated, from bovine pancreas (SIGMA, Cat no. T-8642)
- Penicillin-Streptomycin (10,000 units/ml) (GIBCO, Cat no. 15140-122)
- Phosphate Buffered Saline (PBS Tablets) (Bio Basic Inc., Cat no. D0435)
- Bovine Albumin Fraction V Solution 7.5% (GIBCO, Cat no. 15260-037)
- Cell Freezing medium (SIGMA, Cat no. C6164)
- SeaPlaque agarose (FMC Bioproducts, Cat no. 50100)
- MTT (3-(4,5-dimethylthiazol-2-yl)-2,5-diphenyltetrazolium bromide) (Invitrogen, Cat no. M-6494)
- Trypan blue solution 0.4% (SIGMA, Cat no. T8154)
- V-shaped 96-well microtiter plates (Costar, Cat no. 3897)
- Sterile 6-well cell culture cluster, flat bottom with lid (Costar, Cat no. 3516)
- Tissue Culture Flask 75 cm², phenolic style cap (Corning, Cat no. 430725)
- Tissue Culture Flask 25 cm², phenolic style cap (Corning, Cat no. 430372)
- Sterile pipette 2ml, 5 ml and 10 ml (Costar, Cat no. 4486, 4487 and 4488)

2. Materials and reagents for reverse transfection of siRNA into mammalian cells

- Serine Threonine Kinase siARRAY RTF (Dharmacon, Cat no. H-004400)
- Membrane Trafficking siARRAY RTF (Dharmacon, Cat no. H-005500)
- DharmaFECT Transfection Reagent 1 (Dharmacon, Cat no. T-2001-01)
- DharmaFECT Cell Culture Reagent (Dharmacon)

3. Reagents for nucleic acid extraction

- SDS (Pharmacia Biotech, Cat no. 17-1313-01)
- Sodium acetate anhydrous (SIGMA, Cat no. S-2889)
- TRIZMA Hydrochloride (SIGMA, Cat no. T-7149)
- Glycogen (USB, Cat no. 16445)
- Guanidine Thiocyanate Ultrapure (USB, Cat no. 75818)
- Sodium chloride (BDH Laboratory Supplies, Cat no. 102415K)
- EDTA Tetrasodium Dihydrate (USB, Cat no. 15700)
- Tris, Ultra Pure, Molecular Biology Grade (Research Organics, Cat no. 9680T)
- Boric acid, ACS Reagent (Research Organics, Cat no. 1748B)
- Phenol, Saturated (PIERCE, Cat no. 17914)
- Ethanol (BDH Laboratory Supplies, Cat no. 10107)
- Isopropanol (SIGMA, Cat no. I-9516)
- Chloroform (SIGMA, Cat no. C-2432)
- Iso-Amyl alcohol (BDH Laboratory Supplied, Cat no. 27212)
- Mercaptoethanol (Pharmacia Biolab, Cat no. 17-1317-01)
- TRI REAGENT- RNA/DNA/Protein Isolation (Molecular Research Center, TS120)
- RNeasy Mini Kit (QIAGEN, Cat no. 74104)

4. Reagents for *in vitro* transcription and Reverse Transcription

- RiboMAX Large Scale RNA Production Systems-T7 (Promega, Cat no. P1300)
- ImProm-II Reverse Transcriptase (Promega, Cat no. A3802)
- M-MLV Reverse Transcriptase (Promega, Cat no. M1705)
- RNasin Ribonuclease Inhibitor (Promega, Cat no. N2115)
- Set of dATP, dCTP, dGTP, dTTP (Promega, Catalog no. U1240)
- Random Primers (Promega, Catalog no. C1181)
- Oligo dT 15 primer (Promega, Cat no. C1101)
- Diethylpyrocarbonate (DEPC)
- RQ1 RNase-Free DNase (Promega, Cat no. M6101)

5. Reagents for nucleic acid amplification and quantitation

- AccessQuick RT-PCR System (Promega, Cat no. A1702)
- Eppendorf MasterMix (2.5X) (Eppendorf, Cat no. 0032 002.250)
- Biotools QuantiMix EASY PROBES KIT (BIOTOOLS, Cat no. 10.601)
- QuantiTect Probe RT-PCR Kit (QIAGEN, Cat no. 204443)
- SuperScript III Platinum One-Step Quantitative RT-PCR System (Invitrogen, Cat no. 11732-020)
- SYBR Green PCR Master Mix (Applied Biosystems, Cat no. 4309155)
- TaqMan One-step RT-PCR Master Mix (Applied Biosystems, Cat no. 4309169)

6. Reagents for agarose gel electrophoresis and DNA staining

- GeneRuler 100bp DNA Ladder Plus (Fermentas, Cat no. SM0321)
- 10 bp DNA Ladder (Invitrogen, Cat no. 10821-015)
- Agarose, low EEO, Molecular Biology Grade (Research Organics, Cat no. 1170A)
- SeaKem LE agarose (BioWhittaker Molecular Applications, Cat no. 50004)
- SYBR Green I nucleic acid gel stain (Molecular probes, Cat no. S7563)
- Ethidium Bromide (SIGMA, Cat no. E-1510)

7. Materials and reagents for cloning and transformation in *E.coli*

- One Shot TOP10 Chemically Competent *E.Coli* (Invitrogen, Cat no. C4040-03)
- pGEM-T Easy Vector System for T/A cloning strategy (Promega, Cat no. A1360)
- X-Gal (Promega, Cat no. V3941)
- IPTG (Isopropyl-Thio-B-D-Galactopyranoside) (Eppendorf, Cat no. 0032 006.353)
- Tryptone powder (BIO BASIC INC., Cat no. G211)
- Yeast Extract (GIBCO, Cat no. 20047-056)
- Agar Bacteriological (GIBCO, Cat no. 20001-020)
- FastPlasmid Mini (Eppendorf, Cat no. 955150601)

8. Reagents for nucleotide sequencing

- Perfectprep Gel Cleanup (Eppendorf, Cat no. 955152000)
- ABI PRISM Bigdye Terminator v3.1 Cycle Sequencing Kit (Applied Biosystems, Cat no. 4336917)
- 310 Genetic Analyzer Performance Optimized Polymer 6 (Applied Biosystems, Cat no. 402837)
- Buffer (10X) with EDTA (Applied Biosystems, Cat no. 402824)
- Template Suppression Reagent (TSR) (Applied Biosystems, Cat no. 401674)

9. General materials for molecular biology research

- MicroAmp PCR tube (Perkin Elemer)
- Microcentrifuge tube : 0.5 and 1.5 ml. (AxyGen® Scientific)
- Polypropylene conical tube : 50 and 15 ml. (AxyGen® Scientific)
- Pipette tip : 10 µl, 200 µl and 1000 µl (AxyGen® Scientific)
- Cryotube (Nunc)
- Microscope slide and cover slit (Sail brand)
- Glassware : Beaker, Flask , Cylinder and reagent bottles (Pyrex)

Equipments

- Centrifuge (Beckman GS-6R)
- Refrigerated microcentrifuge (Universal 16R Hettich)
- – 70 °C freezer (Forma Scientific)
- – 20 °C freezer (Philco)
- Inverted Light Microscopy (Nikon)
- DNA Thermal Cyclers 9600 (Perkin Elmer)
- Mastercycler personal (Eppendorf)
- Rotor-Gene RG-3000 (Corbett Research)
- ABI 7500 Real-Time PCR System (Applied Biosystems)
- Gel Doc 1000 UV transilluminator (Biorad)
- Ultrahigh speed centrifugation (55p-72 HIMAC Centrifuge Hitachi)
- Bio Photometer (Eppendorf)
- Class II Microbiological Safety Cabinet (Envair)
- PCR Cabinet (Augusta)
- Orbital incubator S150 (Stuart)
- Perkin-Elmer 310 Sequencer (PE Applied Biosystems)
- CO₂ humidified incubator (TC2323 Shellab)
- Autoclave (Hydroclave MC10 Harvey)
- Hot air oven (Mettler)
- Multi-block heater (Lab-line)
- Balance (PB1502 Mettler Toledo)
- Microwave oven (Sanyo)

Software for bioinformatic and data analysis

- CLUSTAL X program (version 1.8)
- OLIGOS primer design software (version 9.1)
- BioEdit Sequence Alignment Editor (version 7.0.4.1)
- Chromas Lite (version 2.01)

- TreeView (version 1.5.2)
- Molecular Evolutionary Genetics Analysis (MEGA) (version 3.1)
- DNASTAR package software
- 7500 System SDS software (version 1.2; Applied Biosystems)
- Primer Express Software (Version 2.0 ; Applied Biosystems)
- MxPro-Mx3005P QPCR software (version 3.00; Stratagene)
- Rotor-Gene 3000 (version 6.0; Corbett Research)
- GraphPad Prism for Windows (version 4.00)
- SPSS for Windows (version 11.5.0)

Methods

Cell culture

A549 (human alveolar epithelial) and MDCK (Madin-Darby canine kidney) cell lines were cultured in Dulbecco's modified Eagle's medium (DMEM) supplemented with 10% fetal bovine serum (FBS) and 100 units/ml of penicillin-streptomycin. The cells were grown in a humidified atmosphere at 37°C with 5% CO₂.

Cell counting by using hemocytometer

Trypsinize the monolayer and resuspend in medium to give an estimated 1×10^6 cells/ml. Mix the suspension thoroughly to disperse the cells. Clean the surface of the slide and coverslip with 70% alcohol, press the coverslip down over the grooves and semisilvered counting area. Mix the cell sample thoroughly, pipetting vigorously to disperse any clumps and collect 20 μ l into a vial and then mix with 5 μ l of Trypan Blue. Then transfer 10 μ l of the cell suspension to the edge of hemocytometer chamber, expel the suspension and let it be drawn under the coverslip by capillarity. Select a 10X objective lens and focus on the grid line in the chamber. Count the cells lying within 1-mm² area of 4 corners of the grid. Count the cells that lie on the top and left hand lines of each square, but not those on the bottom or right-hand lines, to avoid counting the same cells twice. Calculate the number of cells/ml by divide the amount of cells counted in 4 corner squares by 4 and multiply by 1.25×10^4 . Dilute the cells suspension with complete DMEM medium to yield the desired cell density.

Collection of specimens

Clinical specimens were collected as described below and put into transport medium such as cell culture medium 199 containing 0.5% BSA or PBS with additional antibiotics including Penicillin G (2 X 10⁶ U/liter), Streptomycin 200 mg/liter, polymyxin B (2 x 10⁶ U/liter), gentamicin (250 mg/liter), nystatin (0.5 X 10⁶ U/liter), Ofloxacin HCl (60 mg/liter) and sulfamethoxazole (0.2 g/liter).

- Nasal swab – dry cotton or polyester swab is inserted into the nostril parallel to the palate and left in place for a few seconds. Then it is slowly withdrawn with a rotating motion down the inside of the nose. Specimens from both nostrils are obtained with the same swab. The tip of the swab is put into a vial containing 2-3 ml of transport medium and the applicator stick is broken off.
- Throat swab - the posterior pharynx is swabbed vigorously, and the swab is placed into transport medium
- Tracheal swab - the trachea of live birds is swabbed by inserting a dry cotton or polyester swab into the trachea and gently swabbing the wall, and the swab is placed in transport medium. The trachea of dead animals at slaughter houses can be swabbed after the lungs and trachea have been removed from the animal. The trachea is held in a gloved hand and the swab inserted to its maximal length with vigorous swabbing of the wall. The swabs are placed in transport medium.
- Cloacal swab - the cloaca of live birds is swabbed by inserting a swab deeply into the vent and vigorously swabbing the wall. The swab should be deeply stained with fecal material and is then placed in transport medium.
- Tissue samples- tissue samples are best frozen immediately without transport medium and later ground in transport medium prior to inoculation of eggs or tissue culture. Small samples of tissue (~20 mg) are suspended in 1 mL of transport medium for homogenization.

Processing clinical material for virus isolation

- Nasal, throat, tracheal and cloacal swabs

The specimens were supplemented with 1/10 volume of 10X concentrated antibiotics. Vigorously agitate 1-2ml collection vial with swab on vortex mixer. Then leave at room temperature for 30 minutes to settle. Inoculate the specimen or extract RNA and then store the remainder at -70°C.

- Tissue samples

Tissues were cut and weight (~20 mg) and then homogenized by using a sterile homogenizer, making a 10% suspension with transport medium. Add 1/10 volume of 10x antibiotic mixture. Transfer the specimen to a centrifuge tube and centrifuge at 400xg for 10 minutes to remove extraneous materials. Collect supernatant for inoculation or RNA extraction and then store an aliquot at -70°C.

Virus isolation by using MDCK cells culture

- Preparation of MDCK cells in tissue culture flasks

MDCK cells were cultured in a T-75 flask until a confluent monolayer of MDCK cells was observed (approximately 10^7 cells). Decant medium and wash the cells with 5 ml of Phosphate buffered saline (PBS). Then 3 ml of trypsin-EDTA (pre-warmed to 37°C) were added and distributed over the entire cell sheet by gently rocking the flask. The flask was incubated at 37°C with 5% CO₂ for 5-10 minutes until the cells were detached from the plastic surface. The flask may need to be shaken or tapped in order to detach the cells. The detached cells were investigated by using inverted light microscope. 7 ml of complete Dulbecco's modified Eagle's medium (DMEM) supplemented with 10% fetal bovine serum (FBS) and 100 units/ml of penicillin-streptomycin was added into the flask to inactivate the activity of trypsin. Pipette up and down gently to resuspend and break up cell clumps. Count cells by using hemacytometer under microscope. Transfer the cells suspension containing 600,000 cells into a T-25 flask and then add of complete DMEM with 10%FBS and 100 units/ml of penicillin-streptomycin to a final volume of 5 ml per T-25 flask. Incubate the flask overnight in a humidified atmosphere at 37°C with 5% CO₂.

- Virus inoculation into MDCK cells culture

One day after cell preparation, check the confluent monolayer of MDCK (70-90%) with microscope at 40X magnification. Remove media from MDCK culture flask and wash twice with 3 ml of PBS. Inoculate 500 μ L of each specimen (tissue suspension, nasopharyngeal suction or swab medium) into a T-25 using sterile pipettes. Allow the inoculum to absorb at 37°C for 1 hour with rocking the flask every 10 minutes. Add 5 ml of complete DMEM with 10%FBS and 100 units/ml of penicillin-streptomycin containing additional 2 μ g/ml of TPCK-trypsin to a T-25 flask. Incubate the flask in a humidified atmosphere at 37°C with 5% CO₂ for 2-5 days. Observe daily for the cytopathogenic effect (CPE) occurred on the integrity of the MDCK monolayer.

- Harvesting of supernatants

Harvest the cell culture if 3+ CPE (extensive holes of the monolayer and large number of free floating cells) or 4+ CPE (complete destruction of the monolayer) was observed by collecting supernatant fluid and adding stabilizer such as glycerol gelatin or bovine serum albumin to a final concentration of 0.5%. Harvest the supernatant by day 6 or 7, even if no CPE was observed. Centrifuge the tubes at 3,000 rpm for 5 minutes to remove excess cells. Collect the supernatant and perform a hemagglutination test. Record the HA titer, pipette the positive supernatant into cryotubes and store in -70°C within the day of harvesting. If no HA was present, passage up to 2 more times.

Virus isolation by using embryonated chicken eggs

- Candling of eggs

Examine 9-11 day old of pathogen-free embryonated chicken eggs with an egg candler and place with blunt end up into egg trays. Discard any eggs that are infertile, have cracks, are underdeveloped or that appear to have a porous shell. Incubate the eggs at 35°C until inoculation.

- Inoculation of eggs

Place eggs with blunt end up into egg trays and label each egg with a specific identification number (3 eggs per specimen). Wipe the tops of the eggs with 70% ethanol and punch a small hole in the shell over the air sac. Aspirate 600 μ L of processed specimen (tissue suspension, nasopharyngeal suction or swab medium) with additional 40 μ g of gentamycin into a tuberculin syringe with a 22 gauge, 1.5 inch needle. Holding the egg up to the candler, locate the embryo. Then, insert the needle into the hole of the egg. Using a short stabbing motion, pierce the amniotic membrane and inoculate 100 μ L into the amniotic cavity. Withdraw the needle about 0.5 inches and inoculate 100 μ L of the specimen into the allantoic cavity. Inoculate the other two eggs in the same manner with the same syringe and needle for a total of three eggs inoculated per specimen. Discard syringe into a proper safety container and seal the holes punched in the eggs with a drop of glue. Incubate the eggs at 35°C for 2-3 days

- Harvesting of inoculated chicken eggs

After eggs incubation at 35°C for 2-3 days, eggs were chilled at 4°C overnight or 4 hours before harvesting. Label a 15 ml plastic tube for each egg with the specimen number. Then, clean off the top of each egg with 70% ethanol. Break the shell over the air sac with sterile forceps and push aside the allantoic membrane with sterile pipette tip. Using a 10 ml pipette, aspirate the allantoic fluid as much as possible (5-10 ml per egg) and place in a labeled plastic tube. Centrifuge harvested allantoic fluids at 3,000 rpm for 5 minutes to remove excess blood and tissues. Collect the supernatant and perform a hemagglutination test. Record the HA titer, pipette the positive allantoic fluid into cryotubes and store in -70°C within the day of harvesting. If no HA was present, passage up to 2 more times.

- Isolated viruses and standard strains used in this study

Virus strains	Accession (HA)	Accession (NA)
A/chicken/Nakorn-Pathom/Thailand/CU-K1/04 (H5N1)	AY590563	AY590564
A/chicken/Nakorn-Patom/Thailand/CU-K2/2004 (H5N1)	AY590568	AY590567
A/chicken/Nakorn-Patom/Thailand/CU-K3/2004 (H5N1)	AY590576	AY660557
A/chicken/Ayutthaya/Thailand/CU-23/04 (H5N1)	AY770991	AY770992
A/crow/Thailand/CU-KAF3/2004 (H5N1)	AY590572	AY660554
A/quail/Thailand/CU-KTH/2004 (H5N1)	AY590573	AY590562
A/white peafowl/Thailand/CU-11/2004 (H5N1)	AY590570	AY660555
A/kalij pheasant/Thailand/CU-4/2004 (H5N1)	AY590569	AY660558
A/openbill/Thailand/CU-2/2004 (H5N1)	AY590577	AY660556
A/chicken/Suphanburi/Thailand/CU-1/04 (H5N1)	DQ083550	DQ083586
A/duck/Thailand/CU-2/2004 (H5N1)	AY779048	AY779049
A/chicken/Bangkok/Thailand/CU-3/04 (H5N1)	DQ083551	DQ083587
A/crow/Bangkok/Thailand/CU-4/04 (H5N1)	DQ083552	DQ083588
A/duck/Chonburi/Thailand/CU-5/04 (H5N1)	DQ083553	DQ083589
A/chicken/Bangkok/Thailand/CU-6/04 (H5N1)	DQ083554	DQ083590
A/chicken/Chonburi/Thailand/CU-7/04 (H5N1)	DQ083555	DQ083591
A/chicken/Prachinburi/Thailand/CU-8/04 (H5N1)	DQ083556	DQ083592
A/chicken/Suphanburi/Thailand/CU-9/04 (H5N1)	DQ083557	DQ083593
A/chicken/Chachoengsao/Thailand/CU-10/04 (H5N1)	DQ083558	DQ083594
A/chicken/Chachoengsao/Thailand/CU-11/04 (H5N1)	DQ083559	DQ083595
A/chicken/Nakhon Sawan/Thailand/CU-12/04 (H5N1)	DQ083560	DQ083596
A/chicken/Nakhon Sawan/Thailand/CU-13/04 (H5N1)	DQ083561	DQ083597
A/chicken/Nakhon Pathom/Thailand/CU-14/04 (H5N1)	DQ083562	DQ083598
A/crow/Bangkok/Thailand/CU-15/04 (H5N1)	DQ083563	DQ083599
A/white peafowl/Bangkok/Thailand/CU-16/04 (H5N1)	DQ083564	DQ083600
A/chicken/Saraburi/Thailand/CU-17/04 (H5N1)	DQ083565	DQ083601
A/Kalji Pheasant/Bangkok/Thailand/CU-18/04 (H5N1)	DQ083566	DQ083602
A/Ostrich/Samut Prakan/Thailand/CU-19/04 (H5N1)	DQ083567	DQ083603
A/chicken/Bangkok/Thailand/CU-20/04 (H5N1)	DQ083568	DQ083604
A/chicken/Thailand/CU-21/2004 (H5N1)	AY779050	AY779051
A/chicken/Ayutthaya/Thailand/CU-24/04 (H5N1)	DQ083569	DQ083605
A/crow/Bangkok/Thailand/CU-25/04 (H5N1)	DQ083570	DQ083606
A/rollers/Bangkok/Thailand/CU-26/04 (H5N1)	DQ083571	DQ083607
A/chicken/Saraburi/Thailand/CU-27/04 (H5N1)	DQ083572	DQ083608
A/white peafowl/Bangkok/Thailand/CU-29/04 (H5N1)	DQ083573	DQ083609
A/ostrich/Samut Prakan/Thailand/CU-31/04 (H5N1)	DQ083574	DQ083610
A/crow/Bangkok/Thailand/CU-35/04 (H5N1)	DQ083575	DQ083611
A/chicken/Lopburi/Thailand/CU-38/04 (H5N1)	DQ083576	DQ083612
A/chicken/Nakhon Sawan/Thailand/CU-39/04 (H5N1)	DQ083577	DQ083613
A/chicken/Ratchaburi/Thailand/CU-68/04 (H5N1)	DQ083578	DQ083614
A/duck/Nakhon Pathom/Thailand/CU-71/04 (H5N1)	DQ083579	DQ083615
A/chicken/Chonburi/Thailand/CU-73/04 (H5N1)	DQ083580	DQ083616
A/duck/Saraburi/Thailand/CU-74/04 (H5N1)	DQ083581	DQ083617
A/chicken/Prachinburi/Thailand/CU-104/04 (H5N1)	DQ083582	DQ083618
A/pigeon/Samut Prakan/Thailand/CU-202/04 (H5N1)	DQ083583	DQ083619
A/sparrow/Phang-Nga/Thailand/CU-203/04 (H5N1)	DQ083584	DQ083620
A/Mynas/Ranong/Thailand/CU-209/04 (H5N1)	DQ083585	DQ083621
A/chicken/Thailand/Kanchanaburi/CK-160/2005 (H5N1)	DQ334760	DQ334762
A/quail/Thailand/Nakhon Pathom/QA-161/2005 (H5N1)	DQ334768	DQ334770

- Isolated viruses and standard strains used in this study (continued)

Virus strains	Accession (HA)	Accession (NA)
A/chicken/Thailand/Nontaburi/CK-162/2005(H5N1)	DQ334776	DQ334778
A/leopard/Suphanburi/Thailand/Leo-1/04(H5N1)	AY646175	AY646176
A/tiger/Suphanburi/Thailand/Ti-1/04(H5N1)	AY646167	AY646168
A/tiger/Thailand/CU-T3/2004(H5N1)	AY842935	AY842936
A/tiger/Thailand/CU-T4/04(H5N1)	AY972539	AY972543
A/tiger/Thailand/CU-T5/04(H5N1)	AY972540	AY972544
A/tiger/Thailand/CU-T6/04(H5N1)	AY972541	AY972545
A/tiger/Thailand/CU-T7/2004(H5N1)	AY866475	AY866476
A/tiger/Thailand/CU-T8/04(H5N1)	AY972542	AY972546
A/Thailand/2(SP-33)/2004(H5N1)	AY555153	AY555152
A/Thailand/3(SP-83)/2004(H5N1)	AY577314	AY577315
A/Thailand/4(SP-528)/2004(H5N1)	AY626143	AY577316
A/duck/Hong Kong/308/78 (H5N3)	-	-
A/avian/NY/01 (H5N2)	AY296078	AY300940
A/Chicken/Mexico/31381-3/94 (H5N2)	-	-
A/shoveler/Egypt/03 (H5N2)	-	-
A/ Fujian/411/2002 (H3N2)	DQ865966	-
A/chicken/Netherland/1/2003 (H7N7)	-	-
A/turkey/Wisconsin/66 (H9N2)	DQ067444	DQ067439
A/canine/Florida/242/2003(H3N8)	DQ124157	DQ124159
A/canine/Florida/43/2004(H3N8)	DQ124190	DQ124151
A/canine/Texas/1/2004(H3N8))	DQ124196	-
A/canine/Iowa/13628/2005(H3N8)	DQ146419	DQ146420
A/Ohio/1983 (H1)	-	-
A/WSN/1933 (H1)	-	-
A/Wyoming/3/2003 (H3)	-	-
A/Victoria/3/1975 (H3)	-	-
A/turkey/England/69 (H3)	-	-
A/swine/Nebraska/209/98 (H3)	-	-
A/equine/Alaska/1/91 (H3)	-	-
A/mallard/NY/37/1983 (H4)	-	-
A/turkey/MN/1066/1980 (H4)	-	-
A/Duck/Vietnam/NCVDCDC76/2005 (H4)	-	-
A/pheasant/NJ/1335/1998 (H5)	-	-
A/Duck/Vietnam/NCVDCDC90/2005 (H6)	-	-
A/turkey/VA/4529/2002 (H7)	-	-
A/Teal/Egypt/0457/2003 (H10)	-	-
A/Shoveler/Egypt/0600/2004 (H10)	-	-
A/Duck/Vietnam/NCVDCDC72/2005 (H11)	-	-
A/Teal/Egypt/0688/2004 (H11)	-	-

Determination of viral titers by Hemagglutination (HA) test

The traditional method for identifying influenza field isolates takes advantage of the property that the hemagglutinin (HA) protein agglutinates erythrocytes. Hemagglutination test was performed in a V-shaped 96-well microtiter plates as the following: 100 μ l of each specimen suspension (allantoic fluid or cells supernatant) was pipetted into well A1-H1. Then add 50 μ l of phosphate buffered saline (PBS) into the remaining well (A2-H12). Then 2-fold serially dilution of the specimen suspension was performed by pipette 50 μ l of the sample from the first column into the second column and mix by pipette up and down several times. Repeat the same dilution procedure from the second column to the last column. After that, add 50 μ l of 50% chicken's or turkey's red blood cells into each individual well by using multichannel pipettors. Mix the suspension by gently shaking the plate back and forth for a few times. Then incubate the plate at room temperature for 30 minutes and then determine the result. When the virus is present, it agglutinates with red blood cells yielding a cloudy well (positive result), whereas the negative result will be a red compact dot that falls at the bottom of the well. The highest dilution of virus that causes complete hemagglutination is considered the HA titration end point. The HA titer is the reciprocal of the dilution of virus in the last well with complete hemagglutination.

Determination of viral infectivity by Egg Infective Dose₅₀ (EID₅₀)

The EID₅₀ is defined as that dilution of a virus required to infect 50% of a given batch of inoculated eggs. Briefly, perform 10-fold serial dilution of sample from 10⁻³ to 10⁻⁸ with phosphate buffered saline in a final volume of 1 ml. Inoculate 100 μ l of each sample dilution into 5 eggs per dilution. Incubate the eggs at 35°C for 2-3 days and then chill at 4 °C overnight. Harvest 100 μ l of allantoic fluids obtained from each egg and then perform hemagglutination (HA) test. Record the result and calculate the EID₅₀/mL of virus suspension using Reed-Muench method.

Determination of viral infectivity by plaque assay

Briefly, seed MDCK cell at density of 5×10^5 cells/ well into each of a 6-well cell culture plate and then incubate overnight in a humidified atmosphere at 37°C with 5% CO_2 . On the next day, perform 10-fold serial dilution of sample from 10^{-1} to 10^{-6} with DMEM medium in a final volume of 0.5 ml. Remove culture medium from each well of 6-well plate and then wash once with phosphate buffered saline (PBS). Add 0.5 ml of each sample dilution into each well and incubate in a humidified atmosphere at 37°C with 5% CO_2 for 1 hour with occasionally mixing every 10 minutes in order to let the virus adsorb into the cells. During adsorption period, prepare 1.6% SeaPlaque agarose by microwave and place in $45\text{-}55^\circ\text{C}$ water bath. Place 2X MEM medium and Bovine Albumin Fraction V Solution 7.5% in 37°C water bath. After 1 hour of adsorption, remove the sample suspension and wash once with PBS (optional). Mix equal volume of 1.6% agarose and 2X MEM medium and then add trypsin TPCK-treated at final concentration of $1 \mu\text{g/ml}$ and Bovine Albumin Fraction V Solution at 5% final concentration. After that, add 3 ml of agarose/medim suspension into each well. Leave the plate until the agarose become solidifies. Invert plates and incubate a humidified atmosphere at 37°C with 5% CO_2 for 2-3 days. After 3 days of incubation, check for white-spot plaques in each well of the plate. Remove agar from each well and then stain with 0.05% crystal violet in 10% formaldehyde. Incubate at room temperature for 10 minutes and then indirectly wash the plate with sterile water. Examine the plaques on each well and calculate for pfu/ml.

RNA and DNA by using TRI REAGENT LS

TRI REAGENT LS is a complete and ready to use reagent for the simultaneous isolation of RNA, DNA and proteins from liquid samples of human, animal, plant, yeast, bacterial and viral origin. A biological sample is homogenized or lysed in TRI REAGENT LS and the lysate is separated into aqueous and organic phases by chloroform addition and centrifugation. RNA remains exclusively in the aqueous phase, DNA in the interphase and protein in the organic phase. RNA is precipitated from the aqueous phase by the addition of isopropanol and the RNA pellet is washed with ethanol and solubilized. DNA and proteins are subsequently precipitated from the interphase and organic phase with ethanol and isopropanol, washed with ethanol and solubilized. The details of extraction procedures were described below.

Mix 0.75 ml of TRI REAGENT LS with 0.25 ml of liquid sample (supernatant from cell culture, allantoic fluid or transport media) or use 0.3 ml of TRI REAGENT LS per 10 cm² area of cell culture dish when isolate RNA/DNA/protein from monolayer cells. Lyse cells by passing the suspension several times through a pipette. Store the lysate / homogenates for 5 minutes at room temperature to permit the complete dissociation of nucleoprotein complexes. Then, supplement the lysate with 0.2 ml of chloroform, cover the tube tightly and shake vigorously for 15 seconds. Store the resulting mixture at room temperature for 15 minutes. Centrifuge the resulting mixture at 12,000xg for 15 minutes at 4°C. Following centrifugation, the mixture was separated into a lower red, phenol-chloroform phase, interphase and the colorless upper aqueous phase. RNA remains exclusively in the aqueous phase whereas DNA and proteins are in the interphase and organic phase, respectively.

- RNA extraction

Transfer the aqueous phase to a fresh tube and save the interphase and organic phase at 4°C for subsequent isolation of DNA and proteins. Precipitate RNA from the aqueous phase by mixing with 0.5 ml of isopropanol. Store samples at room temperature for 5-10 minutes and centrifuge at 12,000 g for 8 minutes at 4°C. RNA precipitate (often invisible before centrifugation) forms a gel-like or white pellet on the side and bottom of the tube. Remove the supernatant and wash RNA pellet once with 1 ml of 75% ethanol by vortexing and subsequent centrifugation at 12,000 g for 5 minutes at 4°C. Remove the ethanol wash and briefly air-dry the RNA pellet for 3 - 5 minutes. Dissolve RNA in 30 µl of RNase-free water or diethyl pyrocarbonate (DEPC)-treated water by passing the solution a few times through a pipette tip and incubating for 10-15 minutes at 55-60°C and then store in -70°C.

- DNA extraction

The DNA is isolated from the interphase and phenol phase separated from the initial homogenate as described in the RNA isolation protocol. Remove the remaining aqueous phase overlying the interphase and precipitate DNA from the interphase and organic phase with 0.3 ml of 100% ethanol and mix samples by inversion. Next, store the samples at room temperature for 2-3 minutes and sediment DNA by centrifugation at 2,000 g for 5 minutes at 4°C. Remove the phenol-ethanol supernatant and save it at 4°C for the protein isolation. Wash the DNA pellet twice with 1 ml of 0.1 M sodium citrate in 10% ethanol. At each wash, store the DNA pellet in the washing solution for 30 minutes at room temperature with periodic mixing and centrifuge at 2,000 g for 5 minutes at 4°C. Following these two washes, suspend the DNA pellet in 1.5 ml of 75% ethanol, store for 10 - 20 minutes at room temperature with periodic mixing and centrifuge at 2,000 g for 5 minutes at 4°C. Remove the ethanol wash and briefly air-dry the DNA pellet by keeping tubes open for 3 - 5 minutes at room temperature. Dissolve the DNA pellet in 50 µl of 8 mM NaOH by slowly passing through a pipette. Remove insoluble material by centrifugation at 12,000 g for 10 minutes and transfer the resulting supernatant containing DNA to a new tube and then store in -20°C.

Reverse transcription (cDNA synthesis)

For each 20 µl reverse transcription (RT) reaction, combine RNA template up to 1 µg with primer (0.5 µg of oligo (dT)₁₅ primer or 0.5 µg of random hexamer or 20 pmol of gene-specific primer) and nuclease-free water to a final volume of 10 µl. Incubate the tube in a controlled-temperature heat block at 70°C for 5 minutes and then quick chill and hold on ice for at least 5 minutes. Prepare reverse transcription mixture consisting of 4 µl of ImProm-II 5X reaction buffer, 2.5 µl of 25 mM MgCl₂, 2.5 µl of 10 mM dNTP mix, 0.5 µl of RNasin Ribonuclease Inhibitor (40 u/µl) and 1 µl of ImProm II Reverse Transcriptase (200 u/µl). For each individual reaction, add 10 µl of reverse transcription mix into the 10 µl of template + primer mix to yield the final volume of 20 µl. Incubate the reaction at 37°C (for oligo (dT) primer and random hexamer) or 42°C (for gene-specific primer) for 60 minutes. Then heat-inactivate the ImProm-II Reverse Transcriptase by incubating at 70°C for 15 minutes. Store the cDNA at -20°C.

DNA amplification by conventional Polymerase Chain Reaction (PCR)

Briefly, one microlitre of DNA sample was combined with a reaction mixture containing 10 µl of Eppendorf MasterMix (2.5X), 0.5 µM of each primer, additional 1 mM of MgCl₂ and sterile distilled water to a final volume of 25 µl. Amplification of the target gene was carried out in an automated thermocycler, Mastercycler personal (Eppendorf, Axygen, USA) under the following conditions: After an initial 3 minutes of denaturation step at 94°C, 40 cycles of amplification were performed, each including 30 seconds of denaturation at 94°C, 30 seconds of annealing at 45-60°C (depends on the T_m of the primers) and 30 -180 seconds (depends on the amplicon length, approximately 30 seconds for 500 bp in length) of extension at 72°C, followed by a final 10 minutes extension at 72°C.

Single step Reverse Transcription-Polymerase Chain Reaction (RT-PCR)

RT-PCR was performed simultaneously in a single-step reaction using the AccessQuick RT-PCR System (Promega, Madison, WI). Primers specific for the target gene were used at a final concentration of 0.5 µM each. Five microlitres of RNA sample were combined with a reaction mixture containing 12.5 µl of AccessQuick Master Mix, 5 U of RNase inhibitor, 5 U of AMV Reverse Transcriptase, additional 1 mM MgCl₂ and RNase-free (DEPC-treated) water was added in a final volume of 25 µl. One-step RT-PCR was carried out in a Mastercycler personal (Eppendorf, Axygen, USA). Cycling conditions included a reverse transcription step at 48°C for 45 minutes. After an initial denaturation step at 95°C for 2 minutes in order to activate the *Tfl* DNA polymerase, amplification was performed during 40 cycles including denaturation (94°C for 30 seconds), annealing (45-60°C for 30 seconds, depends on the T_m of the primers) and extension (72°C for 30-120 seconds, depends on the amplicon length), followed by final extension at 72°C for 10 minutes.

Agarose gel electrophoresis

A total of 10 µl of amplified product was mixed with 5 µl of loading buffer and run on a 2% agarose gel (molecular biology grade) at 100 Volts for 40-60 minutes. After electrophoresis the DNA bands were stained with ethidium bromide for 10 minutes and visualized by UV transillumination.

Purification of amplified product

The PCR products of interest were cut and purified from agarose gel using the Perfectprep Gel Cleanup (Eppendorf). After DNA was stained with ethidium bromide and visualized by UV transillumination, the DNA band of interest was cut and combined with 400 μ l of binding buffer. Then incubate the tube at 50°C for 10 minutes until the gel was completely melted. Add 150 μ l of isopropanol into the DNA+binding buffer mixture and then load all of the suspension into the spin column. Centrifuge at 8,000 rpm for 1 minute and then discard the flow through. Reassemble the column and then add 750 μ l of wash buffer containing ethanol into the column. Centrifuge at 8,000 rpm for 1 minute and then discard the flow through. Reassemble the column and centrifuge at 13,000 rpm for 5 minutes in order to dry the membrane of the column. Finally, the DNA was eluted by adding 40 μ l of elution buffer and then centrifuge at 8,000 rpm for 1 minute.

Measurement of DNA / RNA concentrations by UV spectrophotometry

Concentration of the DNA and RNA were determined by measuring the absorption at 260 nm in a UV spectrophotometer (Bio Photometer; Eppendorf). The DNA or RNA was diluted 1:5 or 1:10 by nuclease-free water in a final volume of 50 μ l to yield a reliable OD₂₆₀ ranging from 0.2 to 0.8. The concentration of double-stranded DNA was calculated according to the formula: 1 OD₂₆₀ = 50 μ g/ml dsDNA. The concentration of single stranded RNA was calculated due to the formula: 1 OD₂₆₀ = 50 μ g/ml RNA.

Nucleotide sequencing

The sequencing reaction was performed by using ABI PRISM Bigdye Terminator v3.1 Cycle Sequencing Kit (Applied Biosystems). Briefly, 10 ng of purified DNA or 500 ng of plasmid DNA was combined with 1 μ l of 10 μ M of sequencing primer, 2 μ l of 5X sequencing buffer, 4 μ l of Bigdye Terminator v3.1 and sterile water to a final volume of 10 μ l. The sequencing reaction was carried out in the Gene Amp PCR System 9600 (Perkin-Elmer) under the following condition: 25 cycles of sequencing amplification, each including 10 seconds of denaturation at 96°C, 5 seconds of annealing at 50°C and 4 minutes of extension at 60°C. After, the sequencing reactions were precipitated and purified, the sequencing products were subjected to detect by a Perkin Elmer 310 Sequencer (Perkin-Elmer) and analyzed by Chromas Lite software (version 2.01).

Cloning of PCR products with pGEM-T Easy vector

The pGEM®-T Easy Vector Systems (Promega) is a convenient system for the cloning of PCR products. The vector contains a single 3' terminal thymidine (T) at both ends. These single 3'-T overhangs at the insertion site greatly improve the efficiency of ligation of a PCR product into the plasmids by preventing recircularization of the vector and providing a compatible overhang for PCR products generated by certain thermostable polymerases including *Taq*, *Tfl* and *Tth*. The DNA of interest was amplified based on Polymerase Chain Reaction (PCR) using *Taq* polymerase in order to insert the 3'-A overhangs at both ends of the amplified product for facilitating TA cloning strategy. After electrophoresis and gel purification of the amplified DNA, the concentration of the purified DNA was determined by measuring the absorption at 260 nm in a UV spectrophotometer (Bio Photometer; Eppendorf). Ligation reaction was set up by combining 5 µl of 2X Rapid Ligation Buffer, 50 ng of pGEM-T Easy Vector, 3 Weiss units of T4 DNA Ligase, optimized concentration of purified DNA (approximately, the molar ratio of purified DNA: vector at 3:1 was used) and deionized water to a final volume of 10 µl. Mix the reactions by pipetting and then incubate overnight at 4°C. On the next day, transformation was performed by mixing 2 µl of the ligation reaction with 50 µl of thawed competent cells (One Shot TOP10 Chemically Competent *E. Coli*; Invitrogen). Incubate the suspension on ice for 20 minutes and then heat shock the cells for 45-50 seconds at exactly 42°C. After that, immediately, return the tube to ice for 2 minutes and then add 950 µl of SOC medium to recover the cells. Incubate for 1.5 hours at 37°C with shaking (~200 rpm). Plate 100 µl of transformation culture onto duplicate LB plates supplement with 100 µg/ml of ampicillin, 0.5 mM of IPTG and 80 µg/ml of X-Gal. If a higher number of colonies is desired, the cells may be pelleted by centrifugation at 1,000 ×g for 10 minutes, resuspended in 200 µl of SOC medium, and 100 µl plated on each of 2 plates. Incubate the plates overnight (16-24 hours) at 37°C and then select white colonies which contain the vector with inserted DNA of interest. Culture the selected colonies in 2 ml of LB broth containing 100 µg/ml of ampicillin by incubation overnight (16-18 hours) at 37°C. On the next day, plasmids were extracted from the bacterial culture.

Extraction and purification of plasmids DNA from bacterial culture

Plasmid was extracted and purified by using FastPlasmid Mini Kit (Eppendorf). Briefly, 2 ml of bacterial culture containing the plasmid of interest were centrifuged at 8,000xg for 1 minute and then discard the supernatant. After that, add 400 μ l of lysis buffer containing enzyme into the cell pellets and mix vigorously by vortexing for 30 seconds. Incubate the tube at room temperature for 3-5 minutes until the suspension become clear. Pipette all of the suspension into the spin column and centrifuge at 8,000xg for 30 seconds. Discard the flow through and reassemble the spin column. Add 750 μ l of wash buffer containing ethanol into the spin column and then centrifuge at 8,000xg for 30 seconds. Discard the flow through, reassemble the spin column and then centrifuge at 13,000xg for 5 minutes in order to dry the membrane of the column. Finally, the plasmid DNA was eluted by adding 50 μ l of elution buffer into the membrane and then centrifuge at 8,000xg for 1 minute. Concentration of the plasmid DNA was determined by measuring OD_{260} and then calculated the amount (copies/ μ l) of the plasmid by using the formula: the concentration of plasmid (g/ μ l) was divided by lengths (bp) of the recombinant plasmid (length of vector + length of insert), divided by 660 and then by multiplied by 6.02×10^{23} . The known concentration (copies/ μ l) of plasmid can be used as a standard DNA for DNA quantitation based on real-time PCR.

RNA production based on *in vitro* transcription

Standard RNA of interest was generated by using RiboMAX Large Scale RNA Production Systems- T7 (Promega). According to the construction of pGEM-T Easy vector, this plasmid contains promoters for RNA polymerase (T7 and SP6) flanking multiple cloning sites in opposite directions. Therefore, the production of certain RNA target can be performed by insertion of the target gene into the pGEM-T Easy vector. The process start with the amplification and purification of the gene of interest, then ligation of purified DNA into pGEM-T Easy vector. After that, the recombinant plasmid was transformed into a competent *E.coli* cells. The white colonies which contain the gene of interest were selected and cultured overnight in LB broth containing ampicillin.

Then plasmids DNA were extracted and purified from bacterial culture. The purified plasmids were linearized by digestion with the appropriate restriction endonuclease (such as *Pst* I, *Sal* I or *Nde* I) followed by a clean up procedure. Then the linearized plasmids were used as a template for RNA production by *in vitro* transcription. Briefly, assemble the reaction components appropriate for T7 RNA Polymerase at room temperature in a 1.5 ml microcentrifuge tube as the following: 4 μ l of T7 Transcription 5X buffer, 6 μ l of 25 mM rNTPs mix (ATP, CTP, GTP and UTP), enzyme T7 RNA polymerase, 5 μ g of linearized plasmid and nuclease-free water in a final volume of 20 μ l. Pipette gently to mix the reaction components and incubate at 37°C for 4 hours. Then linearized plasmid DNA can be removed by digestion with 5 units of RQ1 RNase-Free DNase at 37°C for 30 minutes. Then the *in vitro* transcribed RNA was extracted by phenol/ chloroform and precipitated by ethanol. Finally, the RNA was dissolved by 50 μ l of nuclease-free (DEPC-treated) water. Concentration of the *in vitro* transcribed RNA was determined by measuring OD₂₆₀ and then calculated the amount (copies/ μ l) of the plasmid by using the formula: the concentration of RNA (g/ μ l) was divided by lengths (bp) of the transcribed RNA, divided by 340 and then by multiplied by 6.02×10^{23} . The known concentration (copies/ μ l) of *in vitro* transcribed RNA can be used as a standard RNA for quantitation based on real-time RT-PCR.

Single step real-time RT-PCR using SYBR Green I dye with melting curve analysis

One step Real-time RT-PCR using SYBR Green I fluorescence dye with melting curve analysis was performed by using SYBR Green PCR Master Mix (Applied Biosystems). A combination of 3.0 μ l of RNA sample with a reaction mixture containing 10 μ l of 2X SYBR Green PCR Master Mix, 0.5 μ l of 40X MultiScribe and RNase Inhibitor, each primer at a final concentration of 0.5 μ M, additional 1.5 mM MgCl₂ and RNase-free water was used in a final volume of 20 μ l. Cycling conditions included a reverse transcription step at 48°C for 45 minutes. After an initial denaturation step at 95°C for 10 minutes, amplification was performed during 40 cycles including denaturation (94°C for 15 seconds), annealing (50-60°C for 30 seconds) and extension (72°C for 40 seconds). A fluorescent signal of SYBR Green I was obtained once per cycle at the end of extension step.

After amplification, melting curve analysis was performed on the products by heating to 95°C for 15 seconds, cooling to 60°C for 1 minute, followed by a temperature increase to 95°C with a temperature transition rate of 0.5°C /second while continuously collecting the fluorescent signal. Data acquisition and analysis of real-time PCR assay were carried out with 7500 System SDS Software version 1.2 (Applied Biosystems).

Single step multiplex real-time RT-PCR detection using TaqMan probes

A single step multiplex real-time RT-PCR was performed using the TaqMan One Step PCR Master Mix containing ROX as a passive reference (Applied Biosystems). Sets of primers and TaqMan MGB probes specific for each gene of interest were used in multiplex format. Each primer and probe was used at a final concentration of 0.5 and 0.25 μM , respectively. A combination of 3 μl of RNA sample with a reaction mixture containing 10 μl of 2X TaqMan PCR Master Mix, 0.5 μl of 40X MultiScribe and RNase Inhibitor, additional 1.25mM MgCl_2 , 0.25mM dNTPs and RNase-free water was used in a final volume of 20 μl . One-step multiplex real-time RT-PCR was performed on 7500 Real-Time PCR System (Applied Biosystems). Cycling conditions included a reverse transcription step at 48°C for 45 min. After an initial denaturation step at 95 °C for 10 min in order to activate the AmpliTaq Gold DNA polymerase, amplification was performed during 40 cycles including denaturation (94°C for 15 seconds), annealing (55 °C for 30 seconds) and extension (72 °C for 40 seconds). Multiple fluorescent signals were obtained once per cycle at the end of the extension step with detectors corresponding to the fluorescent dyes labeled in each probe. Data acquisition and analysis of the real-time PCR assay were performed using the 7500 System SDS Software Version 1.2 (Applied Biosystems).

Quantitation of viral loads or gene expression by real-time RT-PCR

The concentration of *in vitro* transcribed RNA was determined by measuring OD₂₆₀. After the amount of RNA (copies/ μ l) was calculated, the RNA was 10-fold serially diluted from 10⁸-10 copies/ μ l and served as RNA standards to construct a standard curve for quantitation based on real-time RT-PCR. Quantitation of the gene of interest by real-time RT-PCR was carried out in a Rotor Gene RG-3000 (Corbett Research). A single step real-time RT-PCR was performed using SuperScript III Platinum One-Step Quantitative RT-PCR System (Invitrogen). The reaction mixture comprised 1 μ l of RNA template combined with 10 μ l of 2X Reaction Mix, 0.4 μ l of SuperScript III RT/Platinum® Taq Mix, each primer at a final concentration of 0.5 μ M, probe at a final concentration of 0.25 μ M, 0.4 μ l of ROX Reference Dye, additional 2 mM MgSO₄ and RNase free water in a final volume of 20 μ l. Cycling conditions included a reverse transcription step at 50°C for 30 minutes. After an initial denaturation step at 95 °C for 10 min in order to activate the HotStartTaq DNA polymerase, amplification was performed during 40 cycles including denaturation (94°C for 15 seconds), annealing/extension (60°C for 30 seconds). Data acquisition and analysis of the real-time RT-PCR assay were performed using the Rotor-Gene Version 6.0 (Corbett Research). Each fluorescent reporter signal was measured against the internal reference dye (ROX) signal to normalize for non-PCR-related fluorescence fluctuations between wells. The threshold cycle represented the refraction cycle number at which a positive amplification reaction was measured and set at 10 times the standard deviation of the mean baseline emission calculated for amplification cycles 3-15.

CHAPTER IV

RESULTS

Molecular characterization of H5N1 influenza A virus in Thailand 2004

H5N1 influenza A virus isolated from chicken in Nakorn-Pathom province, Thailand in 2004 termed as “A/Chicken/Nakorn-Pathom/Thailand/CU-K2/04” was selected for whole genome sequencing and used as a representative of the strain that responsible for the outbreak among poultry in Thailand 2004. Firstly, lung tissue of infected chicken was homogenized and virus isolation was performed by using embryonated chicken eggs. Then RNA extracted from allantoic fluids was used as a template for reverse transcription using universal primer specific for all segments of influenza viral genes. Therefore, the cDNAs of the 8 segment genes were generated simultaneously in the same reverse transcription reaction. After that cDNAs were used as a template for amplification by conventional Polymerase Chain Reaction (PCR) using specific primers for each target gene. The sequences and positions of each specific primer were summarized in Table 5 and Figure 6. These primers were designed based on the nucleotide sequences of the previously strains obtained from GenBank database. After amplification, the PCR products were analyzed by agarose gel electrophoresis and then the bands of interest were cut and purified. After that, each purified DNA fragment was subjected to direct sequencing using specific primers in both directions (Table 5). Finally, the sequences obtained from each fragment were assembled in order to generate full-length sequences for genetic characterization and phylogenetic analysis.

As for the genome sequence analysis, all 8 segments of A/Chicken/Nakorn-Pathom/Thailand/CU-K2/04 were sequenced and analyzed. A previous report had clarified that A/Chicken/Hong Kong/ H5N1/ 97 was similar to the A/Goose/Guangdong/ 1/96 virus, and both shared an ancestor with the goose pathogen [40]. For this reason, we retrospectively compared the genome sequences of A/Chicken/Nakorn-Pathom/Thailand/CU-K2/04 to its ancestors as well as other H5N1 sequences obtained during the outbreaks in the past few years and stored in the GenBank database.

Table 5 Sequence of primers used for whole genome amplification and sequencing

PCR Fragment	Product size (bp)	Primer for Sequencing	Sequence (5'→3')	Tm (°C)
PB2 (F5'/ R1+)	1080	PB2-F5'	5' -AgCAAAAgCAggTCAATTATATTC- 3'	64
		PB2-R1+	5' -TTTggAggTTgCCTgTAAgC- 3'	60
PB2 (F3 / R3')	1390	PB2-F3	5' -gTAGATATATgCAAaggCAgCA- 3'	60
		PB2-F41	5' -gTAGCAATggTgTTCTCACAg- 3'	62
		PB2-R51	5' -ACCTgCgTCCTTTCCAAgAA- 3'	60
		PB2-R3'	5' -AgTAGAAAACAAaggTCgTTTTTAAAC- 3'	66
PB1 (F5'/R4)	1500	PB1-F5'	5' -AgCAAAAgCAaggCAAACCATTg- 3'	66
		PB1-R2	5' -AgCTCTgTATCTTgTgAgTTA- 3'	58
		PB1-R4	5' -ATCACTgTAACTCCAATgCTC- 3'	60
PB1 (F3+ / R3')	1000	PB1-F3+	5' -TCCTCTgATgATTTTCgCTCTC- 3'	62
		PB1-R3'	5' -AgTAGAAACAaggCATTTTTTCA- 3'	60
PA (F5' / R2)	1200	PA-F5'	5' -AgCAAAAgCAggTACTgATCCg- 3'	68
		PA-R11	5' -ggCATCCATCAgCAAgAACTT- 3'	62
		PA-R2	5' -CTgTgATACTgTTTCAgATCg- 3'	60
PA (F3 / R3')	1100	PA-F3	5' -TggAAgCAggTgCTggCAg- 3'	62
		PA-R3	5' -CTCATTTCCATgCCCCATTTTC- 3'	60
		PA-R3'	5' -AgTAGAAAACAaggTACTTTTTTgg- 3'	64
HA (F5' / R2+)	1100	H5-F5'	5' -AgCAAAAgCAggggTCTgATCTg- 3'	70
		H5-R2+	5' -CATCTACCATTCCCTgCCATCC- 3'	68
HA (F3 / R3')	850	H5-F3	5' -ACTCCAATGGGGGCGATAAAC- 3'	64
		H5-R3'	5' -AgTAGAAAACAaggTgTTTTTAACTAC- 3'	72
NP (F5' / R11)	900	NP-F5'	5' -AgCAAAAgCAgggTAgATAATC- 3'	62
		NP-R11	5' -CACAAgCAggCAAgCAggAC- 3'	64
NP (F2 / R3')	1000	NP-F2	5' -TgATgCCACATACCgAgAAC- 3'	62
		NP-R3'	5' -AgTAGAAACAaggTATTTTTCT- 3'	60
NA (F5' / R1)	650	N1-F5'	5' -AgCAAAAgCAggAgTTTAAATg- 3'	62
		N1-R1	5' -TgATAgTgTCTgTTATTAATgCC- 3'	60
NA (F2 / R3')	1000	N1-F2	5' -gTTTgAgTCTgTTgCTTggTC- 3'	62
		N1-R3'	5' -AgTAGAAAACAaggAgTTTTTgAAC- 3'	66
M (F5'/ R3')	1130	M-F5'	5' -AgCAAAAgCAggTAgATgTTg- 3'	60
		M-R3'	5' -AgTAGAAAACAaggTAgTTTTTTAC- 3'	62
NS (F5' / R3')	900	NS-F5'	5' -AgCAAAAgCAgggTgACAAAAAC- 3'	66
		NS-R3'	5' -AgTAGAAAACAaggTgTTTTTTAT- 3'	62
Universal primer for influenza cDNA synthesis			5' -AgCAAAAgCAgg- 3'	36

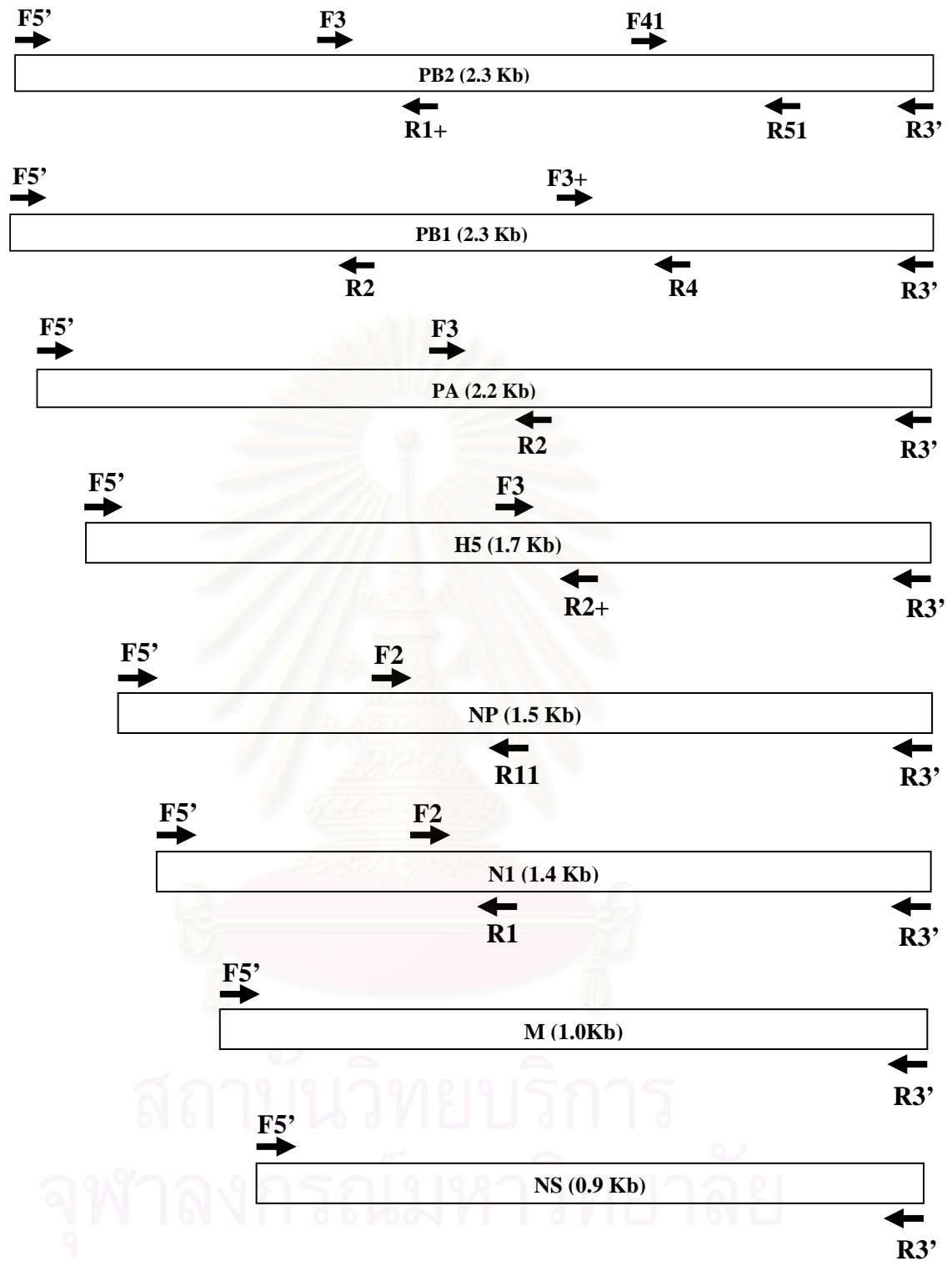


Figure 6 Schematic maps represent position of primers specific for each gene segment of H5N1 influenza A virus.

Phylogenetic analysis of A/Chicken/Nakorn-Pathom/Thailand/CU-K2/04 strain

The nucleotide sequences were analyzed by using maximum parsimony algorithm. Phylogenetic analysis of each gene segment of A/Chicken/Nakorn-Pathom/Thailand/CU-K2/04 compared to H5N1/1997, H5N1/2001 and H5N1/2003-4. Phylogenetic analysis of HA and NA gene segments of A/Chicken/Nakorn-Pathom/Thailand/ CU-K2/04 was performed on viruses collected in 1997, 2001 and 2003-2004. HA and NA of A/Chicken/Nakorn-Pathom/Thailand/CU-K2/04 display 97% similarity to the A/Human/Vietnam/1196/04 and closely share the group with the partial sequences of A/Chicken/Nakorn-Pathom/Thailand/CU-K1/04, A/Human/Thailand/KAN1/04 and A/Human/Thailand/SP33/04 (Figure 7-14). For this reason, A/Chicken/Nakorn-Pathom/Thailand/CU-K2/04 has proven to be the cause of the newly emerging H5N1, totally different from the AI isolates in 1997, which was responsible for the Thai bird flu epidemic and thus caused a deadly disease of humans.

Furthermore, the NA gene of A/Chicken/Nakorn-Pathom/Thailand/ CU-K2/04 is clustered with both Chicken and Human H5N1 of 2004 and hence with A/Duck/China/E319.2/03. In addition, when compared to other genes, the NA gene of A/Chicken/Nakorn-Pathom/Thailand/CU-K2/04 showed the closest relation to its ancestors, A/Goose/Guangdong/1//96 and A/Goose/Guangdong/3 /97.

Apart from the phylogenetic analysis of HA and NA, other viral internal genes potentially responsible for its pathogenicity, virulence and a potential mode of transmission among avian populations and from birds to humans, were also analyzed [51]. Based on the molecular evolution of 8 viral gene segments, all 7 segments of A/Chicken/Nakorn-Pathom/Thailand/CU-K2/04 designated PB2, PB1, PA, NP, NA M and NS had evolved more rapidly than HA (Figure 8-13). There was a limited number of nucleotide sequence changes in the HA molecule compared to other genes. However, HA only formed a cluster to viruses collected in 2003-2004. It may be newly derived from the unknown source of those of the previous years. This particular relatedness ought to be further elucidated.

On the other hand, the NS gene or the non-structural gene of A/Chicken/Nakorn-Pathom/Thailand/CU-K2/04 had the most pronounced changes in nucleotide sequences. Various nucleotides have abruptly modified into a unique direction (the deletion of 15 nucleotides or 5 amino acids). When examined closely, the NS gene was obviously separated into only 2 groups, one was a viral group of 1997 and the others were viruses of more recent years based on the deletion (viruses collected during the year 2000-2001). However, the relatedness of NS was more stabilized than that of other gene segments (Figure 14). Even so, the genes, NA and M1, of this appear to have evolved into a group related more closely to the 2000-2001 outbreak than that of 1997 (Figure 8 and 13). The NP gene of A/Chicken/Nakorn-Pathom/Thailand/CU-K2/04 was once again clustered within the same group of A/Duck/China/E319.2/03 and very distinct from other Hong Kong isolates of 1997 (Figure 12). Similarly, the phylogenetic relatedness of PA and M2 of A/Chicken/Nakorn-Pathom/Thailand/CU-K2/04 were phylogenetically related to A/Duck/China/E319.2/03 (Figure 11, 13) while its NA, NS, NP and M1, are on the adjoining node with both A/Duck/China/E319.2/03 and the highly pathogenic A/Human/Vietnam/1196/04. This result had suggested that A/Chicken/Nakorn-Pathom/Thailand/CU-K2/04 was clustered with the animal and human viruses of 2003-2004.

Hence, this is surmised to be the continuation of the bird flu epidemic of the year 2003-2004. The phylogenetic analysis results of the internal genes; PB2, PB1, PA, NS, NP and M of A/Chicken/Nakorn-Pathom/Thailand/CU-K2/04 were similar with respect to A/Duck/China/E319.2/03. Consequently, A/Chicken/Nakorn-Pathom/Thailand/CU-K2/04 is speculated to be a reassortant virus that recruited HA from the unknown source of avian viruses collected in 2004.

HA gene

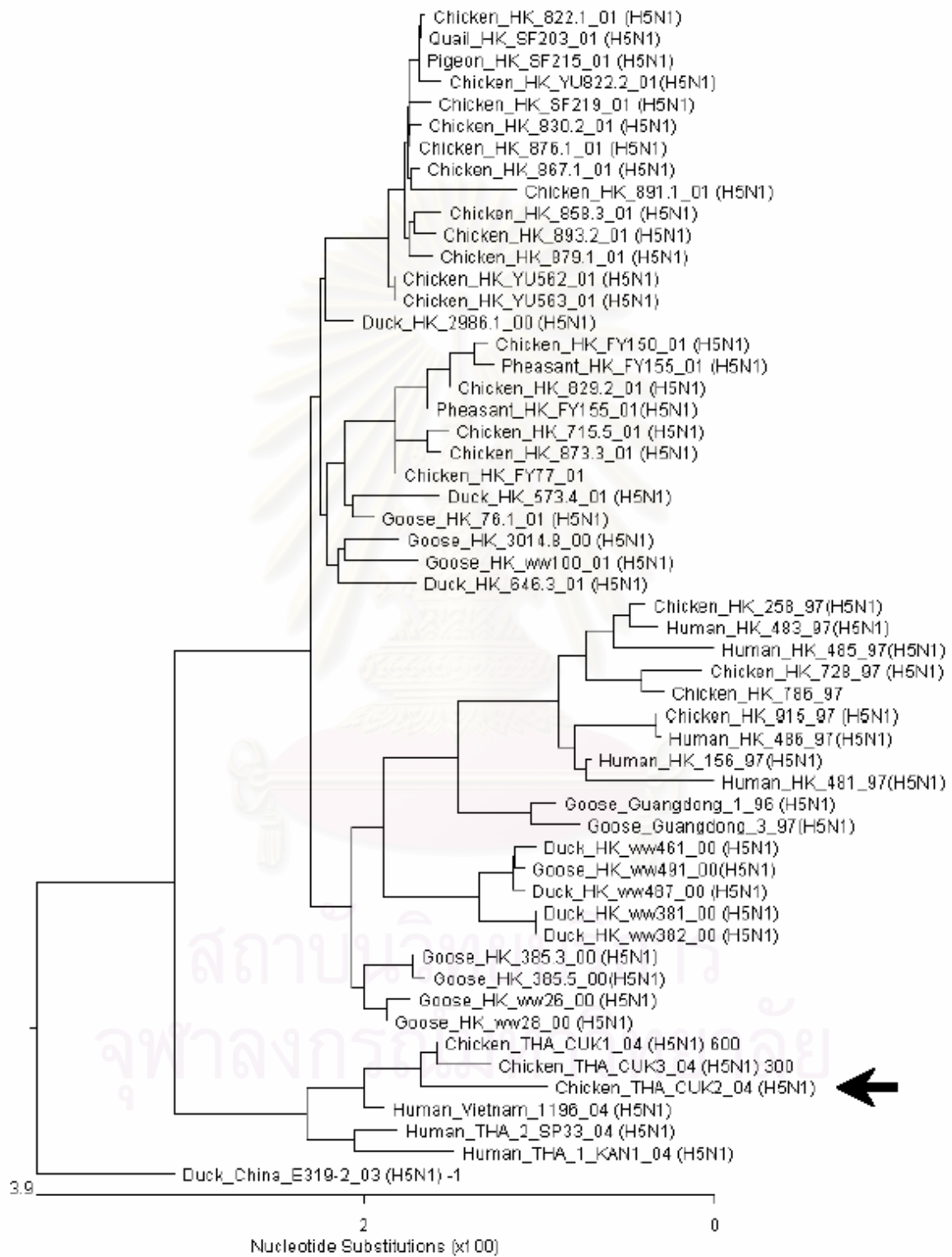


Figure 7 Phylogenetic tree of HA gene of A/Chicken/Nakorn-Pathom/Thailand/CU-K2/04.

NA gene

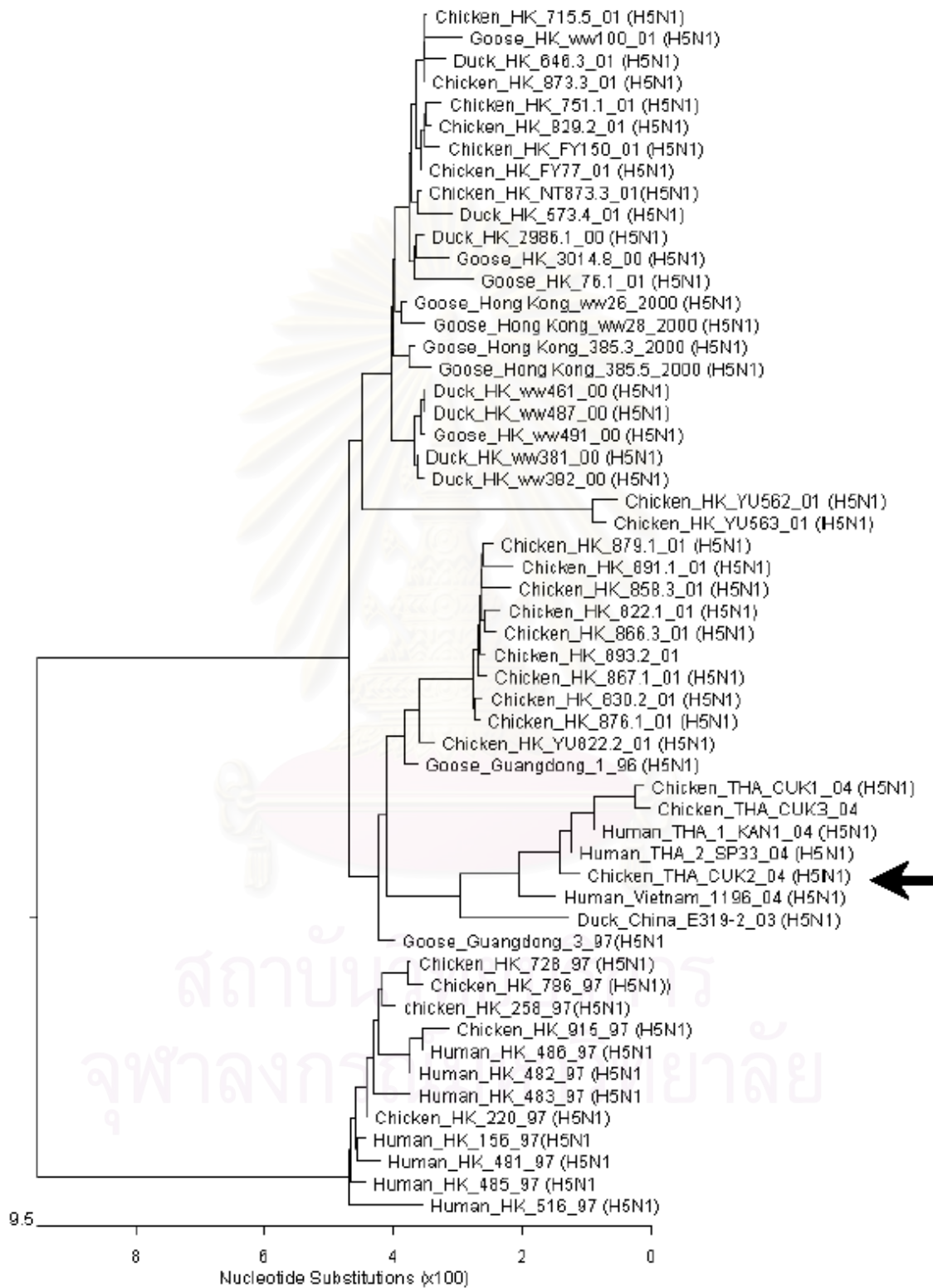


Figure 8 Phylogenetic tree of NA gene of A/Chicken/Nakorn-Pathom/Thailand/CU-K2/04.

PB2 gene

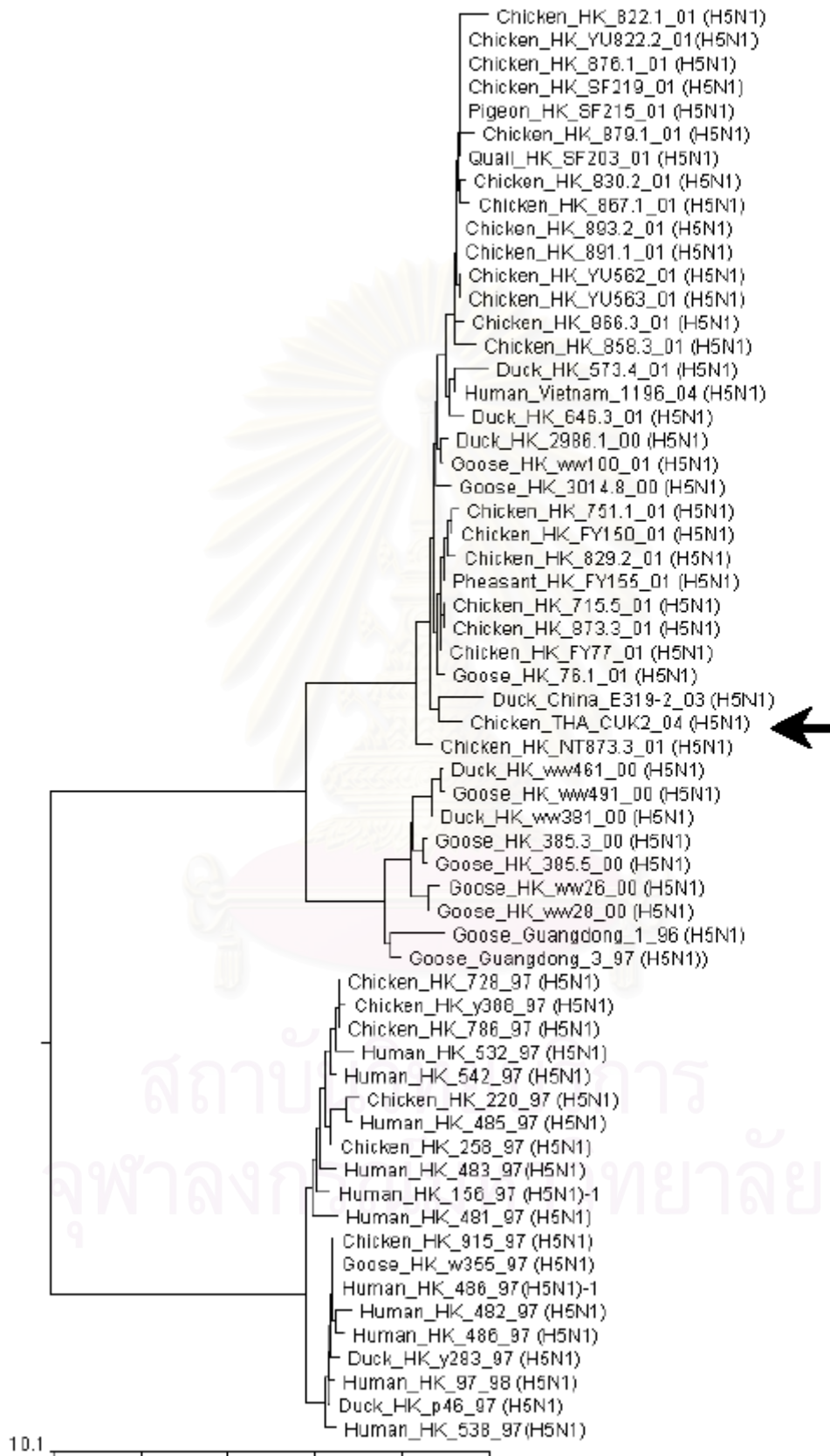


Figure 9 Phylogenetic tree of PB2 of A/Chicken/Nakorn-Pathom/Thailand/CU-K2/04.

PB1 gene

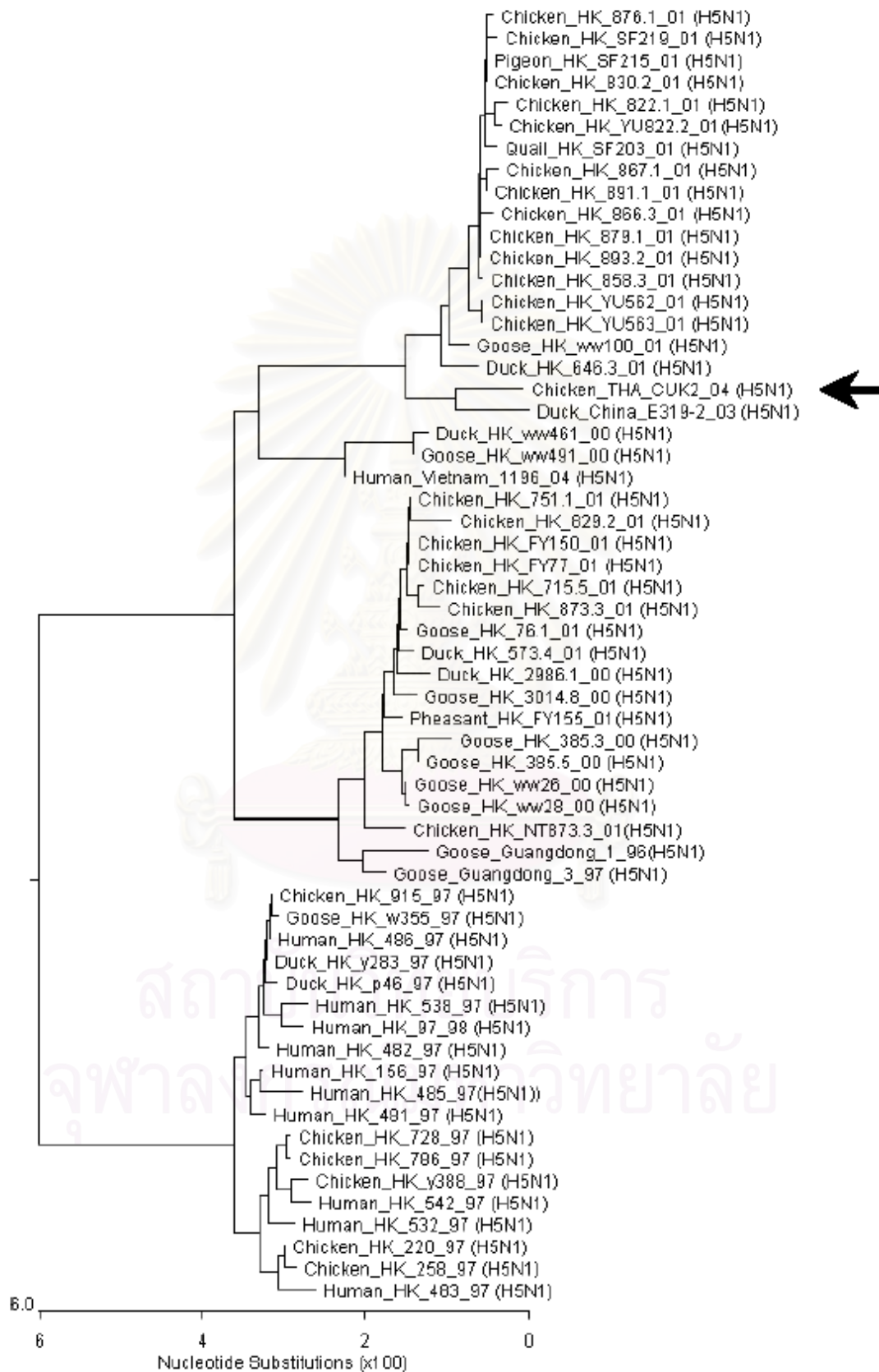


Figure 10 Phylogenetic tree of PB1 of A/Chicken/Nakorn-Pathom/Thailand/CU-K2/04.

PA gene

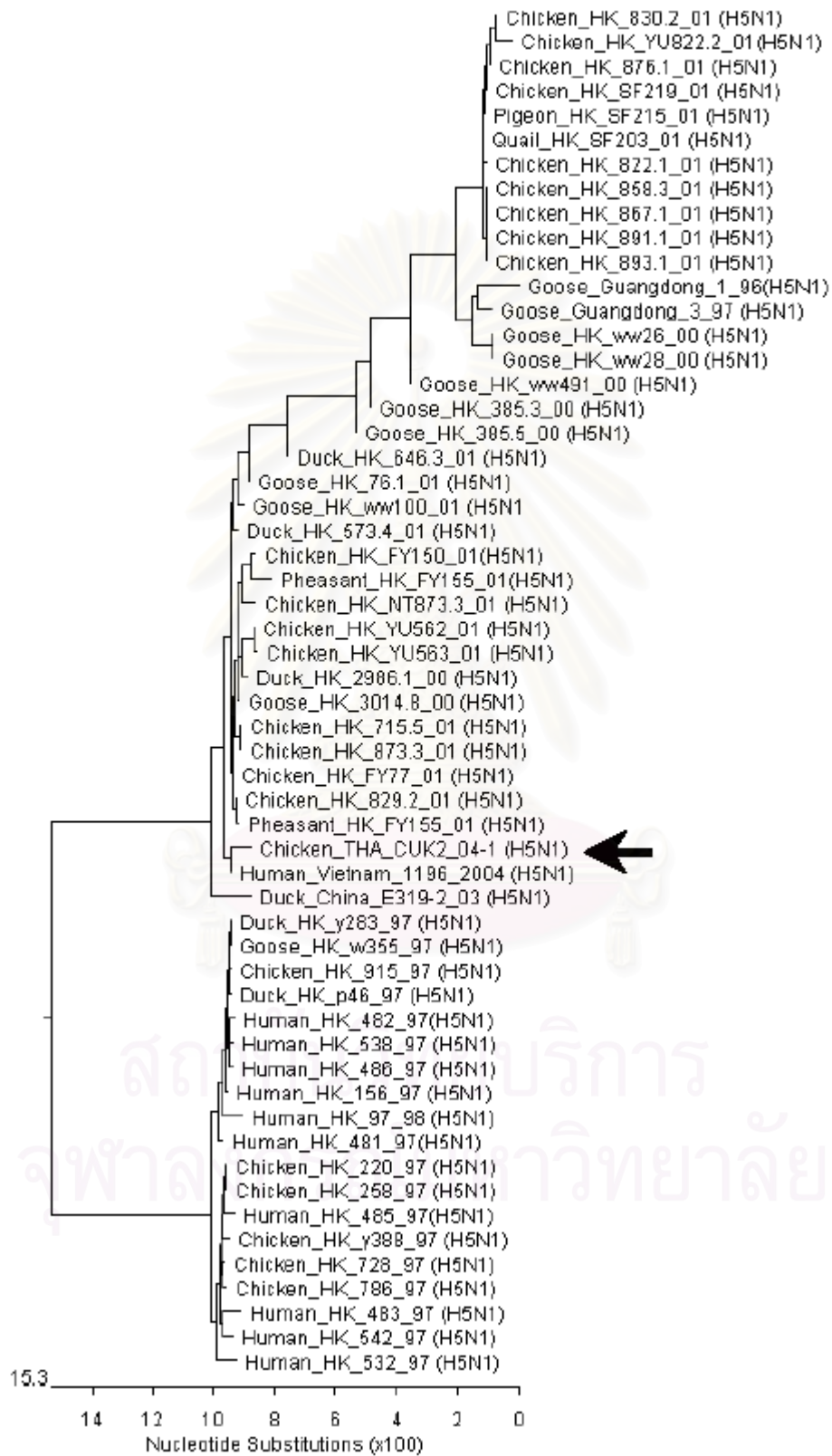


Figure 11 Phylogenetic tree of PA of A/Chicken/Nakorn-Pathom/Thailand/CU-K2/04.

NP gene

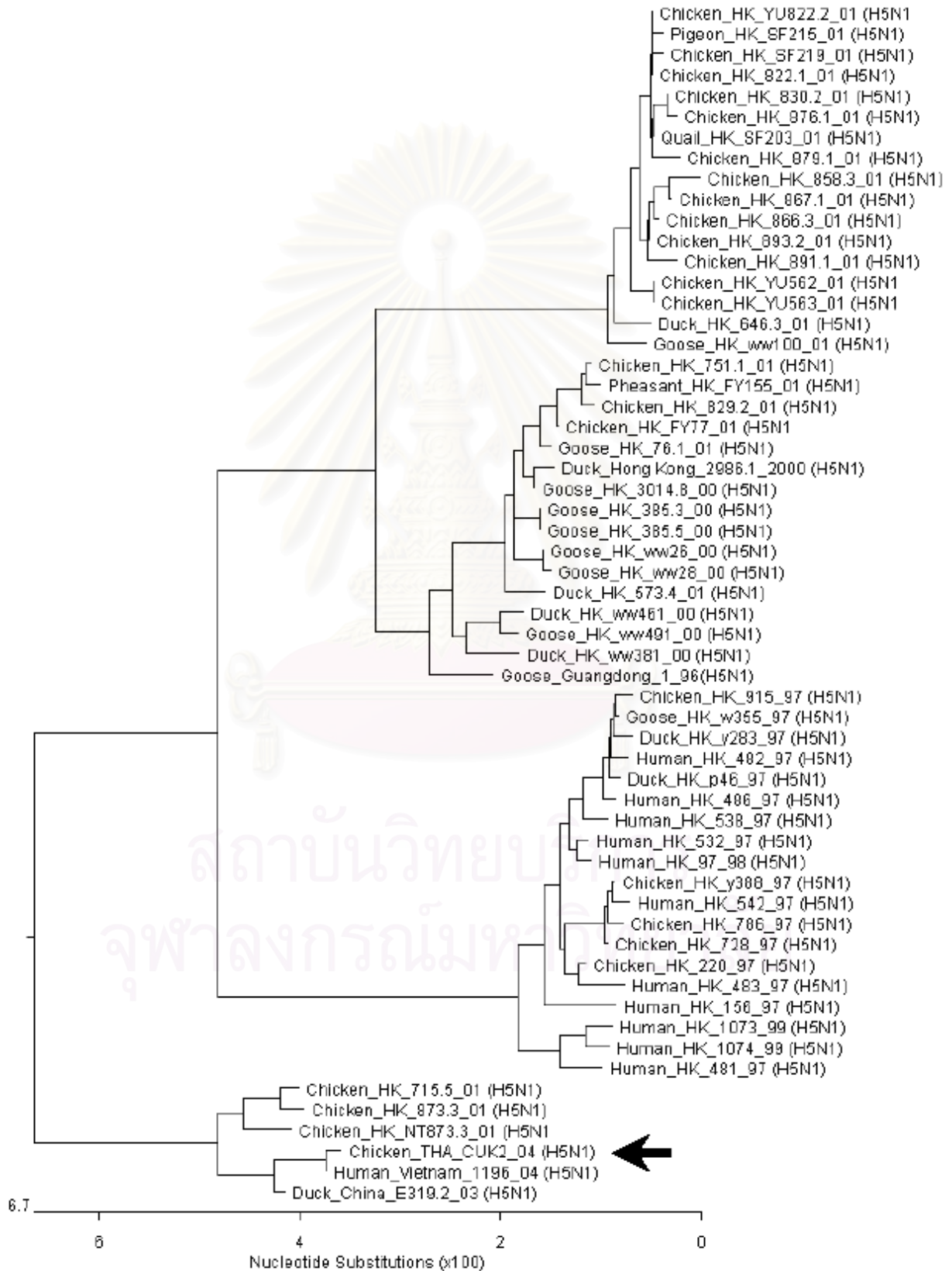


Figure12 Phylogenetic tree of NP of A/Chicken/Nakorn-Pathom/Thailand/CU-K2/04.

M gene

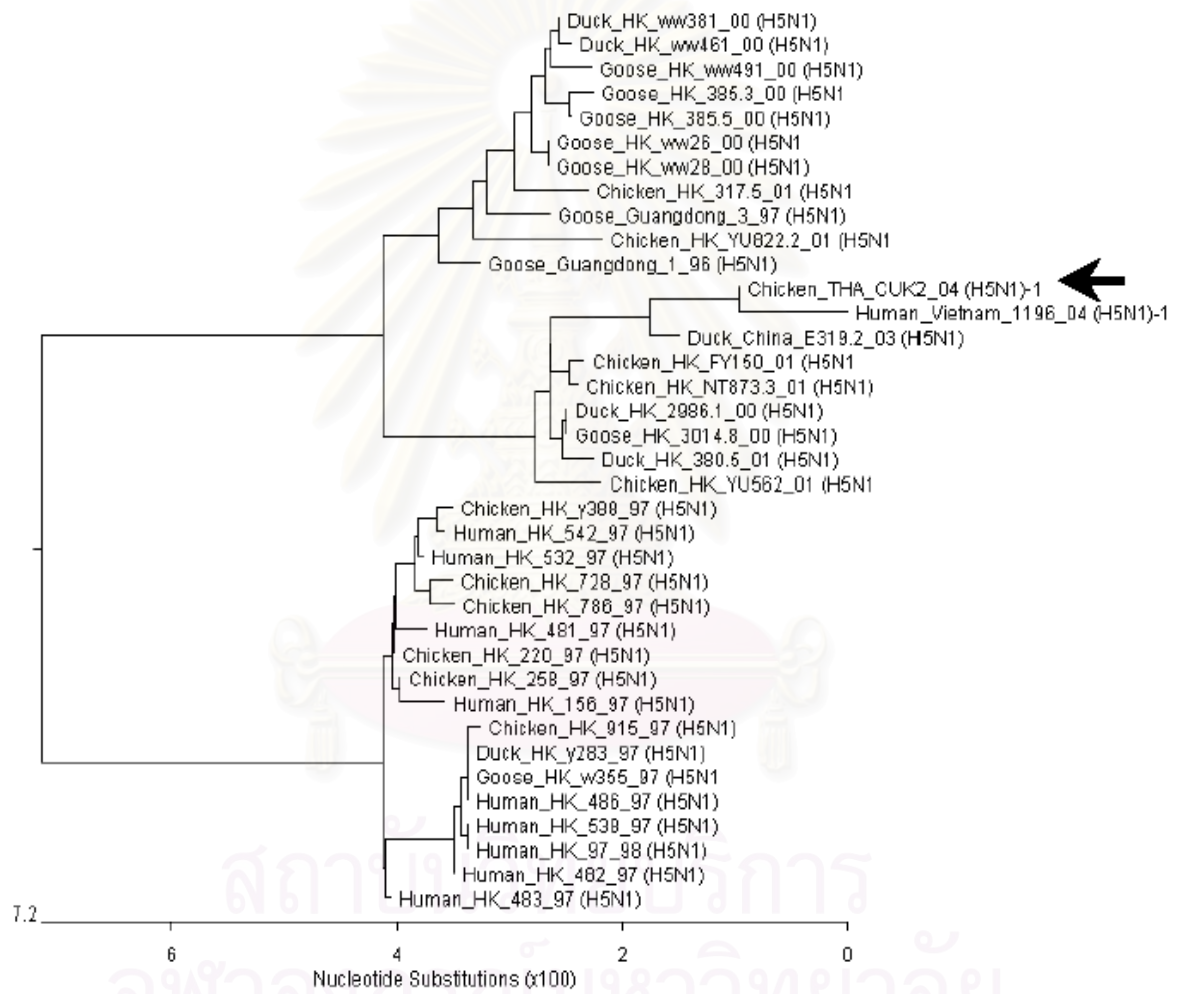


Figure13 Phylogenetic tree of M of A/Chicken/Nakorn-Pathom/Thailand/CU-K2/04.

NS gene

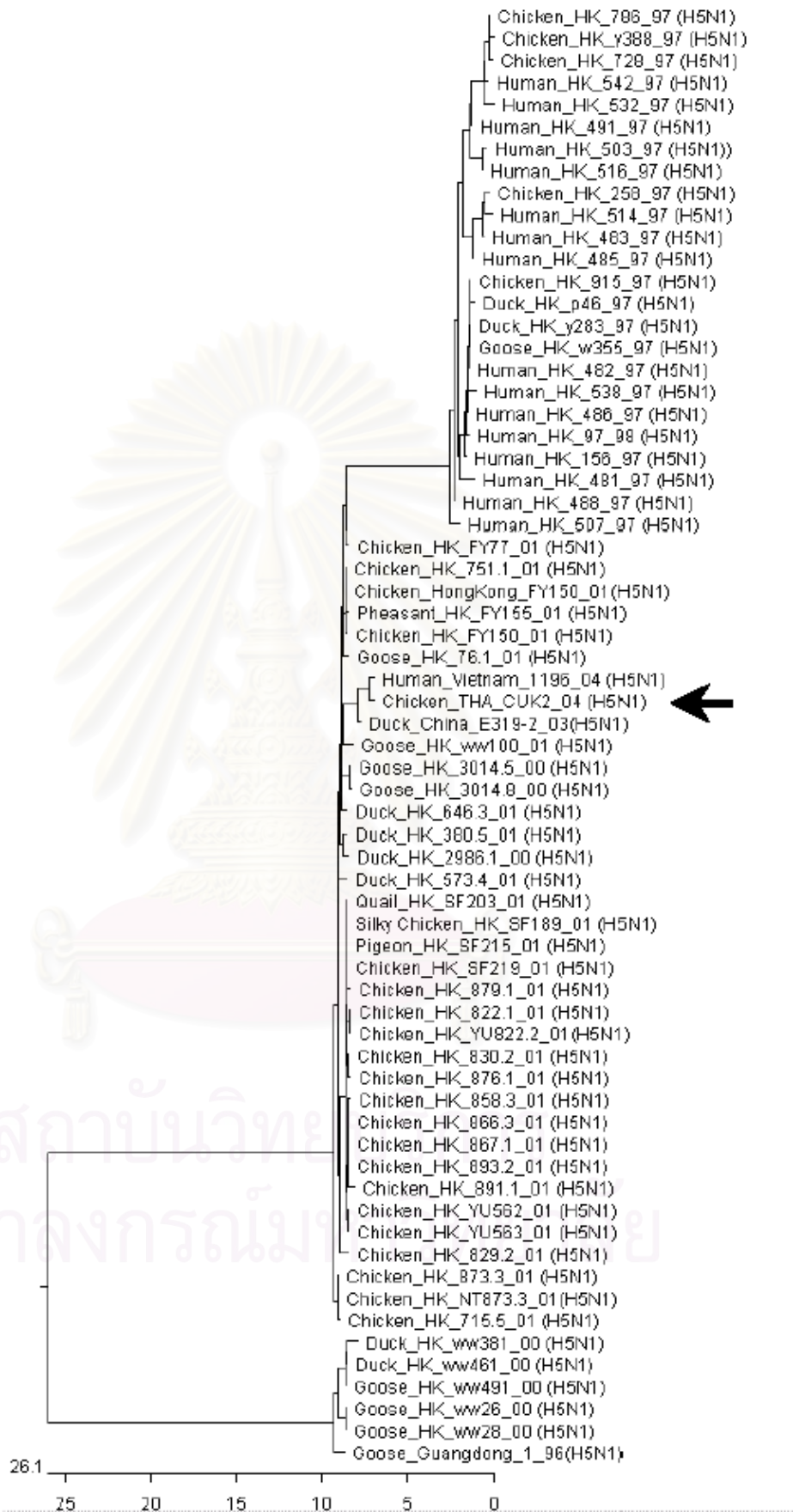


Figure14 Phylogenetic tree of NS of A/Chicken/Nakorn-Pathom/Thailand/CU-K2/04.

Characterization of deduced amino acid sequences

The important residues of deduced amino acids are summarized in Table 6. The deduced amino acid analysis of HA revealed the common HA cleavage site of A/Chicken/Nakorn-Pathom/Thailand/CU-K2/04. Its HA cleavage sites contain polybasic amino acid insertion “SPQREERRRKKR” similar to the published amino acid sequences responsible for the highly pathogenic characteristic (Figure 15). The cleavage site of HA associated with viral virulence as well as amino acid 627 of PB2 has been well documented [75].

Amino acid sequence analysis of neuraminidase (NA) had shown an exceptional finding with a 20-amino-acid deletion at the stalk region rather than one comprising 19-amino acid-deletion as known in previously highly pathogenic viruses. In contrast with the low pathogenic (LPAI) H5N1 viruses circulating in wild bird populations, there were no such deletions of the same epitope. The 19-amino-acid-deletion in the NA gene of A/Chicken/Hong Kong/258/97 was associated with the virus transmitted to humans [76]. Since our result suggested that although A/Chicken/Nakorn-Pathom/Thailand/CU-K2/04 lacked the 20 amino acids from the NA gene, it was still a highly pathogenic virus. The deletion of 20 amino acids from the NA gene had never been found in those viruses collected in the course of 1997-2000 (Figure 16). The association of this 20-amino-acid deletion to the viral pathogenesis should be further elucidated for other strains of avian influenza viruses.

There was a 5-amino-acid deletion in NS. As mentioned, we found 5 amino acids deleted from NS. (Figure17). This type of deletion had not been detected in viruses of previous outbreaks in 1997 and early 2000. But the later years, from 2000 to 2003, almost all viruses had such a deletion in the NS gene including A/Chicken/Nakorn-Pathom/Thailand/CU-K2/04. Interestingly, the virus of the same group was evolved based on the differences in these 5 amino acid residues “AIASS/V”. Furthermore, A/Chicken/Nakorn-Pathom/Thailand/CU-K2/04 and H5N1 of wild birds and ducks of 2000 and 2001 proved pathogenic to humans, but none of the reported H5N1 viruses isolated from human in 1997 display this 5-amino-acid deletion in the NS molecule.

Table 6 Amino acid sequences analysis of A/Chicken/Nakorn-Pathom/Thailand/CU-K2/04

Gene	Residues	Position	Characteristic
HA	Cleavage site	321-331	SPQRERRRKKR/G
	Receptor binding site	222	Q
		224	G
	N-link Glycosylation sites	154-156	NST
NA	Stalk region 20 amino acid deletion		Yes
	Oseltamivir resistance	274	H
M	Amantadine resistance	26	I
		27	V
		30	A
		31	N
NS	5 amino acid deletion	80-84	Yes
	Virulence determinant	92	D
		C-terminal	ESEV
PB2	Replication efficiency in mammals	627	E

HA gene cleavage site

	47 Sequences	40	350	360	3
96	Goose_Guangdong_1_96 (H5N1)	TGLRNT	PQRERRR	KKRGLF	GAIAGFIEGGW
96	Goose_Guangdong_3_97 (H5N1)	TGLRNT	PQRERRR	KKRGLF	GAIAGFIEGGW
	Chicken_HK_258_97 (H5N1)	TGLRNAP	PQRERRR	KKRGLF	GAIAGFIEGGW
97	Chicken_HK_728_97 (H5N1)	TGLRNT	PQRERRR	KKRGLF	GAIAGFIEGGW
	Chicken_HK_786_97 (H5N1)	TGLRNT	PQRERRR	KKRGLF	GAIAGFIEGGW
	Chicken_HK_915_97 (H5N1)	TGLRNT	PQRERRR	KKRGLF	GAIAGFIEGGW
	Human_HK_156_97 (H5N1)	TGLRNT	PQRERRR	KKRGLF	GAIAGFIEGGW
	Human_HK_481_97 (H5N1)	TGLRNT	PQRERRR	KKRGLF	GAIAGFIEGGW
00	Human_HK_483_97 (H5N1)	TGLRNAP	PQRERRR	KKRGLF	GAIAGFIEGGW
	Human_HK_485_97 (H5N1)	TGLRNT	PQRERRR	KKRGLF	GAIAGFIEGGW
	Human_HK_486_97 (H5N1)	TGLRNT	PQRERRR	KKRGLF	GAIAGFIEGGW
	Duck_HK_2986.1_00 (H5N1)	TGLRNT	PQRERRR	KKRGLF	GAIAGFIEGGW
	Duck_HK_ww381_00 (H5N1)	TGLRNT	PQRERRR	KKRGLF	GAIAGFIEGGW
	Duck_HK_ww382_00 (H5N1)	TGLRNT	PQRERRR	KKRGLF	GAIAGFIEGGW
	Duck_HK_ww461_00 (H5N1)	TGLRNT	PQGERRR	KKRGLF	GAIAGFIEGGW
	Duck_HK_ww487_00 (H5N1)	TGLRNT	PQGERRR	KKRGLF	GAIAGFIEGGW
	Goose_HK_3014.8_00 (H5N1)	TGLRNT	PQRERRR	KKRGLF	GAIAGFIEGGW
	Goose_HK_385.3_00 (H5N1)	TGLRNT	PQREGRR	KKRGLF	GAIAGFIEGGW
	Goose_HK_385.5_00 (H5N1)	TGLRNT	PQREGRR	KKRGLF	GAIAGFIEGGW
	Goose_HK_ww491_00 (H5N1)	TGLRNT	PQGERRR	KKRGLF	GAIAGFIEGGW
	Goose_HK_ww26_00 (H5N1)	TGLRNT	PQRERRR	KKRGLF	GAIAGFIEGGW
Goose_HK_ww28_00 (H5N1)	TGLRNT	PQRERRR	KKRGLF	GAIAGFIEGGW	
01	Chicken_HK_715.5_01 (H5N1)	TGLRNT	PQRERRR	KKRGLF	GAIAGFIEGGW
	Chicken_HK_822.1_01 (H5N1)	TGLRNT	PQRERRR	KKRGLF	GAIAGFIEGGW
	Chicken_HK_829.2_01 (H5N1)	TGLRNT	PQRERRR	KKRGLF	GAIAGFIEGGW
	Chicken_HK_830.2_01 (H5N1)	TGLRNT	PQRERRR	KKRGLF	GAIAGFIEGGW
	Chicken_HK_858.3_01 (H5N1)	TGLRNT	PQRERRR	KKRGLF	GAIAGFIEGGW
	Chicken_HK_867.1_01 (H5N1)	TGLRNT	PQRERRR	KKRGLF	GAIAGFIEGGW
	Chicken_HK_873.3_01 (H5N1)	TGLRNT	PQRERRR	KKRGLF	GAIAGFIEGGW
	Chicken_HK_876.1_01 (H5N1)	TGLRNT	PQRERRR	KKRGLF	GAIAGFIEGGW
	Chicken_HK_879.1_01 (H5N1)	TGLRNT	PQRERRR	KKRGLF	GAIAGFIEGGW
	Chicken_HK_891.1_01 (H5N1)	TGLTNT	PQRERRR	KKRGLF	GAIAGFIEGGW
	Chicken_HK_893.2_01 (H5N1)	TGLRNT	PQRERRR	KKRGLF	GAIAGFIEGGW
	Chicken_HK_FY150_01 (H5N1)	TGLRNT	PQRERRR	KKRGLF	GAIAGFIEGGW
	Chicken_HK_FY77_01 (H5N1)	TGLRNT	PQRERRR	KKRGLF	GAIAGFIEGGW
	Chicken_HK_SF219_01 (H5N1)	TGLRNT	PQRERRR	KKRGLF	GAIAGFIEGGW
	Chicken_HK_YU562_01 (H5N1)	TGLRNT	PQRERRR	KKRGLF	GAIAGFIEGGW
	Chicken_HK_YU563_01 (H5N1)	TGLRNT	PQRERRR	KKRGLF	GAIAGFIEGGW
	Chicken_HK_YU822.2_01 (H5N1)	TGLRNT	PQRERRR	KKRGLF	GAIAGFIEGGW
03-04	Duck_HK_573.4_01 (H5N1)	TGLRNT	PQRERR-	KKRGLF	GAIAGFIEGGW
	Duck_HK_646.3_01 (H5N1)	TGLRNT	PQRERRR	KKRGLF	GAIAGFIEGGW
	Goose_HK_76.1_01 (H5N1)	TGLRNT	PQRERRR	KKRGLF	GAIAGFIEGGW
	Goose_HK_ww100_01 (H5N1)	TGLRNT	PQRERRR	KKRGLF	GAIAGFIEGGW
	Duck_China_E319-2_03 (H5N1)	TGLRNS	PQRERR-	KRGLF	GAIAGFIEGGW
	Chicken_THA_CUK1_04 (H5N1)	TGLRNS	PQRERRR	KKRGLF	GAIAGFIEGGW
	Chicken_THA_CUK2_04 (H5N1)	TGLRNS	PQRERRR	KKRGLF	GAIAGFIEGGW
	Human_Vietnam_1196_04 (H5N1)	TGLRNS	PQRERRR	KKRGLF	GAIAGFIEGGW
	Human_THA_2_SP33_04 (H5N1)	TGLRNS	PQRERRR	KKRGLF	GAIAGFIEGGW
	Human_THA_1_KAN1_04 (H5N1)	TGLRNS	PQRERRR	KKRGLF	GAIAGFIEGGW

Figure 15 Alignments of deduced amino acid sequences of the HA cleavage site.

NA gene 20 amino acid deletion

55 Sequences		50	60	70	80	
96	Goose_Guangdong_1_96 (H5N1)	SHSIQTGNQHQAEPCNQSI	IITYENNTWVNQTYVNI	SNTN	NFL	
	Goose_Guangdong_3_97 (H5N1)	SHSIQTGNQHQAEPCNQSI	IITYENNTWVNQTYVNI	SNTN	NFL	
97	Chicken_HK_220_97 (H5N1)	SHIIQTWHPNQPEPCNQSI	-----	-----	----NFY	
	chicken_HK_258_97 (H5N1)	SHIIQTWHPNQPEPCNQSI	-----	-----	----NFY	
	Chicken_HK_728_97 (H5N1)	SHIIQAWHPNQPEPCNQSI	-----	-----	----NFY	
	Chicken_HK_786_97 (H5N1)	SHIIQAWHPNQPEPCNQSI	-----	-----	----NFY	
	Chicken_HK_915_97 (H5N1)	SHIIKTWHPNQPEPCNQSI	-----	-----	----NFY	
	Human_HK_156_97 (H5N1)	SHIIQTWHPNQPEPCNQSI	-----	-----	----NFY	
	Human_HK_481_97 (H5N1)	SHTIQTWHPNQPEPCNQSI	-----	-----	----NFY	
	Human_HK_482_97 (H5N1)	SHIIKTWHPNQPEPCNQSI	-----	-----	----NFY	
	Human_HK_483_97 (H5N1)	SHIIQTWHPNQPEPCNQSI	-----	-----	----NFY	
	Human_HK_485_97 (H5N1)	SHIIQTWHPNQPEPCNQSI	-----	-----	----NFY	
	Human_HK_486_97 (H5N1)	SHIIKTWHPNQPEPCNQSI	-----	-----	----NFY	
	Human_HK_516_97 (H5N1)	SHIIQTWHPNQPEPCNQSI	-----	-----	----NFY	
	00	Duck_HK_2986.1_00 (H5N1)	SHSIQTGNQHQAEPCNQSI	IITYENNTWVNQTYVNI	SNTN	NFL
		Duck_HK_ww381_00 (H5N1)	SHSIQTGNQHQAEPCNQSI	IITYENNTWVNQTYVNI	SNTN	NFL
		Duck_HK_ww382_00 (H5N1)	SHSIQTGNQHQAEPCNQSI	IITYENNTWVNQTYVNI	SNTN	NFL
		Duck_HK_ww461_00 (H5N1)	SHSIQTGNQHQAEPCNQSI	IITYENNTWVNQTYVNI	SNTN	NFL
Duck_HK_ww487_00 (H5N1)		SHSIQTGNQHQAEPCNQSI	IITYENNTWVNQTYVNI	SNTN	NFL	
Goose_HK_3014.8_00 (H5N1)		SHSIQTGNQHQAEPCNQSI	IITYENNTWVNQTYVNI	SNTN	NFL	
Goose_HK_385.3_00 (H5N1)		SHSIQTGNQHQAEPCNQSI	IITYENNTWVNQTYVNI	SNTN	NFL	
Goose_HK_385.5_00 (H5N1)		THSIQTGNQHQAEPCNQSI	IITYENNTWVNQTYVNI	SNTN	NFL	
Goose_HK_ww26_00 (H5N1)		SHSIQTGNQHQAEPCNQSI	IITYENNTWVNQTYVNI	SNTN	NFL	
Goose_HK_ww28_00 (H5N1)		SHSIQTGNQHQAEPCNQSI	IITYENNTWGNQTYVNI	SNTN	NLL	
Goose_HK_ww491_00 (H5N1)		SHSIQTGNQHQAEPCNQSI	IITYENNTWVNQTYVNI	SNTN	NFL	
01		Chicken_HK_715.5_01 (H5N1)	SHSIQTGNQHQAEPCNQSI	IITYENNTWVNQTYVNI	SNTN	NFL
	Chicken_HK_751.1_01 (H5N1)	SHSIQTGNQHQAEPCNQSI	IITYENNTWVNQTYVNI	SNTN	NLL	
	Chicken_HK_829.2_01 (H5N1)	SHSIQTGNQHQAEPCNQSI	IITYENNTWVNQTYVNI	SNTN	NLL	
	Chicken_HK_873.3_01 (H5N1)	SHSIQTGNQHQAEPCNQSI	IITYENNTWVNQTYVNI	SNTN	NFL	
	Chicken_HK_FY150_01 (H5N1)	SHSIQTGNQHQAEPCNQSI	IITYENNTWVNQTYVNI	SNTN	NLL	
	Chicken_HK_FY77_01 (H5N1)	SHSIQTGNQHQAEPCNQSI	IITYENNTWVNQTYVNI	SNTN	NFL	
	Chicken_HK_NT873.3_01 (H5N1)	SHSIQTGNQHQAEPCNQSI	IITYENNTWVNQTYVNI	SNTN	NFL	
	Chicken_HK_YU562_01 (H5N1)	SHSIQKMNQHQTEPCNQSI	IITYENNTWVNQTYVNI	SNTN	NFL	
	Chicken_HK_YU563_01 (H5N1)	SHSIQKMNQHQTEPCNQSI	IITYENNTWVNQTYVNI	SNTN	NFL	
	Chicken_HK_YU822.2_01 (H5N1)	SHSIQTGNQHQAEPCNQSI	IITYENNTWVNQTYVNI	SNTN	NFL	
	Chicken_HK_822.1_01 (H5N1)	SHSIQTGNQHQAEPCNQSI	-----	-----	----IGNTN	
	Chicken_HK_830.2_01 (H5N1)	SHSIQTGNQHQAEPCNQSI	-----	-----	----IGNTN	
	Chicken_HK_858.3_01 (H5N1)	SHSIQTGNQHQAEPCNQSI	-----	-----	----IGNTN	
	Chicken_HK_866.3_01 (H5N1)	SHSIQTGNQHQAEPCNQSI	-----	-----	----IGNTN	
	Chicken_HK_867.1_01 (H5N1)	SHSIQTGNQHQAEPCNQSI	-----	-----	----IGNTN	
	Chicken_HK_876.1_01 (H5N1)	SHSIQTGNQHQAEPCNQSI	-----	-----	----IGNTN	
Chicken_HK_879.1_01 (H5N1)	SHSIQTGNQHQAEPCNQSI	-----	-----	----IGNTN		
Chicken_HK_891.1_01 (H5N1)	SHSIQTGNQHQAEPCNQSI	-----	-----	----IGNTN		
Chicken_HK_893.2_01 (H5N1)	SHSIQTGNQHQAEPCNQSI	-----	-----	----IGNTN		
03-04	Duck_HK_573.4_01 (H5N1)	SHSIQIGNQHQAEPCNQSI	IITYENNTWVNQTYVNI	SNTN	NFL	
	Duck_HK_646.3_01 (H5N1)	SHSIQTGNQHQVPEPCNQSI	IITYENNTWVNQTYVNI	SNTN	NFL	
	Goose_HK_76.1_01 (H5N1)	SHSIQTGNQHQAEPCNQSI	IITYENNTWVNQTYVNI	SNTN	NFL	
	Goose_HK_ww100_01 (H5N1)	SHSIQTGNQHQAEPCNQSI	IITYENNTWVNQTYVNI	SNTN	NFL	
	Duck_China_E319-2_03 (H5N1)	SHSIQTRNQHQAEPCNQSI	-----	-----	----ISNTN	
	Chicken_THA_CUK1_04 (H5N1)	SHSIHTGNQHQAEPCNQSI	-----	-----	----ISNTN	
	Chicken_THA_CUK2_04 (H5N1)	SHSIHTGNQHQAEPCNQSI	-----	-----	----ISNTN	
	Chicken_THA_CUK3_04 (H5N1)	SHSIHTGNQHQAEPCNQSI	-----	-----	----ISNTN	
	Human_Vietnam_1196_04 (H5N1)	-----	-----	-----	-----	
	Human_THA_1_KAN1_04 (H5N1)	SHSIHTGNQHQAEPCNQSI	-----	-----	----ISNTN	
Human_THA_2_SP33_04 (H5N1)	SHSIHTGNQHQAEPCNQSI	-----	-----	----ISNTN		

Figure 16 Alignments of deduced amino acid sequences of the NA stalk region.

NS gene 5 amino acid deletion

		Consensus	NTLGLDIETATRAGKQIVERILEEESDEALKM----PAPRYLTDMTLE
		56 Sequences	60 70 80 90 100
96	}	Goose_Guangdong_1_96 (H5N1)	STLGLDLRVATMEGKKIVEDILKSETNENLKIASSPAPRYITDMSIE
		Chicken_HK_258_97 (H5N1)	STLGLDIRATATREGKHIVERILEEESDEALKMTIASVPAPRYLAEMTLE
		Chicken_HK_728_97 (H5N1)	STLGLDIRAATREGKHIVERILEEESDEALKMTIASVPAPRYLAEMTLE
		Chicken_HK_786_97 (H5N1)	STLGLDIRAATREGKHIVERILEEESDEALKMTIASVPAPRYLAEMTLE
		Chicken_HK_915_97 (H5N1)	STLGLDIRATATREGKHIVERILEEESDEALKMTIASVPAPRYLTEMPTLE
		Chicken_HK_y388_97 (H5N1)	STLGLDIRAATREGKHIVERILEEESDEALKMTIASVPAPRYLAEMTLE
		Duck_HK_p46_97 (H5N1)	STLGLDIRATATREGKHIVERILEEESDEALKMTIASVPAPRYLTEMPTLE
		Duck_HK_y283_97 (H5N1)	STLGLDIRATATREGKHIVERILEEESDEALKMTIASVPAPRYLTEMPTLE
		Goose_HK_w355_97 (H5N1)	STLGLDIRATATREGKHIVERILEEESDEALKMTIASVPAPRYLTEMPTLE
		Human_HK_156_97 (H5N1)	STLGLDIRATATREGKHIVERILEEESDEALKMTIASVPAPRYLTEMPTLE
97	}	Human_HK_481_97 (H5N1)	STLGLDIRATATREGKHIVERILEEESDEALKMTIASVPAPRYLTEMPTLE
		Human_HK_482_97 (H5N1)	STLGLDIRATATREGKHIVERILEEESDEALKMTIASVPAPRYLTEMPTLE
		Human_HK_483_97 (H5N1)	STLGLDIRATATREGKHIVERILEEESDEALKMTIASVPAPRYLAEMTLE
		Human_HK_485_97 (H5N1)	STLGLDIRATATREGKHIVERILEEESDEALKMTIASVPAPRYLAEMTLE
		Human_HK_486_97 (H5N1)	STLGLDIRATATREGKHIVERILEEESDEALKMTIASVPAPRYLTEMPTLE
		Human_HK_488_97 (H5N1)	STLGLDIRATATREGKHIVERILEEESDEALKMTIASVPAPRYLTEMPTLE
		Human_HK_491_97 (H5N1)	STLGLDIRAATREGKHIVERILEEESDEALKMTIASVPAPRYLTEMPTLE
		Human_HK_503_97 (H5N1)	NTLGLDIRAATREGKHIVERILEEESDEALKMTIASVPAPRYLTEMPTLE
		Human_HK_507_97 (H5N1)	STLGLDIRATATREGKHIVERILEEESDEALKMTIASVPAPRYLTEMPTLE
		Human_HK_514_97 (H5N1)	STLGLDIRATATREGKHIVERILEEESDEALKMTIASVPAPRYLAEMTLE
00	}	Duck_HK_ww381_00 (H5N1)	STLGLDLRVATMEGKKIVEDILKNETNENLKIASSPAPRYITDMSIE
		Duck_HK_ww461_00 (H5N1)	STLGLDLRVATMEGKKIVEDILKNETNENLKIASSPAPRYITDMSIE
		Duck_HK_2986.1_00 (H5N1)	NTLGLDIETATRAGKQIVERILEEESDEALKM----PAPRYLTDMTLE
		Goose_HK_ww26_00 (H5N1)	NTLGLDLRVATMEGKKIVEDILKSETNENLKIASSPAPRYITDMSIE
		Goose_HK_ww28_00 (H5N1)	NTLGLDLRVATMEGKKIVEDILKSETNENLKIASSPAPRYITDMSIE
		Goose_HK_ww491_00 (H5N1)	STLGLDLRVATMEGKKIVEDILKNETNENLKIASSPAPRYITDMSIE
		Goose_HK_3014.5_00 (H5N1)	NTLGLDIETATRAGKQIVERILEEESDEALKM----PAPRYLTDMTLE
		Goose_HK_3014.8_00 (H5N1)	NTLGLDIETATRAGKQIVERILEEESDEALKM----PAPRYLTDMTLE
		Chicken_HK_715.5_01 (H5N1)	NTLGLDIETATRAGKQIVERILEEESDEALKM----PAPRYLTDMTLE
		Chicken_HK_751.1_01 (H5N1)	NTLGLDIETATCAGKQIVERILEEESDEALKM----PAPRYLTDMTLE
01	}	Chicken_HK_822.1_01 (H5N1)	NTLGLDIETATRAGKQIVERILEEESDEALKM----PAPRYLTDMTLE
		Chicken_HK_829.2_01 (H5N1)	NTLGLDIETATCAGKQIVERILEEESDEALKM----PAPRYLTDMTLE
		Chicken_HK_830.2_01 (H5N1)	NTLGLDIETATRAGKQIVERILEEESDEALKM----PAPRYLTDMTLE
		Chicken_HK_858.3_01 (H5N1)	NTLGLDIETATRAGKQIVERILEEESDEALKM----PAPRYLTDMTLE
		Chicken_HK_866.3_01 (H5N1)	NTLGLDIETATRAGKQIVERILEEESDEALKM----PAPRYLTDMTLE
		Chicken_HK_867.1_01 (H5N1)	NTLGLDIETATRAGKQIVERILEEESDEALKM----PAPRYLTDMTLE
		Chicken_HK_873.3_01 (H5N1)	NTLGLDIETATRAGKQIVERILEEESDEALKM----PAPRYLTDMTLE
		Chicken_HK_876.1_01 (H5N1)	NTLGLDIETATRAGKQIVERILEEESDEALKM----PAPRYLTDMTLE
		Chicken_HK_879.1_01 (H5N1)	NTLGLDIEPATRAGKQIVERILEEESDEALKM----PAPRYLTDMTLE
		Chicken_HK_891.1_01 (H5N1)	NTLGLDIETATRAGKQIVERILEEESDEALKM----PAPRYLTDMTLE
03-04	}	Chicken_HK_893.2_01 (H5N1)	NTLGLDIETATRAGKQIVERILEEESDEALKM----PAPRYLTDMTLE
		Chicken_HK_8F219_01 (H5N1)	NTLGLDIETATRAGKQIVERILEEESDEALKM----PAPRYLTDMTLE
		Chicken_HK_YU562_01 (H5N1)	NTLGLDIETATRAGKQIVERILEEESDEALKM----PAPRYLTDMTLE
		Chicken_HK_YU563_01 (H5N1)	NTLGLDIETATRAGKQIVERILEEESDEALKM----PAPRYLTDMTLE
		Chicken_HK_YU822.2_01 (H5N1)	NTLGLDIETATRAGKQIVERILEEESDEALKM----PAPRYLTDMTLE
		Pheasant_HK_FY155_01 (H5N1)	NTLGLDIETATCAGKQIVERILEEESDEALKM----PAPRYLTDMTLE
		Pigeon_HK_SF215_01 (H5N1)	NTLGLDIETATRAGKQIVERILEEESDEALKM----PAPRYLTDMTLE
		Quail_HK_SF203_01 (H5N1)	NTLGLDIETATRAGKQIVERILEEESDEALKM----PAPRYLTDMTLE
		Duck_HK_380.5_01 (H5N1)	NTLGLDIETATRAGKQIVERILEEESDEALKV----PAPRYLTDMTLE
		Duck_HK_573.4_01 (H5N1)	NTLGLDIETATRAGKQIVERILEEESDEALKM----PAPRYLTDMTLE
03-04	}	Duck_HK_646.3_01 (H5N1)	NTLGLDIETATRAGKQIVERILEEESDEALKM----PAPRYLTDMTLE
		Goose_HK_76.1_01 (H5N1)	NTLGLDIETATRAGKQIVERILEEESDEALKM----PAPRYLTDMTLE
		Goose_HK_ww100_01 (H5N1)	NTLGLDIETATRAGKQIVERILEEESDEALKM----PAPRYLTDMTLE
		Duck_China_B319-2_03 (H5N1)	NTLGLDIETATRAGKQIVERILEEESDEALKV----PAPRYLTDMTLE
		Human_Vietnam_1196_04 (H5N1)	NTLGLDIETATRAGKQIVERILEEESDKALKM----PAPRYLTDMTLE
		Chicken_THA_CUK2_04 (H5N1)	NTLGLDIETATRAGKQIVERILEEESDKALKM----PAPRYLTDMTLE

Figure 17 Alignments of deduced amino acid sequence of NS.

In summary, the whole genome sequencing of the *A/Chicken/Nakorn-Pathom/Thailand/CU-K2/04* and its genetic sequence analysis has been presented in this study. The sequences obtained from this study were submitted into the GenBank database (assigned accession numbers as PB2: AY590581, PB1: AY590582, PA: AY551934, HA: AY590568, NP: AY590579, NA: AY590567, M: AY590578 and NS: AY590580). The HA and NA genes of this virus are similar to those isolated from the outbreak in humans in Vietnam and in Thailand 2004, whereas the internal genes are similar to viruses found in the aquatic and terrestrial birds in recent years particularly *A/Duck/China/E319.2/2003*. The entire nucleotide sequences of these viruses are dissimilar to *A/Chicken/HKG/97* or the ancestor, *A/Goose/Guangdong/96-97*, except some unique amino acid residues and the relation found in NA. Instead, *A/Chicken/Nakorn-Pathom/Thailand/CU-K2/04* is more closely related to viruses from the outbreaks of 2000-2001 than the truncated lineage viruses of the year 1997.



สถาบันวิทยบริการ
จุฬาลงกรณ์มหาวิทยาลัย

Molecular diagnosis for H5N1 avian influenza A viruses detection

According to the early 2004 outbreak of H5N1 avian influenza A virus in Thailand, there is a requirement for sensitive and rapid diagnostic techniques to verify the clinical diagnosis of H5N1 influenza A virus and improve the quality of surveillance systems. After the whole genome characterization of H5N1 influenza A virus, the nucleotide sequences of Matrix (M), Hemagglutinin (H5) and Neuraminidase (N1) genes of A/Chicken/Nakorn-Pathom/Thailand/CU-K2/04 were exclusively analyzed and then multiple aligned with H5N1 and other subtypes of influenza A viral nucleotide sequences obtained from the GenBank database in order to select the primers and probes used in molecular diagnosis of H5N1 influenza A viruses.

Single step multiplex RT-PCR for H5N1 influenza A virus detection

The aim of this study was to develop a rapid, cost-saving and effective method based on single step multiplex RT-PCR for influenza A virus subtype H5N1 detection. The term multiplex PCR refers to the inclusion of more than one primer set in an amplification reaction, to detect the presence of more than one gene or genome segment in a single pathogen, or in more than one pathogen [77]. The primers used in the multiplex PCR reaction should have the same T_m and following the general guidelines for primer designation (Appendix A). Moreover, the amplified DNA fragments should be clearly separated by agarose gel electrophoresis.

Using the nucleotide sequences of A/Chicken/Nakorn-Pathom/Thailand/CU-K2/04 and nucleotide sequences available in the GenBank database, multiple sequence alignments of the H5, N1 and M genes were performed using the CLUSTAL X program (version 1.8). M primers were selected from conserved regions of over 50 known sequences corresponding to different subtypes of influenza A virus while H5 and N1 primers were designed from invariant regions of over 30 known sequences specific for influenza A virus subtype H5 and N1. The primers were chosen and analyzed using the OLIGO primer design software (version 9.1) to ensure that they could be combined in a multiplex format under the same PCR condition. The selected primer set will be used in single-step RT-PCR for simultaneous detection in multiplex format corresponding to sequences specific for M, H5 and N1.

- Selection of candidate multiplex primer sets

Several primer corresponding to M, H5 and N1 were designed and synthesized for combining in multiplex format. Each multiplex primer system consists of each pair of primer specific for M, H5 and N1 yielding different PCR product sizes which should be clearly separated by agarose gel electrophoresis. Totally, 12 systems of the multiplex primer set were selected and tested for the efficiency of amplification in multiplex format. Primer compositions in each multiplex system were summarized in Table 7 whereas the positions of each primer were illustrated in Figure 18.

Figure 19 showed the amplification of multiplex RT-PCR obtained from 12 multiplex primer sets by using RNA of A/Chicken/Nakorn-Pathom/Thailand/CU-K2/04 as a template. The result of agarose gel electrophoresis revealed that multiplex system 5, 7 and 12 yielded favorable 3 discrete bands corresponding to M, H5 and N1 which clearly separated in 2% agarose gel (Figure 19). After that these 3 systems (5, 7 and 12) were subjected to test for their specificity with H5N1 and other subtypes of influenza A viruses. We found that the Matrix primers used in system 5 and 7 failed to amplify the matrix gene of some subtypes of influenza A viruses such as H3N2, H7N7 and H9N2. Only the system-12 provided favorable result, therefore this system was further optimized to use in multiplex RT-PCR for H5N1 influenza A virus detection.

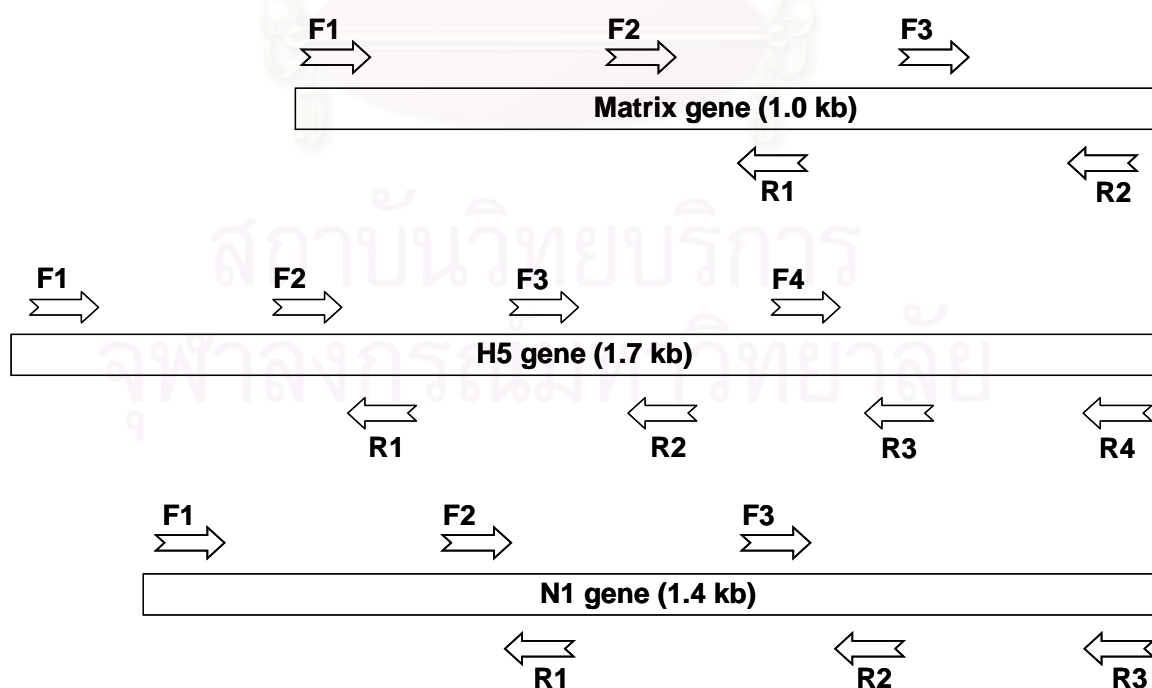


Figure 18 Schematic maps of candidate primers used in multiplex RT-PCR

Table 7 Primers compositions in each multiplex RT-PCR systems

System	M	H5	N1
1	F2/R1 (180 bp)	F3/R4 (817 bp)	F3/R3 (370 bp)
2	F2/R2 (480 bp)	F2/R2 (836 bp)	F2/R2 (627 bp)
3	F1/R1 (680 bp)	F4/R4 (327 bp)	F2/R3 (890 bp)
4	F2/R1 (180 bp)	F3/R2 (351 bp)	F2/R2 (627 bp)
5	F2/R2 (480 bp)	F3/R2 (351 bp)	F2/R2 (627 bp)
6	F2/R1 (180 bp)	F4/R4 (327 bp)	F2/R2 (627 bp)
7	F2/R2 (480 bp)	F4/R4 (327 bp)	F2/R2 (627 bp)
8	F2/R2 (480 bp)	F3/R3 (679 bp)	F2/R3 (890 bp)
9	F2/R1 (180 bp)	F3/R3 (679 bp)	F3/R3 (370 bp)
10	F2/R1 (180 bp)	F3/R2 (351 bp)	F2/R1 (131 bp)
11	F3/R2 (276 bp)	F3/R2 (351 bp)	F2/R2 (627 bp)
12	F3/R2 (276 bp)	F4/R3 (189 bp)	F2/R1 (131 bp)

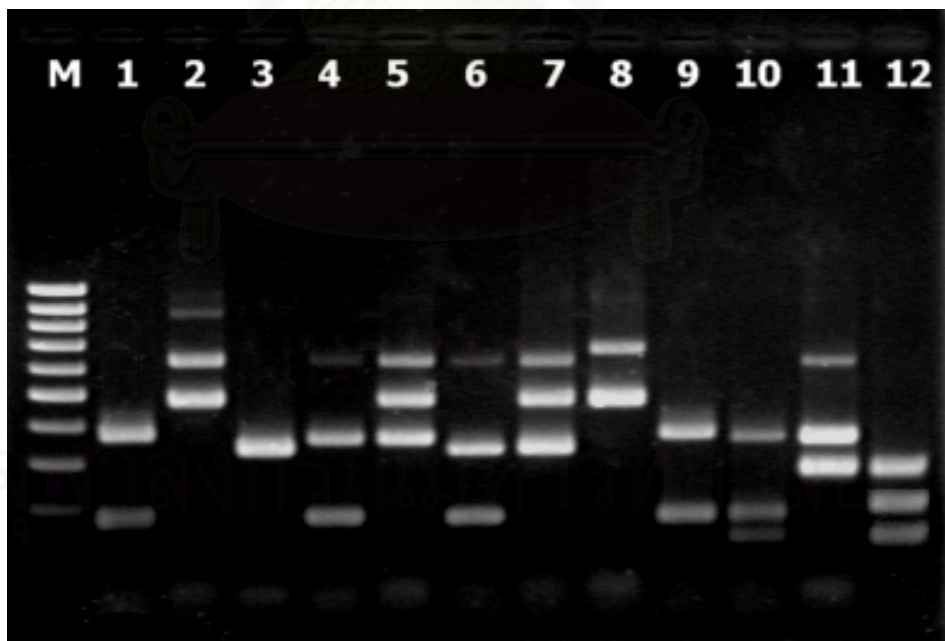


Figure 19 Band patterns of PCR products amplified by 12 systems of multiplex RT-PCR.

- Construction of positive controls

The genes of influenza A virus (A/chicken/Nakorn-Patom/Thailand/CU-K2/2004 (H5N1)) were used to construct plasmid DNAs by inserting the H5 (nt 898-1715), N1 (nt 539-1431) and M (nt 510-990) genes into the pGEM-T Easy Vector (Promega). *In vitro* transcription was performed by using RiboMAX™ Large Scale RNA Production System-T7 (Promega) following the manufacturer's recommendations (Chapter III). Then the *in vitro* transcribed RNA of M, H5 and N1 were used as a positive control for optimization of multiplex RT-PCR (Figure 20). The concentration of the *in vitro* transcribed RNAs was calculated by measuring absorbance at 260 nm. The RNAs were then serially diluted ten fold, ranging from 10^8 -10 copies/ μ L to perform sensitivity tests.

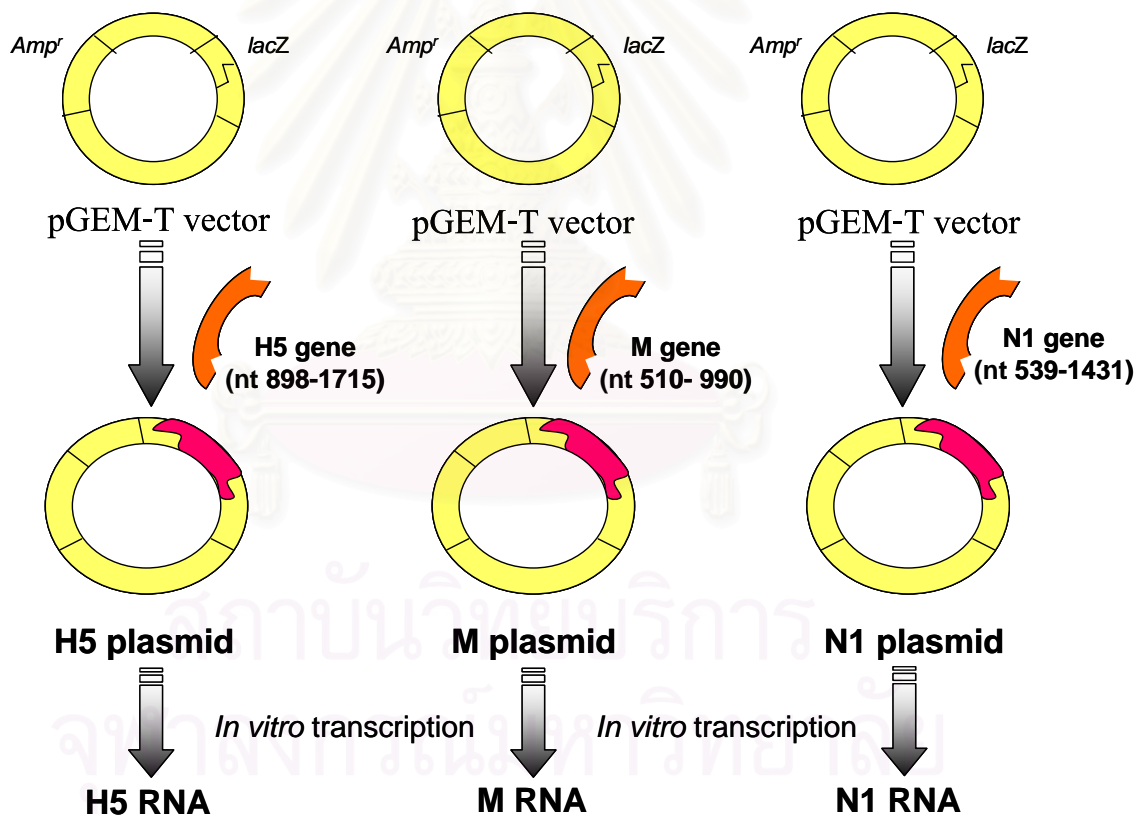


Figure 20 Schematic diagrams represent the construction of positive controls for Matrix (M), Hemagglutinin (H5) and Neuraminidase (N1) genes.

- **Optimization of the multiplex RT-PCR conditions**

For maximum efficiency of amplification in multiplex RT-PCR system 12, several factors including each primer concentration (0.25-0.75 μ M), additional Mg²⁺ concentration (ranging from 0.5 – 3.0 μ M) and thermocycling condition (annealing at 53, 55, 58 or 60°C) were subjected to be optimized by using *in vitro* transcribed RNA as a positive control.

According to the result of optimization (data not shown), Multiplex RT-PCR was performed in a single-step reaction using the AccessQuick RT-PCR System (Promega). Sets of primers specific for the H5, N1 and M genes of influenza A virus subtype H5N1 (Table 8) were used at a final concentration of 0.5 μ M each. A combination of 5.0 μ L of RNA sample with a reaction mixture containing 12.5 μ L of AccessQuick Master Mix, 5 U of RNase inhibitor, 5 U of AMV Reverse Transcriptase, 1.0 mM additional MgCl₂ and RNase-free water was used in a final volume of 25 μ L. One-step multiplex RT-PCR was carried out in a Mastercycler personal (Eppendorf). Cycling conditions included a reverse transcription step at 48°C for 45 minutes. After an initial denaturation step at 95°C for 2 minutes in order to activate the *Tfl* DNA polymerase, amplification was performed during 40 cycles including denaturation (94°C for 30 seconds), annealing (55°C for 30 seconds) and extension (72°C for 30 seconds), followed by final extension at 72°C for 10 minutes. Then, a total of 10 μ L of PCR product was added to loading buffer and run on a 2% agarose gel at 100 Volts for 60 minutes. After electrophoresis the DNA bands were stained with ethidium bromide and visualized by UV transillumination.

- **Interpretation of the band pattern from multiplex RT-PCR.**

The oligonucleotide primer sets summarized in Table 8 were selected for amplification in multiplex format of the 276-, 189- and 131-bp PCR products, corresponding to the influenza A virus M, H5 and N1 genes, respectively. A band pattern of 276, 189 and 131 bp obtained from multiplex RT-PCR can be interpreted as influenza A virus subtype H5N1, whereas other subtypes of influenza A virus will only yield a 276-bp band of the matrix gene. (Figure 21)

Table 8 Multiplex RT-PCR primers set for H5N1 influenza A virus detection

Target gene	Oligo name	Primer sequence	Amplicon length (bp)
M	CU-MF ₇₁₈	5' -TGATCTTCTTGAAAATTTGCAG-3'	276
	CU-MR ₉₉₃	5' -TGTTGACAAAATGACCATCG-3'	
H5	CU-H5F ₁₄₀₀	5' -GACTCAAATGTCAAGAACCTTTA-3'	189
	CU-H5R ₁₅₉₀	5' -CCACTTATTTCTCTCTKTTTA-3'	
N1	CU-N1F ₅₃₉	5' -GTTTGAGTCTGTTGCTTGGTC-3'	131
	CU-N1R ₆₄₆	5' -TGATAGTGTCTGTTATTATGCC-3'	

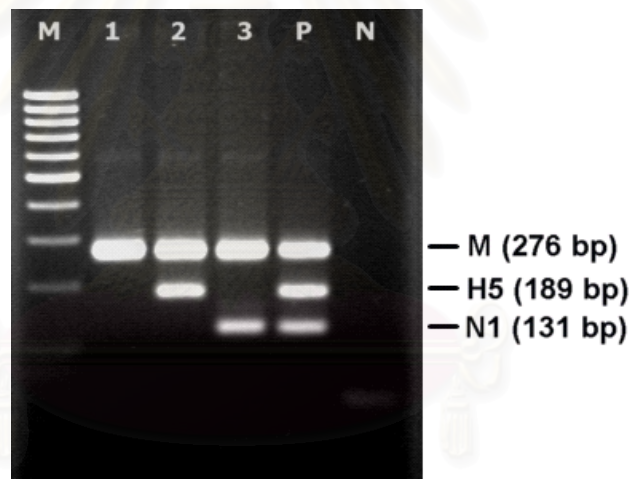


Figure 21 Interpretation of influenza A virus in a panel of clinical isolates using single step multiplex RT-PCR. Lane M:100-bp ladder. Lane 1: influenza A virus (non-H5N1). Lane 2: influenza A virus (H5). Lane 3: influenza A virus (N1). Lane P: positive control of influenza A virus (H5N1). Lane N: Negative control.

- **Specificity test of multiplex RT-PCR**

The specificity of this assay was evaluated by cross-reaction tests showing no cross-reactivity to total human genomic DNA or Respiratory Syncytial Virus (RSV), types A and B (data not shown). Moreover, H3N2, H7N7 and H9N2 subtypes yield only a 276 bp band of matrix gene. An inactivated influenza A/Fujian/411/2002 (H3N2) was provided by the Department of Microbiology, Faculty of Medicine Siriraj Hospital, Mahidol University Bangkok, Thailand. The cDNAs of avian influenza A/chicken/Netherland/1/03 (H7N7) and influenza A/turkey/Wisconsin/66 (H9N2) were provided by the Department of Virology, Erasmus Medical Centre, Rotterdam, The Netherlands. This indicated absence of cross-reactivity to other subtypes of influenza A virus. The results show that this assay can be applied to specifically detect both avian influenza A virus and human influenza A virus subtype H5N1. No significant false positive or non-specific bands were observed in any of the samples tested (Figure 22).

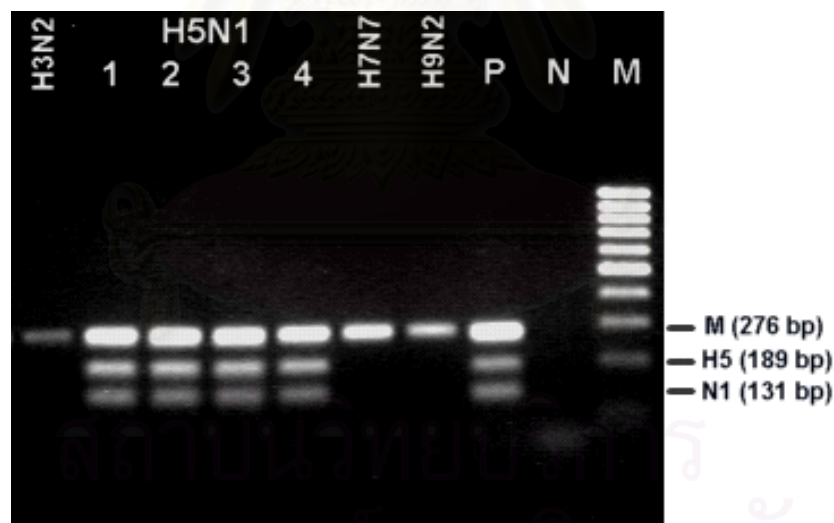


Figure 22 Specificity test of influenza A virus subtype H5N1 detected by multiplex RT-PCR from avian and human specimens. Control subtypes of H3N2, H7N7 and H9N2 were as indicated on top of the lanes. Lane 1: influenza A/chicken (H5N1), Lane 2: influenza A/duck (H5N1), Lane 3: influenza A/crow (H5N1), Lane 4: human influenza A virus (H5N1). Lane P: positive control, Lane N: Negative control and Lane M: 100-bp ladder.

- **Clinical sample test of multiplex RT-PCR**

Twenty eight influenza A virus subtype H5N1 specimens used to test in this study were collected during the 2004 outbreak in Thailand, comprising 17 samples of chicken, 2 each from duck and crow, the others from ostrich, open bill, quail, Kalij pheasant, Indian roller, tiger and leopard. All avian and tiger specimens were isolated by the virology unit, Faculty of Veterinary Science, Chulalongkorn University, Bangkok, Thailand. Three RNA samples of human influenza A virus subtype H5N1 were also collected during the 2004 outbreak in Thailand. All 3 human H5N1 influenza viral RNAs were provided by the Department of Medical Sciences (DMSc) Ministry of Public Health, Nonthaburi, Thailand.

All of H5N1 influenza specimens can be efficiently detected by the multiplex RT-PCR (Figure 23). All positive specimens were subjected to nucleotide sequencing and BLAST search for confirmation of the H5N1 subtype detection. Some sequences obtained in this study have been submitted to GenBank database and assigned accession numbers (Chapter III).



Figure 23 Representative results of H5N1 multiplex RT-PCR tested with several clinical specimens. Lane M: 100-bp ladder, lane 1: chicken isolate, lane 2: duck isolate, lane 3: crow isolate, lane 4: ostrich isolate, lane 5: open bill isolate, lane 6: quail isolate, lane 7: kali pheasant isolate, lane 8: Indian roller isolate, lane 9: tiger isolate, lane 10: human isolate, lane +: positive control and lane -: negative control.

- Sensitivity test of multiplex RT-PCR

The sensitivity of the multiplex PCR assay was evaluated by 10-fold serial dilution of the standard *in vitro* transcribed RNAs of M, H5 and N1. As expected, intensities of DNA bands decreased with increased dilution of the RNA standards. The DNA bands were visible at RNA standard dilutions as low as 10^3 copies/ μ L (Figure 24).

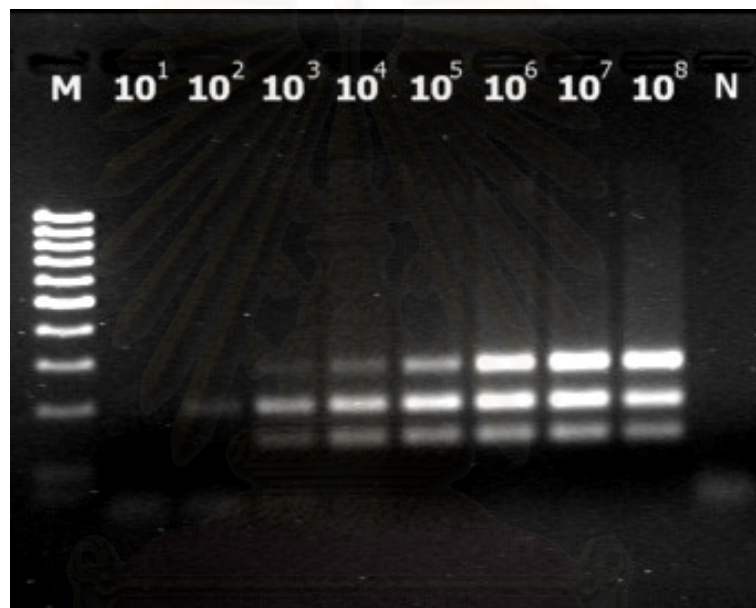


Figure 24 The sensitivity of multiplex RT-PCR detection was evaluated by 10-fold serial dilutions ranging from 10^8 – 10^1 copies/ μ L of the RNA standard. RNA dilutions were as indicated on top of the lanes. Lane M: 100-bp ladder. Lane N: Negative control.

จุฬาลงกรณ์มหาวิทยาลัย

Multiplex real-time RT-PCR for H5N1 influenza A virus detection

In this study, the diagnostic method was further developed for an even more rapid, specific and sensitive assay based on a single step multiplex real-time RT-PCR using primers and triple fluorescent labeled TaqMan MGB probes corresponding to the M, H5 and N1 genes in order to detect H5N1 influenza A virus.

A TaqMan MGB probe is an oligonucleotide with a reporter fluorescent dye attached to the 5' end and a non-fluorescent quencher attached to the 3' end. The probe is coupled with a minor groove binder, which enhances the T_m of the probe. The fluorescent signal increases when the probe is cleaved by the 5' to 3' exonuclease activity of Taq DNA polymerase during the PCR reaction, thereby separating the reporter dye from the quencher. Applying the multiplex primers from the above study and TaqMan MGB probes labeled with 3 different fluorescent reporter dyes (FAM, VIC and NED which have emission wavelength at 518, 552 and 575 nm, respectively) for specific targets corresponding to M, H5 and N1. Therefore, molecular diagnosis of H5N1 influenza A virus based on a single step multiplex real-time RT-PCR using TaqMan MGB probes should yields more efficient, specific and sensitive assay for rapid detection and quantitation of the viral load in the original specimen.

- **TaqMan MGB probe designation**

TaqMan MGB probes were designed following the general guideline described in (Appendix A). Using the nucleotide sequences available in the GenBank database and sequences obtained from the previous study [10, 16], multiple sequence alignments of the H5, N1 and M genes were performed using the CLUSTAL X program (version 1.8). M probe was selected from the conserved regions of over 75 known sequences corresponding to different subtypes of influenza A virus whereas H5 and N1 probes were chosen from the invariant regions of over 50 known sequences specific for influenza A virus subtypes H5 and N1. Both primers and probes were chosen and analyzed using the primer design software (OLIGOS version 9.1) and Primer Express Software version 2.0 (Applied Biosystems) to ensure that they could be combined in a multiplex format. The primers and probes used in this study are shown in Table 9 and Figure 25.

Table 9 Multiplex real-time RT-PCR primers and probes for H5N1 influenza detection

Target gene	Oligo name	Sequence (5' → 3')	Strand
M	CU-MF ₇₁₈	5' -TGATCTTCTTGAAAATTTGCAG-3'	sense
	CU-MR ₉₀₉	5' -CCGTAGMAGGCCCTCTTTTCA-3'	anti-sense
	CU-MP ₈₃₉	FAM -TTGTGGATTCTTGATCG- MGB	sense
H5	CU-H5F ₁₄₀₀	5' -GACTCAAATGTCAAGAACCCTTTA-3'	sense
	CU-H5R ₁₅₉₀	5' -CCACTTATTTCTCTCTCTKTTTA-3'	anti-sense
	CU-H5P ₁₅₃₅	VIC -ACGGAACGTATGACTAC- MGB	sense
N1	CU-N1F ₅₃₉	5' -GTTTGAGTCTGTTGCTTGGTC-3'	sense
	CU-N1R ₆₆₉	5' -TGATAGTGTCTGTTATTATGCC-3'	anti-sense
	CU-N1P ₆₃₇	NED -TTGTATTTCAATACAGCCAC- MGB	anti-sense

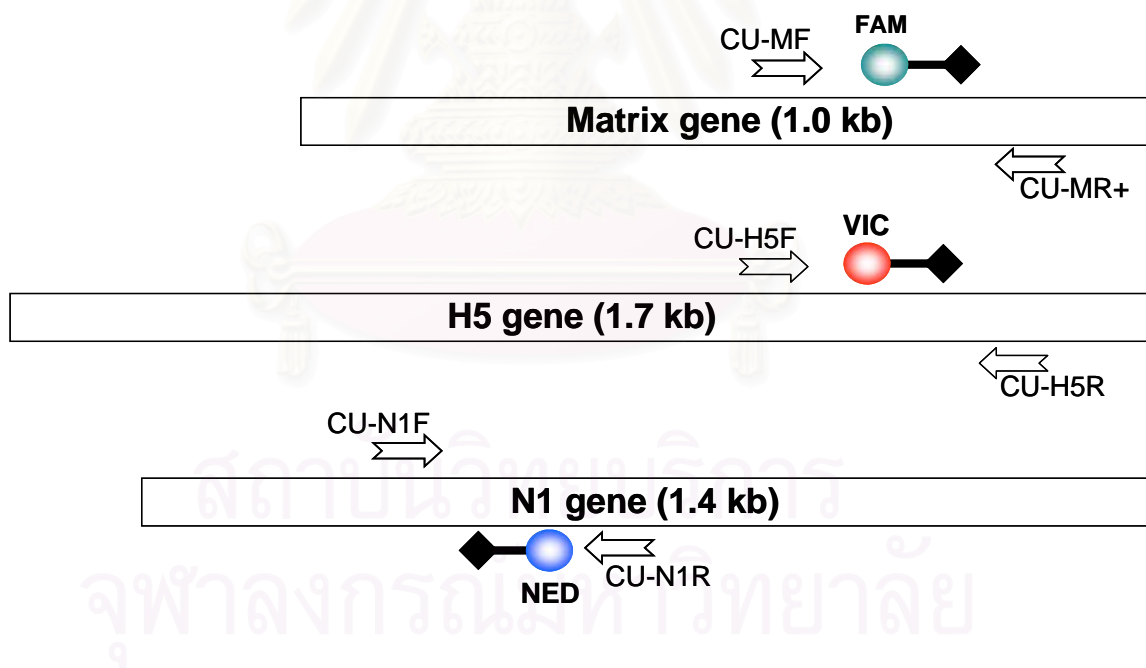


Figure 25 Schematic maps of primers and probes used in multiplex real-time RT-PCR for H5N1 influenza A virus detection. M probe was labeled with FAM (emission wavelength at 518 nm), H5 probe was labeled with VIC (emission wavelength at 552 nm) and N1 probe was labeled with NED (emission wavelength at 575 nm).

- **Optimization of the multiplex real-time RT-PCR conditions**

For maximum efficiency of amplification in multiplex real-time RT-PCR, several factors including each primer concentration (0.25-0.75 μM), each probe concentration (0.1 – 0.5 μM), additional Mg^{2+} concentration (ranging from 0.5 – 3.0 μM) and thermocycling condition (annealing at 55, 58 or 60°C) were subjected to be optimized by using *in vitro* transcribed RNA as a positive control.

According to the result of optimization (data not shown), A single-step multiplex real-time RT-PCR was performed using the TaqMan One Step PCR Master Mix containing ROX as a passive reference (Applied Biosystems). Three sets of primers and TaqMan MGB probes specific for the M, H5 and N1 genes of influenza A virus subtype H5N1 were used in multiplex format. Each primer and probe was used at a final concentration of 0.5 μM and 0.25 μM , respectively. A combination of 3.0 μl RNA sample with a reaction mixture containing 10 μl of 2X TaqMan PCR Master Mix, 0.5 μl of 40X MultiScribe and RNase Inhibitor, additional 1.25 mM MgCl_2 , 0.25 mM dNTPs and RNase-free water was used in a final volume of 20 μl . One-step multiplex real-time RT-PCR was carried out on 7500 Real-Time PCR System (Applied Biosystems). Cycling conditions included a reverse transcription step at 48°C for 45 minutes. After an initial denaturation step at 95°C for 10 minutes in order to activate the AmpliTaq Gold DNA polymerase, amplification was performed during 40 cycles including denaturation (94°C for 15 seconds), annealing (55°C for 30 seconds) and extension (72°C for 40 seconds). Multiple fluorescent signals were obtained once per cycle at the end of the extension step with detectors corresponding to FAM, VIC and NED. Data acquisition and analysis of the real-time PCR assay were performed using the 7500 System SDS Software version 1.2 (Applied Biosystems). Each fluorescent reporter signal was measured against the passive reference dye (ROX) signal to normalize for non-PCR-related fluorescence fluctuations between wells.

- **Interpretation of single step multiplex real-time RT-PCR detection**

The primers and probes summarized in Table 9 were selected for real-time PCR detection in multiplex format of the FAM, VIC and NED fluorescent signals, corresponding to the influenza A virus matrix (M), hemagglutinin (H5) and neuraminidase (N1) genes, respectively. A triple fluorescent signals resulting from multiplex real-time RT-PCR can be interpreted as influenza A virus subtype H5N1 (Figure 26A), whereas other subtypes of influenza A virus will only yield a FAM signal of the matrix gene (Figure 26B).

- **Specificity test of Multiplex real-time RT-PCR**

The specificity of multiplex real-time RT-PCR assay was evaluated by cross-reaction tests showing no cross-reactivity to human total RNA, Newcastle disease virus (NDV), respiratory syncytial virus (RSV) subgroups-A and B, infectious bursal disease virus (IBDV), infectious bronchitis virus (IBV) or non-inoculated allantoic fluid (data not shown). Moreover, other influenza subtypes including A/Fujian/411/02 (H3N2), A/duck/Thailand/249/04 (H4N6), A/chicken/Netherlands/1/03 (H7N7), A/turkey/Wisconsin/66 (H9N2) and A/duck/Thailand/1812/04 (H10N9) yielded only a FAM fluorescent signal of the M gene indicating influenza A virus but not subtype H5N1 (Figure 26B and Table 10). This indicates absence of cross-reactivity to other subtypes of influenza A virus. No significant false positive or non-specific signal was observed in any of the samples tested. Taken together, these results indicate high specificity of the primers and probes used in the multiplex real-time RT-PCR assay.

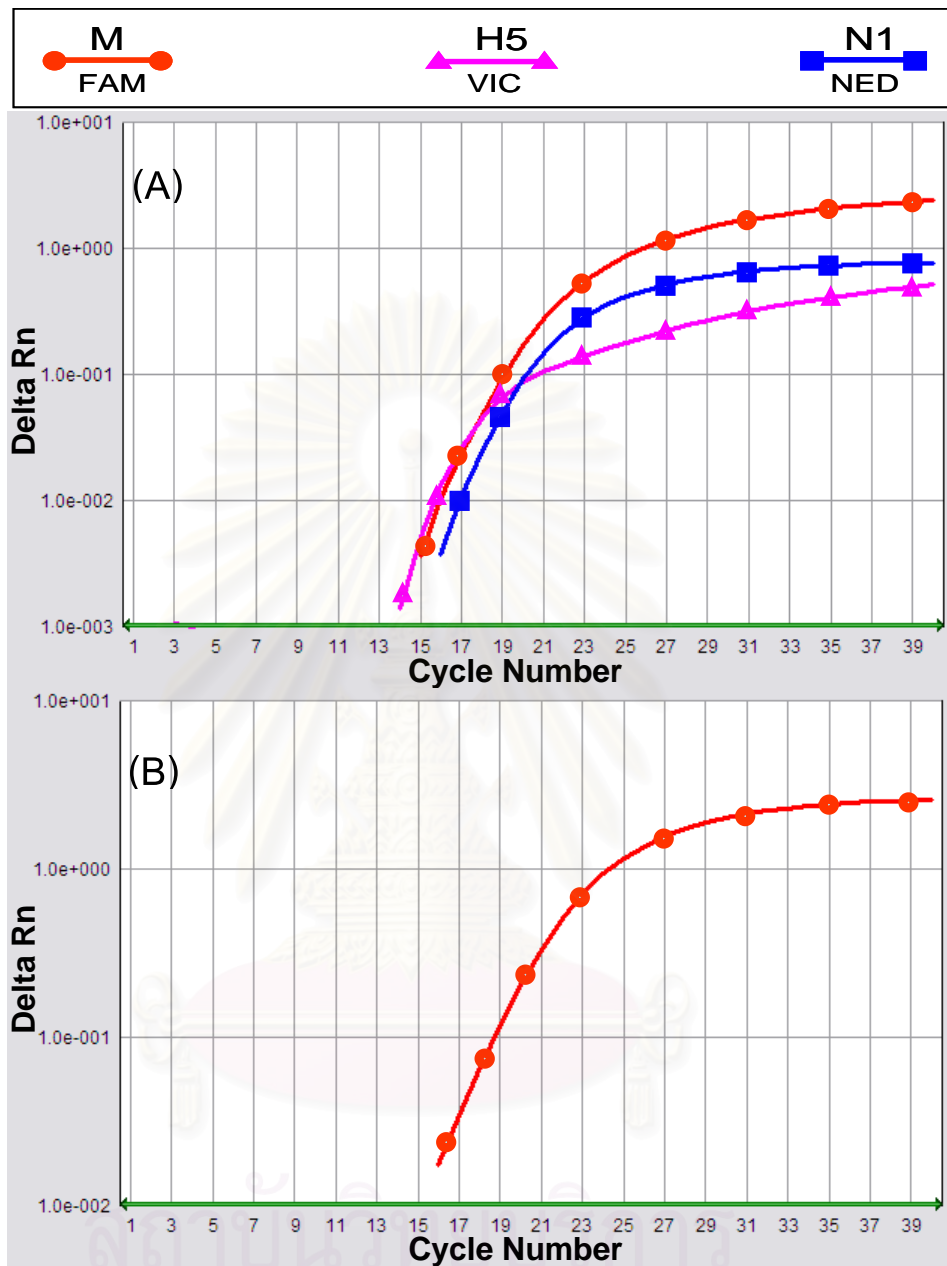


Figure 26 Representative results obtained from single step multiplex real-time RT-PCR. (A) Influenza A virus subtype H5N1 yielded triple fluorescent signals of FAM, VIC and NED corresponding to M, H5 and N1 respectively. (B) Other subtypes of influenza A virus (non-H5N1) yielded only a FAM fluorescent signal of M gene.

- **Clinical sample test of multiplex real-time RT-PCR**

Allantoic fluids obtained from 75 specimens of avian influenza A virus subtype H5N1 used in this study were isolated from humans (N=4), tigers (N=7), a leopard (N=1) and several avian species (including chickens (N=16), laying hens (N=4), fighting cocks (N=2), ducks (N=27), crows (N=6), ostriches (N=2), one each of pheasant, quail, open bill, white peafowl, Indian roller and kalij pheasant) during the 2004 outbreak in Thailand (Chapter III). These specimens were isolated and provided by the Faculty of Veterinary Science, Chulalongkorn University, Bangkok, Thailand; the Department of Livestock Development, Bangkok, Thailand and the Department of Medical Sciences (DMSc), Ministry of Public Health, Nonthaburi, Thailand.

All of the H5N1 specimens were effectively detected by the multiplex real-time RT-PCR detection (Table 10). All positive specimens were subjected to nucleotide sequencing for confirmation of the H5N1 subtype detection. Several sequences have been submitted to GenBank and assigned accession numbers (Chapter III). The clinical samples tested in this assay were isolated from humans, tigers, a leopard and various avian species thus representing the influenza A virus subtype H5N1 in a wide host range. Hence, this method can be used to detect not only avian influenza A virus (H5N1) but also human influenza A virus (H5N1).

- **Sensitivity test of multiplex real-time RT-PCR**

The genes of influenza A virus (A/chicken/Nakorn-Patom/Thailand/ CU-K2/2004 (H5N1)) were used to construct plasmid DNAs by inserting the H5 (nt 898-1715), N1 (nt 539-1431) and M (nt 516-993) genes into the pGEM-T Easy Vector (Promega). *In vitro* transcription was performed by using RiboMAX™ Large Scale RNA Production System-T7 (Promega) following the manufacturer's recommendations (Chapter III). The concentration of the transcribed RNAs was calculated by measuring absorbance at 260 nm. The *in vitro* transcribed RNA of M, H5 and N1 RNAs were then serially diluted ten fold, ranging from 10^8 - 10 copies/ μ l to perform sensitivity tests. As expected, the threshold cycle (Ct) increased in direct proportion to the dilution of the RNA standards. The fluorescent signal can be detected at RNA standard dilutions as low as 10^2 copies/ μ l in a multiplex real-time RT-PCR assay (data not shown).

Table 10 Specificity test of multiplex real-time RT-PCR

Sample name	Fluorescent signal		
	FAM (M)	VIC (H5)	NED (N1)
A/ Fujian/411/2002 (H3N2)	+	-	-
A/duck/Thailand/249/04 (H4N6)	+	-	-
A/chicken/Netherland/1/2003 (H7N7)	+	-	-
A/turkey/Wisconsin/66 (H9N2)	+	-	-
A/duck/Thailand/1812/04 (H10N9)	+	-	-
A/chicken/Nakorn-Patom/Thailand/CU-K2/04(H5N1)	+	+	+
A/chicken/Ayutthaya/Thailand/CU-23/04(H5N1)	+	+	+
A/chicken/Thailand/CU-21/2004 (H5N1)	+	+	+
A/tiger/Suphanburi/Thailand/Ti-1/04(H5N1)	+	+	+
A/tiger/Thailand/CU-T3/04(H5N1)	+	+	+
A/tiger/Thailand/CU-T4/04(H5N1)	+	+	+
A/tiger/Thailand/CU-T5/04(H5N1)	+	+	+
A/tiger/Thailand/CU-T6/04(H5N1)	+	+	+
A/tiger/Thailand/CU-T7/04(H5N1)	+	+	+
A/tiger/Thailand/CU-T8/04(H5N1)	+	+	+
A/leopard/Suphanburi/Thailand/Leo-1/04(H5N1)	+	+	+
A/duck/Thailand/CU-2/2004 (H5N1)	+	+	+
A/Kalji pheasant/Bangkok/Thailand/04(H5N1)	+	+	+
A/open bill/Bangkok/Thailand/04(H5N1)	+	+	+
A/white peafowl/Bangkok/Thailand/04(H5N1)	+	+	+
A/crow/Bangkok/Thailand/04(H5N1)	+	+	+
A/Thailand/2(SP-33)/04(H5N1)	+	+	+
A/Thailand/3(SP-83)/04(H5N1)	+	+	+
A/Thailand/4(SP-528)/04(H5N1)	+	+	+
Newcastle disease virus (NDV)	-	-	-
Respiratory syncytial virus (RSV)	-	-	-
Infectious bursal disease virus (IBDV)	-	-	-
Infectious bronchitis virus (IBV)	-	-	-
Virus-free allantoic fluid	-	-	-
Uninfected human RNA	-	-	-

Discrimination of HPAI and LPAI by real-time RT-PCR with melting analysis

Identification of highly pathogenic avian influenza (HPAI) and low pathogenic avian influenza (LPAI) is essential for investigation during avian influenza A virus outbreaks. The HA protein appears to be the most important protein in molecular determining the virulence of avian influenza viruses. Comparison of the complete sequence of HA from the two virus strains responsible for the different degrees of severity of the disease, demonstrated that the highly pathogenicity was determined by the insertion and substitution of basic amino acid residues in the HA cleavage site. Currently, determination of inserted basic amino acids within the HA cleavage site of HPAI relies on nucleotide sequencing. Direct sequencing is relatively time consuming and laborious; hence it is not suitable for local and regional diagnostic laboratories receiving large numbers of samples that may contain HPAI or LPAI subtype H5N1. In this study, a rapid diagnostic assay was developed to discriminate between HPAI and LPAI subtype H5 viruses by one-step real-time RT-PCR with melting curve analysis.

- **Designation of H5 primers for melting curve analysis**

Real-time PCR with melting curve analysis (Appendix A) was first described in 1997 [78]. Melting temperature (T_m) values are directly related to the %GC contents, the length of PCR products and $MgCl_2$ concentration [79]. Based on H5 amino acid sequences comparison between HPAI and LPAI, revealed that the highly pathogenicity was determined by the insertion and substitution of multiple basic amino acid residues in the HA cleavage site. Therefore, H5 primers flanking the cleavage site were designed from conserved region of both HPAI and LPAI strains. Using the nucleotide sequences available in the GenBank database and sequences obtained from previous study, multiple alignments of the H5 genes were performed using the CLUSTAL X program. The primers were analyzed for self-complementary and primer-dimers using Oligo software and tested for specificity by BLAST. The selected primers (Table 11) were used for amplification which allowed the amplification of a 124- bp or 112- bp products corresponding to HPAI and LPAI, respectively. Therefore, the PCR product sizes and %GC content within the amplicons were different, allowed the discrimination between HPAI and LPAI by melting curve analysis (Figure 27).

Table 11 Primers flanking the cleavage site of H5 gene for discrimination of HPAI and LPAI by melting curve analysis.

Oligo name	Primer sequence	Amplicon length (bp)
CU-H5F ₁₀₀₁	5' - AACAGATTAGTCCTTGCGACTG - 3'	124 bp (HPAI)
CU-H5R ₁₀₂₄	5' - CATCTACCATTCCCTGCCATCC - 3'	112 bp (LPAI)



Figure 27 Schematic alignment between nucleotide sequences obtained from HPAI and LPAI strains. The HPAI strain contains 12 nucleotides insertion which responsible for the 4 basic amino acid residues at the cleavage site of hemagglutinin.

- **Construction of positive control for HPAI and LPAI**

A sample previously identified as influenza A/chicken/ Nakorn-Patom/Thailand/ CU-K2/04(H5N1) [16] served as a control of HPAI where as influenza A/duck/Hong Kong/308/78 (H5N3) served as a control of LPAI for developing and optimizing the assays. The H5 genes of each strain were used to construct plasmid DNAs by inserting the H5 (nt 914-1728) gene into the pGEM-T Easy Vector (Promega). *In vitro* transcription was performed by using RiboMAX Large Scale RNA Production System-T7 (Promega) following the manufacturer's recommendations (Chapter III). Then the in vitro transcribed H5 RNA of HPAI and LPAI strains were used as a positive control for optimization of the real-time RT-PCR with melting curve analysis.

- **Optimization of the real-time RT-PCR with melting curve analysis**

For maximum efficiency of real-time RT-PCR with melting curve analysis for discrimination between HPAI and LPAI, several factors including each primer concentration (0.25-0.75 μM), additional Mg^{2+} concentration (ranging from 0.5 – 3.0 μM) and thermocycling condition (annealing at 55, 58, 60, 65 or 68°C) were subjected to be optimized by using *in vitro* transcribed RNA as a positive control.

According to the result of optimization (data not shown), one step real-time RT-PCR using SYBR Green I fluorescence dye with melting curve analysis was performed by using SYBR Green PCR Master Mix (Applied Biosystems). Each primer was used at a final concentration of 0.5 μM . A combination of 3.0 μl of RNA sample with a reaction mixture containing 10 μl of 2X SYBR Green PCR Master Mix, 0.5 μl of 40X MultiScribe and RNase Inhibitor, additional 1.5 mM MgCl_2 and RNase-free water was used in a final volume of 20 μl . Cycling conditions included a reverse transcription step at 48°C for 45 minutes. After an initial denaturation step at 95°C for 10 minutes, amplification was performed during 40 cycles including denaturation (94°C for 15 seconds) and annealing/extension (68°C for 40 seconds). A fluorescent signal of SYBR Green I was obtained once per cycle at the end of extension step. After amplification, melting curve analysis was performed on the products by heating to 95°C for 15 seconds, cooling to 60°C for 1 minute, followed by a temperature increase to 95°C with a temperature transition rate of 0.5°C /second while continuously collecting the SYBR Green fluorescent signal. Data acquisition and analysis of real-time PCR assay were carried out with 7500 System SDS Software version 1.2 (Applied Biosystems). SYBR Green I fluorescent signal was measured against the internal reference dye (ROX) signal to normalize for non-PCR-related fluorescence fluctuations occurring from well to well.

- Validation of real-time RT-PCR with melting curve analysis

Three preliminary real-time PCR assays with melting curve analysis revealed that a pair of primers (CU-H5F₁₀₀₁/CU-H5R₁₀₂₄), which yield an amplified product within the cleavage site of H5 was effective to discriminate between the melting peaks of HPAI and LPAI (Figure 28). In addition, the reaction occurred without any unexpected PCR product or primer dimers. The mean T_m values for HPAI and LPAI were 77.43 °C and 79.57 °C, respectively. Therefore, the cut-off value was set at 78.50 °C (mid-point between HPAI and LPAI) and used it to interpret the pathogenicity of unknown samples.

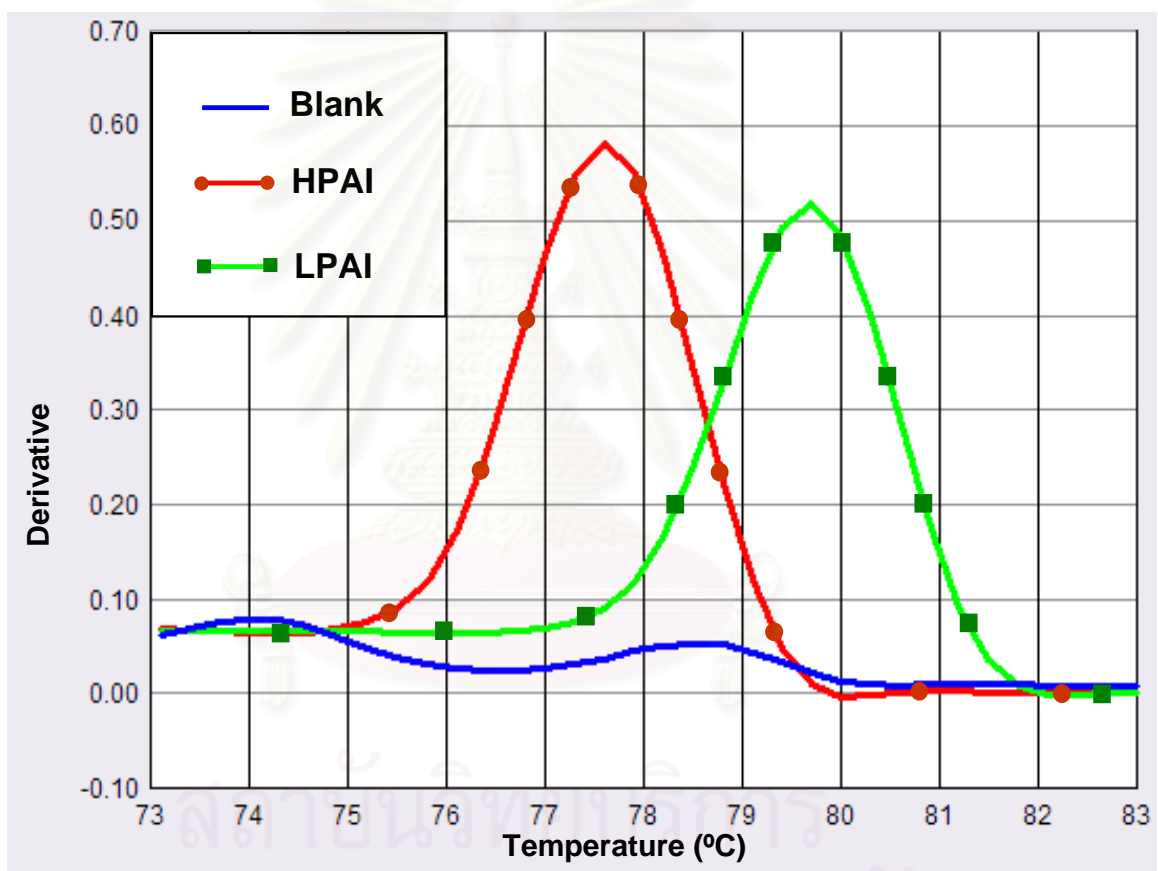


Figure 28 Discrimination between HPAI and LPAI by melting analysis based on one step real-time RT-PCR using SYBR Green I fluorescent dye. The melting point peaks were clearly separated between HPAI and LPAI using CU-H5F₁₀₀₁/CU-H5R₁₀₂₄ primers.

- **Clinical sample test of real-time RT-PCR with melting curve analysis**

Seventy eight specimens of influenza A virus were used to validate the assay. The 75 HPAI samples were isolated during the 2004 outbreak in Thailand and 3 LPAI samples including A/avian/NY/01 (H5N2), A/Chicken/Mexico/31381-3/94 (H5N2) and A/shoveler/Egypt/03 (H5N2) were provided by the Influenza Branch, DVRD/NCID, CDC, Atlanta, GA. Melting curve analysis revealed that all H5N1 isolates from the 2004 outbreak in Thailand were interpreted as HPAI, whereas 3 samples of H5N2 subtype were classified as LPAI. The T_m varied from 77.2 to 78.1°C for HPAI and 78.75 to 79.5°C for LPAI. The melting curve analysis results were completely concordant with the results of direct sequence analysis of the H5 gene for all samples tested.

- **Specificity test of real-time RT-PCR with melting curve analysis**

The specificity of this assay was evaluated by cross-reaction tests showing no cross-reactivity to total RNA of human, New Castle Disease Virus (NDV) or Respiratory Syncytial Virus (RSV), types A and B (data not shown). There were no unwanted fluorescent signals that interfered with the discrimination assay. Moreover, viral RNA extracted from other subtypes of influenza A viruses (H1-H4 and H6-H15) were tested. The assay yield specific for the H5 subtype, since no amplification was detected from other subtypes of influenza (data not shown).

- **Sensitivity test of real-time RT-PCR with melting curve analysis**

The standard *in vitro* transcribed RNAs were serially diluted ten fold, ranging from 10^9 - 10^0 copies/ μ L to perform sensitivity tests. As expected, the threshold cycle (Ct) increased with the increased dilution of the RNA standards. The fluorescent signal can be detected at RNA standard dilutions as low as 10^2 copies/ μ L (data not shown).

- Variation of melting temperature (T_m)

The mean T_m values for HPAI and LPAI were 77.43 °C and 79.57 °C, respectively. Therefore, the cut-off value was set at 78.50 °C (mid-point between HPAI and LPAI) and used it to interpret the pathogenicity of unknown samples. The result of melting curve analysis revealed that all of the samples tested were interpreted as HPAI. The variations of T_m found in intra- and inter-assay were presented in Table 12. The intra-assay variation was indicated from assay with more than one sample of HPAI. The intra-assay variation of LPAI was not determined because no LPAI sample available. The inter-assay variation was calculated from the T_m of the positive control of HPAI and LPAI between independent triplicate assays. The coefficient of variation (CV) of T_m (inter-assay) was 0.27 and 0.29 for HPAI and LPAI, respectively (Table 12).

Table 12 Intra- and inter-assay variation of melting temperature (T_m)

Strain	%GC contents Mean (SD)	Variation of T _m (°C)					
		Intra-assay		Inter-assay			
		Interval	Range	Interval	Range	Mean (SD)	CV
HPAI	43.44 (0.29)	77.20-78.10	0.90	77.20-77.60	0.4	77.43 (0.21)	0.27
LPAI	49.11	-	-	79.30-79.70	0.4	79.57 (0.23)	0.29

Molecular characterization and molecular diagnosis of H3N8 canine influenza

According to the previous study, the emergence of canine influenza virus (CIV) in the United States during 2004 was initially associated with outbreaks of canine respiratory tract disease in dog racetracks and soon thereafter in many other settings and locations. The disease is caused by viruses closely related to equine influenza A virus, subtype H3N8. The HA gene of H3N8 canine influenza A virus has a 96% nucleotide sequence identity with that of equine influenza (Figure 29), suggesting that the entire virus was directly transmitted from horses to dogs without reassorting with other strains [13, 17, 18].

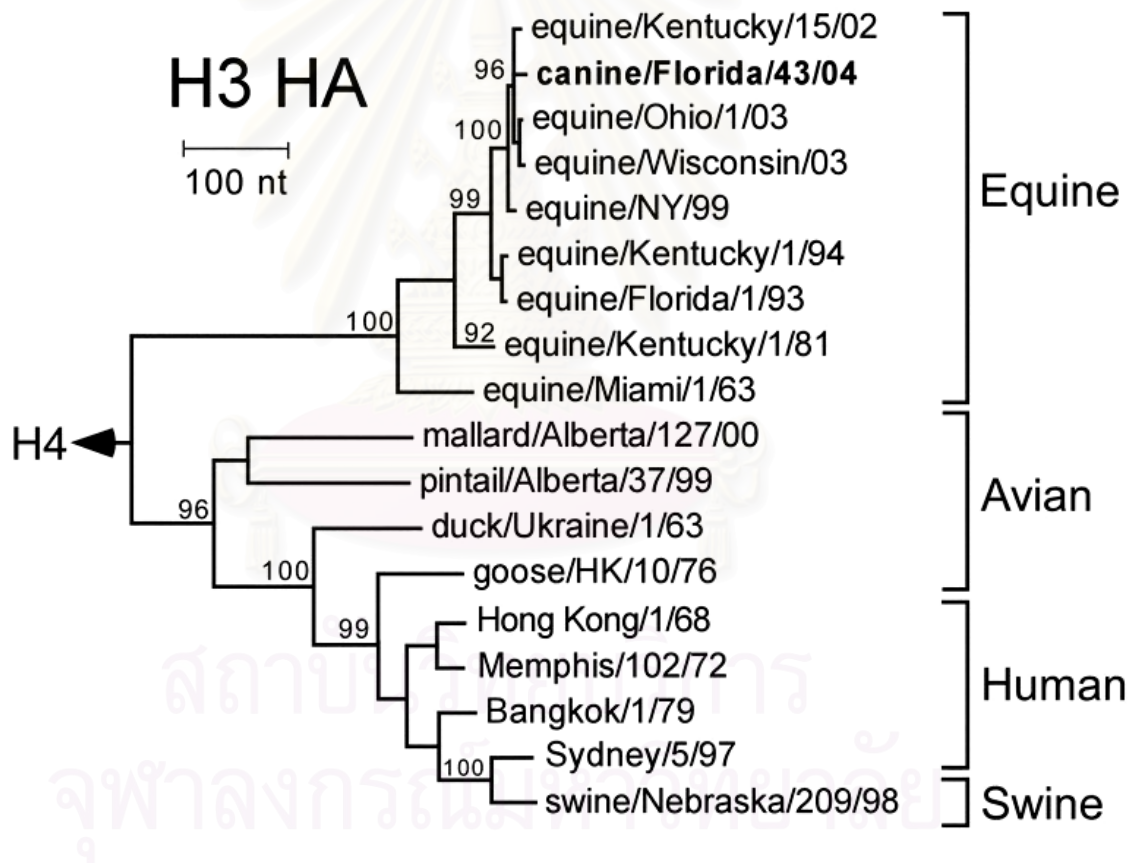


Figure 29 Phylogenetic tree of H3 gene of canine influenza (A/canine/Florida/43/04). The full-length gene of H3 genes of influenza A viruses isolated from several host species including equine, avian, swine and human were multiple aligned with canine influenza [13].

Isolation and characterization of influenza A subtype H3N8 viruses from non-greyhound dogs with respiratory disease in Florida

Canine influenza virus subtype H3N8 (CIV) firstly emerged in the United States in 2004, causing multiple outbreaks of respiratory disease in racing greyhound dogs. Serologic evidence indicated virus circulation in dog breeds besides racing greyhounds but the virus was not isolated from affected animals. In this study, we investigated two outbreaks of respiratory disease in an animal shelter and veterinary clinic in the State of Florida that involved dog breeds other than greyhounds. The aim of this study was to isolate and characterize canine influenza from these dogs and compare the isolates to those from greyhounds to determine genetic diversity.

- **Clinical presentation of infected dogs**

Postmortem examinations were performed on six mixed breed dogs that died in April and May 2005 during a canine influenza outbreak in a shelter facility in northeast Florida, and on one pet Yorkshire Terrier dog that died in May 2005 during a canine influenza outbreak in a veterinary clinic in southeast Florida. Postmortem examination of the six shelter dogs and one pet dog revealed pulmonary congestion and edema, but no intrathoracic or pulmonary hemorrhage. Histological examination revealed rhinitis, tracheitis, bronchitis, bronchiolitis, and suppurative bronchopneumonia. There was epithelial cell necrosis and erosion in the trachea, bronchi, bronchioles, and bronchial glands, and these tissues were infiltrated by neutrophils and macrophages.

- **Laboratory diagnosis by real-time RT-PCR and viral isolation**

Frozen lung tissues from each of the seven dogs examined postmortem were thawed and homogenized. Total RNA extracted from each tissue was subjected to test for the presence of canine influenza by real-time RT-PCR using primers and probes specific for M and H3 genes (as described below). Real-time RT-PCR for eukaryotic 18S rRNA was performed using commercially available assay reagents (VIC/TAMRA) (TaqMan®, Applied Biosystems) for detection of endogenous 18S rRNA as an internal control for RNA extraction from the tissues.

The lungs from all seven dogs revealed the presence of canine influenza virus, because the influenza M gene and the canine influenza H3 gene were amplified in the real-time RT-PCR assays. Lung tissue from specific pathogen-free dogs did not show evidence of amplification of influenza virus genes. MDCK cultures and embryonated chicken eggs were inoculated with these lung homogenates to identify the presence of viable influenza virus. Cytopathology was noted in the MDCK cell monolayer on the third passage of the lung homogenate from one of the shelter dogs that died after 3 days of pneumonia. Influenza A virus (later identified as subtype H3N8) was recovered from the supernatant and the isolate was named *A/canine/Jacksonville/05* (H3N8). After two passages in embryonated chicken eggs, influenza A virus was recovered from the lung homogenate of the pet dog that also died of pneumonia 3 days after onset. This virus was named *A/canine/Miami//05* (H3N8). These isolates provided for the first time virologic evidence of canine influenza virus infection in non-greyhound dogs.

Nucleotide sequences analysis of H3 gene of the canine influenza

Sequence analyses of *A/canine/Jacksonville/05* and *A/canine/Miami//05* revealed that their hemagglutinin (H3) gene nucleotide sequences were 98% identical to the *A/canine/FL/242/03*, *A/canine/FL/43/04*, *A/canine/TX/04*, and *A/canine/Iowa/05* isolates recovered from the lungs of racing greyhounds that died of pneumonia during influenza outbreaks at tracks in 2004 and 2005 [13, 19].

Phylogenetic comparisons of the H3 genes showed that *A/canine/Jacksonville/05* and *A/canine/Miami//05* viruses from non-greyhound dogs were clustered with the greyhound isolates and contemporary equine isolates, forming a distinct group from the older equine viruses isolated in the early 1990's (Figure 30A). Furthermore, the *canine/Jacksonville/05*, *canine/Miami/05*, and *canine/IA/05* isolates were more closely related to *canine/TX/04* than to either *canine/FL/04* or *canine/FL/03*. The three 2005 HA genes formed a subgroup that appears to branch off from the earlier 2003 and 2004 canine viruses with nucleotide differences at 10 sites. Most of the nucleotide changes are silent, as can be appreciated by the shorter branch lengths in the phylogenetic tree constructed using amino acid sequence data (Figure 30A and 30B).

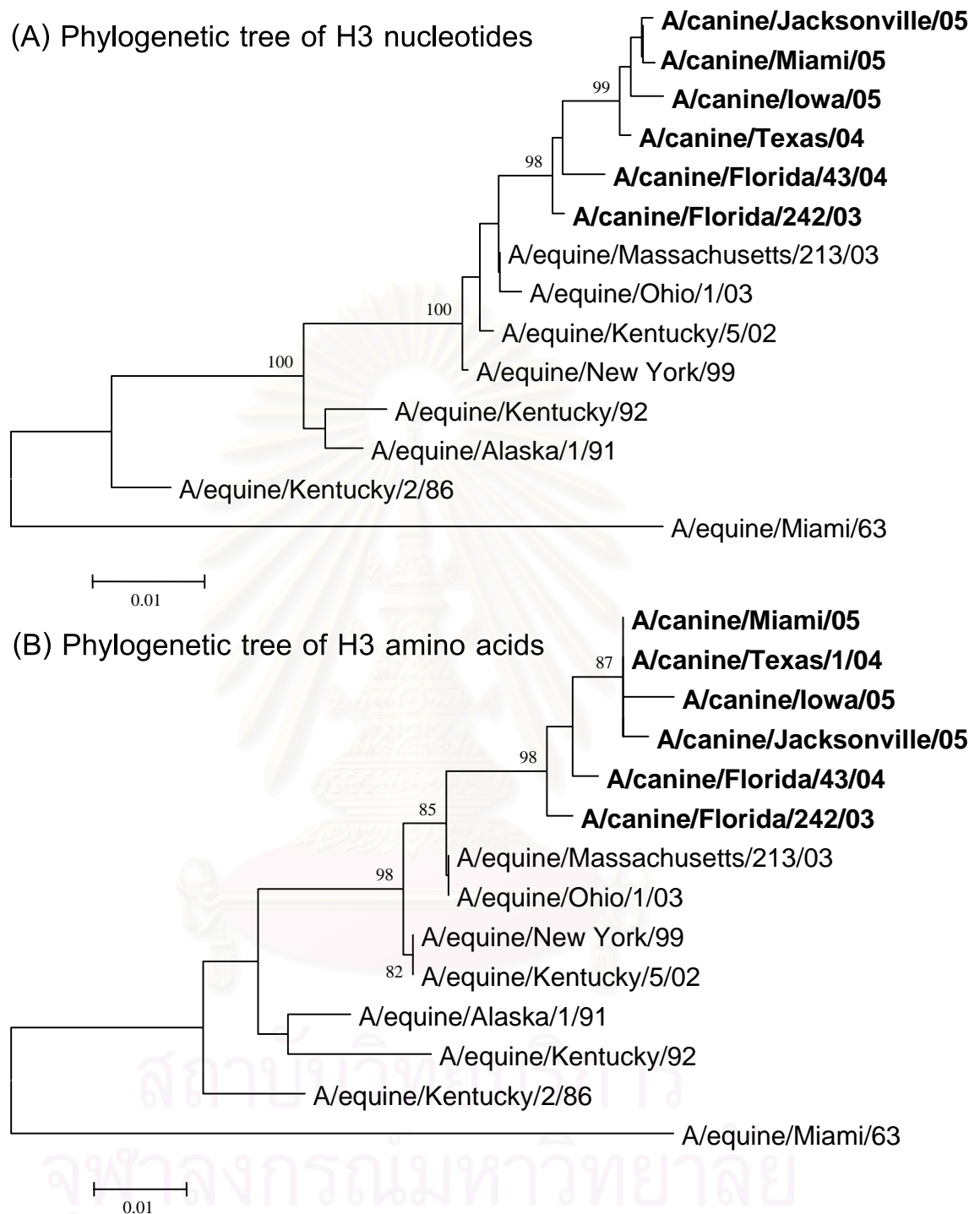


Figure 30 Phylogenetic relationships among the H3 hemagglutinin genes. (A) Nucleotide tree of the canine influenza virus H3 genes with contemporary and older equine H3 genes. (B) Amino acid tree of the canine influenza virus H3 protein with contemporary and older equine H3 proteins. Bootstrap analysis values $\geq 80\%$ was shown. The bar scale denotes substitutions per site.

- **Amino acid sequence analysis of H3 hemagglutinin of canine influenza**

The deduced amino acid sequences of the H3 HAs from the six available CIV isolates were compared to each other to identify changes with possible functional significance. There were five amino acid substitutions conserved in all six canine isolates that differentiated them from contemporary equine influenza viruses (Table 13). These conserved substitutions were I15M, N83S, W222L, I328T, and N483T, and can be considered as a signature of the circulating CIV H3 HA. Phylogenetic comparisons of the mature H3 protein showed that the canine/Jacksonville/05, canine/Miami/05, and canine/IA/05 viruses formed a subgroup with the canine/TX/04 isolate (Figure 30B). Three amino acid changes (L118V, K261N, and G479E) differentiated this subgroup from the earlier canine/FL/04 and canine/FL/03 isolates (Table 13). Two amino acid changes (F79L and G218E) differentiated the 2005 isolates from their canine/TX/04 root. Furthermore, the canine/Jacksonville/05 and canine/Miami/05 isolates from non-greyhound dogs differed from the canine/IA/05 greyhound isolate by one amino acid change, R492K. Finally, canine/Jacksonville/05 differed from canine/Miami/05 at a single amino acid, S107P.

Table 13 Amino acid differences among H3 hemagglutinins of canine and contemporary equine influenza viruses.

Virus isolates	H3 Amino acid positions										
	15	83	107	118	218	222	261	328	479	483	492
A/equine/KY/5/02	I	N	S	L	G	W	K	I	G	N	R
A/equine/MA/213/03	I	N	S	L	G	W	K	I	G	N	R
A/equine/OH/1/03	I	N	S	L	G	W	K	I	G	N	R
A/canine/FL/242/03	M	S	S	L	G	L	K	T	G	T	R
A/canine/FL/43/04	M	S	S	L	G	L	K	T	G	T	R
A/canine/TX/1/04	M	S	S	V	G	L	N	T	E	T	R
A/canine/IA/05	M	S	S	V	E	L	N	T	E	T	R
A/canine/Miami/05	M	S	S	V	E	L	N	T	E	T	K
A/canine/Jacksonville/05	M	S	P	V	E	L	N	T	E	T	K

Molecular diagnosis of H3N8 canine influenza A viruses

The standard method for virologic diagnosis of influenza is virus isolation by inoculation of respiratory tract secretions into Madin Darby Canine Kidney (MDCK) cell cultures or embryonated chicken eggs, followed by assays to detect the presence of the amplified progeny virus, such as ELISA, immunofluorescence or hemagglutination inhibition [72, 77]. Furthermore, clinical specimens for virus isolation must be collected within the first few days of infection because the neutralizing antibody response of the host effectively abrogates viral infectivity in tissues and secretions within one week of infection. Consequently, the standard method is extremely laborious and often impractical as a means to diagnose canine influenza on individual animals. Serologic diagnosis of canine influenza by virus neutralization, hemagglutination inhibition (HI) test or ELISA, among others, provides only retrospective data which do not facilitate prompt intervention and appropriate case management although it can be a valuable tool to guide population health interventions. Therefore, specific and sensitive virus detection systems that provide a rapid diagnosis of canine influenza infection are urgently needed. In this study, a rapid, sensitive and specific assay was developed for molecular diagnosis of canine influenza virus subtype H3 based on a single step TaqMan real-time RT-PCR.

- **H3 primers and TaqMan probe designation**

Multiple sequence alignments of the H3 gene from various subtypes and from diverse species were performed using the CLUSTAL X program (Version 1.8). The H3 hemagglutinin gene-specific primers and probe set were selected to specifically match equine and canine influenza A virus genes and mismatch the homologous avian and human genes (Table 14). Primer design software (OLIGOS Version 9.1) and the web based analysis tools (Exiqon; <http://lnatools.com>) were used for melting temperature (T_m) calculation and prediction of secondary structure as well as self-hybridization.

Table 14 H3 primers & probe for H3N8 canine influenza detection by real-time RT-PCR

Oligo name	Sequence (5'→3')	Application
Ca-H3-F ₃₉₀	5' -TATGCATCGCTCCGATCCAT-3'	Real-time RT-PCR
Ca-H3-R ₄₉₀	5' -GCTCCACTTCTTCCGTTTTGA-3'	
Ca-H3-P ₄₃₀	FAM-AATTCACAGCAGAGGGATTACATGGACAG-BHQ1	
H3-F ₁	5' -TATTCGTCTCAGGGAGCAAAGCAGGGG-3'	<i>In vitro</i>
T7/H3-R ₄₉₀	5' -TGTAATACGACTCACTATAGGGCTCCACTTCTTCCGTTTTGA-3'	transcription

- **Construction of positive control**

The genes of canine influenza A virus (A/canine/Florida/242/2003(H3N8)) were used to generate the PCR amplicons for H3 (nt 1-487) by using primers linked with T7 promoter (Table 14). Then the purified PCR amplicons of H3 was used as a template for *in vitro* transcription by using Riboprobe *in vitro* Transcription System-T7 (Promega), followed by DNase treatment and purification. Then the *in vitro* transcribed H3 RNA was used as a positive control to validate the assay.

- **Optimized condition of the real-time RT-PCR for canine influenza detection**

A single-step real-time RT-PCR was performed by using the Quantitect Probe RT-PCR Kit containing ROX as a passive reference dye (QIAGEN). In each real-time RT-PCR reaction, 5 µl of RNA sample were used as a template to combine with a reaction mixture containing 10 µl of 2X QuantiTech Probe RT-PCR Master Mix, 0.2 µl of QuantiTech RT Mix, H3 primers at final concentration of 0.4 µM, H3 probe at final concentration of 0.1 µM and RNase-free water in a final volume of 20 µl. One-step real-time RT-PCR was performed in the Mx3005P Real-Time QPCR System (Stratagene). Cycling conditions included a reverse transcription step at 50°C for 30 minutes. After an initial denaturation step at 95°C for 15 minutes in order to activate the HotStarTaq DNA polymerase, amplification was performed during 40 cycles including denaturation (94°C for 15 seconds) and annealing/extension (60°C for 30 seconds). The FAM (emission wavelength 518 nm for H3 detection) fluorescent signal was obtained once per cycle at the end of the extension step. Data acquisition and analysis of the real-time PCR assay were performed using the Mx3005P software version 2.02 (Stratagene).

- **Specificity test of real-time RT-PCR for canine influenza detection**

In order to test the specificity of the H3 primers/probe set for canine influenza A virus (H3N8), multiple subtypes of influenza A viruses were tested by real-time RT-PCR. The results show that H3 primers/probe set yielded a positive amplification signal only with canine and equine influenza subtype H3N8 (Table 15). No significant amplification signals were observed in samples containing human or avian H3 strains suggesting that the H3 primer/probe are specific for the canine and equine lineages. Samples with a variety of other viral HA subtypes failed to yield amplification signals, further confirming the specificity of the assay.

Table 15 Specificity test of canine H3 primers/probe set

Subtypes	Strain Name	Host	Real-time RT-PCR (H3)
H1	A/Ohio/1983	Human	-
	A/WSN/1933	Human	-
H3	A/Wyoming/3/2003	Human	-
	A/Victoria/3/1975	Human	-
	A/turkey/England/69	Avian	-
	A/swine/Nebraska/209/98	Swine	-
	A/equine/Alaska/1/91	Equine	+
	A/canine/FL/242/2003	Canine	+
H4	A/mallard/NY/37/1983	Human	-
	A/turkey/MN/1066/1980	Avian	-
	A/Duck/Vietnam/NCVDCDC76/2005	Avian	-
H5	A/chicken/Thailand/CUK2/2004	Avian	-
	A/pheasant/NJ/1335/1998	Avian	-
H6	A/Duck/Vietnam/NCVDCDC90/2005	Avian	-
H7	A/turkey/VA/4529/2002	Avian	-
H10	A/Teal/Egypt/0457/2003	Avian	-
	A/Shoveler/Egypt/0600/2004	Avian	-
H11	A/Duck/Vietnam/NCVDCDC72/2005	Avian	-
	A/Teal/Egypt/0688/2004	Avian	-

- Sensitivity test of real-time RT-PCR for canine influenza detection

The *in vitro* transcribed RNA concentration was determined by UV absorption spectroscopy at 260 nm. The RNAs were then serially diluted 10-fold, ranging from 10^8 to 10^1 copies/ μl . Then 1 μl of each standard RNA dilutions was used as a template to study the sensitivity of the real-time RT-PCR assay. As expected, the threshold cycle (Ct) increased in direct correlation with the dilution of the RNA standards. The fluorescent signals can be detected at H3 RNA standard dilutions as low as 10^2 copies/ PCR reaction (Figure 31).

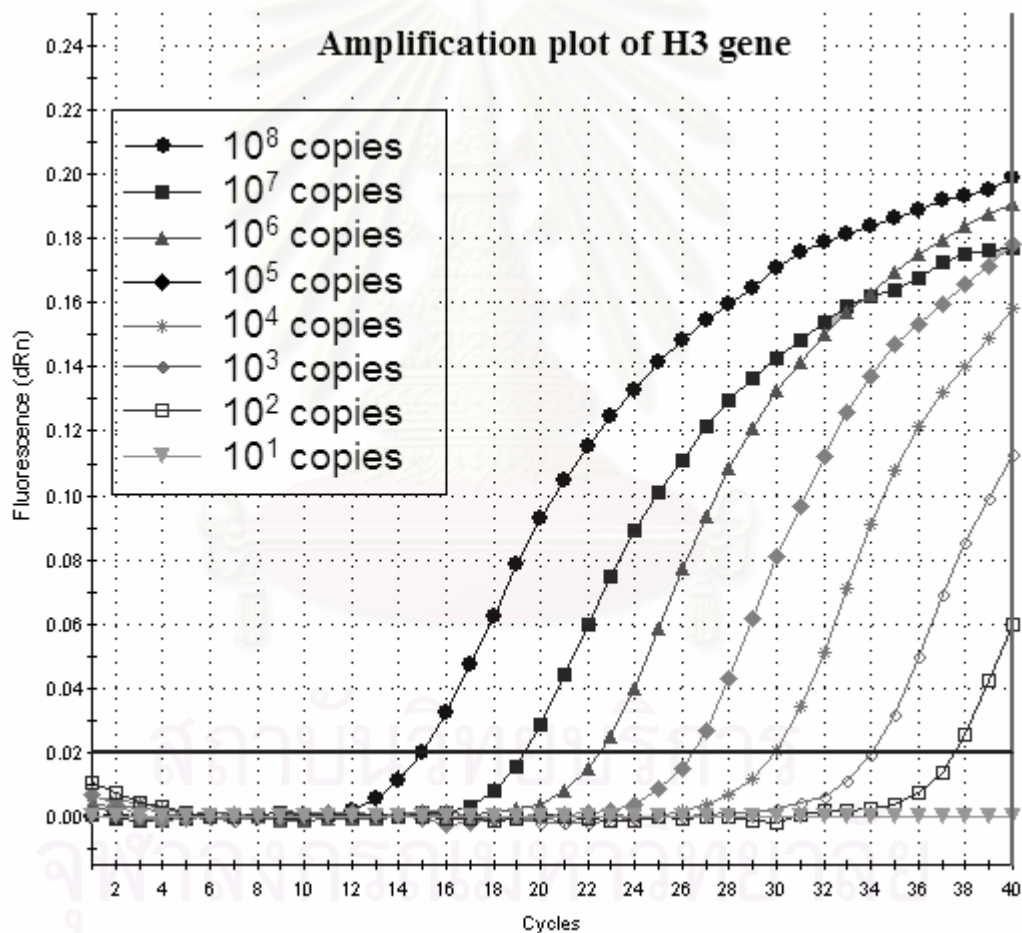


Figure 31 Amplification plots of H3 gene obtained from the amplification of 10-fold serially diluted *in vitro* transcribed H3 RNA standards. The result revealed that the sensitivity of the real-time RT-PCR was 10^2 copies/ μl .

- Evaluation of real-time RT-PCR performance

The standard curves H3 gene was constructed by plotting the logarithm of initial RNA concentrations against the threshold cycle (Ct) obtained from each dilution (Figure 32). The slope of the standard curve is used to determine the PCR reaction efficiency, which is theoretically exponential; 100% amplification efficiency would imply doubling of amplicon concentration each cycle. The standard curves with a slope between approximately -3.1 and -3.6 are typically acceptable for most applications requiring accurate quantification (90 -110 % reaction efficiency). An Rsq value is the fit of all data to the standard curve plot. If all the data lie perfectly on the line, the Rsq will be 1.00. As the data fall further from the line, the Rsq decreases. An Rsq value ≥ 0.985 is acceptable for most assays. The H3 standard curve yielded a slope of -3.423 (efficiency= 95.9%) and Rsq= 0.999. These values indicate satisfactory amplification efficiency and overall performance of the real-time RT-PCR assay for canine influenza detection.

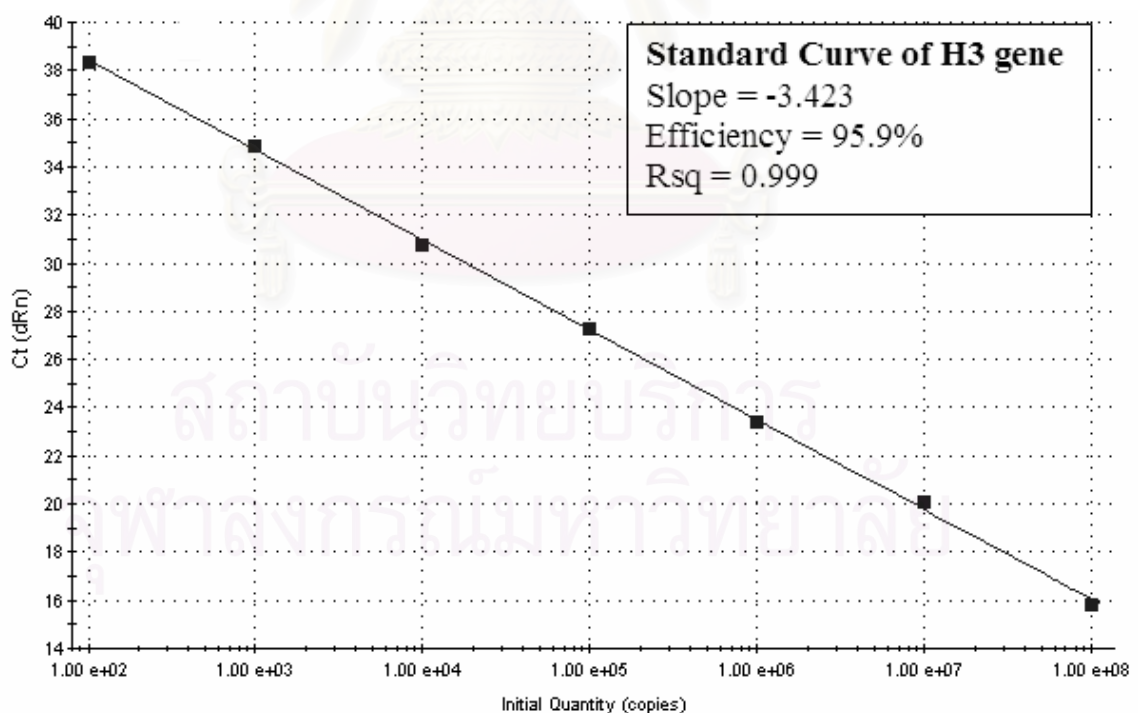


Figure 32 Standard curves of H3 gene was constructed by plotting the log of starting RNA concentrations against the threshold cycle (Ct) obtained from each dilution.

- **Clinical sample test of real-time RT-for canine influenza detection**

To evaluate the performance of the real-time RT-PCR test in postmortem specimens from dogs with acute respiratory disease, sixty canine lung tissue samples submitted for virologic diagnosis during 2005 were tested for the presence of canine influenza A virus by real-time RT-PCR and virus isolation. CIV was detected by real-time RT-PCR with both M and H3 genes from a total of 12 out of 60 samples (20%) whereas no amplification signal was detected with these probes in the remaining 48 samples. Aliquots from the tissue homogenates were injected into the allantois of embryonated chicken eggs and inoculated onto MDCK cells to culture CIV as described previously. Only 2 out of 12 samples that were positive for canine influenza by real-time RT-PCR yielded CIV. The low frequency of virus isolation from tissues containing CIV RNA may be attributed to the relatively late stage of infection at which animals were submitted for postmortem exam, allowing the neutralization of virus by the host immune response.

In conclusion, the single step real-time RT-PCR assay described in this study provides a rapid, sensitive and cost-effective approach for canine influenza A virus (H3N8) detection. Rapid laboratory diagnosis of canine influenza A virus (H3N8) infections in the early stage of the disease can yield information relevant to patient clinical management and facility biosecurity protocols.

CHAPTER V

CONCLUSION AND DISCUSSION

Molecular characterization of H5N1 influenza A virus in Thailand 2004

The genome of influenza A virus contains 8 double stranded RNA segments. Each RNA segment carries a particular gene constellation responsible for viral surface proteins, replication and assembly. While HA and NA molecules are responsible for viral surface proteins, other 6 viral internal genes; PB2, PB1, PA, NP, M and NS are required for viral replication and assembly. The replicative complex such as PB2, PB1 and PA together with NP play a crucial role in viral infectivity of the different host range environments [80].

The first known H5 virus (H5N3) was isolated from Tern in 1961, A/tern/South Africa/61. It was shown highly pathogenic in chickens [81]. Since H5N1 with the high degree of pathogenicity has been associated with multiple basic amino acids at the cleavage site of HA, "QRKKR". We found that by now, this cleavage site in H5 of A/Chicken/Nakorn-Pathom/Thailand/CU-K2/04 had changed into "QRERRRKKR" by inserting additionally basic amino acids into the sequence and hence still furthering relatively pathogenicity [40].

In comparison, A/Chicken/NakornPathom/Thailand/CU-K2/04 and H5N1 viruses isolated from Vietnam, 2004 may be a virus from ducks having undergone reassortment in the course of 2000-2003 whereas receiving the HA from the recent outbreak in Vietnam 2004 [82]. Furthermore, The NA gene has only been shown to be closely related to the group of A/Goose/Guangdong/1/96 and A/Goose/Guangdong/3/97 (H5N1), the ancestor viruses. Previously, H5N1 has been associated with multiple outbreaks in a short period of time providing newly emerged viruses circulating in Hong Kong and China in 2000-2001. Although the correct origin of the outbreak cannot be determined, we speculate that on the evolutionary scale this virus is genetically linked to duck viruses of the recent years. These findings will prove invaluable for future analysis of these viruses although the reservoir of H5 as yet remains to be identified.

The twenty-amino-acid deletion of the NA molecule has been reported (Figure 16). However, these findings have been previously described [80]. The result suggests that the avian influenza isolated in Thailand 2004 was an emerged virus derived from those collected in 2001. Although, A/Chicken/Nakorn-Pathom/Thailand/ CU-K2/04 has no relation to the early outbreak of 1997 but shows remarkable similarity with the avian viruses of the year 2000-2001. These remarkable findings have been shown by the phylogenetic analysis and amino acid sequences of PB2, PA, NP and M2. The 2001 surveillance report on outbreaks in the Hong Kong live-bird market suggested another hit of H5N1 in the very near future by H5N1 and as predicted it occurred in 2003-2004. Conclusively, A/Chicken/Nakorn-Pathom/Thailand/CU-K2/04 had recently evolved from viral lineages of the years, 2000-2003.

The NS gene was important in regulating the host cell response triggered by virus infection. The NS1 protein has been suggested to perform an accessory function for the optimal replication of the virus in its host. The C- terminus of the NS protein played an important role in inhibiting of IFN expression [83]. The ESEV residues in the c-terminal and Asp92 of NS1 were observed in virus isolated from Thailand, implying that this isolate was highly virulent but sensitive to IFN and TNF- α treatment [84]. The 5-amino-acid deletion in NS of HPAI H5N1 in Hong Kong has been previously described [80]. In 1997 viruses, no deleted sequences were detected but this deletion was clearly identified in the 2000-2001 viruses (Figure 17). However, the associated function of the 5-amino-acid deletion of the NS protein still requires additional investigation. Although, the function of NS after 5-amino-acid deletion is still unknown, somehow it played a major part in the evolution of NS. It is noteworthy that all new H5N1 viruses were evolved with this 5-amino-acid deletion.

The CU-K2 isolate contains Glu627 of PB2 which may indicate that the virus had less efficient replication capability in mammalian host. Moreover, substitution within residues including Leu26, Val27, Ala30, and Ser31 of the M2 ion channel protein were used to predict for Amantadine-resistant mutants [85]. The Oseltamivir resistant mutant based on the substitution of His to Tyr at position 274 of neuraminidase was not observed in the CU-K2 isolate. The result revealed that the CU-K2 isolate was resistant to amantadine but sensitive to Oseltamivir, implying different anti-viral drug administration during clinical treatment of infected patients.

To our conclusion, the phylogenetic analyses subsequent to the sequencing of the 8 gene segments of H5N1 have demonstrated the genetic relation of the virus to the H5N1 viruses of the early outbreaks. Hence, the H5N1 of Thailand collected in the early 2004 represents a continuation of the viral lineage collected in 2000-2001 from Hong Kong and China and share an epidemic occurrence with the Vietnamese bird flu rather than that of the lineage viruses from 1997.



สถาบันวิทยบริการ
จุฬาลงกรณ์มหาวิทยาลัย

Molecular diagnosis of H5N1 influenza A virus

The conventional diagnostic methods for influenza detection comprise the use of embryonated fowl egg or MDCK cells inoculated with the virus, subsequent induction of virus culture stained with immunofluorescent dye and antigen subtyping based on haemagglutination inhibition (HI). These methods are sensitive and accurate but are also time-consuming and tedious. Commercially available of immunofluorescence assay (IFA) and Enzyme Linked Immunosorbant assay (ELISA) are applied for rapid detection of influenza virus but have proven less sensitive and specific than virus culture [77, 86, 87].

A number of molecular methods can be employed for the rapid and specific detection of influenza viruses, the majority of which are based on PCR methodology (Table 16). Each of these methods has advantages and disadvantages, and some, or all, of these factors may influence the method of choice. When selecting which assay to use, there are several factors that should be taken into consideration. These include the requirement for qualitative, semi-quantitative or quantitative data, and the nature and number of samples to be analysed. In addition, the available time and resources of the laboratory and the skill of the staff involved must also be considered [77].

Table 16 Properties of molecular methods suitable for detection of influenza viruses

Method	Advantages	Disadvantages
Hybridisation	High specificity Flexible formats Inexpensive	Sensitivity Time-consuming
PCR	Sensitive and specific Allows further product analysis	Qualitative, not usually quantitative
Multiplex PCR	Sensitive and specific Tests >1 target per assay Allows further product analysis	Requires extensive optimisation to ensure no false negatives or primer competition May be limited by product size
PCR-EIA	Sensitive and specific High throughput Not limited by product size Can be multiplexed	Does not allow further product analysis Requires additional evaluation/validation before use
Real-time PCR	Sensitive and specific Rapid Can be quantitative Can be multiplexed	Requires specialised equipment Product analysis not always feasible
NASBA	Sensitive and specific Can be quantitative	Three enzymes used Time-consuming RNA product analysis less feasible
Microarrays	Sensitive and specific Tests many targets per assay	Requires specialised equipment and extensive development Does not allow further product analysis

In times of influenza A virus subtype H5N1 outbreak, preparations for outbreak termination and re-emergence prevention are crucial. Therefore, a rapid, accurate and cost saving molecular diagnostic method is important for large-scale screening and surveillance of the outbreak of this virus.

Multiplex RT-PCR for H5N1 influenza A virus detection

This study describes simultaneous amplification of 3 target genes (H5, N1 and M) in multiplex format for influenza A virus subtype H5N1 detection. The primer set for multiplex RT-PCR was selected so that the amplified products could be clearly separated in an agarose gel. The sizes of the A-type Matrix gene, the H5- and N1-subtype specific DNA fragments were 276, 189 and 131 bp, respectively. Since the present method has been carried out in a single-tube, single-step process (RT-PCR), the risk of carryover contamination was considerably reduced. Moreover, a single-step process has also proven less time consuming than the two-step process.

A single step multiplex RT-PCR can be performed on a less costly instrument and allows simultaneously detection the influenza A virus H5, N1 and M genes. Hence, influenza A virus subtype H5N1 detection based on a single step multiplex RT-PCR may be more appropriate for large-scale molecular screening in those areas unable to afford advanced real-time PCR or NASBA instruments.

In conclusion, the single step multiplex RT-PCR assay described in this study provides a rapid, cost saving and effective way for simultaneous detection of the M, H5 and N1 genes in multiplex format, thus rendering it feasible and attractive for large-scale screening, particularly in times of influenza A virus subtype H5N1 outbreak. However, this molecular diagnostic method utilizes primer sets specific for the detection of the currently endemic influenza A virus subtype H5N1 strain. The primer sets in this study target the haemagglutinin and neuraminidase genes which have experienced a high rate of evolution. Therefore, it may be necessary to re-evaluate the primer sequences to accommodate for the genetic variation of influenza A viruses.

Application of multiplex RT-PCR for H5N1 influenza detection

This technique was applied for efficiently detection and initial identification of H5N1 influenza viruses isolated from several infected host species during various outbreaks occurred during the 2004 until the present time. Therefore, the multiplex RT-PCR was performed and cited as a reference method for H5N1 influenza virus detection in several research studies including:

- Determination of H5N1 influenza A virus infection in tigers during the outbreak of this virus in Sriracha tiger zoo at Chonburi province, Thailand [49].
- Detection and genetic characterization of H5N1 influenza A viruses isolated from zoo tigers in Thailand [88].
- Identification and genetic characterization of influenza A viruses (H5N1) isolated from 3rd wave of Thailand avian influenza outbreaks [89].
- Determination of H5N1 avian influenza in naturally infected domestic cat [11].
- Detection of H5N1 influenza A virus from infected human plasma [90].
- Screening of avian influenza in food markets with live birds [91].
- This technique was reviewed in current methods for the rapid diagnosis of bioterrorism-related infectious agents [92].
- Development of the single step multiplex RT-PCR assay for detecting H5 and H7 avian influenza A viruses [93].

Multiplex real-time RT-PCR for H5N1 influenza A virus detection

This study described a single-step multiplex real-time RT-PCR for H5N1 influenza A virus detection. The selected primers and 3 TaqMan MGB probes labeled with FAM, VIC and NED corresponding to M, H5 and N1 were used in multiplex format for simultaneous detection of triple fluorescent signals. The advantages of real-time RT-PCR lie in the rapidity, high specificity and high sensitivity. Moreover, the assay provides quantitative data suitable for absolute or relative quantitation of viral loads in clinical specimens.

The primers and probes used in this study target the hemagglutinin (H5) and neuraminidase (N1) genes which have experienced a high rate of evolutionary changes and the primers and probe of the matrix (M) gene were selected from the conserved region of all subtypes of influenza A viruses. Thus, there is no suitable region for a conventional TaqMan probe (25-30 bp in length). Basically, the T_m of the TaqMan probe should be 10° C higher than that of the primer. Therefore, TaqMan MGB was used instead as this probe is shorter in length and coupled with a minor groove binder which enhances the T_m of the probe. Moreover, TaqMan MGB has a non-fluorescent quencher attached to the 3' end which will not interfere with fluorescent signal detection.

This technique was developed based on the ABI Real-time PCR system (Applied Biosystems), which contains a unique fluorescent detector (especially detector for NED reporter dye). The NED reporter dye may not be suitable for detector in other real-time PCR instruments such as Mx3005P (Stratagene), Roter gene 3000 (Corbett Research), i-Cycler iQ (BioRad), Smart Cycler (Cepheid), Mastercycler Ep realplex (Eppendorf) and Light Cycler (Roche). However, the particular probe can be carried out on other real-time PCR platforms by modification with appropriate reporter dyes instead (Appendix A).

The single step real-time real-time RT-PCR provided several advantages over the conventional multiplex RT-PCR in terms of less time consuming because post-PCR processing steps are not required resulting in decrease the risk of contamination. Moreover, utilizing of TaqMan probe yielded more specificity and sensitivity of the assay. Finally, the real-time RT-PCR assay provided accurate quantitative data whereas the conventional RT-PCR yielded just semi-quantitative data.

Application of real-time RT-PCR for H5N1 influenza A virus detection

One of the applications of this technique was the quantitation of influenza A viral RNA isolated from infected tiger tissues by using real-time RT-PCR (unpublished data). The real-time RT-PCR assay allowed linear quantitation of influenza matrix RNA in the range 10^{10} - 10^2 copies/reaction of standard *in vitro* transcribed matrix RNA. To determine the amount of viral RNA in several tiger tissues, RNA extracted from each tissue sample was analyzed based on real-time RT-PCR and the results were normalized according to the 28S rRNA gene-specific amplification. The slopes of the standard curves for matrix gene of influenza virus and 28S rRNA gene were -3.50 and -3.31, respectively (mean of 3 consecutive experiments), with R^2 value >0.99 in both cases (Figure 33).

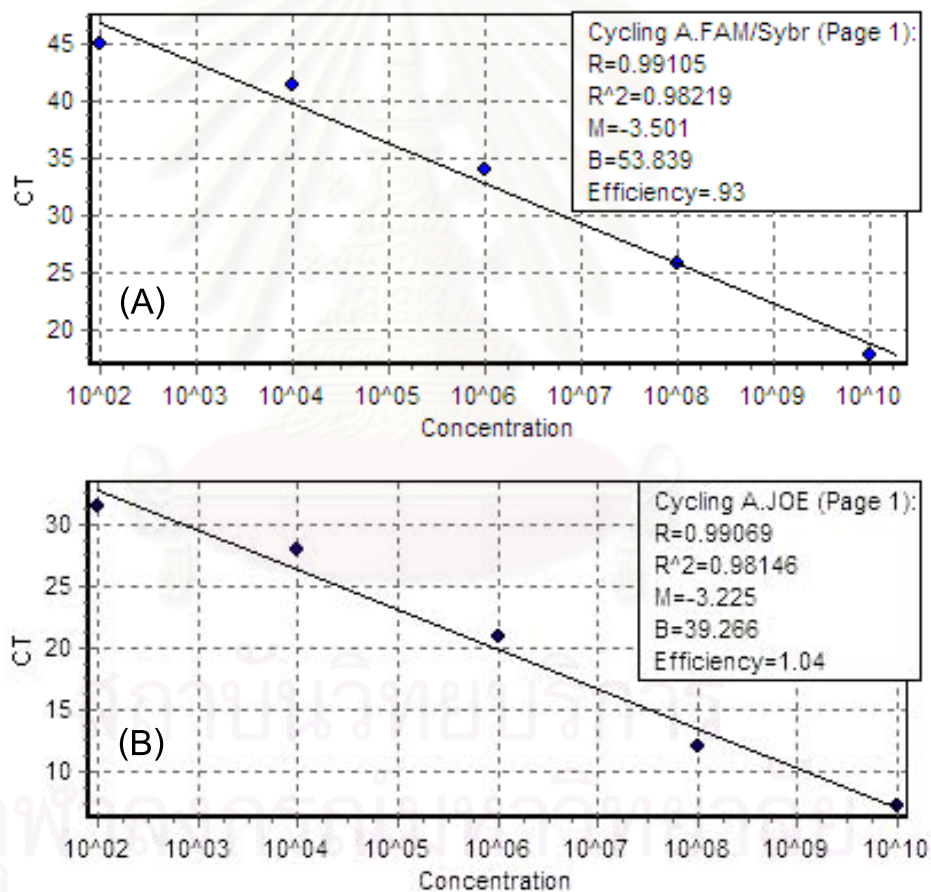


Figure 33 Standard curve for matrix (A) and 28S rRNA (B) based on real-time RT-PCR assay. Serially diluted of *in vitro* transcribed RNAs corresponding to matrix and 28S rRNA were amplified and analyzed in real time. The threshold cycle (Ct) values were plotted against copy number in order to construct the standard curve.

Absolute quantitation by real-time RT-PCR was performed on tissues obtained from various organs of infected tigers and leopard in order to determine tissue tropism of the H5N1 influenza distribution in a leopard and tigers (Table 17). Unfortunately, we could not collect every organ and types of organs obtained from each individual tigers are not exactly the same. Therefore, determination of tissue tropism could not be compared. However, the results implied that the H5N1 influenza A viruses could be detected in several organs with slightly alteration in the viral loads.

Table 17 Normalized viral RNA in different tissue organs of infected tigers and leopard.

Organ	Leopard	Tiger 1	Tiger 2	Tiger 3	Tiger 4
Brain	2.12E-04	2.89E-06	No sample	No sample	No sample
Lung	8.86E-06	7.08E-06	8.16E-06	9.75E-02	No sample
Trachea	No sample	No sample	No sample	2.63E-01	1.61E-01
Liver	No sample	2.27E-07	2.39E-08	No sample	9.78E+01
Spleen	7.90E-09	No sample	No sample	5.04E-01	5.38E-01
Kidney	No sample	No sample	No sample	2.28E-04	1.17E-02
Lymph node	No sample	No sample	No sample	No sample	1.11E-02
Heart	No sample	5.47E-06	2.57E-07	2.64E-01	No sample
Pancreas	No sample	No sample	No sample	3.04E-02	6.86E-03

Evaluation of primer and probe sequences

According to rapid accumulations of nucleotide substitutions (antigenic drift) within the gene segments (especially HA and NA genes) of the influenza A virus, it is crucial to monitor the complementary between the sequences of primer/probe and the nucleotide sequences of the virus in order to avoid false negative results obtained from RT-PCR and real-time RT-PCR detection. Therefore, the primers and probes used in the single step multiplex RT-PCR and real-time RT-PCR were multiple aligned with nucleotide sequences obtained from H5N1 influenza A viruses isolated from several host species and several provinces during the 2004-2006 outbreaks in Thailand.

The results of multiple alignments of matrix primers and probe (Figure 34) revealed the matrix TaqMan MGB probe (CU-MP₈₃₉) yielded perfect complementary with all strains used. The matrix forward primer (CU-MF₇₁₈) was almost perfect complement with all strains aligned except only one non-significant mismatch at the 5'-end with A/chicken/Thailand/PC-168/2006(H5N1) strain, whereas the matrix reverse primer (CU-MR₉₀₉) showed only one mismatch within the internal regions with 3 strains of virus, including A/chicken/Bangkok/Thailand/CU-3/04(H5N1), A/chicken/Nontaburi/Thailand/CK-162/2005(H5N1) and A/chicken/Thailand/NP-172/2006(H5N1). Because only one nucleotide mismatch at 5'-end and internal position are not significant affect the specificity and sensitivity of the primer, thus implying that the matrix primers and probe can be used to detect all strains of H5N1 influenza A viruses during 2004-2006 outbreaks in Thailand.

From multiple alignments of neuraminidase(N1) primers and probe (Figure 35) revealed that the N1 forward primer (CU-N1F₅₃₉) yielded perfect complement with all strains used whereas N1 TaqMan probe (CU-N1P₆₃₇) and N1 reverse primer (CU-N1R₆₆₉) showed only one mismatch in internal position with A/chicken/Thailand/PC-170/2006(H5N1) and A/chicken/Thailand/NP-172/2006(H5N1), respectively. These implied that the N1 primers and probe can be used to detect all strains of H5N1 influenza A viruses during 2004-2006 outbreaks in Thailand.

According to the multiple alignments of hemagglutinin (H5) primers and probe (Figure 36) revealed that H5 TaqMan MGB probe (CU-H5P₁₅₃₅) yielded perfect complementary with all strains used. The H5 forward primer (CU-H5F₁₄₀₀) was almost perfect complement with all strains aligned except only one non-significant mismatch at third position from the 5'-end with A/quail/Nakhon Pathom/Thailand/QA-161/2005(H5N1) whereas the H5 reverse primer (CU-H5R₁₅₉₀) showed only one mismatch within the internal regions or 5'-end with 7 strains of virus, including A/crow/Bangkok/Thailand/CU-4/04(H5N1), A/crow/Bangkok/Thailand/CU-15/04(H5N1), A/kalij pheasant/Thailand/CU-4/2004(H5N1), A/kalji pheasant/Bangkok/Thailand/CU-18/04(H5N1), A/white peafowl/ Bangkok/Thailand/CU-16/04(H5N1), A/white peafowl/ Bangkok/Thailand/CU-29/04(H5N1) and A/chicken/Thailand/PC-170/2006(H5N1). Because only one nucleotide mismatch at 5'-end or internal position are not significant affect the specificity and sensitivity of the primer, thus implying that the H5 primers and probe can be used to detect all strains of H5N1 influenza A viruses during 2004-2006 outbreaks in Thailand.

Taken together, the M, H5 and N1 primers and probes used in this study seem to be able to detect H5N1 influenza A viruses during 2004-2006 outbreaks in Thailand and might be able to continuously detect the virus in the current outbreak until the occurrence of new variants containing significant nucleotide sequence mismatch with the primers and probes.

สถาบันวิทยบริการ
จุฬาลงกรณ์มหาวิทยาลัย

Strains of virus	CU-MF ₇₁₈	CU-MP ₈₃₉	CU-MR ₉₀₉
A/chicken/Nakorn-Patomb/Thailand/CU-K2/2004 (H5N1)	TAATCTTCTTGAAAAATTGCAG	TTGTGGATTCTTGATCG	TGAAAAGAGGGCCTGCTACGG
A/chicken/Ayutthaya/Thailand/CU-23/04 (H5N1)
A/chicken/Chonburi/Thailand/CU-7/04 (H5N1)
A/chicken/Prachinburi/Thailand/CU-8/04 (H5N1)
A/chicken/Suphanburi/Thailand/CU-9/04 (H5N1)
A/chicken/Chachoengsao/Thailand/CU-10/04 (H5N1)
A/chicken/Bangkok/Thailand/CU-3/04 (H5N1)	A.....
A/chicken/Nakhon Sawan/Thailand/CU-12/04 (H5N1)
A/chicken/Saraburi/Thailand/CU-17/04 (H5N1)
A/chicken/Lopburi/Thailand/CU-38/04 (H5N1)
A/chicken/Ratchaburi/Thailand/CU-68/04 (H5N1)
A/chicken/Thailand/2/04 (H5N1)
A/little grebe/Thailand/Phichit-01/2004 (H5N1)
A/duck/Chonburi/Thailand/CU-2/04 (H5N1)
A/duck/Chonburi/Thailand/CU-5/04 (H5N1)
A/duck/Nakhon Pathom/Thailand/CU-71/04 (H5N1)
A/duck/Saraburi/Thailand/CU-74/04 (H5N1)
A/crow/Bangkok/Thailand/CU-4/04 (H5N1)
A/crow/Bangkok/Thailand/CU-15/04 (H5N1)
A/crow/Bangkok/Thailand/CU-25/04 (H5N1)
A/crow/Bangkok/Thailand/CU-35/04 (H5N1)
A/pigeon/Samut Prakan/Thailand/CU-202/04 (H5N1)
A/sparrow/Phang-Nga/Thailand/CU-203/04 (H5N1)
A/Mynas/Ranong/Thailand/CU-209/04 (H5N1)
A/kalji pheasant/Bangkok/Thailand/CU-18/04 (H5N1)
A/white peafowl/Bangkok/Thailand/CU-16/04 (H5N1)
A/white peafowl/Bangkok/Thailand/CU-29/04 (H5N1)
A/ostrich/Samut Prakan/Thailand/CU-19/04 (H5N1)
A/ostrich/Samut Prakan/Thailand/CU-31/04 (H5N1)
A/rollers/Bangkok/Thailand/CU-26/04 (H5N1)
A/leopard/Suphanburi/Thailand/Leo-1/04 (H5N1)
A/tiger/Suphanburi/Thailand/Ti-1/04 (H5N1)
A/tiger/Thailand/CU-T3/2004 (H5N1)
A/tiger/Thailand/CU-T7/2004 (H5N1)
A/cat/Thailand/KU-02/04 (H5N1)
A/Thailand/1 (KAN-1)/2004 (H5N1)
A/Thailand/2 (SP-33)/2004 (H5N1)
A/Thailand/SP83/2004 (H5N1)
A/Thailand/Ran353/2004 (H5N1)
A/Thailand/5 (KK-494)/2004 (H5N1)
A/Thailand/Chaiyaphum/622/2004 (H5N1)
A/Thailand/Prachinburi/6231/2004 (H5N1)
A/Thailand/676/2005 (H5N1)
A/Thailand/NK165/2005 (H5N1)
A/quail/Thailand/Nakhon Pathom/QA-161/2005 (H5N1)
A/chicken/Kanchanaburi/Thailand/CK-160/2005 (H5N1)
A/chicken/Nontaburi/Thailand/CK-162/2005 (H5N1)	G.....
A/chicken/Thailand/NP-172/2006 (H5N1)T.....
A/chicken/Thailand/PC-168/2006 (H5N1)	C.....
A/chicken/Thailand/PC-170/2006 (H5N1)

Figure 34 Multiple alignments of matrix primers and probe with nucleotide sequences of matrix genes obtained from various strains of H5N1 influenza A viruses isolated during 2004-2006 outbreaks in Thailand. Dots represent identical nucleotide residues.

Strains of virus	CU-N1F ₅₃₉	CU-N1P ₆₃₇	CU-N1R ₆₆₉
A/chicken/Nakorn-Patom/Thailand/CU-K2/2004 (H5N1)	GTTTGAGTCTGTTGGCTTGGTC	GTGGCTGTATTGAAATACAA	GGCATAAATAACAGACACTATCA
A/chicken/Ayutthaya/Thailand/CU-23/04 (H5N1)
A/chicken/Ayutthaya/Thailand/CU-24/04 (H5N1)
A/little grebe/Thailand/Phichit-01/2004 (H5N1)
A/duck/Thailand/CU-2/2004 (H5N1)
A/duck/Chonburi/Thailand/CU-5/04 (H5N1)
A/duck/Nakhon Pathom/Thailand/CU-71/04 (H5N1)
A/duck/Saraburi/Thailand/CU-74/04 (H5N1)
A/duck/Thailand/KU-KPS/2004 (H5N1)
A/crow/Bangkok/Thailand/2004 (H5N1)
A/crow/Bangkok/Thailand/CU-4/04 (H5N1)
A/crow/Bangkok/Thailand/CU-15/04 (H5N1)
A/crow/Bangkok/Thailand/CU-25/04 (H5N1)
A/crow/Bangkok/Thailand/CU-35/04 (H5N1)
A/pigeon/Samut Prakan/Thailand/CU-202/04 (H5N1)
A/pigeon/Thailand/KU-03/04 (H5N1)
A/sparrow/Phang-Nga/Thailand/CU-203/04 (H5N1)
A/Mynas/Ranong/Thailand/CU-209/04 (H5N1)
A/open bill/Bangkok/Thailand/2004 (H5N1)
A/kalji pheasant/Bangkok/Thailand/2004 (H5N1)
A/kalji pheasant/Bangkok/Thailand/CU-18/04 (H5N1)
A/white peafowl/Bangkok/Thailand/2004 (H5N1)
A/ostrich/Samut Prakan/Thailand/CU-19/04 (H5N1)
A/ostrich/Samut Prakan/Thailand/CU-31/04 (H5N1)
A/white peafowl/Bangkok/Thailand/CU-16/04 (H5N1)
A/white peafowl/Bangkok/Thailand/CU-29/04 (H5N1)
A/rollers/Bangkok/Thailand/CU-26/04 (H5N1)
A/leopard/Suphanburi/Thailand/Leo-1/04 (H5N1)
A/tiger/Suphanburi/Thailand/Ti-1/04 (H5N1)
A/tiger/Thailand/CU-T3/2004 (H5N1)
A/tiger/Thailand/CU-T7/2004 (H5N1)
A/Tiger/Thailand/VSMU-1-SPB/2004 (H5N1)
A/cat/Thailand/KU-02/04 (H5N1)
A/dog/Thailand-Suphanburi/KU-08/04 (H5N1)
A/Thailand/1 (KAN-1)/2004 (H5N1)
A/Thailand/2 (SP-33)/2004 (H5N1)
A/Thailand/3 (SP-83)/2004 (H5N1)
A/Thailand/4 (SP-528)/2004 (H5N1)
A/Thailand/5 (KK-494)/2004 (H5N1)
A/Thailand/LPEN-2004/2004 (H5N1)
A/Thailand/676/2005 (H5N1)
A/Thailand/NK165/2005 (H5N1)
A/Thailand/NKPE/2005 (H5N1)
A/Thailand/NKNE/2005 (H5N1)
A/Thailand/PPPE/2005 (H5N1)
A/Thailand/PPNE/2005 (H5N1)
A/Thailand/MA60/2005 (H5N1)
A/chicken/Thailand/Kanchanaburi/CK-160/2005 (H5N1)
A/quail/Thailand/Nakhon Pathom/QA-161/2005 (H5N1)
A/chicken/Thailand/Nontaburi/CK-162/2005 (H5N1)
A/chicken/Thailand/MP-172/2006 (H5N1)	C.....
A/chicken/Thailand/PC-168/2006 (H5N1)
A/chicken/Thailand/PC-170/2006 (H5N1)

Figure 35 Multiple alignments of neuraminidase (N1) primers and probe with nucleotide sequences of N1 genes obtained from various strains of H5N1 influenza A viruses isolated during 2004-2006 outbreaks in Thailand. Dots represent identical nucleotide residues.

Strains of virus	CU-H5F ₁₄₀₀	CU-H5P ₁₅₃₅	CU-H5R ₁₅₉₀
A/chicken/Nakorn-Patom/Thailand/CU-R2/2004 (H5N1)	GACTCAAATGTC AAGAACCTTTA	ACGGAACGTATGACTAC	TAAAAAGAGAGGAAATAAGTGG
A/chicken/Thailand/CH-2/2004 (H5N1)
A/chicken/Bangkok/Thailand/CU-3/04 (H5N1)
A/chicken/Ayutthaya/Thailand/CU-23/04 (H5N1)
A/little grebe/Thailand/Phichit-01/2004 (H5N1)
A/duck/Thailand/CU-2/2004 (H5N1)
A/duck/Chonburi/Thailand/CU-5/04 (H5N1)
A/duck/Nakhon Pathom/Thailand/CU-71/04 (H5N1)
A/duck/Saraburi/Thailand/CU-74/04 (H5N1)
A/crow/Bangkok/Thailand/CU-4/04 (H5N1)C.....
A/crow/Bangkok/Thailand/CU-15/04 (H5N1)A.....
A/crow/Bangkok/Thailand/CU-25/04 (H5N1)
A/crow/Bangkok/Thailand/CU-35/04 (H5N1)
A/pigeon/Thailand/KU-03/04 (H5N1)
A/pigeon/Samut Prakan/Thailand/CU-202/04 (H5N1)
A/sparrow/Phang-Mga/Thailand/CU-203/04 (H5N1)
A/Mynas/Ranong/Thailand/CU-209/04 (H5N1)
A/openbill/Thailand/CU-2/2004 (H5N1)A.....
A/kalij pheasant/Thailand/CU-4/2004 (H5N1)A.....
A/kalji pheasant/Bangkok/Thailand/CU-18/04 (H5N1)A.....
A/white peafowl/Bangkok/Thailand/CU-16/04 (H5N1)A.....
A/ostrich/Samut Prakan/Thailand/CU-19/04 (H5N1)
A/ostrich/Samut Prakan/Thailand/CU-31/04 (H5N1)
A/rollers/Bangkok/Thailand/CU-26/04 (H5N1)
A/white peafowl/Bangkok/Thailand/CU-29/04 (H5N1)A.....
A/leopard/Suphanburi/Thailand/Leo-1/04 (H5N1)
A/tiger/Suphanburi/Thailand/Ti-1/04 (H5N1)
A/tiger/Thailand/CU-T3/2004 (H5N1)
A/tiger/Thailand/CU-T7/2004 (H5N1)
A/tiger/Thailand/SPB-1 (H5N1)
A/cat/Thailand/KU-02/04 (H5N1)
A/dog/Thailand-Suphanburi/KU-08/04 (H5N1)
A/Thailand/1 (KAN-1)/2004 (H5N1)
A/Thailand/2 (SP-33)/2004 (H5N1)
A/Thailand/3 (SP-83)/2004 (H5N1)
A/Thailand/4 (SP-528)/2004 (H5N1)
A/Thailand/5 (KK-494)/2004 (H5N1)
A/quail/Nakhon Pathom/Thailand/QA-161/2005 (H5N1)T.....
A/chicken/Kanchanaburi/Thailand/CK-160/2005 (H5N1)
A/chicken/Nontaburi/Thailand/CK-162/2005 (H5N1)
A/Thailand/676/2005 (H5N1)
A/Thailand/NK165/2005 (H5N1)
A/Thailand/NKFE/2005 (H5N1)
A/Thailand/NKNP/2005 (H5N1)
A/Thailand/PPPE/2005 (H5N1)
A/Thailand/PPNE/2005 (H5N1)
A/Thailand/HA20/2005 (H5N1)
A/chicken/Thailand/NP-172/2006 (H5N1)
A/chicken/Thailand/PC-168/2006 (H5N1)
A/chicken/Thailand/PC-170/2006 (H5N1)A.....
A/chicken/Nakhonphanom/NIAHL13718/2006 (H5N1)

Figure 36 Multiple alignments of hemagglutinin (H5) primers and probe with nucleotide sequences of H5 genes obtained from various strains of H5N1 influenza A viruses isolated during 2004-2006 outbreaks in Thailand. Dots represent identical nucleotide residues.

Discrimination between HPAI and LPAI by real-time RT-PCR with melting analysis

Conventionally, the standard method used to determine whether an avian influenza virus is highly pathogenic involves the intravenous inoculation of a minimum of eight susceptible 4- to 8-week old chickens with infectious virus. If the virus lethal for at least 75% (six of the eight) chickens within 10 days, the virus strain is considered to be highly pathogenic. Because the highly pathogenic of H5N1 avian influenza, a bio-safety level 3 laboratory for animal experiment is required in order to perform the pathogenicity test. Thus, performing such test in animal will be impossible in areas lack of the BSL3 laboratory for animal. An additional test involves sequencing of HA gene of the virus. All highly pathogenic avian influenza viruses contain a multiple basic amino acid insertion at the cleavage site, which known to be associated with high lethality. However, nucleotide sequencing is time-consuming and required several manipulation steps including amplification, gel electrophoresis, purification and cycle sequencing, thus rendering the risks of contaminations during the process and may not suitable for large scale screening in outbreak areas. Therefore, the real-time RT-PCR with melting curve analysis described here may served as a rapid and simple screening method based on the differences in %GC content and amplicon length within the cleavage site of H5 gene resulting in distinct T_m values for discrimination between HPAI and LPAI. Moreover, the coefficient of variation (CV) of T_m (inter-assay) was 0.27 and 0.29 for HPAI and LPAI, respectively; indicating high reproducibility of the assay.

There are a few variations occurred within the cleavage site of high pathogenic avian influenza (HPAI) strain (Figure 37), which may affect the melting curve and melting temperature (T_m) obtained from these strains. T_m value depends on %GC contents within the PCR amplicon. Higher %GC contents leads to higher melting temperature.

Therefore, the %GC contents within the PCR product amplified by CU-H5F₁₀₀₁ and CU-H5R₁₀₂₄ primer set were analyzed in order to estimate the alteration of T_m values of these strains (Figure 37). Analysis of %GC contents revealed that LPAI (PQRE----TR) contains %GC content higher than 45 leading to T_m value higher than 79°C, whereas conventional insertion of HPAI (PQRERRRKKR) yielded %GC approximately 43.55 leading to T_m of 77.5°C. Other variations including “PQREKRRKKR”, “PQRERKRKK” and “PLRER-RRKR” HPAI variants contains %GC lower than 43 resulting in T_m shift to lower than 77°C. Therefore, the variants of HPAI HA cleavage sites yielded a little alteration of T_m from the conventional HPAI but more clearly distinguishable from LPAI strain because the T_m values of these HPAI variants shift to lower temperature.

		Cleavage site	↓	%GC
LPAI	A/avian/NY/118547-11/01 (H5N2)	P Q R E - - - - T R	G	46.43
	A/duck/Minnesota/1525/81	* * * * - - - - * * *		48.21
	A/gull/Pennsylvania/4175/83	* * * * - - - - * K *		45.54
HPAI	A/Goose/Guangdong/1/96	* * * * R R R K K * *		44.35
	A/chicken/Nakorn-Patom/Thailand/CU-K2/04	* * * * R R R K K * *		43.55
	A/cat/Thailand/KU-02/04	* * * * R R R K K * *		43.55
	A/tiger/Thailand/CU-T7/04	* * * * R R R K K * *		43.55
	A/dog/Thailand-Suphanburi/KU-08/04	* * * * R R R K K * *		43.55
	A/chicken/Thailand/PC-168/06	* * * * R R R K K * *		44.35
	A/openbill/Thailand/CU-2/04	* * * * K R R K K * *		42.74
	A/chicken/Thailand/Nontaburi/CK-162/05	* * * * K R R K K * *		41.94
	A/Thailand/NK165/05	* * * * K R R K K * *		41.94
	A/Chicken/Thailand/PC-170/06	* * * * K R R K K * *		41.94
	A/whitepeafowl/Bangkok/Thailand/CU-16/04	* * * * R K R K K * *		42.74
	A/KaljiPheasant/Bangkok/Thailand/CU-18/04	* * * * R K R K K * *		42.74
	A/chicken/Thailand/NP-172/06	* L * * R - R R K * *		41.32
	A/chicken/Nongkhai/NIAH400802/07	* L * * R - R R K * *		41.32

Figure 37 Variations of the multiple basic amino acids insertion within the cleavage site of the hemagglutinin (H5). Stars represent identical amino acid residues.

In conclusion, the melting curve analysis real-time RT-PCR described here provides a rapid, accurate and high-throughput approach to discriminate between HPAI and LPAI. This assay is particularly attractive for large-scale screening of suspected subtype H5 influenza A virus during outbreaks, in order to initially identify candidate LPAI that could be used as vaccine strains.

Molecular characterization and molecular diagnosis of H3N8 canine influenza

Isolation and characterization of influenza A subtype H3N8 viruses from non-greyhound dogs with respiratory disease in Florida

In this study, we report for the first time the isolation and characterization of canine influenza virus from non-greyhound dogs. H3N8 viruses were isolated from non-greyhound dogs involved in fatal canine influenza outbreaks in a shelter and veterinary clinic in Florida in May 2005.

Since the viral hemagglutinin is a critical determinant of the host specificity of influenza virus [56], we compared the nucleic acid and deduced amino acid sequences for the canine and equine H3 to identify residues that may be associated with efficient replication in different species or dog breeds. There were five conserved amino acid substitutions in all of the canine viruses that differentiated them from contemporary equine viruses: I15M, N83S, W222L, I328T, and N483T. The substitution of methionine for isoleucine at position 15 maintains the hydrophobicity of the residue and is of unknown functional significance. Position 83 located within antigenic site E of human H3 has been implicated in antigenic drift [94]. The substitution of serine for asparagine at position 83 in canine H3 maintains the polar nature of the residue, but the functional significance in the evolution of canine influenza is not immediately apparent. The substitution of leucine for tryptophane at position 222 represents a non-conservative change adjacent to the sialic acid binding pocket, suggesting a potential modulator function in adaptation of equine influenza virus to canine sialic acid receptors. This leucine substitution has also been reported in avian influenza subtype H4 infection of pigs [95] and subtype H9 infection of humans [96]. The strictly conserved isoleucine at position 328 near the cleavage site of the equine H3 hemagglutinin has been replaced by threonine in all of the canine isolates, suggesting the potential importance of threonine in recognition of the HA cleavage site by canine proteases. The replacement of asparagine with threonine at position 483 results in the loss of a glycosylation site in the HA2 subunit that is conserved in all other HA subtypes.

The phylogenetic tree of the canine and equine influenza HA genes shows that the canine genes from the two Florida 2005 isolates formed a clade with high bootstrap support that included canine/TX/04 virus and canine/IA/05. Three amino acid substitutions in the H3 differentiated this group from the earlier isolates: L118V, K261N, and G479E. Positions 118 and 261 are located in the HA1 subunit of canine H3, while position 479 is in the HA2 subunit. The HA1 subunit of human H3 contains the antibody-binding sites where amino acid substitutions occur at high frequency, presumably due to escape from humoral immune responses [97]. Although there is no evidence for high variability at positions 118 and 261, neighboring positions 121 (antigenic site D) and 262 (antigenic site E) are sites of frequent positive selection in human H3 genes. The 2005 isolates from non-greyhound dogs differed from the 2005 Iowa greyhound isolate by one amino acid change at position 492 in the HA2 subunit. The two non-greyhound isolates differed from each other by substitution of proline for serine at position 107 in the HA1 subunit of canine/Jax/05. Serine is conserved at position 107 in all other equine and canine H3 isolates except for A/Equine/Jilin/1/89 which has a threonine substitution (Guo et al., 1992). Canine/Jax/05 is antigenically distinct from the other canine isolates, which may be partially related to the proline substitution at position 107. However, there is no serologic evidence that residue 107 modulates the antigenicity of human, swine or equine H3 HAs.

With the introduction and sustained transmission of the H3N8 influenza virus in dogs, the H3 HA became the most broadly distributed subtype in mammalian species; including humans, swine, horses and dogs. Continued virologic and serologic surveillance will be important to monitor the evolution of canine influenza virus in the dog population and its impact on the health of this species as well as the possible transmission to other species.

Molecular diagnosis of H3N8 canine influenza

Canine influenza (H3N8) emerged recently in the United States as a cause of respiratory tract disease outbreaks in dogs. The aim of this study was to develop and evaluate a single step real-time RT-PCR for rapid detection of canine influenza A virus. Primers and TaqMan probe corresponding to hemagglutinin (H3) genes were used for specific detection of canine influenza. The assay was evaluated using cultured virus material as well as clinical specimens from naturally or experimentally infected dogs. Most importantly, the assay with H3 primers and probe detected as few as 10^2 copies / μ l of canine influenza virus as compared to standard *in vitro* transcribed H3 RNA. This assay compared favorably to traditional virus isolation in cell culture from postmortem specimens. Whereas 12 of 60 canine lung specimens (20%) identified CIV sequences in H3 probe assays, only 2 of 60 specimens yield CIV by isolation. In summary, the newly developed real-time RT-PCR is a rapid, sensitive and specific assay to diagnose canine influenza A virus (H3N8) infection in diagnostic laboratories and research settings. The availability of improved molecular diagnostic assays for canine influenza will facilitate virologic surveillance for this pathogen. Rapid laboratory diagnosis of canine influenza A virus (H3N8) infections in the early stage of the disease can yield information relevant to patient clinical management and facility bio-security protocols.

In conclusion, this study reported the molecular characterization and molecular diagnosis of recently emerged influenza A viruses including H5N1 avian influenza and H3N8 canine influenza. The molecular characterization provided crucial information of the nucleotide and deduced amino acid sequences which represent general and particular characteristics of the viruses in terms of subtyping, antigenicity, pathogenicity, binding affinity, ability of transmission and resistance against anti-viral treatment. In addition, the nucleotide sequences can be used to construct a phylogenetic tree representing genetic evolution and relationship among several virus strains. Moreover, these sequences were submitted into GenBank database for further investigation and information sharing between laboratories. The molecular diagnosis based on RT-PCR and real-time RT-PCR were rapid, specific and sensitive assays suitable for immediate detection and large scale screening in order to control and prevent severe outbreaks of H5N1 avian influenza and H3N8 canine influenza viruses.

REFERENCES

- [1] Nicholson KG, Wood JM, Zambon M. Influenza. Lancet 2003;362:1733-1745.
- [2] Turner D, Wailoo A, Nicholson K, Cooper N, Sutton A, Abrams K. Systematic review and economic decision modelling for the prevention and treatment of influenza A and B. Health Technol Assess 2003;7: 1-170.
- [3] Lamb RA, Krug R. Orthomyxoviridae: the viruses and their replication. In: Knipe DM, Howley PM (Eds.), Fundamental Virology, 725–770. 2001.
- [4] Fleming DM, Chakraverty P, Sadler C, Litton P. Combined clinical and virological surveillance of influenza in winters of 1992 and 1993-1994. BMJ 1995;29:290-291.
- [5] Webster RG, Bean WJ, Gorman OT, Chambers TM, Kawaoka Y. Evolution and ecology of influenza A viruses. Microbiol Rev 1992;56:152–179.
- [6] Webster RG, Laver WG, Air GM, Schild GC. Molecular mechanisms of variation in influenza viruses. Nature 1982;296:115–121.
- [7] Webby RJ, Webster RG. Emergence of influenza A viruses. Philos Trans R Soc Lond B Biol Sci 2001;356:1817-1828.
- [8] Kemble G, Greenberg H. Novel generations of influenza vaccines. Vaccine 2003;21:1789–1795.
- [9] Trampuz A, Prabhu RM, Smith TF, Baddour LM. Avian influenza: a new pandemic threat?. Mayo Clin Proc 2004;79:523-350.
- [10] Keawcharoen J, Oraveerakul K, Kuiken T, Fouchier RA, Amonsin A, Payungporn S, Noppornpanth S, Wattanodorn S, Theambooniers A, Tantilertcharoen R, Pattanarangsarn R, Arya N, Ratanakorn P, Osterhaus DM, Poovorawan Y. Avian influenza H5N1 in tigers and leopards. Emerg Infect Dis 2004;10:2189-91.
- [11] Songserm T, Amonsin A, Jam-on R, Sae-Heng N, Meemak N, Pariyothorn N, Payungporn S, Theambooniers A, Poovorawan Y. Avian Influenza H5N1 in Naturally Infected Domestic Cat. Emerg Infect Dis 2006;12:681-683.

- [12] Songserm T, Amonsin A, Jam-on R, Sae-Heng N, Pariyothorn N, Payungporn S, Theamboonlers A, Chutinimitkul S, Thanawongnuwech R, Poovorawan Y. Fatal avian influenza A H5N1 in a dog. Emerg Infect Dis 2006;12:1744-1747.
- [13] Crawford PC, Dubovi EJ, Castleman WL, Stephenson I, Gibbs EPJ, Chen L, Smith C, Hill RC, Ferro P, Pompey J, Bright RA, Medina M-J, Influenza Genomics Group, Johnson CM, Olsen CW, Cox NJ, Klimov AI, Katz JM, Donis RO. Transmission of equine influenza virus to dogs. Science 2005;310:482-485.
- [14] Claas EC, Osterhaus AD, van Beek R, De Jong JC, Rimmelzwaan GF, Senne DA, Krauss S, Shortridge KF, Webster RG. Human influenza A (H5N1) virus related to highly pathogenic avian influenza virus. Lancet 1998;351:472-477.
- [15] Tran TH, Nguyen TL, Nguyen TD, Luong TS, Pham PM, Nguyen VC, Pham TS, Vo CD, Le TQ, Ngo TT, Dao BK, Le PP, Nguyen TT, Hoang TL, Cao VT, Le TG, Nguyen DT, Le HN, Nguyen KT, Le HS, Le VT, Christiane D, Tran TT, Menno de J, Schultsz C, Cheng P, Lim W, Horby P, Farrar J; World Health Organization International Avian Influenza Investigative Team. Avian influenza A (H5N1) in 10 patients in Vietnam. N Engl J Med 2004; 350:1179-1188.
- [16] Viseshakul N, Thanawongnuwech R, Amonsin A, Suradhat S, Payungporn S, Keawchareon J, Oraveerakul K, Wongyanin P, Plitkul S, Theamboonlers A, Poovorawan Y. The genome sequence analysis of H5N1 avian influenza A virus isolated from the outbreak among poultry populations in Thailand. Virology 2004;328:169-176.
- [17] Enserink M. Epidemiology. Horse flu virus jumps to dogs. Science 2005;309:2147.
- [18] Hampton T. Equine influenza jumps to canines. JAMA 2005;294:2015.
- [19] Yoon KJ, Cooper VL, Schwartz KJ, Harmon KM, Kim WI, Janke BH, Strohbehn J, Butts D, Troutman J. Influenza virus infection in racing greyhounds. Emerg Infect Dis 2005;11:1974-1976.

- [20] Clark A. Canine influenza virus surfaces. J Am Vet Med Assoc 2005;227:1377-1378.
- [21] Joly C. Canine influenza virus. Vet Rec 2005;157:527.
- [22] Steinhauer DA, Skehel JJ. Genetics of influenza viruses. Annu Rev Genet 2002;36:305–332.
- [23] Ludwig S, Planz O, Pleschka S, Wolff T. Influenza-virus-induced signaling cascades: targets for antiviral therapy?. Trends in Molecular Medicine 2003;9:46-52.
- [24] Baigent SJ, McCauley JW. Influenza type A in humans, mammals and birds: determinants of virus virulence, host-range and interspecies transmission. Bioessays 2003;25:657-671.
- [25] Fouchier RA, Munster V, Wallensten A, Bestebroer TM, Herfst S, Smith D, Rimmelzwaan GF, Olsen B, Osterhaus AD. Characterization of a novel influenza A virus hemagglutinin subtype (H16) obtained from black-headed gulls. J Virol 2005;79:2814–2822.
- [26] Holmes EC, Ghedin E, Miller N, Taylor J, Bao Y, St George K, Grenfell BT, Salzberg SL, Fraser CM, Lipman DJ, Taubenberger JK. Whole-genome analysis of human influenza A virus reveals multiple persistent lineages and reassortment among recent H3N2 viruses. PLoS Biol 2005; 3:300.
- [27] Reid AH, Fanning TG, Hultin JV, Taubenberger JK. Origin and evolution of the 1918 "Spanish" influenza virus hemagglutinin gene. Proc Natl Acad Sci USA 1999;96:1651- 1656.
- [28] Kawaoka Y, Krauss S, Webster RG. Avian-to-human transmission of the PB1 gene of influenza A viruses in the 1957 and 1968 pandemics. J Virol 1989;63:4603-4608.
- [29] Alexander DJ. A review of avian influenza in different bird species. Vet Microbiol 2000;74:3-13
- [30] Rott R. The pathogenic determinant of influenza virus. Veterinary Microbiolog 1992;33:303-310.

- [31] Horimoto T, Rivera E, Pearson J, Senne D, Krauss S, Kawaoka Y, Webster RG. Origin and molecular changes associated with emergence of a highly pathogenic H5N2 influenza virus in Mexico. *Virology* 1995;213:22-30.
- [32] Horimoto T, Nakayama K, Smeekens SP, Kawaoka Y. Proprotein-processing endoproteases PC6 and furin both activate hemagglutinin of virulent avian influenza viruses. *J Virol* 1994;68:6074-6078.
- [33] Wood JM, Robertson JS. From lethal virus to lifesaving vaccine: the development of inactivated influenza vaccines for pandemic influenza. *Nature Rev Microbiol* 2004;2:842-847.
- [34] Swayne DE. Pathobiology of H5N2 Mexican avian influenza virus infections of chickens. *Veterinary Pathology* 1997;34:557-567
- [35] Easterday BC, Hinshaw VS, Halvorson DA. Influenza. In: Calnek BW, Barnes HJ, Beard CW, McDougald LR, & Saif YM (Eds.), *Diseases of Poultry*, 583-605. Iowa: Iowa State University Press, 1997.
- [36] Horimoto T, Kawaoka Y. Influenza: lessons from past pandemics, warnings from current incidents. *Nat Rev Microbiol* 2005;3:591-600.
- [37] Yuen KY, Chan PK, Peiris M, Tsang DN, Que TL, Shorridge KF, Cheung PT, To WK, Ho ET, Sung R, Cheng AF. Clinical features and rapid viral diagnosis of human disease associated with avian influenza A H5N1 virus. *Lancet* 1998;351:467-471.
- [38] Buxton Bridges C, Katz JM, Seto WH, Chan PK, Tsang D, Ho W, Mak KH, Lim W, Tam JS, Clarke M, Williams SG, Mounts AW, Bresee JS, Conn LA, Rowe T, Hu-Primmer J, Abernathy RA, Lu X, Cox NJ, Fukuda K. Risk of influenza A (H5N1) infection among health care workers exposed to patients with influenza A (H5N1), Hong Kong. *J Infect Dis* 2000;181:344-348.
- [39] Subbarao K, Klimov A, Katz J, Regnery H, Lim W, Hall H, Perdue M, Swayne D, Bender C, Huang J, Hemphill M, Rowe T, Shaw M, Xu X, Fukuda K, Cox N. Characterization of an avian influenza A (H5N1) virus isolated from a child with a fatal respiratory illness. *Science* 1998;279:393-396.

- [40] Xu X, Subbarao, Cox NJ, Guo Y. Genetic characterization of the pathogenic influenza A/Goose/Guangdong/1/96 (H5N1) virus: similarity of its hemagglutinin gene to those of H5N1 viruses from the 1997 outbreaks in Hong Kong. Virology 1999;261:15-19.
- [41] Cauthen AN, Swayne DE, Schultz-Cherry S, Perdue ML, Suarez DL. Continued circulation in China of highly pathogenic avian influenza viruses encoding the hemagglutinin gene associated with the 1997 H5N1 outbreak in poultry and humans. J Virol 2000;74:6592-6599.
- [42] Sturm-Ramirez KM, Ellis T, Bousfield B, Bissett L, Dyrting K, Rehg JE, Poon L, Guan Y, Peiris M, Webster RG. Reemerging H5N1 influenza viruses in Hong Kong in 2002 are highly pathogenic to ducks. J Virol 2004;78:4892-4901.
- [43] Peiris JS, Guan Y, Yuen KY. Severe acute respiratory syndrome. Nat Med 2004;10:88-97.
- [44] World Health Organization. H5N1 avian influenza: Timeline of major events. Available from http://www.who.int/csr/disease/avian_influenza/timeline2007_04_02.pdf
- [45] Li KS, Guan Y, Wang J, Smith GJ, Xu KM, Duan L, Rahardjo AP, Puthavathana P, Buranathai C, Nguyen TD, Estoepongastie AT, Chaisingh A, Auewarakul P, Long HT, Hanh NT, Webby RJ, Poon LL, Chen H, Shortridge KF, Yuen KY, Webster RG, Peiris JS. Genesis of a highly pathogenic and potentially pandemic H5N1 influenza virus in eastern Asia. Nature 2004;430:209-213.
- [46] Mase M, Tsukamoto K, Imada T, Imai K, Tanimura N, Nakamura K, Yamamoto Y, Hitomi T, Kira T, Nakai T, Kiso M, Horimoto T, Kawaoka Y, Yamaguchi S. Characterization of H5N1 influenza A viruses isolated during the 2003-2004 influenza outbreaks in Japan. Virology 2005;332:167-176.
- [47] Chen H, Deng G, Li Z, Tian G, Li Y, Jiao P, Zhang L, Liu Z, Webster RG, Yu K. The evolution of H5N1 influenza viruses in ducks in southern China. Proc Natl Acad Sci USA 2004;101:10452-10457.

- [48] World Health Organization. Cumulative number of confirmed human cases of H5N1 avian influenza reported to WHO. Available from http://www.who.int/entity/csr/disease/avian_influenza/country/en/
- [49] Thanawongnuwech R, Amonsin A, Tantilertcharoen R, Damrongwatanapokin S, Theamboonlers A, Payungporn S, Nanthapornphiphat K, Ratanamungklanon S, Tunak E, Songserm T, Vivatthanavanich V, Lekdumrongsak T, Kesdangsakonwut S, Tunhikorn S, Poovorawan Y. Probable tiger-to-tiger transmission of avian influenza H5N1. Emerg Infect Dis 2005;11:699-701.
- [50] Kuiken T, Rimmelzwaan G, van Riel D, van Amerongen G, Baars M, Fouchier R, Osterhaus A. Avian H5N1 influenza in cats. Science 2004;306:241.
- [51] Shortridge KF, Zhou NN, Guan Y, Gao P, Ito T, Kawaoka Y, Kodihalli S, Krauss S, Markwell D, Murti KG, Norwood M, Senne D, Sims L, Takada A, Webster RG. Characterization of avian H5N1 influenza viruses from poultry in Hong Kong. Virology 1998;252:331-342.
- [52] Herrler G, Hausmann J, Klenk HD. Sialic acid as receptor determinant of ortho- and paramyxoviruses. In: Rosenberg A (Ed.), Biology of the Sialic Acids, 315-336. Plenum Press NY, 1995.
- [53] Gambaryan A, Yamnikova S, Lvov D, Tuzikov A, Chinarev A, Pazynina G, Webster R, Matrosovich M, Bovin N. Receptor specificity of influenza viruses from birds and mammals: new data on involvement of the inner fragments of the carbohydrate chain. Virology 2005;334: 276-283.
- [54] Ito T, Kawaoka Y, Nomura A, Otsuki K. Receptor specificity of influenza A viruses from sea mammals correlates with lung sialyloligosaccharides in these animals. J Vet Med Sci 1999;61: 955-958.
- [55] Kim JA, Ryu SY, Seo SH. Cells in the respiratory and intestinal tracts of chicken have different proportions of both human and avian influenza virus receptors. J Microbiol 2005;43:366-369.
- [56] Suzuki Y, Ito T, Suzuki T, Holland RE Jr, Chambers TM, Kiso M, Ishida H, Kawaoka Y. Sialic acid species as a determinant of the host range of influenza A viruses. J Virol 2000;74:11825-11831.

- [57] Rust MJ, Lakadamyali M, Zhang F, Zhuang X. Assembly of endocytic machinery around individual influenza viruses during viral entry. Nat Struct Mol Biol 2004;11:567-573.
- [58] Haque ME, Koppaka V, Axelsen PH, Lentz BR. Properties and Structures of the Influenza and HIV Fusion Peptides on Lipid Membranes: Implications for a Role in Fusion. Biophys J 2005; 89:3183-94.
- [59] Whittaker G, Bui M, Helenius A. The role of nuclear import and export in influenza virus infection. Trends Cell Biol 1996;6:67-71.
- [60] Drake JW. Rates of spontaneous mutation among RNA viruses. Proc Natl Acad Sci USA 1993; 90: 4171-4175.
- [61] Palese P, Garcia-Sastre A. Influenza vaccines: present and future. J Clin Invest 2002;110:9-13.
- [62] Thomas RE, Jefferson TO, Demicheli V, Rivetti D. Influenza vaccination for health-care workers who work with elderly people in institutions: a systematic review. Lancet Infect Dis 2006;6:273-279.
- [63] World Health Organization. Recommended composition of influenza virus vaccines for use in the 2006–2007 influenza season. Available from <http://www.who.int/csr/disease/influenza/2007northreport.pdf>
- [64] Kilbourne ED. Future influenza vaccines and the use of genetic recombinants. Bull World Health Organ 1969;41:643-645.
- [65] Maassab H, Heilman C, Herlocher M. Cold-adapted influenza viruses for use as live vaccines for man. Adv Biotechnol Processes 1990;14:203–242.
- [66] Murphy BR, Coelingh K. Principles underlying the development and use of live attenuated cold-adapted influenza A and B virus vaccines. Viral Immunol 2002;15:295–323.
- [67] Pinto LH, Holsinger LJ, Lamb LA. Influenza virus M2 protein has ion channel activity. Cell 1992; 69:517– 528.
- [68] Moscona A. Oseltamivir resistance--disabling our influenza defenses. N Engl J Med 2005;353:2633-2636.

- [69] Allwinn R, Preiser W, Rabenau H, Buxbaum S, Sturmer M, Doerr HW. Laboratory diagnosis of influenza--virology or serology?. Med Microbiol Immunol 2002;191:157-160.
- [70] Steininger C, Kundi M, Aberle SW, Aberle JH, Popow-Kraupp T. Effectiveness of reverse transcription-PCR, virus isolation, and enzyme-linked immunosorbent assay for diagnosis of influenza A virus infection in different age groups. J Clin Microbiol 2002;40:2051-2056.
- [71] Frisbie B, Tang YW, Griffin M, Poehling K, Wright PF, Holland K, Edwards KM. Surveillance of childhood influenza virus infection: what is the best diagnostic method to use for archival samples?. J Clin Microbiol 2004;42:1181-1184.
- [72] World Health Organization. WHO manual on animal influenza diagnosis and surveillance. Available from: <http://www.who.int/csr/resources/publications/influenza/en/whocdscsrncs20025rev.pdf>.
- [73] Julkunen I, Pyhala R, Hovi T. Enzyme immunoassay, complement fixation and hemagglutination inhibition tests in the diagnosis of influenza A and B virus infections, Purified hemagglutinin in subtype-specific diagnosis. J Virol Methods 1985;10:75-84.
- [74] Julkunen I, Hovi T, Seppala I, Makela O. Immunoglobulin G subclass antibody responses in influenza A and parainfluenza type 1 virus infections. Clin Exp Immunol 1985;60:130-138.
- [75] Hatta M, Gao P, Halfmann P, Kawaoka Y. Molecular basis for high virulence of Hong Kong H5N1 influenza A viruses. Science 2001;293:1840-1842.
- [76] Matrosovich MN, Zhou N, Kawaoka Y, Webster R. The surface glycoproteins of H5 influenza viruses isolated from humans, chicken, and wild aquatic birds have distinguishable properties. J Virol 1999;73:1146-1155.
- [77] Ellis JS, Zambon MC. Molecular diagnosis of influenza. Rev Med Virol 2002;12:375-389.
- [78] Ririe KM, Rasmussen RP, Wittwer CT. Product differentiation by analysis of DNA melting curves during the polymerase chain reaction. Anal Biochem 1997;245:154-160.

- [79] Wittwer CT, Herrmann MG, Moss AA, Rasmussen RP. Continuous fluorescence monitoring of rapid cycle DNA amplification. Biotechniques 1997;22:134–138.
- [80] Guan Y, Peiris M, Lipatov AS, Ellis TM, Dyrting KC, Krauss S, Zhang LJ, Webster RG, Shortridge KF. Emergence of multiple genotypes of H5N1 avian influenza viruses in Hong Kong SAR. Proceedings of National Academic of Sciences 2002;99:8950-8955.
- [81] Becker WB. The isolation and classification of Tern virus: influenza A-Tern South Africa. 1961. J Hyg (Lond) 1966;64:309-320.
- [82] Hien TT, Nguyen TL, Nguyen TD, et al. Avian influenza A (H5N1) in 10 patients in Vietnam. N Engl J Med 2004;350:1179-1188.
- [83] Giess GK, Salvatore M, Tumpey TM, Carter VS, Wang X, Basler CF, Taubenberger JK, Bumgarner RE, Pales P, Katze MG, Garcia-Sastre A. Cellular transcriptional profiling in influenza A virus-infected lung epithelial cells: The role of the non-structural NS1 protein in the evasion of the host innate defense and its potential contribution to pandemic influenza. Proceedings of National Academic of Sciences 2002;99:10736-10741.
- [84] Krug RM. Virology. Clues to the virulence of H5N1 viruses in humans. Science 2006;311:1562-1563.
- [85] Scholtissek C, Quack G, Klenk HD, Webster RG. How to overcome resistance of influenza A viruses against adamantane derivatives. Antiviral Res 1998;37:83–95.
- [86] Herrmann B, Larsson C, Zwegyberg BW. Simultaneous detection and typing of influenza viruses A and B by a nested reverse transcription-PCR: comparison to virus isolation and antigen detection by immunofluorescence and optical immunoassay (FLU OIA). J Clin Microbiol 2001;39:134-138.
- [87] Wright KE, Wilson GA, Novosad D, Dimock C, Tan D, Weber JM. Typing and subtyping of influenza viruses in clinical samples by PCR. J Clin Microbiol 1995;33:1180-1184.

- [88] Amonsin A, Payungporn S, Theamboonlers A, Thanawongnuwech R, Suradhat S, Pariyothorn N, Tantilertcharoen R, Damrongwatanapokin S, Buranathai C, Chaisingh A, Songserm T, Poovorawan Y. Genetic characterization of H5N1 influenza A viruses isolated from zoo tigers in Thailand. Virology 2006;344:480-491.
- [89] Amonsin A, Chutinimitkul S, Pariyothorn N, Songserm T, Damrongwatanapokin S, Puranaveja S, Jam-On R, Sae-Heng N, Payungporn S, Theamboonlers A, Chaisingh A, Tantilertcharoen R, Suradhat S, Thanawongnuwech R, Poovorawan Y. Genetic characterization of influenza A viruses (H5N1) isolated from 3rd wave of Thailand AI outbreaks. Virus Res 2006;122:194-199.
- [90] Chutinimitkul S, Bhattarakosol P, Srisuratanon S, Eiamudomkan A, Kongsomboon K, Damrongwatanapokin S, Chaisingh A, Suwannakarn K, Chieochansin T, Theamboonlers A, Poovorawan Y. H5N1 influenza A virus and infected human plasma. Emerg Infect Dis 2006;12:1041-1043.
- [91] Wang M, Di B, Zhou DH, Zheng BJ, Jing H, Lin YP, Liu YF, Wu XW, Qin PZ, Wang YL, Jian LY, Li XZ, Xu JX, Lu EJ, Li TG, Xu J. Food markets with live birds as source of avian influenza. Emerg Infect Dis 2006;12:1773-1775.
- [92] Fan J, Kraft AJ, Henrickson KJ. Current methods for the rapid diagnosis of bioterrorism-related infectious agents. Pediatric clinics of North America 2006;53:817.
- [93] Thontiravong A, Payungporn S, Keawcharoen J, Chutinimitkul S, Wattanodorn S, Damrongwatanapokin S, Chaisingh A, Theamboonlers A, Poovorawan Y, Oraveerakul K. The single-step multiplex reverse transcription-polymerase chain reaction assay for detecting H5 and H7 avian influenza A viruses. Tohoku J Exp Med 2007;211:75-79.
- [94] Plotkin JB, Dushoff J. Codon bias and frequency-dependent selection on the hemagglutinin epitopes of influenza A virus. Proc Natl Acad Sci U S A 2003;100:7152-7157.

- [95] Karasin AI, Brown IH, Carman S, Olsen CW. Isolation and characterization of H4N6 avian influenza viruses from pigs with pneumonia in Canada. J Virol 2000;74:9322-9327.
- [96] Peiris M, Yuen KY, Leung CW, Chan KH, Ip PL, Lai RW, Orr WK, Shortridge KF. Human infection with influenza H9N2. Lancet 1999;354:916-917.
- [97] Bush R, Bender C, Subbarao K, Cox N J, Fitch WM. Predicting the evolution of human influenza A. Science 1999;286:1921-1925.
- [98] Guo Y, Wang M, Kawaoka Y, Gorman O, Ito T, Saito T, Webster RG. Characterization of a new avian-like influenza A virus from horses in China. Virology 1992;188:245-255.
- [99] Myers TW, Gelfand DH. Reverse transcription and DNA amplification by a *Thermus thermophilus* DNA polymerase. Biochemistry 1991;30:7661-7666.
- [100] Hannon GJ. RNA interference. Nature 2002;418:244-251.
- [101] McManus MT, Sharp PA. Gene silencing in mammals by small interfering RNAs. Nature Rev Genet 2002;3:737-747.
- [102] Dykxhoorn DM, Novina CD, Sharp PA. Killing the messenger: short RNAs that silence gene expression. Nature Rev Mol Cell Biol 2003;4:457-467.
- [103] Fire A, Xu S, Montgomery MK, Kostas SA, Driver SE, Mello CC. Potent and specific genetic interference by double-stranded RNA in *Caenorhabditis elegans*. Nature 1998;391:806-811.
- [104] Vaucheret H, Beclin C, Fagard M. Post-transcriptional gene silencing in plants. J Cell Sci 2001;114:3083-3091.
- [105] Elbashir SM, Harborth J, Lendeckel W, Yalcin A, Weber K, Tuschl T. Duplexes of 21-nucleotide RNAs mediate RNA interference in cultured mammalian cells. Nature 2001;411:494-498.
- [106] Bernstein E, Caudy AA, Hammond SM, Hannon GJ. Role for a bidentate ribonuclease in the initiation step of RNA interference. Nature 2001;409:363-366.
- [107] Nykanen A, Haley B, Zamore PD. ATP requirements and small interfering RNA structure in the RNA interference pathway. Cell 2001;107:309-321.

- [108] Echeverri CJ, Perrimon N. High-throughput RNAi screening in cultured cells: a user's guide. Nat Rev Genet 2006;7:373-384.
- [109] Mittal V. Improving the efficiency of RNA interference in mammals. Nat Rev Genet 2004;5:355-365.
- [110] Sachse C, Echeverri CJ. Oncology studies using siRNA libraries: the dawn of RNAi-based genomics. Oncogene 2004;23:8384-8391.
- [111] Sachse C, Krausz E, Kronke A, Hannus M, Walsh A, Grabner A, Ovcharenko D, Dorris D, Trudel C, Sonnichsen B, Echeverri CJ. High-throughput RNA interference strategies for target discovery and validation by using synthetic short interfering RNAs: functional genomics investigations of biological pathways. Methods Enzymol 2005;392:242-277.
- [112] Conner SD, Schmid SL. Regulated portals of entry into the cell. Nature 2003;422:37-44.
- [113] Brodsky FM, Chen CY, Knuehl C, Towler MC, Wakeham DE. Biological basket weaving: formation and function of clathrin-coated vesicles. Annu Rev Cell Dev Biol 2001;17:517-568.
- [114] Nabi IR, Le PU. Caveolae/raft-dependent endocytosis. J Cell Biol 2003;161:673-677.
- [115] Rust MJ, Lakadamyali M, Zhang F, Zhuang X. Assembly of endocytic machinery around individual influenza viruses during viral entry. Nat Struct Mol Biol 2004;11:567-573.
- [116] Salcini AE, Chen H, Iannolo G, De Camilli P, Di Fiore PP. Epidermal growth factor pathway substrate 15, Eps15. Int J Biochem Cell Biol 1999;3:805-809.
- [117] Le Roy C, Wrana JL. Clathrin- and non-clathrin-mediated endocytic regulation of cell signaling. Nat Rev Mol Cell Biol 2005;6:112-126.
- [118] Chen H, Slepnev VI, Di Fiore PP, De Camilli P. The interaction of epsin and Eps15 with the clathrin adaptor AP-2 is inhibited by mitotic phosphorylation and enhanced by stimulation-dependent dephosphorylation in nerve terminals. J Biol Chem 1999;274:3257-3260.

- [119] Polo S, Confalonieri S, Salcini AE, Di Fiore PP. EH and UIM: endocytosis and more. Sci STKE 2003;2003:re17.
- [120] Pucharcos C, Estivill X, de la Luna S. Intersectin 2, a new multimodular protein involved in clathrin-mediated endocytosis. FEBS Lett 2000;478:43-51.
- [121] Apodaca G. Endocytic traffic in polarized epithelial cells: role of the actin and microtubule cytoskeleton. Traffic 2001;2:149-159.
- [122] Gorovoy M, Niu J, Bernard O, Profirovic J, Minshall R, Neamu R, Voynov-Yasenetskaya T. LIM kinase 1 coordinates microtubule stability and actin polymerization in human endothelial cell. J Biol Chem 2005;280:26533-26542.
- [123] Bokoch GM. Biology of the p21-activated kinases. Annu Rev Biochem 2003;72:743-781.
- [124] Pelkmans L. Secrets of caveolae- and lipid raft-mediated endocytosis revealed by mammalian viruses. Biochim Biophys Acta 2005;1746:295-304.
- [125] Pelkmans L, Fava E, Grabner H, Hannus M, Habermann B, Krausz E, Zerial M. Genome-wide analysis of human kinases in clathrin- and caveolae/raft-mediated endocytosis. Nature 2005;436:78-86
- [126] Agaisse H, Burrack LS, Philips JA, Rubin EJ, Perrimon N, Higgins DE. Genome-wide RNAi screen for host factors required for intracellular bacterial infection. Science 2005;309:1248-1251.



APPENDICES

สถาบันวิทยบริการ
จุฬาลงกรณ์มหาวิทยาลัย

APPENDIX A

Molecular biology techniques

Polymerase Chain Reaction (PCR)

The polymerase chain reaction (PCR) is a relatively simple technique that amplifies a DNA template to produce specific DNA fragments *in vitro*. Traditional methods of cloning a DNA sequence into a vector and replicating it in a living cell often require days or weeks of work, but amplification of DNA sequences by PCR requires only hours. While most biochemical analyses, including nucleic acid detection with radioisotopes, require the input of significant amounts of biological material, the PCR process requires very little. Thus, PCR can achieve more sensitive detection and higher levels of amplification of specific sequences in less time than previously used methods. These features make the technique extremely useful, not only in basic research, but also in commercial uses, including genetic identity testing, forensics, industrial quality control and *in vitro* diagnostics. Basic PCR has become commonplace in many molecular biology labs where it is used to amplify DNA fragments and detect DNA or RNA sequences within a cell or environment. However, PCR has evolved far beyond simple amplification and detection, and many extensions of the original PCR method have been described.

- **Conventional PCR**

The PCR process was originally developed to amplify short segments of a longer DNA molecule. A typical amplification reaction includes the target DNA, a thermostable DNA polymerase, two oligonucleotide primers, deoxynucleotide triphosphates (dNTPs), reaction buffer and magnesium. Once assembled, the reaction is placed in a thermal cycler, an instrument that subjects the reaction to a series of different temperatures for varying amounts of time. This series of temperature and time adjustments is referred to as one cycle of amplification. Each PCR cycle theoretically doubles the amount of targeted sequence (amplicon) in the reaction.

Each cycle of PCR includes steps for template denaturation, primer annealing and primer extension (Figure 38). The initial step denatures the target DNA by heating it to 94°C or higher for 15 seconds to 2 minutes. In the denaturation process, the two intertwined strands of DNA separate from one another, producing the necessary single-stranded DNA template for replication by the thermostable DNA polymerase. In the next step, the temperature is reduced to approximately 40–60°C. At this temperature, the oligonucleotide primers can form stable associations (anneal) with the denatured target DNA and serve as primers for the DNA polymerase. This step lasts approximately 15–60 seconds. Finally, the synthesis of new DNA begins as the reaction temperature is raised to the optimum for the DNA polymerase. For most thermostable DNA polymerases, this temperature is in the range of 68–74°C. The extension step lasts approximately 1–2 minutes. The next cycle begins with a return to 94°C for denaturation.

Each step of the cycle should be optimized for each template and primer pair combination. If the temperature during the annealing and extension steps are similar, these two steps can be combined into a single step in which both primer annealing and extension take place. After 20–40 cycles, the amplified product may then be analyzed for size, quantity, sequence, etc., or used in further experimental procedures.

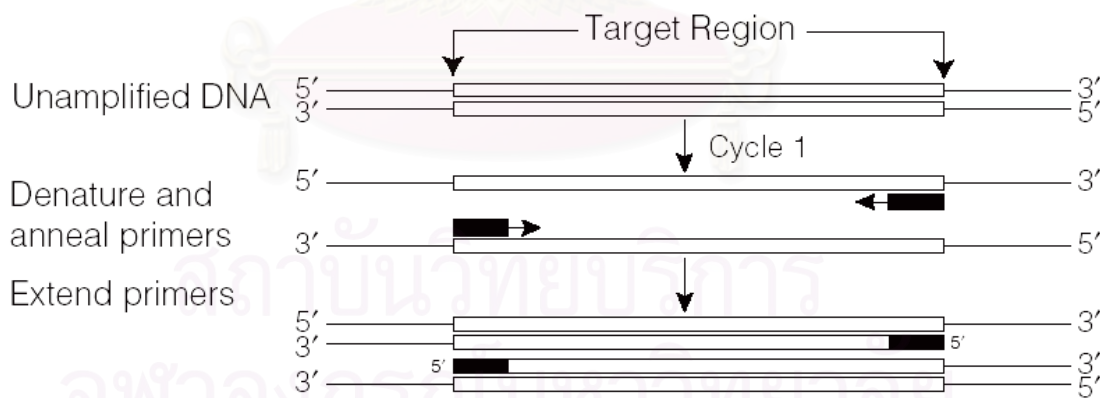


Figure 38 Schematic diagram of the PCR process

- RT-PCR

In order to apply PCR to the study of RNA, the RNA sample must first be reverse transcribed to cDNA to provide the necessary DNA template for the thermostable polymerase (Figure 39). This process is called reverse transcription (RT), hence the name RT-PCR.

Avian myeloblastosis virus (AMV) or Moloney murine leukemia virus (M-MLV or MuLV) reverse transcriptases are generally used to produce a DNA copy of the RNA template using random primers, an oligo (dT) primer or a sequence-specific primer. Alternatively, some thermostable DNA polymerases (e.g., Tth DNA polymerase) possess a reverse transcriptase activity, which can be activated under certain conditions, namely using manganese instead of magnesium as a cofactor [99]. After this initial reverse transcription step has produced the cDNA template, basic PCR is carried out to amplify the target sequence. The efficiency of the first-strand synthesis reaction, which can be related to the quality of the RNA template, will also significantly impact the results of the subsequent amplification.

First Strand Synthesis:

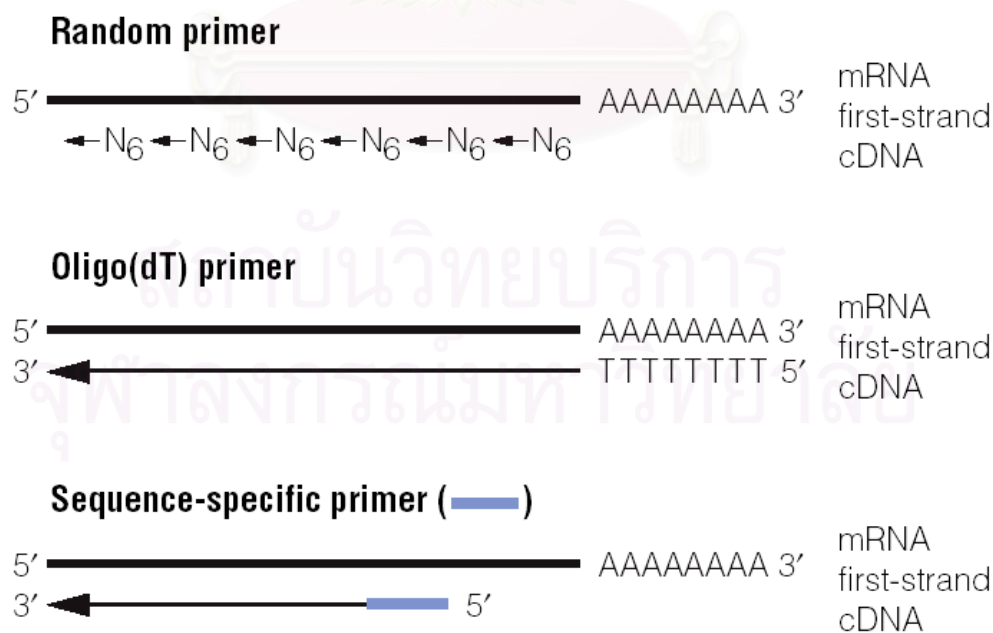


Figure 39 Schematic diagram of reverse transcription process

- **Multiplex PCR**

Multiplex PCR is a powerful technique that enables amplification of two or more products in parallel in a single reaction tube [77]. The primers used in the multiplex PCR reaction should have the same T_m and following the general guidelines for primer designation. Moreover, the amplified DNA fragments should be clearly separated by agarose gel electrophoresis (Table 18).

Table 18 Guidelines for agarose gel analysis of multiplex PCR products

Minimum different in size of PCR products	Maximum size of fragments	Concentration of agarose
>200 bp	2000 bp	1.3%
>100-200 bp	1000 bp	1.4-1.6%
>50-100 bp	750 bp	1.7-2.0%
20-50 bp	500 bp	2.5-3.0%
<20 bp	250 bp	3.0-4.0%

Quantitative real-time PCR

The use of fluorescently labeled oligonucleotide probes or primers or DNA binding fluorescent dyes, such as SYBR Green, to detect and quantitate a PCR product allows quantitative PCR to be performed in real time. The more PCR products present the stronger the fluorescent intensity of the reaction. Measuring the increase in signal intensity during the exponential phase of the PCR reaction allows the researcher to determine the amount of genetic material present at the beginning of the reaction. DNA-binding dyes are easy to use but do not differentiate between specific and nonspecific PCR products. Fluorescently labeled nucleic acid probes have the advantage that they react with only specific PCR products.

Using any of the developed chemistries, the increase in fluorescence emission during the PCR reaction can be detected in real-time. The computer software constructs amplification plots using the fluorescence signal that are collected during each cycle of the PCR amplification (Figure 40).

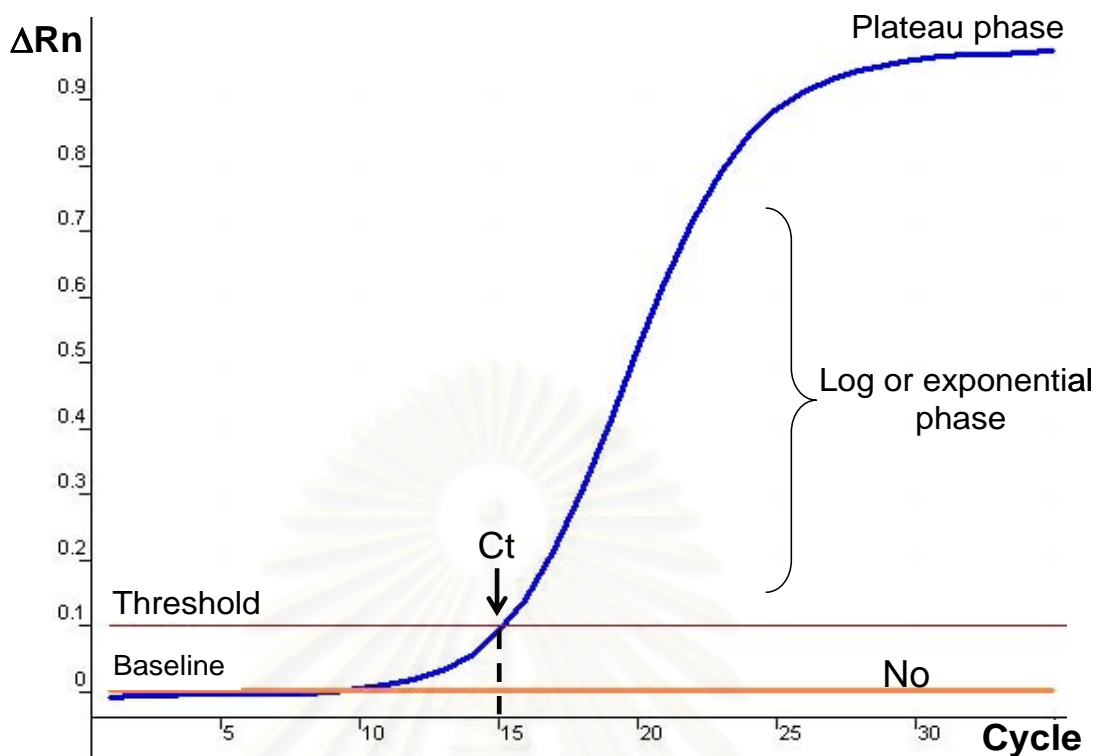


Figure 40 Schematic representative of amplification plot and the important terminology associated with real-time PCR analysis.

According to the amplification plot (Figure 40), there are several important terms associated with the data analysis of real-time PCR assay as the following.

- Baseline: the baseline is defined as the PCR cycles in which a reporter fluorescent signal is accumulating but is beneath the limits of detection of the instrument. By default, the software sets the baseline from cycles 3 to 15.
- ΔR_n : the software calculates a ΔR_n by using $\Delta R_n = R_{nf} - R_{nb}$, R_{nf} is the fluorescence emission of the product at each time point and R_{nb} is the fluorescence emission of the baseline. The ΔR_n values are plotted against the cycle number.
- Threshold: an arbitrary threshold is chosen by the computers, based on the variability of the baseline. Conventionally, it is calculated as ten-times the standard deviation of the average signal of the baseline fluorescent signal between cycles 3 to 15. A fluorescent signal that is detected above the threshold level is considered as a real signal which can be used to define the threshold cycle (Ct).

- **Threshold cycle (Ct):** this is defined as the fractional PCR cycle number at which the reporter fluorescence is greater than the minimal detection (threshold) level. The Ct is the basic principle of real-time PCR and is an essential component in producing accurate and reproducible data. The presence of more template at the beginning of reaction leads to a fewer number of cycles reaching the threshold level.

As reaction components become limiting, the rate of the target amplification decreases until the PCR reaction is no longer generating template at an exponential rate (plateau phase) and there is little or no increase in PCR product. This is the main reason why real-time PCR is a more reliable measurement of starting copy number than an endpoint measurement of the accumulated PCR product.

Commonly used detection chemistries in real-time PCR

As the popularity of Real-time PCR technology has grown over the last several years, a number of companies have developed products to ease the process and time requirements for quantitative real-time PCR (qPCR).

SYBR Green I dye

SYBR Green is a fluorescent dye that non-specifically binds to the minor groove of double-stranded DNA. Thus amplicon production is measured by the increase in fluorescence intensity of this DNA binding dye in a non-sequence specific manner.

At high temperatures, during the DNA denaturation step, the SYBR Green dye molecules are unbound and exhibit little fluorescence. During the renaturation (annealing) step, as the temperature cools to allow the primers to bind, a few dye molecules begin to bind, resulting in a low fluorescence signal. As the complementary strands are synthesized (elongation), SYBR green molecules are rapidly incorporated into the new DNA and the increase in fluorescence can be measured in real time. When the cycle returns to the high temperature denaturation step, the dye molecules are released and the signal returns to background levels (Figure 41A).

Advantages of SYBR Green:

- Simple and cost-effective
- Can be applied for discrimination by using melting curve analysis

Disadvantage of SYBR Green:

- Used in single-plex reaction
- Detection of non-specific amplification

TaqMan probe

TaqMan probes are oligonucleotides that contain a fluorescent dye on the 5' end (typically) and a quenching dye on the 3' end. While the probe is intact, the close proximity of the reporter and the quencher prevent the emission of fluorescence via fluorescence resonance energy transfer (FRET). TaqMan probes anneal to an internal region of a PCR product, thus when the Taq polymerase with exonuclease activity replicates a template on which TaqMan is bound, the probe is cleaved, releasing the reporter dye from the quencher.

During the high temperature denaturation step there is no binding of the probe to the DNA. As the temperature cools during the renaturation (annealing) step, the primers and the TaqMan probe anneal. At this stage, the fluorescent signal from the reporter is quenched by the close proximity of the quencher. The synthesis of DNA results in the displacement and hydrolysis of the labeled probe by the polymerase, thus releasing the signal from the reporter once separated from the quencher (Figure 41B).

Advantages of TaqMan probe:

- Detects only amplification of specific product
- Hybridization and cleavage does not interfere with accumulation of the product
- Can be used in multi-color labeled probes for multiplex detection

Disadvantages of TaqMan probe:

- Requires that specific probes be generated for each template

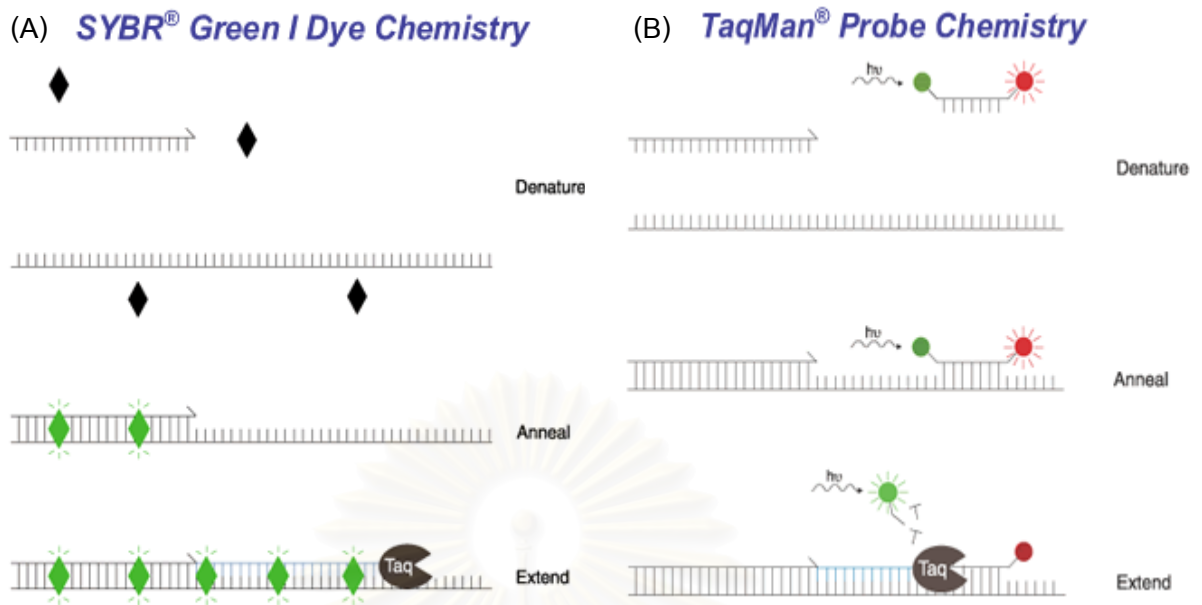


Figure 41 Detection chemistries commonly used in real-time PCR. (A) Detection mechanism of SYBR Green dye chemistry. (B) Detection mechanism of TaqMan probe chemistry.

Melting curve analysis

Following the amplification reaction with SYBR Green dye, the melting curve analysis is performed by slightly increasing the temperature in order to melt the double-stranded PCR products into single-stranded DNA coupled with continuous detection of the fluorescence signal until the temperature reaches 95°C. The result is a plot of raw fluorescence data versus temperature (Figure 42A). This view of the data may appear difficult to interpret; therefore the plot is then converted into a plot of negative first derivative of raw fluorescence against increasing temperature during the melting process (Figure 42B). This curve is easier to determine the melting peak and melting temperature of the PCR products. Melting temperature (T_m) of the DNA is the temperature where 50% of the DNA is single stranded. The T_m of the PCR product depends on several factors including %GC content within the amplicon, length of the amplicon and Mg^{2+} concentration. Therefore, if PCR products consist of identical and homogeneous molecules, a single melting peak will be detected.

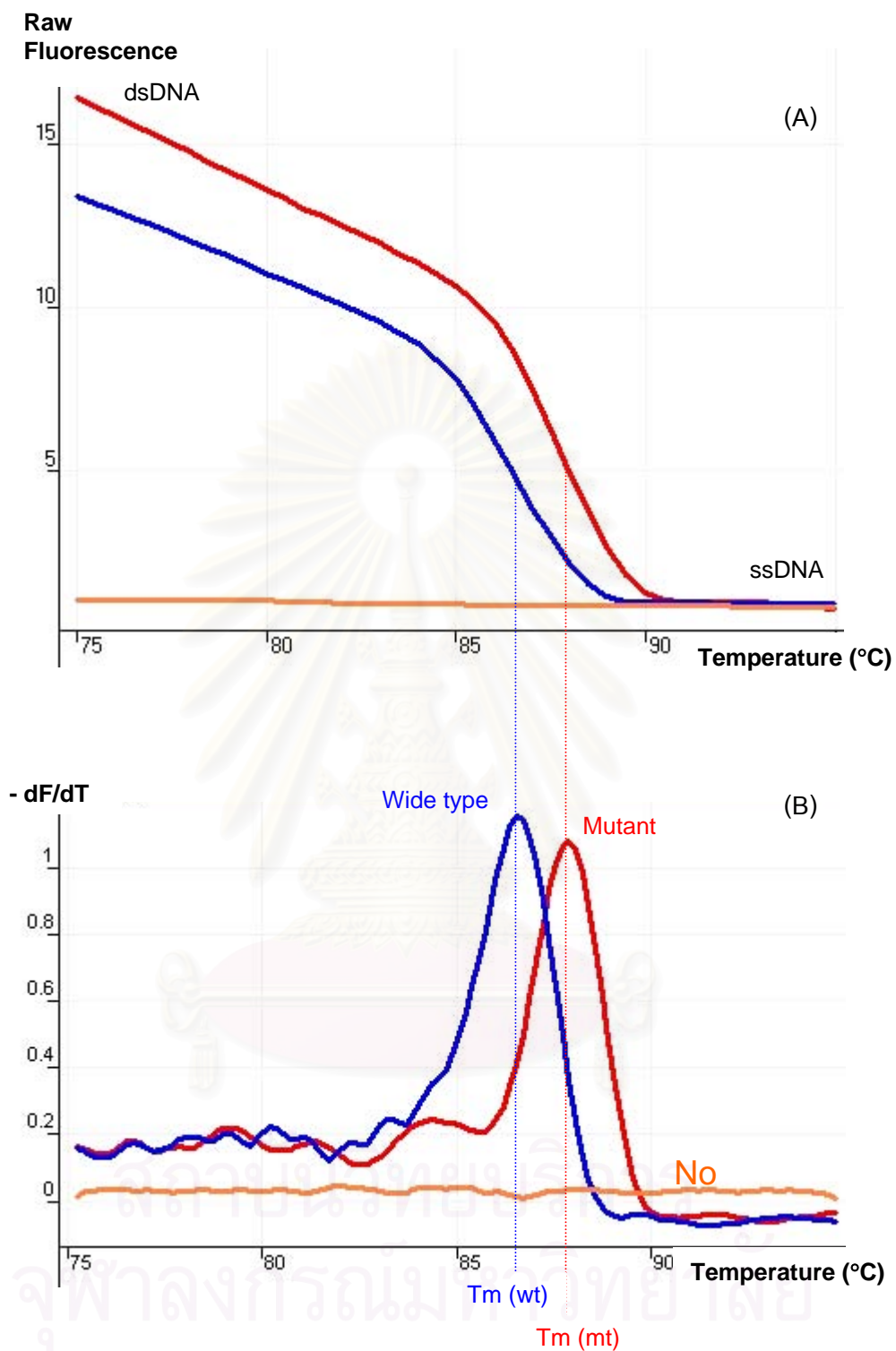


Figure 42 Representative of real-time PCR with melting curve analysis. (A) Change of raw fluorescence signal plotted as a function of increasing temperature. (B) The negative first deviation of raw fluorescence plotted against increasing temperature showed a discrimination of melting peak between wide type and mutant strains.

On the other hand, the presence of more than one population of PCR products will be reflected as multiple melting peaks. In this way, the melting curve analysis can be used to differentiate between specific and non-specific amplicons based on the melting peak and T_m of the PCR products. Moreover, the melting curve analysis can be further applied in several applications including discrimination between wild type and mutant (deletion or insertion) and strains or subtypes identification of several pathogens.

Multiplex real-time PCR

The term multiplex real-time PCR is used to describe the use of multiple fluorogenic probes for the detection of multiple amplicons in a single tube. The main advantages of multiplexing over single-target analysis are the ability to provide internal controls, lower reagent costs and preservation of precious samples. The main restrictions of this technique are the limited number of available fluorophores, fluorescence emission from quenching dyes and the common use in real-time instruments of a monochromatic light source. Conventionally, only four-color multiplex reactions are usually possible, of which one color may be used as a passive reference dye control (Table 19).

Table 19 Multiplex fluorescence reporters dyes suitable for each instrument

Real-time PCR company	Fluorescence dye			Passive Reference dye
	Target 1	Target 2	Target 3	
Applied Biosystems (ABI)	FAM	HEX / JOE / VIC	NED	ROX
Corbett Research (Roter Gene)	FAM	HEX / JOE / VIC	Cy5	ROX
Stratagene (Mx)	FAM	HEX / JOE / VIC	Cy5	ROX
BioRad (iCycler iQ)	FAM	HEX / JOE / VIC	Cy5	ROX
Cepheid (Smart Cycler)	FAM	HEX / JOE / VIC	Cy5	ROX
Eppendorf (Mastercycler realplex)	FAM	HEX / JOE / VIC	Cy5	ROX
Roche (Light Cycler)	LC Red 640	LC Red 670	LC Red 705	ROX

ROX Passive Reference dye

The passive reference dye is not linked to any amplification effect. Therefore, the fluorescence from this dye should be constant throughout the amplification reaction. Provided equal concentration and volume in every well of the reaction, theoretically the fluorescence intensity for the reference dye should be the same in every sample. The target amplification fluorescent signal in the reaction can be normalized to the passive reference dye by dividing the raw fluorescence intensity at each cycle for the dye of target gene by the fluorescence intensity from the passive reference dye at the same cycle in the same tube. This will correct or normalize any signal level differences which may be caused by differences in plastic ware transparency and reflectivity, or volume differences due to pipetting errors. The most commonly used passive reference dye is ROX. Pure ROX dye should be used at a final concentration of 30 nM.

Quantitation of nucleic acids by real-time PCR

Target nucleic acids can be quantified using either absolute quantitation or relative quantitation. Absolute quantitation determines the absolute amount of a target (expressed as a copy number or concentration), whereas relative quantitation determines the ratio between the amount of a target and the amount of a reference nucleic acid, usually a suitable housekeeping gene. This normalized value can then be used to compare, for example, differential gene expression in different samples.

Absolute quantitation

The absolute amount of a target nucleic acid is determined using external standards. The sequence of the standards is usually the same as or very similar to the target sequence, but the primer binding sites of the standards must be identical to those in the target sequence. This ensures that both the standards and the target are amplified with equivalent efficiencies, which is essential for absolute quantitation. A standard curve (plot of Ct value against log of initial amount of standard) is a linear line generated by using different dilutions of the standard (Figure 43). The target and each of the standards are amplified in separate tubes. Quantitation of the amount of target in the “unknown” samples of interest is accomplished by measuring Ct and using the standard curve to determine starting amount of the sample.

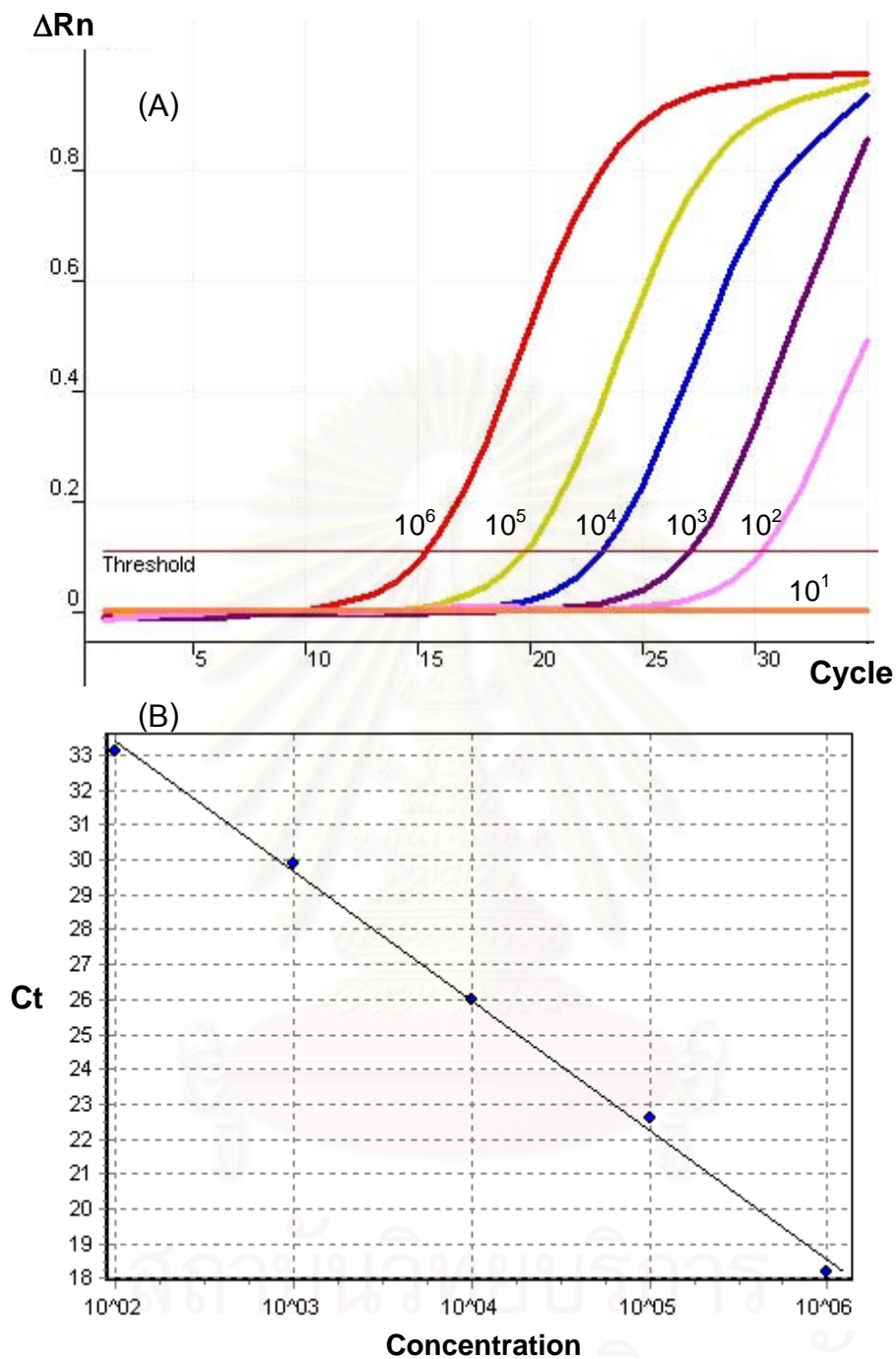


Figure 43 Representative of absolute quantitation by real-time PCR. (A) Amplification plot obtained from 10-fold serial dilution of standard template (10^6 - 10). (B) Standard curve obtained from plotting Ct values against the concentration of each standard dilution.

Generating standard curves

Standard curves can be used in both absolute and relative quantitation. To generate a standard curve, at least 5 different amounts of the standard should be quantified, and the amount of unknown target should fall within the range of the standard curve. Reactions should be carried out in at least triplicate, especially when quantifying standards of low copy number.

For absolute quantitation, the copy number or concentration of the nucleic acids used as standards must be known. In addition, standards should show the following features:

- Primer binding sites identical to the target to be quantified
- Sequence between primer binding sites identical or highly similar to target
- Sequences upstream and downstream from the amplified sequence identical or similar to “natural” target

Plasmid DNA containing the target gene can be used as a standard for generating a standard curve. After determination of plasmid DNA concentration by spectrophotometry (Table 20), the copy number of standard DNA molecules can be calculated using the following formula:

$$(X \text{ g}/\mu\text{l DNA} / [\text{plasmid length in nucleotides} \times 660]) \times 6.022 \times 10^{23} = Y \text{ molecules}/\mu\text{l}$$

Table 20 Spectrophotometric conversions for nucleic acid templates

Types of nucleic acid	Concentration ($\mu\text{g}/\text{ml}$) when $A_{260} = 1$
Double-stranded DNA (dsDNA)	50
Single-stranded DNA (ssDNA)	33
Single-stranded RNA (ssRNA)	40

For quantitation of RNA, *in vitro* transcribed RNA molecules are strongly recommended to use as standards in order to take the variable efficiency of the RT reaction into account. RNA standards can be created by cloning part or the entire transcript of interest into a standard cloning vector. The insert can be generated by RT-PCR from total RNA or mRNA, or by PCR from cDNA. The cloning vector must contain an RNA polymerase promoter such as T7, SP6, or T3. Ensure that *in vitro* transcription of the insert leads to generation of the sense transcript. After *in vitro* transcription, plasmid DNA must be removed completely with RNase-free DNase, since residual plasmid DNA will lead to errors in spectrophotometric determinations of RNA concentration and will also serve as a template in the subsequent PCR. Furthermore, ensure that the RNA used as a standard does not contain any degradation products or aberrant transcripts by checking that it migrates as a single band in gel electrophoresis. After determination of RNA concentration by spectrophotometry (Table 20), the copy number of standard RNA molecules can be calculated using the following formula:

$$(X \text{ g}/\mu\text{l RNA} / [\text{transcript length in nucleotides} \times 340]) \times 6.022 \times 10^{23} = Y \text{ molecules}/\mu\text{l}$$

In addition, the curve must be linear over the whole concentration range. The linearity is denoted by the R squared (Rsq) value (R^2 or Pearson Correlation Coefficient) and should be very close to 1 (≥ 0.985 is acceptable). Ideally, the efficiency of both the standard curve and sample reactions should be between 90 and 110% (slope between -3.1 to -3.6) are acceptable. One hundred percent efficiency implies perfect doubling of amplicon each cycle. If the efficiency is significantly less, this implies the reaction is being slowed in some way, either from inhibitors present in the reaction mix or suboptimal primer sets or reaction conditions. Efficiencies significantly above 100% typically indicate experimenter error (e.g. miscalibrated pipettors, PCR inhibitors, probe degradation, formation of nonspecific products, and formation of primer dimers).

Relative quantitation by comparative threshold (delta-delta Ct) method ($2^{-\Delta\Delta Ct}$)

Comparative threshold method is the most commonly used strategy for relative quantitation in real-time PCR. This method eliminates the need for standard curves and mathematical equations are used to calculate the relative expression levels of a target relative to calibrator such as a non treated control or RNA from normal tissue or a sample at time zero in a time-course study. The amount of target gene in the sample, normalized to an endogenous housekeeping gene (reference gene) and relative to the normalized calibrator, is then given by $2^{-\Delta\Delta Ct}$, where

$$\Delta\Delta Ct = \Delta Ct (\text{sample}) - \Delta Ct (\text{calibrator})$$

$$\Delta Ct (\text{sample}) = Ct (\text{target gene of sample}) - Ct (\text{reference gene of sample})$$

$$\Delta Ct (\text{calibrator}) = Ct (\text{target gene of calibrator}) - Ct (\text{reference gene of calibrator})$$

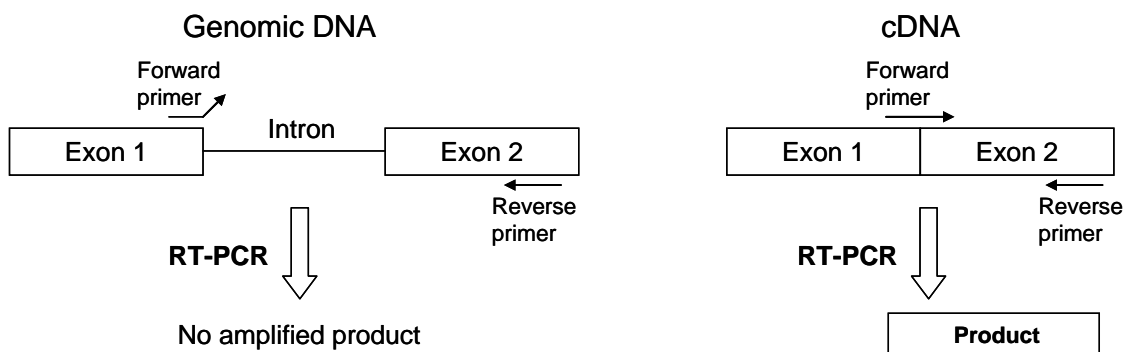
$$\text{Ratio (folds of difference) of sample: calibrator} = 2^{-\Delta\Delta Ct}$$

For this calculation to be valid and in order to obtain reliable results, it is imperative that the amplification efficiencies of the reference and the target gene are approximately equal and at or above 90%. This can be established by calculation of ΔCt (of both and calibrator) varies with template dilution. If the plot of template dilution against ΔCt yield slope < 0.1 , it implies that the efficiencies of the target and reference gene are very similar.

Primer design guidelines:-

- Primer length between 18-30 bp.
- Keep GC content in the range of 40-60%.
- The melting temperature (T_m) of primers should be 55-62°C and within 2°C of each other. The T_m is calculated by using the formula:
$$T_m = 2^\circ\text{C} \times (\text{number of [A+T]}) + 4^\circ\text{C} \times (\text{number of [G+C]})$$
- G or C at the 3' end of primers will increase priming efficiency.
- Avoid runs of an identical nucleotides (3 or more), especially guanine.
- Avoid secondary structure (hairpin, self-complementary and primer dimers).
- Avoid mismatches between the 3' end of the primer and the target-template.
- The 5 nucleotides at the 3' end should have no more than two G and/or C bases.
- Primers should be searched using BLAST and checked for cross-homology.
- Primers should be specific with the target gene and not anneal with other gene.
- In multiplexing, all primers should be designed using the same settings to ensure that they will work optimally under the same cycling conditions.
- In real-time PCR assay, short amplicon length (70-200) is recommended for high efficiency of amplification.
- For RT-PCR, design primer spans an intron/exon boundary, so that one half hybridizes to the 3' end of one exon and the other half to the 5' end of the adjacent exon (Figure 44). Therefore, the primers will only anneal to cDNA synthesized from spliced mRNAs, but not to genomic DNA.
- Alternatively, RT-PCR primers should be designed to flank a region that contains at least one intron. Products amplified from cDNA (no introns) will be smaller than those amplified from genomic DNA (containing introns). If possible, select a target with very long introns: the RNA target may then be preferentially amplified because of the higher PCR efficiency of this shorter PCR product without introns.

Primer spans an intron / exon boundary



Probe spans an intron / exon boundary

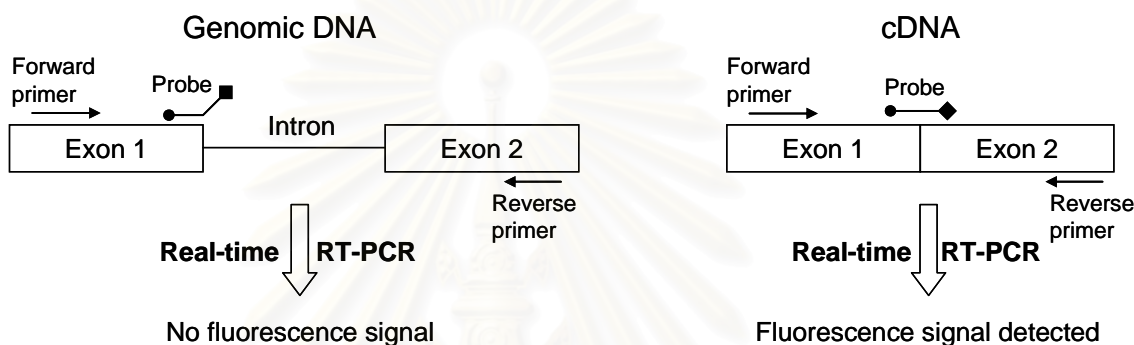


Figure 44 Schematic representation of primer and probe spanning of an intron/exon boundary to eliminate the genomic DNA contamination during RT-PCR or real-time RT-PCR assays.

TaqMan probe design guidelines:-

- Keep G-C content in the 30-80% range.
- The T_m of probe should be 65-72°C (8-10°C higher than the T_m of primers).
- Avoid probes with "G" at the 5' end of the probe. Because "G" adjacent to the reporter dye will quench the reporter fluorescence, even after cleavage.
- Select probes with a Primer Express software-estimated T_m of 65-67 °C.
- Avoid runs of an identical nucleotide. This is especially true for guanine, where runs of four or more should be avoided.
- Design probe as close as possible to the primer without overlapping.
- For TaqMan MGB, select the probe as short as possible (13-20 bp) and calculated T_m (65-70°C) using Primer Express software (Applied Biosystems).
- For real-time RT-PCR, design probe spans an intron/exon boundary (Figure 44).

Fluorescence reporters / quenchers selection

- Select the appropriate quencher for each reporter dye (Table 21).
- Select dyes with excitation/emission maxima compatible with the excitation/detection ranges of the instrument..
- Label least abundant target with the best performing dye (usually FAM)
- For multiplexing, select suitable fluorescence reporters / quenchers for the detector of each real-time PCR instrument in order to avoid spectral overlap between reporter dyes (Table 21).

Table 21 Commonly used fluorescence reporters & quenchers in real-time PCR

Reporters	Excitation (nm)	Emission (nm)	Compatible Quenchers
FAM	494	518	TAMRA BHQ1 MGB
TET	521	538	
JOE	520	548	
VIC	538	552	
HEX	535	553	
NED	546	575	BHQ2 MGB
Cy3	552	570	
TAMRA	560	582	
ROX	587	607	
Texas Red	596	615	
Cy5	643	667	BHQ3

Cloning of PCR products with pGEM-T Easy vector

The pGEM-T Easy Vector Systems (Promega) is a convenient system for the cloning of PCR products. The vector contains a single 3' terminal thymidine (T) at both ends. These single 3'-T overhangs at the insertion site greatly improve the efficiency of ligation of a PCR product into the plasmids by preventing recircularization of the vector and providing a compatible overhang for PCR products generated by certain thermostable polymerases including *Taq*, *Tfl* and *Tth*. Table 22 and Figure 45 show the description of pGEM-T Easy Vector.

Table 22 pGEM-T Easy Vector sequence reference points

Reference points	Positions
T7 RNA polymerase transcription initiation site	1
Multiple cloning region	10-128
SP6 RNA polymerase promoter (-17 to +3)	139-158
SP6 RNA polymerase transcription initiation site	141
M13 Reverse Sequencing Primer binding site	176-197
M13 Forward Sequencing Primer binding site	2949-2972
T7 RNA polymerase promoter (-17 to +3)	2999-3

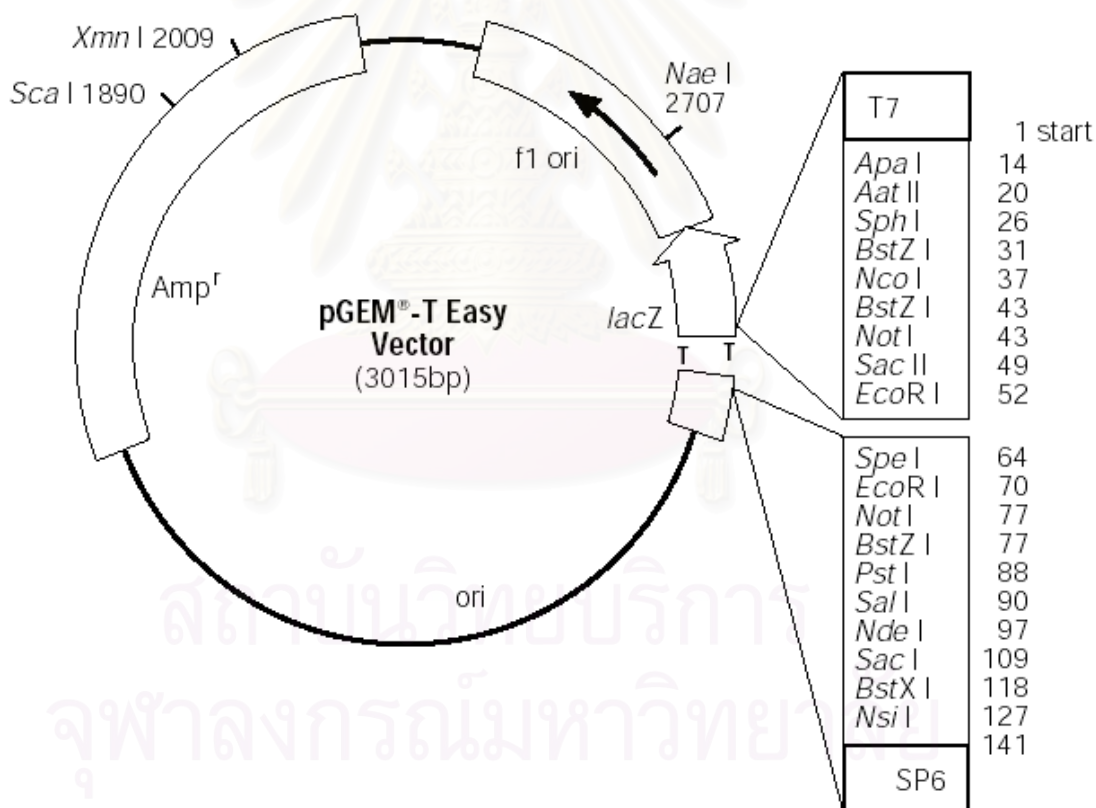


Figure 45 Circle map of pGEM-T Easy vector (Promega)

RNA interference

RNA interference (RNAi) is a process by which double stranded RNA (dsRNA) or small interfering RNA (siRNA) directs the gene-silencing mechanism in eukaryotes, either by inducing the sequence-specific degradation of mRNA or by inhibiting translation [100-102]. This phenomenon was initially observed in *Caenorhabditis elegans* [103], in plants [104] and in mammalian cells [105]. Naturally occurring RNAi is triggered by long dsRNAs which are then processed by the ribonuclease III activity of the Dicer enzyme [106] to generate a 21-22 nucleotides long RNA duplex (21-22 nucleotides long with 2-nt overhang at each 3' end), termed short interfering RNA (siRNA) [105]. Each strand of siRNA contains a 5' phosphate group and a 3' hydroxyly group. These siRNAs are then incorporated into a protein complex, known as the RNA-induced silencing complex (RISC), which in turn uses an ATP-dependent RNA-helicase activity to unwind the duplex siRNA into single-stranded siRNA [107]. The antisense strand of the siRNA guides the RISC to the target mRNA, where the RISC-associated endoribonuclease cleaves the target mRNA at a single site in the centre resulting in the silencing of the target gene (Figure 46).

The natural RNAi process has now expanded as a tool into a widely used in high-throughput screens in both basic and applied molecular biological applications including gene mapping, pathway dissection and functional gene analysis. With in advent of RNAi, genes knockdown (lose of function) in mammalian organism are now accessible to a broader array of researchers and accelerate the progress of discovery biology.

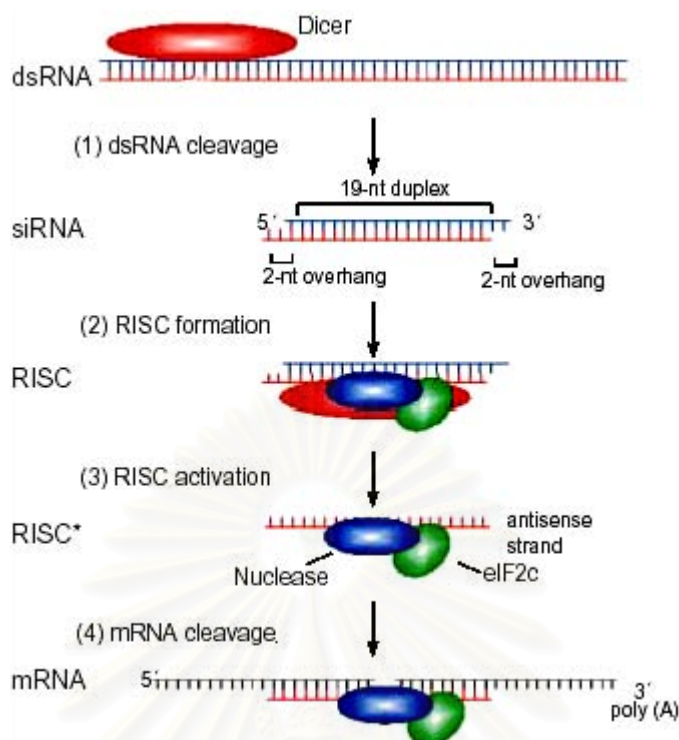


Figure 46 Model for RNA interference triggered by dsRNA. RNAi process can be divided into four stages: (1) dsRNA cleavage by Dicer and generation of siRNA duplex, (2) recruitment of RNAi machinery and formation of RNA-induced silencing complex (RISC), (3) siRNA unwinding and RISC activation, and (4) target mRNA degradation.

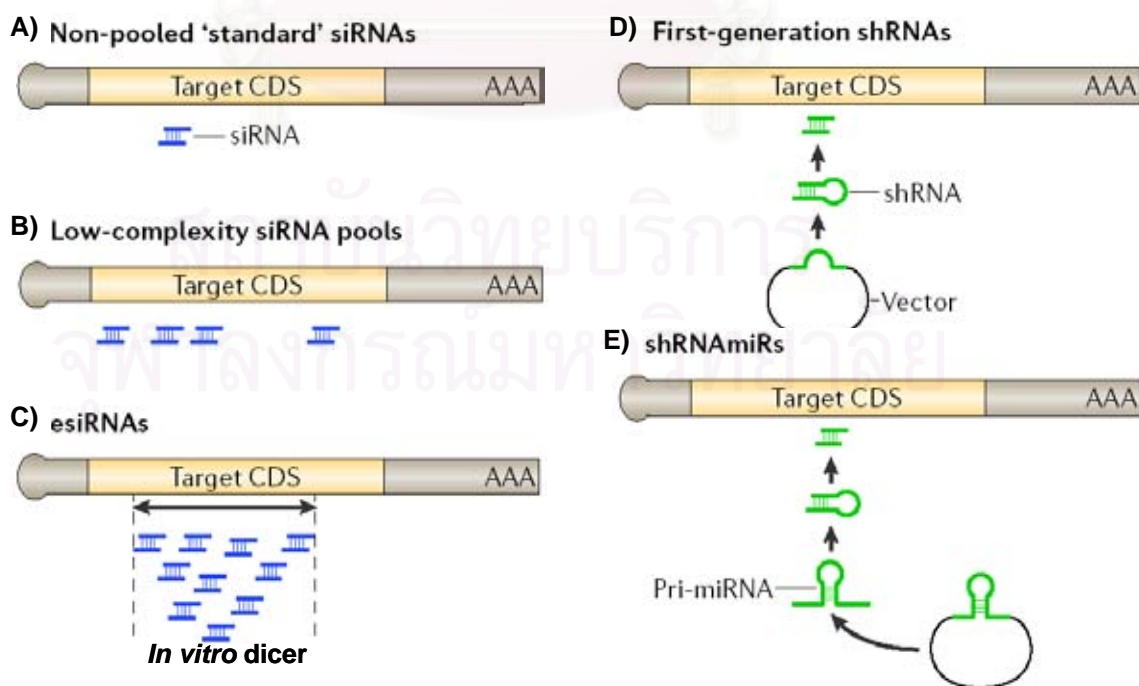


Figure 47 Silencing reagents for RNAi screening [108].

Silencing reagents for RNAi screening

Synthetic siRNA molecules

Most mammalian cell based RNAi studies have used siRNAs that are designed to closely mimic endogenous 21-nt siRNAs with 2-base overhangs at both 3' ends [105].

- Standard single siRNA (Figure 47A)

Experimental validation of this type of siRNAs has typically shown approximately 80-90% probabilities of individual siRNAs yielding a >70% reduction in target mRNA level after 48 hours under standard transfection in human cell lines.

- Low-complexity siRNA pools (3-6 siRNAs) (Figure 47B)

Using multiple siRNAs that target different regions within the same gene, the combined probabilities of achieving >70% silencing are theoretically increased to ~95% or more. Although the concept of using a pool of siRNAs is attractive for achieving a higher probability of strong silencing, this procedure results in higher cost.

- Endonuclease-prepared siRNA (esiRNA) (Figure 47C)

Using of endonuclease-prepared siRNA (esiRNA) takes the pooling concept to a higher level (Kittler, 2004). esiRNAs are generated from 200-500 bp dsRNAs that are transcribed *in vitro* from DNA templates and then digested by either a recombinant Dicer enzyme or bacterial RNase III. The result is a high complexity of siRNA-like molecules which all target the same gene (Figure 47C). This procedure significantly lower siRNAs production costs.

Vector-based shRNA (Figure 47D and 47E)

The advent of shRNA technology has allowed the development of cheaper, renewable RNAi libraries that can be delivered into almost cell lines, enabling sustained silencing over weeks. The shRNA approach is most powerful when combined with viral vector-based delivery, which yielding almost 100% delivery in many cell types. The first generation of shRNA expression vectors were designed to express as hairpin transcripts driven by RNA polymerase III promoters, entering the RNAi pathway as pre-miRNA-like molecules. The second generation of shRNA expression vector integrates an endogenous miRNA (miR-30). This yields "shRNAmiRs" that enter the RNAi pathway as pri-miRNAs and thought to undergo more efficient processing by the RNAi machinery.

Short interfering RNA (siRNA) design guidelines:-

Several groups of researchers have proposed basic rules and additional guidelines for designing effective siRNAs [109]. The basic rules require the generation of two 21-nt sense and antisense oligoribonucleotides that target a region in the gene of interest. It is important that each strand of siRNAs has 2-nt of deoxythymidine(dT) overhangs at 3'end, in order to protect the siRNAs from exonuclease activity. An example siRNA would be: sense 5'-(N19)dTdT-3' and antisense 3'-dTdT(N19)-5', where N is any nucleotide. In addition, overall G+C content in the siRNA should be moderate (30-50%) in order to facilitate an interaction with RISC and unwinding. Other suggestions in the basic rules including the siRNA must avoid targeting certain regions of the mRNA such as introns, both 5' and 3' untranslated regions (UTRs) and regions within 75 bases of the start codon. Finally, to minimize nonspecific effects, a BLAST-search of genome sequence databases should be done to confirm that only one gene is being targeted by the siRNA.

Additional guidelines describe considerations for generating an effective and specific siRNA. First of all, the siRNA should lack internal repeated or palindromic sequences. In addition, an effective siRNA should have high stability (GC rich) at the 5' end of the sense strand and lower stability (AU rich) at the 5' antisense terminus in order to promote anti-sense strand selection by RISC. Moreover, base preferences at specific position in the sense strand should be included in the consideration. For example, a presence of (A) at position 3, (U) at position 10 and an absence of a (G) or (C) at position 19 for promoting anti-sense strand selection and RISC mediated cleavage of mRNA (Figure 48).

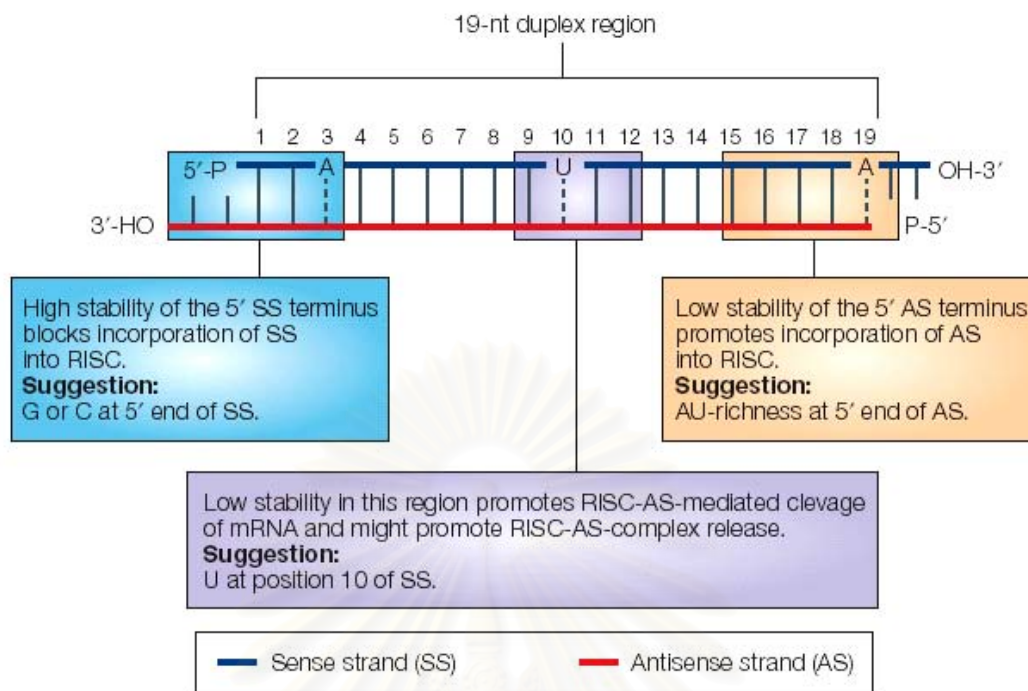


Figure 48 Designation of effective siRNA. A small interfering RNA (siRNA) is a 21 nt dsRNA that contains: a 19-nt duplexed region, symmetric 2-nt overhangs at 3' end, 5'-phosphate (P) and 3'-hydroxyl (OH) groups. The positions of each nucleotide in the 19-nt duplexed region of the sense strand are shown. On the basis of recently established guidelines, an effective siRNA has high stability at the 5' terminus of the sense strand, lower stability at the 5' antisense terminus and at the cleavage site. In addition, the sequence-specific preferences at the following positions on the sense strand are important: the presence of an A at position 19, an A at position 3, and a U at position 10 [109].

สถาบันวิทยบริการ
จุฬาลงกรณ์มหาวิทยาลัย

MTT assay

MTT assay is a simple method for determination of cell number using standard microplate absorbance readers. Determination of cell growth rates is widely used in the testing of drug action, cytotoxic agents and screening other biologically active compounds. Several methods can be used for such determinations, but indirect approaches using fluorescent or chromogenic indicators provide the most rapid and large scale assays. Among such procedures, the MTT assay developed by Mossman is still among one of the most versatile and popular assays.

The MTT assay involves the conversion of the water soluble MTT (3-(4,5-dimethylthiazol-2-yl)-2,5-diphenyltetrazolium bromide) to an insoluble formazan by mitochondrial succinate dehydrogenase, an enzyme which is only active in viable cells. The formazan is then solubilized by SDS-HCL solution, and the concentration was determined by optical density at 570 nm. The intensity of the color developed by the assay was correlated with the number of viable cells. An increased number of viable cells leads to increased metabolic activity and results in a stronger color development. The result is a sensitive assay with excellent linearity up to approximately 10^6 cells per well.



สถาบันวิทยบริการ
จุฬาลงกรณ์มหาวิทยาลัย

APPENDIX B

Virological techniques

Primary isolation of viruses

For clinical samples, the type of specimen and the manner of collection are dependent on the laboratory methods anticipated. Ideally specimens should be collected within two days of onset of symptoms, because most viruses are shed only in the initial stages of illness. Nasal swabs are the easiest specimens to collect for respiratory viruses and are also the best specimens for the majority of the respiratory viruses. For nasal swabs, urogenital calginate swabs are inserted into the nasal passages, gently rotated to absorb mucus and cells, and then vigorously twirled into 1 ml of transport medium. Throat swabs can be obtained with cotton-tipped wooden applicator sticks that are rubbed against the posterior nasopharynx and then placed in the transport medium. The stick can easily be broken off to leave the cotton tip in the medium. Nasopharyngeal aspirates are collected with a neonatal mucus extractor and mucus trap to which transport medium is added. Swabs or scrapings of vesicular lesions are likewise carefully obtained and placed in transport medium.

Specimens should be placed on wet ice and transported to the laboratory for immediate testing. If testing is not possible within 5 days after collection, the specimens should be frozen on dry ice and stored at -70°C until processed, although this may decrease the amount of viable virus.

When processing for viral isolation, the specimens are treated with antibiotics, vigorously mixed, clarified by centrifugation in $1000\times g$ for 3 minutes at 4°C to remove cell debris and bacteria, and inoculated onto appropriate cell culture monolayers. The inoculum is adsorbed to the cell monolayers for 1 hour at ambient temperature, and the cultures are then fed with maintenance medium and incubated at 37°C for several days.

Small variations in media composition and incubation temperature are also important for the successful isolation of certain viruses. For instance, some viruses require prior treatment with trypsin for successful cultivation, and some cells require the presence of trypsin in the medium for them to be sensitive to certain viruses.

Virus isolation for *Orthomyxoviridae*

Influenza A, B and C viruses are spread by aerosol droplets and fomites and are best recovered in roller cultures of MK and MDCK cells and in embryonated eggs. Chick embryo, MDCK and other cells require a fortified medium containing trypsin for optimal sensitivity. The viruses are detected in MK cells by hemadsorption and MDCK cells by hemagglutination test. The embryonated eggs provides an ideal “receptacle” in which to grow influenza viruses, as it is sterile and had a range of tissue types and cavity fluids which both support the replication and allow the concentration of infectious virus. The anatomy of the egg is shown in Figure 49.

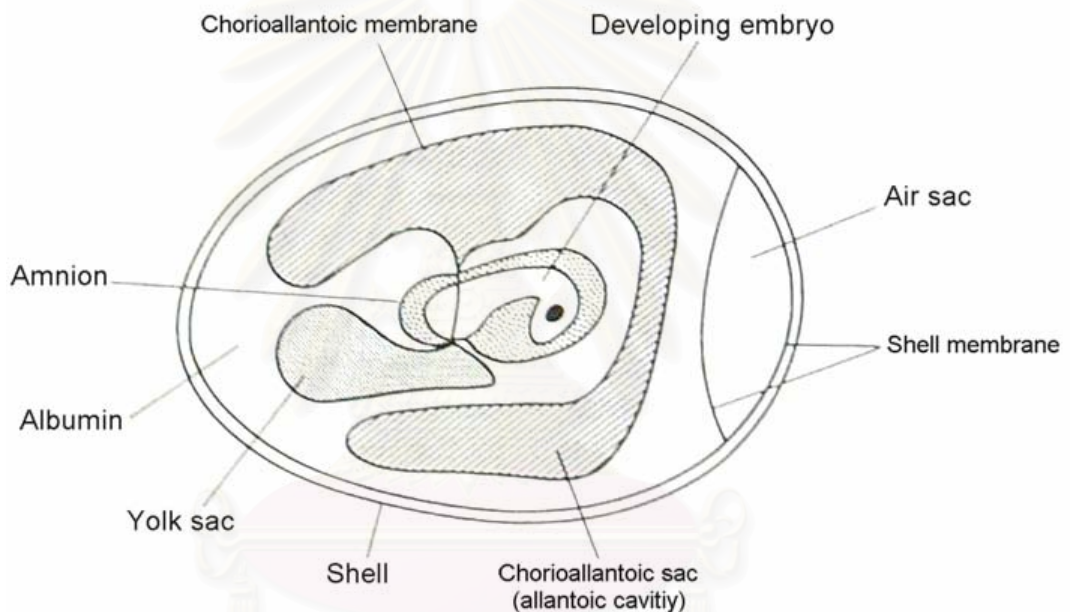


Figure 49 Schematic diagram represent anatomy of embryonated egg.

สภานิติบัญญัติ
จุฬาลงกรณ์มหาวิทยาลัย

Fertile hens' eggs are acquired from a suitable hatchery and incubated at 37°C in an atmosphere of about 62% humidity with a forced (usually fan driven) air circulation. This prevents drying out of the egg and allows for good air exchange in the developing embryo. The embryo and developing membranes and cavities go through a variety of anatomical changes up to hatching. Particular sites of injection are therefore optimal at various times in the development of the embryo, e.g. influenza viruses are inoculated into the chorioallantoic sac of a 9-11 day embryo. The procedure of egg inoculation can be divided up into a series of steps.

- Eggs are candled to check for viability and to determine the positions of the embryo, membranes and blood vessels. Dead eggs will have little or no vasculature and have a characteristic translucent appearance. Darkly stained eggs are usually heavily contaminated. Candling is carried out in a darkened room using a light box which has one small egg-shaped hole surrounded by a piece of foam on which the egg is placed. Rotating the egg immediately reveals its anatomical make-up.
- Eggs are disinfected with alcohol and marked on the shell in preparation for the drilling of holes, care being taken to avoid areas rich in blood vessels.
- The virus is injected via the appropriate route, and the hole is covered with glue.
- Contaminated eggs (which appear 24 hours post inoculation) are discarded.
- Eggs are chilled and harvested 2-5 days post infection.

Determination of viral titers

For most virology experiments, it is essential to know the concentration of the total or infectious virus particles present in any given virus suspension. Such quantitation forms the basis for example of determining one-step growth curves, examining the neutralization of virus infectivity, assessing the activity of chemotherapeutic agents, monitoring the stages of virus purification and assessing virus pathogenicity. Animal viruses are quantified by either an infectivity assay including Tissue Culture Infective Dose₅₀ (TCID₅₀), Egg Infective Dose₅₀ (EID₅₀) and Lethal Dose₅₀ (LD₅₀) or biological/chemical assays such as haemadsorption, haemagglutination and total protein assay or by direct total virus particle counting using the electron microscope.

Most virologists however, would consider the plaque assay to be the easiest, most accurate and sensitive form of assaying virus infectivity. The plaquing efficiency of some viruses however is often poor and hence other methods are needed.

Infectivity assay

Probably the most important attribute of a virus is its ability to infect and replicate within a cell. The virus replicative cycle is accompanied by a number of biochemical and morphological changes within the cell which usually culminates with cell death. These morphological changes, which are often readily visualized with light microscopy including the virus cytopathic effect (CPE) and may take several forms e.g. cell rounding, cell fusion (syncytia formation) or total cell lysis.

Infectivity assays are designed to allow the calculation of a virus "titer" (the number of infectious units per unit volume (such as plaque forming units per ml). Infectious units are usually thought of as being the smallest amount of virus that will produce a detectable biological effect in the assay. Infectivity assays are of either the quantal or focal type. Quantal assays detect the presence of infectious virus by use of an "all or none" approach. For example; Does a tissue culture monolayer show CPE? Is an egg infected? Has an animal died? Whereas, focal assays rely on the detection and counting of foci of infection e.g. a focus of CPE (plaque) which allows for the quantitative determination of the number of infectious units as opposed to the qualitative approach of the quantal assay.

Virus dilution

Virus titers are determined by making accurate serial dilutions of virus suspensions, the diluent usually being either tissue culture maintenance or growth medium. Such serial dilutions are usually done using factors of 2, 5 or 10, the former obviously giving a more precise titer. For routine use 10-fold dilutions are usually carried out.

When setting up such a dilution series consideration should be given to the final volume of diluent needed for the assay and thus aliquots of 0.9, 4.5, 9.0 ml are usually made in a series of sterile tubes or bottles. In order to conserve virus stocks, it is usual for the first (lowest) dilution in the series to be achieved by the use of 0.1 ml stock suspension. With subsequent dilutions, it is very important to use a new sterile pipette for each transfer and to thoroughly mix each virus dilution before further transfer. Use of the same pipette will transfer millions of virus particles along the series, resulting in a very large dilution error. Once diluted, virus should be assayed as soon as possible although, if necessary, some viruses will withstand storing at 4°C for a few hours before assay. The use of such a storage procedure should obviously be checked to determine if it is suitable for the virus under assay.

Tissue Infective Dose₅₀ (TCID₅₀)

The TCID₅₀ is defined as that dilution of a virus required to infect 50% of a given batch of inoculated cell cultures. The assay relies on the presence and detection of cytocidal virus particles i.e. those capable of causing CPE.

Host cells are grown in confluent healthy monolayers, usually in tubes or 96-well tissue culture grade plastic plates, to which aliquots of virus dilutions are added. The method becomes more accurate with increasing numbers of tubes or wells per dilution, but it is usual to use either 5 or 10 repetitions per dilution.

On incubation, the virus replicates and progeny virions are released into the supernatant, these infecting healthy cells in the monolayer. The CPE is allowed to develop over a period of days (depending on the virus and cell type) at which time the cell monolayers are observed microscopically (they can be fixed and stained if necessary). Tubes are scored for the presence or absence of CPE.

It is thus a quantal assay in that each tube provides only one piece of information, i.e. is there CPE or not? The data is used to calculate the TCID₅₀ of the initial virus suspension by one of two ways- the Reed-Muench and the Spearman-Kärber methods. The calculation does not tell us how many infectious units are present in the original virus suspension but what dilution of virus will give CPE in 50% of the cells inoculated.

Calculation of TCID₅₀ and EID₅₀

Table 23 Data used to calculate TCID₅₀ and EID₅₀

Log of virus dilution	Infected test units	Cumulative infected (A)	Cumulative non-infected (B)	Ratio of A/ (A+B)	Percent infected
-5	5/5	9	0	9/9	100.0
-6	3/5	4	2	4/6	66.7
-7	1/5	1	6	1/7	14.3
-8	0/5	0	11	0/11	00.0

- Reed-Muench method

The dilution in Table 27 that corresponds to the 50% end point obviously lies somewhere between the 10⁻⁶ (66.7% infected) and 10⁻⁷ (14.3% infected) dilutions. The proportionate distance between these two dilutions is calculated in the following manner:

$$\frac{(\% \text{ positive above } 50\%) - 50\%}{(\% \text{ positive above } 50\%) - (\% \text{ positive below } 50\%)} = \text{Proportionate distance}$$

i.e.,

$$\frac{66.7\% - 50\%}{66.7\% - 14.3\%} = 0.3$$

Given that the log of the dilution above 50% is -6, the proportionate distance is 0.3 and the log of the dilution factor is -1 (i.e., serial 10 fold dilutions were used) the 50% end point is now calculated in the following way:

$$(\log \text{ dilution above } 50\%) + (\text{proportionate distance} \times \log \text{ dilution factor}) = \log \text{ ID}_{50}$$

$$(-6) + (0.3 \times -1.0) = -6.3$$

Therefore ID₅₀ = 10^{-6.3}

This is the end point dilution, i.e., the dilution that will infect 50% of the test units inoculated. The reciprocal of this number give rise to the virus titer in terms of infectious doses per unit volume. If the inoculation of virus dilution was 0.1 ml the titer of the virus suspension would therefore be: 10^{6.3} ID₅₀ / 0.1 ml = 10^{7.3} ID₅₀ / ml.

- Spearman-Kärber method

Using the data from table 27, the following formula is used to directly estimate the 50% end point:

$$\text{Highest dilution giving 100\% CPE} + \frac{1}{2} - \frac{\text{total number of test units showing CPE}}{\text{number of test units per dilution}} = \text{ID}_{50}$$

$$-5 + \frac{1}{2} - \frac{9}{5} = -6.3 \text{ ID}_{50} \text{ or } 10^{-6.3} \text{ ID}_{50} \text{ unit / volume}$$

The titer, given a volume of 0.1 ml, therefore: $10^{-6.3} \text{ ID}_{50} \text{ unit} / 0.1 \text{ ml} = 10^{-7.3} \text{ ID}_{50} \text{ unit / ml}$.

The principle involve in the TCID_{50} experiment is the same for either animal deaths (LD_{50}) or infection of developing fertile hen's egg (EID_{50}).

Plaque assay

The plaque assay is an infectivity assay that quantified the number of infectious units in a given virus suspension. Plaques are localized discrete foci of infection denoted by zones of cell lysis or CPE within a monolayer of otherwise healthy tissue culture cells. Each plaque originates from a single infectious virion thus allowing a very precise calculation of the virus titer.

Plaque assays are essentially of two types, suspension assays and monolayer assays. In suspension assays a high concentration of healthy tissue cells, in a small volume, are shaken with a suitable diluted aliquot of virus to allow virus adsorption to take place; cells are seeded onto a tissue culture grade vented Petri dish. The monolayer assay on the other hand requires a small volume of virus diluent to be added to a previously seeded confluent tissue culture cell monolayer for virus adsorption to take place. In both assays, prior to incubation, an overlay medium is added to the cell suspension or cell monolayer. Overlay media, composed of either agar/agarose or methylcellulose solution prevent the formation of secondary plaques by forcing those virus particles released from the initial infected cell to invade adjacent cells as opposed to spreading to other areas of the cell monolayer.

Following the addition of overlay medium, the assay dishes are incubated at an appropriate temperature until plaques are readily discernible. At this point, Petri plates or microplates are “fixed” with formal saline solution and stained with crystal violet solution. Plaques are observed either macro- or microscopically.

For statistical reasons 20-100 plaques per monolayer are ideal to count, although the actual number is often dependent on the size of the plaque and the size of the vessel used for the assay.

The infectivity titer is expressed as the number of plaque forming units per ml (pfu/ml) and is obtained in the following way: [Plaque number x Reciprocal of dilution x Reciprocal of volume in ml]. For example, if there is a mean number of 50 plaques from monolayers infected with 0.1 ml of a 10^{-6} dilution there are [$50 \times 10 \times 10 = 5 \times 10^8$ pfu/ml].

It is essential that the reader experiments to determine the most sensitive and suitable plaque assay for their own virus/cell system as the methods vary in relation to details including:

- Sensitivity of the cell to virus infection- plaquing efficiencies varying from cell to cell.
- The time required for virus adsorption to cells.
- The type of agar used in the overlay medium, i.e. some can be inhibitory for virus replication.
- The time of incubation, i.e. plaques must be visible but discrete.
- The constituents of the medium in which the overlay is dissolved, i.e. some viruses require high Mg^{2+} concentrations for plaque formation.
- The ability of the virus to cause a detectable CPE in tissue culture.
- The ability of the cells to form a confluent monolayer.
- The need to add a protease (e.g. trypsin) to the overlay medium for plaque formation.

Haemagglutination

The ability of some viruses to aggregate various species of red blood cells (RBCs) is referred to as haemagglutination. This effect is brought about by the interaction of specific virus glycoproteins with surface receptors present on the plasma membrane of RBCs. Not all viruses are capable of causing this reaction and those that do may only react with RBCs of particular species and may do so only under stringent conditions of pH and ionic strength.

For the reaction to occur, the virus should be in sufficient concentration to form cross-bridges between RBCs, causing their agglutination. Thus, RBCs left in a hemispherical well unagglutinated will fall to the bottom of the well and form a well-defined RBC pellet. Agglutinated RBCs on the other hand will form a lattice-work structure which coats the sides of the well. The two morphological appearances (pellet and lattice) are easily discernible with the naked eye.

The haemagglutination assay is done by end point titration. Serial two fold dilutions of virus suspension are mixed with an equal volume of RBCs of known concentration and wells are observed for the presence or absence of a lattice. RBCs are routinely used at 0.3% or 0.5%. The end point of the titration can be interpreted by the last dilution showing complete agglutination. The HA titer of a virus suspension is therefore defined as being the reciprocal of the highest dilution which causes complete agglutination and is expressed as the number of HA units per unit volume for a given concentration of RBCs. An example upon which a calculation of the HA titer can be made is shown in Figure 51. The end point in this figure, assuming this to be the highest dilution capable of complete agglutination, is 1/512. If 0.1 ml of virus were added per well, the HA titer would be 512 HA units / 0.1 ml or 5120 HA units/ ml.



Figure 50: Example of result obtained by Hemagglutination assay

APPENDIX C

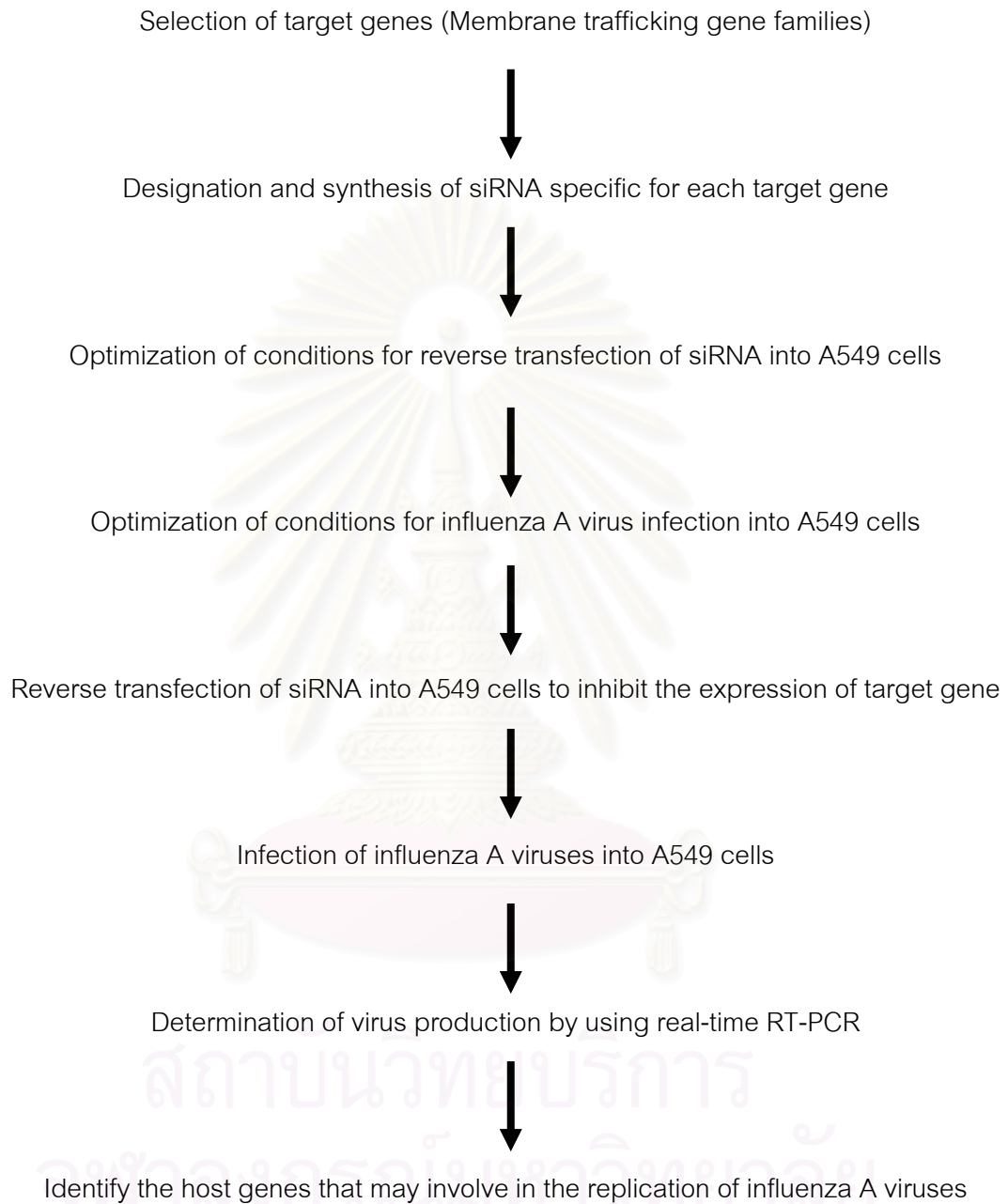
Identification of host genes involving in the replication of influenza A viruses by RNAi screening

RNA interference (RNAi) is a highly conserved pathway used by eukaryotes as a cellular line of defense directed against invading viral genomes or as a method to clear a cell of aberrant transcription products. While the mechanism is not fully understood, RNAi is proving to be an invaluable tool for gene function analysis and target validation. Short RNA duplexes (19-25 bases in length) introduced into mammalian cells in culture led to sequence-specific inhibition of target mRNA without inducing an interferon response. The siRNA-mediated effect has been shown to be stable over time, and silencing may be observed through several cell generations. These properties make siRNA-mediated interference attractive as a method for targeted gene knockdown. The ability to assess gene function by this method represents an innovation that promises to revolutionize and accelerate genome-wide research, drug discovery, therapeutic development, and is now being used in highthroughput experiments with large numbers of siRNAs, or siRNA libraries [110, 111]. Therefore, we applied the RNAi technique to inhibit the expression of host target genes and then monitoring the amount of virus production in order to identify genes that involve in the replication of influenza A viruses.

- **Model for investigation**

A549 (human lung carcinoma) was selected for using as a model in this study for 3 major reasons. The first reason is because this cell can be infected with influenza A viruses and allowed efficiently replication of influenza A virus. Second, the complete human genome provides valuable information for designation of siRNAs specific for each target gene. Finally, the replication of influenza A virus in human cell line may directly represents the natural replication of the virus in infected patients. Therefore, the conceptual model in this study included the A549 cells transfected with specific siRNA in order to knockdown the expression of individual host mRNA, followed by infection with human influenza A viruses and then the amount of virus production was determined in order to identify the host genes involving in the replication of influenza A viruses.

- Conceptual framework for Identification of host genes that may involve in the replication of influenza A viruses



- **Selection of host target genes to be knocked-down**

Several gene families are available for analysis by genome-wide RNAi screening. Membrane trafficking gene family (122 genes) were selected as a primary targets for gene knocked-down by RNAi screening. Because we hypothesized that during influenza viral replication, the genes responsible for the membrane trafficking pathway may involve in the endocytosis and virus assembly step of the replication cycle.

- **Platform of siARRAY siRNA Libraries**

siARRAY siRNA libraries (Dharmacon) consist of prevalidated groups of rationally designed pooled of siRNA reagents consisted of four non-identical siRNAs directed against different regions of the same gene- virtually assuring efficient gene knockdown (Figure 51). Each siRNAs pool is provided in a ready-to-use dried-down form, which can be prepared for silencing studies by resuspending in buffer. Each library is arrayed in a multi-well format that facilitates the rapid preparation of hundreds of silencing reagents for use in small-scale or large-scale studies of entire gene families or specific regulatory pathways. Efficient and potent gene silencing in each case is virtually assured since each siRNA-based reagent is expected to silence target gene expression at the mRNA level by at least 75% when used under optimized transfection and cell culture conditions. This feature promotes savings on assay cost as well as on experimental time, and minimizes uncertainty related to randomly designed siRNA duplexes.

- **Transfection of siRNAs into cells by reverse transfection format (RTF)**

Reverse Transfection Format (RTF) is an efficient siRNA screening technique that requires minimal handling. Pre-validated siRNA reagents (6.25 pmol / well) are provided dried-down in cell culture plates. There is a simple 4 step procedures including: (1) rehydration of siRNA, (2) formation of lipid mediated-siRNA complex, (3) seeding of cell cultures and (4) target gene silencing after 48 hours post transfection (Figure 51).

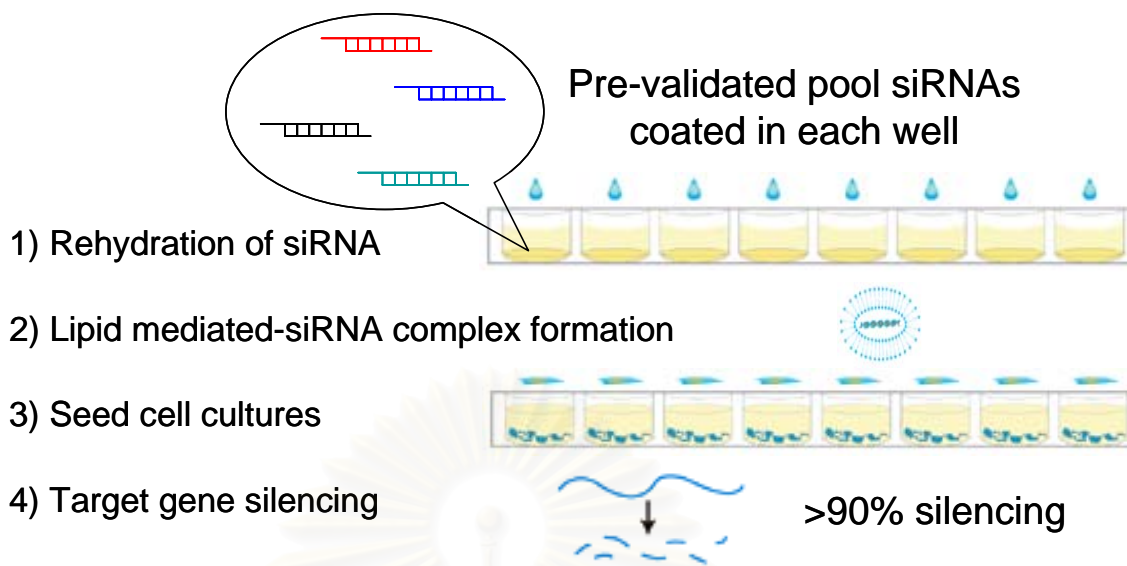


Figure 51 Transfection of siRNAs by reverse transfection format (RTF)

Optimization of siRNA transfection and silencing

For optimization of siRNA transfection condition and silencing efficiency, several factors including cell plating density (1×10^4 or 2.5×10^4 cells/well), amount of transfection reagent (0.2 or 0.4 μl / well) and post transfection periods (48 or 60 hours) were subjected to be optimized by using optimization available from Dharmacon. The optimization plate is a 96-well plate coated with siRNAs controls (Figure 52).

- Wells in row A were coated with non-targeting siRNA which will not silencing any of human gene whereas wells in row B were coated with RISC-free siRNA (modified siRNA molecules that will not incorporated in to the RISC complex). Therefore, wells in row A and B are served as a negative silencing control.

- Wells in row C were coated with siGLO RISC-Free siRNA (modified siRNA which will not incorporated into the RISC complex) labeled with Cy3 fluorescent reporter. Thus wells in row C were used to monitor the transfection efficiency under fluorescence microscope with rhodamine filter.

- Wells in row D, E and F were coated with pools of siRNA targeted GAPDH, Cyclophilin B and Lamin A/C, respectively. These wells served as a positive silencing control.

- Wells in row G and H were an empty well (no siRNAi) which served as a mock transfection control (transfection reagent only) and an untreated control, respectively.

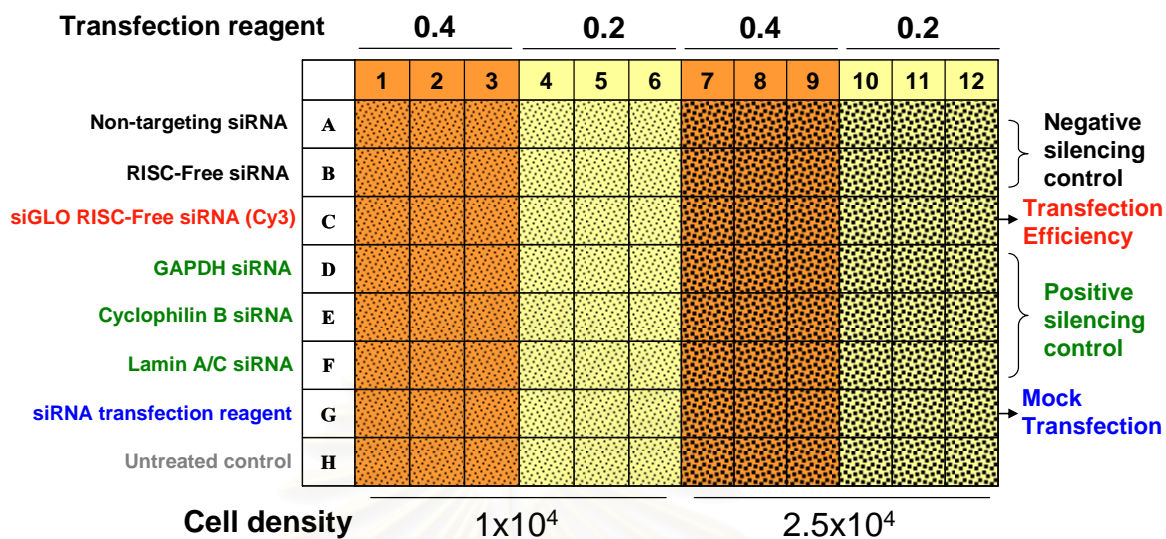


Figure 52 Optimization plate for optimization of the siRNA transfection and silencing efficiency.

- **Determination of siRNA transfection efficiency**

After 48 or 60 hours post-transfection, the plate was observed under fluorescence microscope with rhodamine filter in order to determine the siRNA transfection efficiency (row C) (data not shown). The condition that yields highest transfection efficiency will be used as a condition for transfection.

- **Determination of cell viability by MTT assay**

Because excess amount of transfection reagent may be toxic for transfected cells, therefore, MTT assay was performed for determination of cell viability. The MTT assay involves the conversion of the water soluble MTT (3-(4,5-dimethylthiazol-2-yl)-2,5-diphenyltetrazolium bromide) to an insoluble formazan (dark color) by mitochondrial succinate dehydrogenase, an enzyme which is only active in viable cells. Therefore, more viable cells result in darker color of cell monolayer (Figure 53A). The formazan is then solubilized by SDS-HCL solution, and the concentration was determined by optical density at 570 nm. The intensity of the color developed by the assay was correlated with the number of viable cells (Figure 53B). The condition that yields higher cell viability will be used as a condition for transfection.

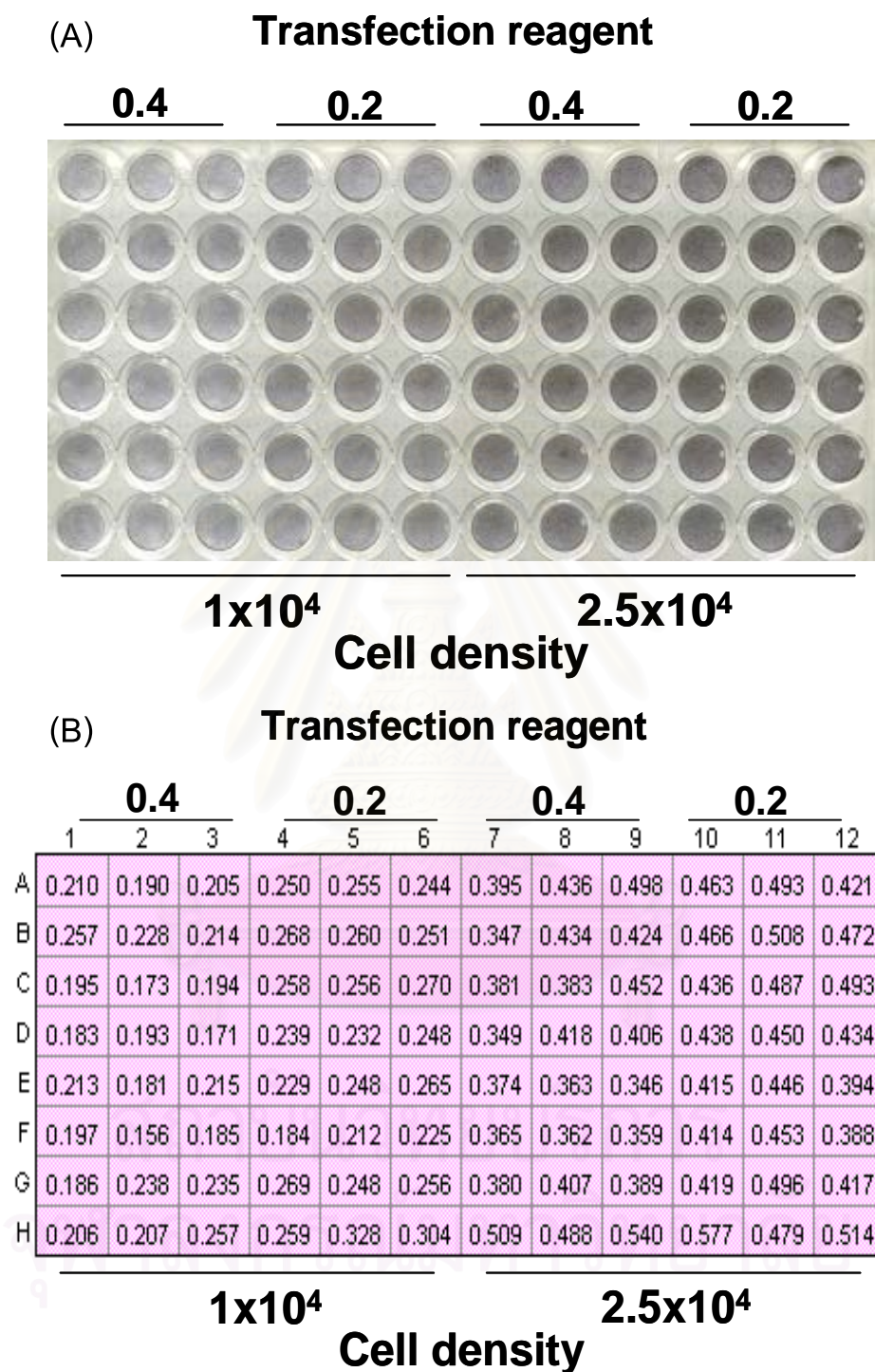


Figure 53 Results of MTT assay obtained from the optimization plate. (A) Pre-solubilized insoluble formazan (dark color) represents amount of viable cells. (B) Optical density at 570 nm obtained after solubilization of formazan with SDS-HCl solution.

- **Determination of silencing efficiency**

Silencing efficiency was performed comparing amount of GAPDH and Cyclophilin B gene between wells of the positive silencing control and negative silencing control. The amounts of GAPDH and Cyclophilin B genes were determined by relative quantitation based on real-time RT-PCR using specific primers and probes (Table 24). Delta Ct method (Appendix A) was used to calculate relative (different ratio) amount of genes (Table 25). The condition that yields highest silencing efficiency will be used as a condition for silencing.

Table 24 Specific primers and probes for GAPDH and Cyclophilin B

Oligo name	Sequence (5'→3') (upper cases = LNA residues)	Product size (cDNA)	Product size (gDNA)
GAPDH-F ₈₅	5'-gtgaagggtcggagtcacacgg-3'	107 bp	1739 bp
GAPDH-P ₁₂₁	HEX-cgcctgggtcaCcacgggctgc-BHQ1		
GAPDH-R ₁₉₁	5'-tcaatgaaggggtcattgatgg-3'		
CPB-F ₄₁₄	5'-gagagaaaggattttggctacaa-3'	181 bp	3375 bp
CPB-P ₄₅₈	HEX-atcaaGgActTcaTgAtcCagg-BHQ1		
CPB-R ₅₉₄	5'-ttggccatgctcaccacagc-3'		

Table 25 Silencing efficiency of the optimization plate obtained from real-time RT-PCR

Cells	TF reagent	Hours	GAPDH		Cyclophilin B	
			Δ Ct	Folds	Δ Ct	Folds
1 × 10 ⁴	0.4	48	7.56	188	6.77	109
		60	6.37	83	5.49	45
	0.2	48	6.36	82	5.40	42
		60	6.30	79	6.61	97
2.5 × 10 ⁴	0.4	48	7.35	163	7.51	182
		60	6.22	74	7.29	156
	0.2	48	6.26	76	7.03	130
		60	5.79	55	6.07	67

- **Optimized conditions for highest siRNA transfection and silencing**

According to the optimization results obtained from fluorescent microscope (determination of siRNA transfection efficiency), together with MTT assay (determination of cell viability) and real-time RT-PCR (determination of silencing efficiency), we consider the conditions in terms of yielding high efficiency of transfection, favorable amount of viable cells and high degree of specific gene silencing. In summary, the optimized condition including:

- Cell seeding density at 2.5×10^4 cells per well
- 0.4 μl / well of transfection reagent
- 48 hours post transfection period

- **Optimization of virus infection condition**

For optimization of virus infection, several factors including strains of human influenza A viruses (Ohio (H1N1) or Victoria (H3N2)), Trypsin concentrations (0.1, 0.25 or 0.5 $\mu\text{g} / \mu\text{l}$) and post infection period (24, 36 and 48 hours) were subjected to tested with the optimization plate as described above. Viability of cells was determined by staining the cell monolayer with crystal violet (CV) and MTT assay (Figure 54). The amount of influenza viral gene (matrix) which represents the replication of the virus was relatively quantitated by real-time RT-PCR using specific primers and probe for M gene (Table 26).

According to the result obtained from the optimization of virus infection, we considered the cell viability from crystal violet and MTT staining and amount of viral RNA detected by real-time RT-PCR assay. We found the optimized condition for virus infection includes:

- Infection with Victoria (H3N2) strain (with MOI of 5)
- Trypsin (TPCK) at final concentration of 1 $\mu\text{g} / \mu\text{l}$
- 24 hours post-infection period

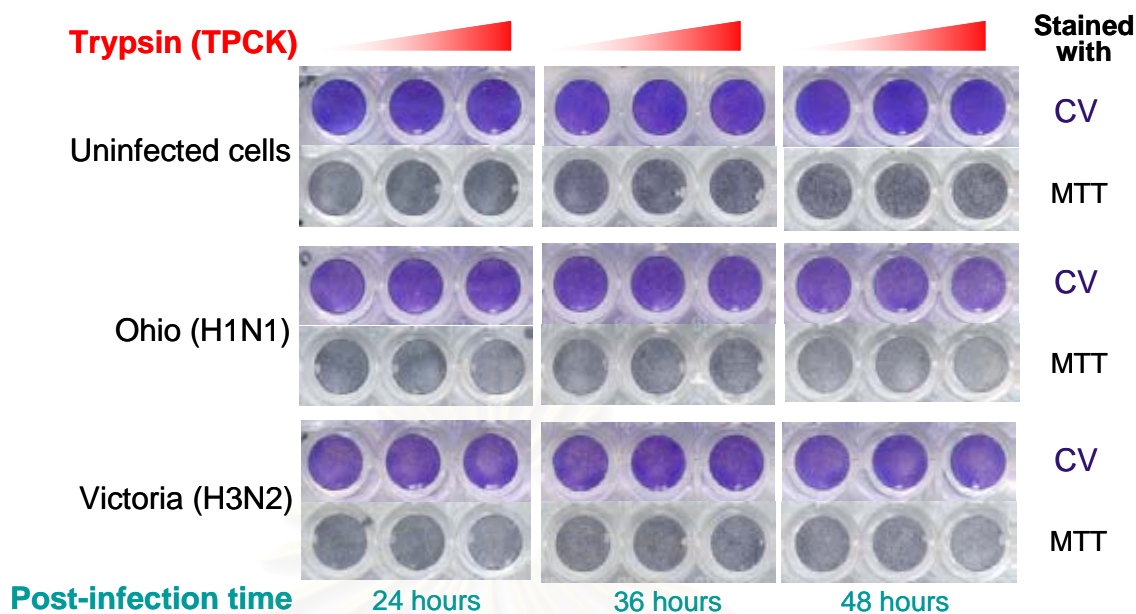


Figure 54 Optimization of condition for virus infection. A549 cells were infected with Ohio (H1N1) or Victoria (H3N2) in different post infection periods and then strained with MTT assay or crystal violet.

Table 26 Quantitation of M gene by real-time RT-PCR (Numbers indicate Ct values; lower Ct represents higher initial amount of gene)

Post infection time	Ct obtained from real-time RT-PCR								
	24 hours			36 hours			48 hours		
Trypsin (TPCK)	1	2.5	5	1	2.5	5	1	2.5	5
Uninfected cells	-	-	-	-	-	-	-	-	-
Ohio (H1N1)	11.48	11.30	11.18	17.05	12.50	11.09	14.06	11.78	10.53
Victoria (H3N2)	13.29	12.90	12.26	12.95	12.50	11.95	12.25	12.05	11.96

- **RNAi screening experiment**

All of siRNAs target the membrane trafficking gene family were pre-validated and synthesized by Dharmacon. After optimization of siRNA transfection and virus infection conditions, the RNAi screening was performed following the optimized condition. Briefly, pools of pre-validated siRNAs (6.25 pmoles per well) specific for each target gene in the membrane trafficking gene family (Table 27) were coated onto each well of a 96-well siARRAY RTF plate (Dharmacon). For reverse transfection of each individual siARRAY RTF plate, a rehydration solution was prepared by combining 2 ml of DharmaFECT Cell Culture Reagent (DCCR) with 32 μ l of DharmaFECT Transfection Reagent (DF) and then mix by pipetting. Transfer 25 μ l of the rehydration solution into each well (the final volume of DharmaFECT Transfection Reagent will be 0.4 μ l/ well) and incubate the plate at room temperature for 30-90 minutes to allow complete rehydration of the siRNAs. During the time of incubation, prepare A549 cells at density of 2.5×10^5 cells/ ml in 15 ml of antibiotic-free complete DMEM medium. After that, seed 100 μ l of the cell suspension into each well of the siARRAY RTF plate (final cell density will be 2.5×10^4 cells /well). Wrap the plate with plastic and then incubate in a humidified atmosphere at 37°C with 5% CO₂ for 48 hours in order to allow siRNA transfection and efficiently silencing of the target genes. After 48 hours of the siARRAY RTF plate incubation, prepare influenza A virus (strain A/Victoria/3/75) suspension by dilution of the virus stock with DMEM medium to yield the desired concentration of 1.25×10^6 pfu/ml (5 multiplicity of infection). Remove the cell culture media from each well of the siARRAY RTF plate. Add 100 μ l of virus suspension into each well by using multi-channels pipettor and then incubate in a humidified atmosphere at 37°C with 5% CO₂ for 1 hour with occasionally shaking to allow the virus to adsorb into the cells. After incubation, remove the virus suspension from each well and then wash by 100 μ l of Phosphate buffered saline (PBS). Add 100 μ l of complete DMEM medium into each well and then incubate in a humidified atmosphere at 37°C with 5% CO₂ for 24 hours in order to allow virus replication occurred. After the time of incubation, cytopathic effect (CPE) occurred on the monolayer of viable cells was determined by MTT assay and the supernatant from each well was harvested for RNA extraction and then followed by real-time RT-PCR detection.

Table 27 Membrane trafficking gene families used as a target for gene knocked-down by RNAi screening

Symbol	Official Name	Location	Accession
ACTR2	ARP2 actin-related protein 2 homolog	2p14	NM_005722
ACTR3	ARP3 actin-related protein 3 homolog	2q14.1	NM_005721
ADAM10	ADAM metallopeptidase domain 10	15q22	NM_001110
AMPH	amphiphysin	7p14-p13	NM_001635
AP1B1	adaptor-related protein complex 1, beta 1 subunit	22q12.2	NM_001127
AP1M1	adaptor-related protein complex 1, mu 1 subunit	19p13.12	NM_032493
AP1M2	adaptor-related protein complex 1, mu 2 subunit	19p13.2	NM_005498
AP2A1	adaptor-related protein complex 2, alpha 1 subunit	19q13.33	NM_014203
AP2A2	adaptor-related protein complex 2, alpha 2 subunit	11p15.5	NM_012305
AP2B1	adaptor-related protein complex 2, beta 1 subunit	17q11.2-q12	NM_001282
AP2M1	adaptor-related protein complex 2, mu 1 subunit	3q28	NM_004068
ARF1	ADP-ribosylation factor 1	1q42	NM_001658
ARF6	ADP-ribosylation factor 6	14q21.3	NM_001663
ARFIP2	ADP-ribosylation factor interacting protein 2	11p15	NM_012402
ARPC1B	actin related protein 2/3 complex, subunit 1B, 41kDa	7q22.1	NM_005720
ARPC2	actin related protein 2/3 complex, subunit 2, 34kDa	2q36.1	NM_005731
ARPC3	actin related protein 2/3 complex, subunit 3, 21kDa	12q24.11	NM_005719
ARPC4	actin related protein 2/3 complex, subunit 4, 20kDa	3p25.3	NM_005718
ARPC5	actin related protein 2/3 complex, subunit 5, 16kDa	1q25.3	NM_005717
ARRB1	arrestin, beta 1	11q13	NM_004041
ARRB2	arrestin, beta 2	17p13	NM_004313
ATM	ataxia telangiectasia mutated	11q22-q23	NM_138293
ATP6VOA1	ATPase, H ⁺ transporting, lysosomal VO subunit a1	17q21	NM_005177
BIN1	bridging integrator 1	2q14	NM_004305
CAMK1	calcium/calmodulin-dependent protein kinase I	3p25.3	NM_003656
CAV1	caveolin 1, caveolae protein, 22kDa	7q31.1	NM_001753
CAV2	caveolin 2	7q31.1	NM_001233
CAV3	caveolin 3	3p25	NM_001234
CBL	Cas-Br-M (murine) ecotropic retroviral transforming sequence	11q23.3	NM_005188
CBLB	Cas-Br-M (murine) ecotropic retroviral transforming sequence b	3q13.11	NM_170662
CBLC	Cas-Br-M (murine) ecotropic retroviral transforming sequence c	19q13.2	NM_012116
CDC42	cell division cycle 42 (GTP binding protein, 25kDa)	1p36.1	NM_001791
CFL1	cofilin 1 (non-muscle)	11q13	NM_005507
CIB1	calcium and integrin binding 1 (calmyrin)	15q25.3-q26	NM_006384
CIB2	calcium and integrin binding family member 2	15q24	NM_006383
CIB3	calcium and integrin binding family member 3	19p13.12	NM_054113
CLTA	clathrin, light polypeptide (Lca)	9p13	NM_001833
CLTB	clathrin, light polypeptide (Lcb)	5q35	NM_001834
CLTC	clathrin, heavy polypeptide (Hc)	17q11-qter	NM_004859
CLTCL1	clathrin, heavy polypeptide-like 1	22q11.21	NM_001835

Symbol	Official Name	Location	Accession
DAB2	disabled homolog 2	5p13	NM_001343
DDEF2	development and differentiation enhancing factor 2	2p24	NM_003887
DIAPH1	diaphanous homolog 1	5q31	NM_005219
DNM1	dynamin 1	9q34	NM_004408
DNM2	dynamin 2	19p13.2	NM_004945
DNM3	dynamin 3	1q24.3	NM_015569
EEA1	early endosome antigen 1, 162kD	12q22	NM_003566
EFS	embryonal Fyn-associated substrate	14q11.2-q12	NM_005864
ELKS	ELKS/RAB6-interacting/CAST family member 1	12p13.3	NM_015064
ENTH	clathrin interactor 1	5q23.1-q33.3	NM_014666
EPN1	epsin 1	19q13.42	NM_013333
EPN2	epsin 2	17p11.2	NM_148921
EPN3	epsin 3	17q21.33	NM_017957
EPS15	epidermal growth factor receptor pathway substrate 15	1p32	NM_001981
EPS15L1	epidermal growth factor receptor pathway substrate 15-like 1	19p13.11	NM_021235
FYN	FYN oncogene related to SRC, FGR, YES	6q21	NM_002037
GAF1	RAB11 family interacting protein 5 (class I)	2p13-p12	NM_015470
GIT1	G protein-coupled receptor kinase interactor 1	17p11.2	NM_014030
GORASP1	golgi reassembly stacking protein 1, 65kDa	3p22-p21.33	NM_031899
GRB2	growth factor receptor-bound protein 2	17q24-q25	NM_002086
HIP1	huntingtin interacting protein 1	7q11.23	NM_005338
HIP1R	huntingtin interacting protein 1 related	12q24	NM_003959
IHPK3	inositol hexaphosphate kinase 3	6p21.31	NM_054111
ITSN1	intersectin 1 (SH3 domain protein)	21q22.1-q22.2	NM_003024
ITSN2	intersectin 2	2pter-p25.1	NM_006277
LIMK1	LIM domain kinase 1	7q11.23	NM_002314
MAP4K2	mitogen-activated protein kinase kinase kinase kinase 2	11q13	NM_004579
MAPK8IP1	mitogen-activated protein kinase 8 interacting protein 1	11p12-p11.2	NM_005456
MAPK8IP2	mitogen-activated protein kinase 8 interacting protein 2	22q13.33	NM_012324
MAPK8IP3	mitogen-activated protein kinase 8 interacting protein 3	16p13.3	NM_015133
NEDD4	neural precursor cell expressed, developmentally down-regulated 4	15q	NM_006154
NEDD4L	neural precursor cell expressed, developmentally down-regulated 4-like	18q21	NM_015277
NSF	N-ethylmaleimide-sensitive factor	17q21	NM_006178
PACSIN1	protein kinase C and casein kinase substrate in neurons 1	6p21.3	NM_020804
PACSIN3	protein kinase C and casein kinase substrate in neurons 3	11p12-p11.12	NM_016223
PAK1	p21/Cdc42/Rac1-activated kinase 1	11q13-q14	NM_002576
PICALM	phosphatidylinositol binding clathrin assembly protein	11q14	NM_007166
PIK3CG	phosphoinositide-3-kinase, catalytic, gamma polypeptide	7q22.3	NM_002649
PIK4CA	phosphatidylinositol 4-kinase, catalytic, alpha polypeptide	22q11.21	NM_002650
PIP5K1A	phosphatidylinositol-4-phosphate 5-kinase, type I, alpha	1q22-q24	NM_003557
PSCD3	pleckstrin homology, Sec7 and coiled-coil domains 3	7p22.1	NM_004227

Symbol	Official Name	Location	Accession
RAB11A	RAB11A, member RAS oncogene family	15q21.3-q22.3	NM_004663
RAB11B	RAB11B, member RAS oncogene family	19p13.2	NM_004218
RAB3A	RAB3A, member RAS oncogene family	19p13.2	NM_002866
RAB3B	RAB3B, member RAS oncogene family	1p32-p31	NM_002867
RAB3C	RAB3C, member RAS oncogene family	5q13	NM_138453
RAB3D	RAB3D, member RAS oncogene family	19p13.2	NM_004283
RAB4A	RAB4A, member RAS oncogene family	1q42-q43	NM_004578
RAB4B	RAB4B, member RAS oncogene family	19q13.2	NM_016154
RAB5A	RAB5A, member RAS oncogene family	3p24-p22	NM_004162
RAB5B	RAB5B, member RAS oncogene family	12q13	NM_002868
RAB5C	RAB5C, member RAS oncogene family	17q21.2	NM_004583
RAB6A	RAB6A, member RAS oncogene family	11q13.3	NM_002869
RAB6B	RAB6B, member RAS oncogene family	3q22.1	NM_016577
RAB7L1	RAB7, member RAS oncogene family-like 1	1q32	NM_003929
RAB8A	RAB8A, member RAS oncogene family	19p13.1	NM_005370
RAB8B	RAB8B, member RAS oncogene family	15q22.2	NM_016530
RAC1	ras-related C3 botulinum toxin substrate 1	7p22	NM_018890
RHOA	ras homolog gene family, member A	3p21.3	NM_001664
ROCK1	Rho-associated, coiled-coil containing protein kinase 1	18q11.1	NM_005406
ROCK2	Rho-associated, coiled-coil containing protein kinase 2	2p24	NM_004850
SH3GLB1	SH3-domain GRB2-like endophilin B1	1p22	NM_016009
SH3GLB2	SH3-domain GRB2-like endophilin B2	9q34	NM_020145
SNAP91	synaptosomal-associated protein, 91kDa homolog	6q14.2	NM_014841
STAU	staufer, RNA binding protein, homolog 1	20q13.1	NM_004602
SYNJ1	synaptojanin 1	21q22.2	NM_003895
SYNJ2	synaptojanin 2	6q25.3	NM_003898
SYT1	synaptotagmin I	12cen-q21	NM_005639
SYT2	synaptotagmin II	1q32.1	NM_177402
TNIK	TRAF2 and NCK interacting kinase	3q26.2-q26.31	XM_039796
VAMP1	vesicle-associated membrane protein 1	12p	NM_014231
VAMP2	vesicle-associated membrane protein 2	17p13.1	NM_014232
VAPA	VAMP (vesicle-associated membrane protein)-associated protein A, 33kDa	18p11.22	NM_003574
VAPB	VAMP (vesicle-associated membrane protein)-associated protein B and C	20q13.33	NM_004738
VAV2	vav 2 oncogene	9q34.1	NM_003371
VIL2	villin 2 (ezrin)	6q25.2-q26	NM_003379
WAS	Wiskott-Aldrich syndrome (eczema-thrombocytopenia)	Xp11.4-p11.2	NM_000377
WASF1	WAS protein family, member 1	6q21-q22	NM_003931
WASF2	WAS protein family, member 2	1p36.11-p34.3	NM_006990
WASF3	WAS protein family, member 3	13q12	NM_006646
PIK3C2G	phosphoinositide-3-kinase, class 2, gamma polypeptide	12p12	NM_004570
MGC9726	RAB7B, member RAS oncogene family	1q32	NM_177403

- **MTT assay**

The MTT assay involves the conversion of the water soluble MTT (3-(4,5-dimethylthiazol-2-yl)-2,5-diphenyltetrazolium bromide) to an insoluble formazan. The formazan is then solubilized, and the concentration determined by optical density at 570 nm. Briefly, remove cell culture medium from each well of the 96-well plate and then replace with 100 μ l of fresh complete DMEM medium. Add 10 μ l of 12 mM MTT stock solution (prepared by mixing 5 mg of MTT with 1 ml of PBS) into each well. Incubate the plate in a humidified atmosphere at 37°C with 5% CO₂ for 4 hours. After incubation, add 100 μ l of SDS-HCl solution (prepared by mixing 1 g of SDS with 10 ml of 0.01 M HCl) into each well and mix thoroughly using the pipette. Incubate the plate in a humidified atmosphere at 37°C with 5% CO₂ for 4 -18 hours. Mix the suspension in each well again using a pipette and read absorbance at 570 nm.

- **Relative quantitation of virus production by real-time RT-PCR**

After 24 hours post-infection, the supernatant of each well was collected and subjected for RNA extraction. Amount of viral RNA production was quantitated by real-time RT-PCR using primers and probe specific for the matrix gene of influenza A viruses. Delta Ct method was used to calculate the relative quantitation of virus production in each individual well compared to mock transfection (Table 28). Delta Ct of M gene was calculated by using Ct obtained from each silenced sample minus with Ct obtained from mock transfection control [Δ Ct = Ct (silenced) – Ct (mock)]. Then the relative quantities of M gene were calculated by $2^{-\Delta$ Ct} formula. The silenced samples that yield significant alteration (at least 5 folds) in the virus production will be considered as candidate genes which may involve in the replication of influenza A virus.

Table 28 Means of delta Ct values obtained from relative quantitation of M gene by real-time RT-PCR

Gene	Δ Ct	Folds	Gene	Δ Ct	Folds	Gene	Δ Ct	Folds
ACTR2	1.98	-3.94	DDEF2	1.03	-2.04	RAB11B	-1.09	0.47
ACTR3	-0.34	0.79	DIAPH1	-1.35	0.39	RAB3A	-0.78	0.58
ADAM10	0.17	-1.13	DNM1	0.76	-1.69	RAB3B	-1.06	0.48
AMPH	-0.39	0.76	DNM2	1.02	-2.03	RAB3C	-0.68	0.62
AP1B1	1.35	-2.55	DNM3	2.66	-6.32	RAB3D	0.37	-1.29
AP1M1	-0.04	0.97	EEA1	0.51	-1.42	RAB4A	1.48	-2.79
AP1M2	1.83	-3.56	EFS	-0.02	0.99	RAB4B	-0.60	0.66
AP2A1	-0.66	0.63	ELKS	-0.40	0.76	RAB5A	-0.23	0.85
AP2A2	0.51	-1.42	ENTH	-0.70	0.62	RAB5B	0.58	-1.49
AP2B1	-0.17	0.89	EPN1	0.61	-1.53	RAB5C	0.25	-1.19
AP2M1	0.63	-1.55	EPN2	2.99	-7.94	RAB6A	-0.56	0.68
ARF1	0.74	-1.67	EPN3	2.57	-5.94	RAB6B	-0.69	0.62
ARF6	-0.50	0.71	EPS15	3.42	-10.70	RAB7L1	0.33	-1.26
ARFIP2	2.18	-4.53	EPS15L1	3.39	-10.48	RAB8A	0.07	-1.05
ARPC1B	0.73	-1.66	FYN	3.77	-13.64	RAB8B	0.17	-1.13
ARPC2	3.64	-12.47	GAF1	0.27	-1.21	RAC1	-0.33	0.80
ARPC3	3.63	-12.38	GIT1	-0.45	0.73	RHOA	-0.23	0.85
ARPC4	-1.05	0.48	GORASP1	-2.09	0.23	ROCK1	1.32	-2.50
ARPC5	-0.44	0.74	GRB2	-1.99	0.25	ROCK2	-0.21	0.86
ARRB1	0.28	-1.21	HIP1	-0.72	0.61	SH3GLB1	0.94	-1.92
ARRB2	0.50	-1.41	HIP1R	2.18	-4.53	SH3GLB2	0.26	-1.20
ATM	1.24	-2.36	IHPK3	1.41	-2.66	SNAP91	-0.72	0.61
ATP6VOA1	1.64	-3.12	ITSN1	1.22	-2.33	STAU	0.11	-1.08
BIN1	1.35	-2.55	ITSN2	3.05	-8.28	SYNJ1	0.43	-1.35
CAMK1	1.75	-3.36	LIMK1	3.12	-8.69	SYNJ2	0.50	-1.41
CAV1	0.57	-1.48	MAP4K2	2.41	-5.31	SYT1	-1.39	0.38
CAV2	1.26	-2.39	MAPK8IP1	-0.41	0.75	SYT2	1.10	-2.14
CAV3	-1.01	0.50	MAPK8IP2	0.94	-1.92	TNIK	-0.54	0.69
CBL	-0.54	0.69	MAPK8IP3	0.86	-1.82	VAMP1	1.07	-2.10
CBLB	0.22	-1.16	NEDD4	1.26	-2.39	VAMP2	0.04	-1.03
CBLC	-0.04	0.97	NEDD4L	0.13	-1.09	VAPA	1.01	-2.01
CDC42	0.22	-1.16	NSF	2.30	-4.92	VAPB	0.85	-1.80
CFL1	-0.43	0.74	PACSIN1	0.95	-1.93	VAV2	0.52	-1.43
CIB1	0.67	-1.59	PACSIN3	1.26	-2.39	VIL2	0.16	-1.12
CIB2	-0.17	0.89	PAK1	2.56	-5.90	WAS	1.59	-3.01
CIB3	1.52	-2.87	PICALM	1.08	-2.11	WASF1	2.29	-4.89
CLTA	-0.47	0.72	PIK3CG	-0.72	0.61	WASF2	-0.64	0.64
CLTB	0.02	-1.01	PIK4CA	0.16	-1.12	WASF3	0.43	-1.35
CLTC	0.20	-1.15	PIP5K1A	-0.50	0.71	PIK3C2G	1.08	-2.11
CLTCL1	0.66	-1.58	PSCD3	-0.80	0.57	MGC9726	-0.91	0.53
DAB2	0.79	-1.73	RAB11A	-0.87	0.55			

- Identification of host genes involving in the replication of influenza A viruses

The results of relative quantitation revealed that there were 12 candidate genes including ARPC2, ARPC3, DNM3, EPN2, EPN3, EPS15, EPS15L1, FYN, ITSN2, LIMK1, MAP4K2 and PAK1. Silencing of these genes resulted in more than 5 folds significant reduction of the virus production (Figure 55). The result implied that these 12 candidate genes may involve in the replication process of influenza A virus.

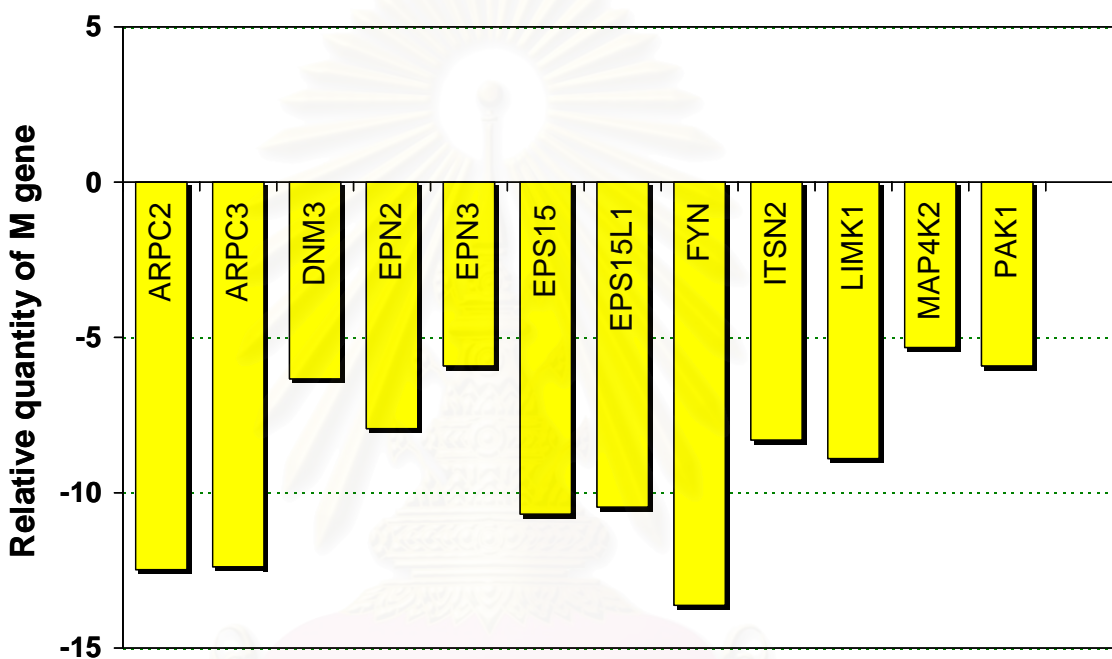


Figure 55 Relative quantification of M gene by real-time RT-PCR. Silencing of these 12 candidate genes yielded significant alteration (more than 5 folds) in the amount of influenza virus production.

- **Possible role of candidate genes in the replication process of influenza**

The RNAi screening was performed using A549 (human lung carcinoma) cells because their genes can be efficiently silenced with siRNA. Two days after transfection (90% transfection efficiency and >70% reduction in messenger RNA), A549 cells were infected with the influenza A virus using a high multiplicity of infection (MOI 5) and then after 24 hours post-infection, viral production in supernatant was determined by real-time RT-PCR. Delta Ct method was used to calculate the relative quantity of influenza viral load in the supernatant. The result revealed that there were 12 candidate target genes which yielded significant alteration (more than 5 folds) in the amount of influenza virus production. Silencing of ARPC2, ARPC3, DNMT3, EPN2, EPN3, EPS15, EPS15L1, FYN, ITSN2, LIMK1, MAP4K2 and PAK1 genes led to significant lower amount of influenza virus production, indicating that these target genes may be required for the process of influenza virus replication.

The replication cycle of influenza A viruses can be divided into 6 major steps, beginning with the attachment of the virus with host cell's receptors, entry of the virus into a host cell, followed by uncoating of the viral components into the cytoplasm. After that the viral RNAs and viral proteins are synthesized by using host cell machinery, then the viral RNAs and proteins are assembled into a new viral progeny and finally release of the infectious progeny virus. We hypothesized that virus replication process required host cell machinery and therefore, several host factors may play a crucial role in the replication. Several genes categorized into membrane trafficking gene family were subjected to be candidate target genes that may involve in the virus entry by endocytosis, transport of vesicle and virus assembly process.

- **Endocytosis of influenza A virus**

There are several endocytic pathways in cells which can be divided into phagocytosis and pinocytosis [112]. Phagocytosis is typically restricted to specialized cells such as macrophages and is mainly employed by cells to internalize large particles such as debris, apoptotic cells and bacteria whereas pinocytosis is responsible for the cell's uptake of fluids, macromolecules and small pathogens such as viruses.

Pinocytosis can occur by several different mechanisms including macropinocytosis, clathrin-mediated endocytosis, caveolin-mediated endocytosis, and clathrin & caveolae independent pathways [112]. Macropinocytosis is a form of regulated endocytosis that involves the formation of large endocytic vesicles after the closure of cell-surface membrane ruffles and often related with growth factor-induced membrane ruffling and protrusion, which then collapse to form vesicles (macropinosomes). Clathrin-mediated endocytosis occurs by the concentration of receptors and bound ligands into clathrin-coated pits (CCPs), which pinch off from the plasma membrane to form clathrin-coated vesicles (CCVs). The CCVs then uncoat and fuse with other endocytic vesicles or endosomes [113]. Caveolin-mediated endocytosis occurs via caveolae, i.e. caveolin-associated membrane invaginations, which pinch off to form endocytic vesicles and fuse with caveolin-containing membrane compartments, referred to as caveosomes [114]. Other clathrin- and caveolin-independent pathways are known to exist but are poorly understood due to the lack of any known marker proteins.

Previous study found that about two thirds (65%) of the endocytosed influenza virus particles associated with clathrin-coated pits (CCPs) for an extended period of time prior to internalization, indicating the endocytosis of the viruses via the clathrin-mediated pathway. The remaining one third (35%) of the influenza virus particles internalize into the cell via clathrin- and caveolin- independent pathway [115]. Therefore, clathrin-mediated endocytosis plays a crucial role in influenza virus entry. According to the results obtained from this study, we found that silencing of DNM3 (Dynamin), EPN2/EPN3 (Epsin), EPS15 (Epidermal growth factor receptor pathway substrate 15) and EPS15L1 (Epidermal growth factor receptor pathway substrate 15-like1) led to significant lower amount of influenza virus production. These genes encode for proteins that required for clathrin-coated pits formation during endocytosis [116-118] (Figure 56 and Table 29). Therefore, silencing of these genes resulted in blocking of influenza virus entry via the clathrin-mediated endocytosis pathway. The result implied that DNM3, EPN2, EPN3, EPS15 and EPS15L1 were associated with and required for influenza virus entry.

- **Transportations of endocytic vesicle**

According to the results obtained from this study, we found that silencing of EPN2/EPN3 (Epsin), DNAM3 (Dynamin) and ITSN2 (Intersectin) led to a significant lower amount of influenza virus production. These genes encode for proteins that are required for vesicle transport [119, 120] (Figure 56 and Table 29). Therefore, silencing of these genes resulted in blocking of influenza virus endocytosis via the vesicle transport pathway. The result implied that EPN2/EPN3, DNAM3 and ITSN2 were associated with and required for influenza virus endocytosis.

- **Roles of cytoskeleton in vesicle and protein transport**

Cytoskeleton is required for multiple cellular events including endocytosis and the transfer of cargo within the endocytic system. Microtubules and actin are required for efficient transcytosis and delivery of proteins to late endosomes and lysosomes [121]. Microtubules are long filamentous elements that are important in organelle localization, as well as transport of cargo between organelles. Movement along microtubules is relatively rapid and can occur over long distances. Actin filaments have also been implicated in localization of intracellular organelles and vesicular transport.

There are several models described roles of actin cytoskeleton in receptor-mediated endocytosis [121]: (1) The actin cytoskeleton may constrain the lateral mobility of receptors, thereby regulating their entry into coated pits. (2) Actin may act as a molecular fence that regulates access to the plasma membrane. Presumably, localized actin depolymerization would be permissive for the formation of coated pits and their subsequent internalization. (3) Actin may act as a scaffold for the assembly of the endocytic machinery or may be required for efficient invagination of the plasma membrane. (4) Actin forms a scaffold that promotes the assembly of dynamin and associated components at the neck of deeply invaginated coated pits. (5) Myosin motors, in conjunction with actin, form a contractile ring that helps pinch off coated vesicles. This event may be regulated by the dynamin GTPase. (6) Myosin motor:actin complexes are required for vesicle detachment and movement into the cytoplasm. (7) Actin polymerization on the coated vesicle promotes vesicle detachment and movement by formation of a comet tail. Therefore, actin dynamics (polymerization and disassembly) are required for vesicular and protein transport.

According to the results obtained from our study, we found that silencing of ARPC2/ARPC3 (Arp2/3 complex), ITSN2 (Intersectin), PAK1 (p21-activated kinases 1), LIMK1 (LIM domain kinase 1) and FYN (FYN oncogene related to SRC) led to a significant lower amount of influenza virus production. ARPC2/ARPC3 and ITSN2 genes encode for proteins that are required for the actin polymerization process [119]. LIMK1 associates with the stability of microtubule and regulates the actin polymerization [122]. PAK1 modulates actin dynamics through activation of the LIMK1 activity [123]. FYN associated with SRC regulates actin disassembly through activation of FAK activity [124]. Therefore, silencing of these genes resulted in blocking of influenza virus endocytosis and protein transport via the alteration of actin dynamics. The result implied that ARPC2/ARPC3, ITSN2, PAK1, LIMK1 and FYN were associated with and required for endocytosis and assembly of influenza virus (Figure 56 and Table 29).

A few candidate genes obtained from this study were concordant with the previous RNAi screening studies that PAK1 and FYN were required for the entry of Simian Virus 40 (SV40) into cells [125] whereas ARPC2/ARPC3 were required for *Listeria monocytogenes* infection [126]. MAP4K2 is not well characterized in terms of its functions. Therefore, we just speculate that this gene may involve in one of the steps in the process of influenza A virus replication.

In conclusion, applying the RNAi screening on membrane trafficking gene family, we identified 12 candidate genes involving in the replication of influenza A virus. This finding provided initial valuable information for the molecular virology regarding the host gene that is responsible for influenza viral replication which may be further applied for novel antiviral drugs in the near future. However, further investigations are required for more details about the interaction between host cell and virus.

Table 29 Possible roles of candidate genes involving in the replication of influenza virus

Symbol	Gene	Cellular functions	Possible association with influenza virus
EPS15	Epidermal growth factor receptor pathway substrate 15	Clathrin coated pit formation	Virus entry
EPS15L1	Epidermal growth factor receptor pathway substrate 15-like 1		
DNM3	Dynamin	Clathrin coated pit	Virus entry and Endosome transport
EPN2	Epsin	Vesicle transport	
EPN3			
ITSN2	Intersectin	Vesicle transport Actin polymerization	Endosome transport and Virus assembly
ARPC2	Arp2/3 complex	Activation of Actin polymerization	
ARPC3			
PAK1	p21-activated kinases 1	Regulation of actin polymerization and microtubule stability	
LIMK1	LIM domain kinase 1		
FYN	FYN oncogene related to SRC	Regulation of actin disassembly	

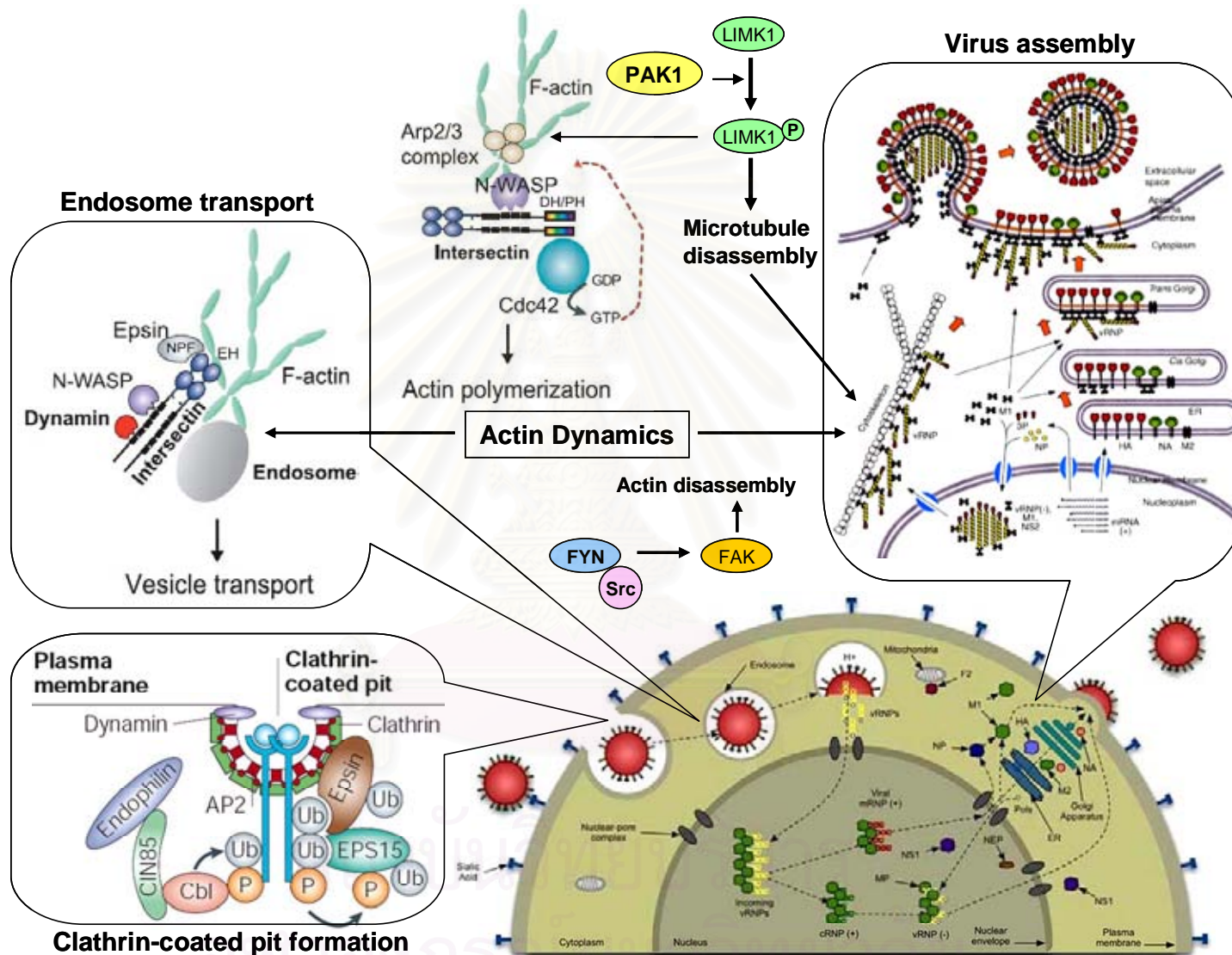


Figure 56 Proposed roles of the candidate genes involving in the replication of influenza A virus [116-124].

BIOGRAPHY

NAME: Sunchai Payungporn
SEX: Male
DATE OF BIRTH: August 31st, 1979
PLACE OF BIRTH: Bangkok, Thailand
NATIONALITY: Thai
E-MAIL ADDRESS: sirius_sun@hotmail.com

EDUCATION:

1998-2002: Bachelor of Science (1st Class Honors) in Biochemistry,
Chulalongkorn University, Thailand
2002-Present: Ph.D. student, Department of Biomedical Science, Faculty of Graduate
School, Chulalongkorn University, Thailand

RESEARCH GRANT: Royal Golden Jubilee Ph.D. program, Thailand Research Fund

PROFESSIONAL EXPERIENCE: A guest researcher in Molecular Genetics Section,
Influenza Branch, Centers for Disease Control and Prevention, Atlanta, GA (2005-2006)

INTERNATIOANAL PRESENTATION:

1. **Poster Presentation:** "Detection, isolation and characterization of influenza A subtype H3N8 viruses from dogs with respiratory disease in a shelter and veterinary clinic in Florida", Respiratory Viruses of Animals Causing Disease in Humans (E7). December 10-15, 2006. Singapore.
2. **Poster Presentation:** "Discrimination between highly and low pathogenic subtype H5 avian influenza A viruses", International Conference on Emerging Infectious Disease. March 19-22, 2006. Atlanta, GA.
3. **Poster Presentation:** "Simultaneous quantitation and genotyping of Hepatitis B virus by real-time PCR and melting curve analysis", The 5th Princess Chulabhorn International Science Congress "Evolving Genetics and Its Global Impact". August 16-20, 2004. Bangkok, Thailand.

PUBLICATIONS (2004-2006): 18 international publications and 2 regional publications